Examining Autophagy and Mitophagy as Inducible Mechanisms of Cellular Remodelling

by

Darin Bloemberg

A thesis

presented to the University of Waterloo

in fulfillment of the

thesis requirement for the degree of

Doctor of Philosophy

in

Kinesiology

Waterloo, Ontario, Canada, 2017

Examining Committee Membership

The following served on the Examining Committee for this thesis. The decision of the Examining Committee is by majority vote.

External Examiner: Dr. Vladimir Ljubicic

Assistant Professor – Department of Kinesiology, McMaster University, Hamilton, Ontario, Canada

Supervisor: Dr. Joe Quadrilatero

Associate Professor – Department of Kinesiology, University of Waterloo, Waterloo, Ontario, Canada

Internal Members: Dr. A. Russell Tupling

Associate Professor – Department of Kinesiology, University of Waterloo, Waterloo, Ontario, Canada

Dr. Paul Spagnuolo

Associate Professor – Department of Food Science, University of Guelph, Guelph, Ontario, Canada

Internal/External Member: Dr. Moira Glerum

Professor – Department of Biology, University of Waterloo, Waterloo, Ontario, Canada

Author's Declaration

This thesis consists of material all of which I authored or co-authored: see Statement of Contributions included in the thesis. This is a true copy of the thesis, including any required final revisions, as accepted by my examiners.

I understand that my thesis may be made electronically available to the public.

Statement of Contributions

Chapter I was written by Darin Bloemberg.

Chapters II-IV were conceived of and designed by Darin Bloemberg and Joe Quadrilatero. Experiments, data collection, data analyses, and figure preparation were performed by Darin Bloemberg. These Chapters were written by Darin Bloemberg and edited by Joe Quadrilatero.

Chapter V was written by Darin Bloemberg and edited by Joe Quadrilatero.

Abstract

Despite an explosion of knowledge regarding the molecular regulation of autophagy since its initial characterization in yeast in the 1990s (including the 2016 Nobel Prize in Physiology or Medicine for Dr Yoshinori Ohsumi), essential questions concerning its biological relevance are unanswered. Importantly, given autophagy's logical links to the beneficial health effects of relative caloric restriction and exercise, progress is being made towards developing autophagy-inducing drugs intended to generally benefit human health. Although many candidates appear to have such effects in model organisms and are well-tolerated by humans, it remains unclear whether these effects are due to autophagy specifically, as direct autophagy-inducing chemicals have not yet been publicly identified. This lack of precise autophagy-targeting chemicals amplifies and confounds the fact that the biological and physiological impacts of *specific* autophagy induction are relatively unexplored. Here, several basic cellular effects resulting from autophagy induction by amino acid starvation or rapamycin (mTOR inhibitor) as well as mitophagy induction by CCCP (depolarizes mitochondrial membranes) were examined. These effects were investigated in Atg7-knockdown C2C12 cells (considered to be autophagy-deficient) and those with Bnip3-knockout.

First, previous research has examined the relationship between autophagy and senescence caused by various stimuli; results have shown that autophagy promotes and attenuates senescence, depending on the study. Although, whether autophagy induction itself causes senescence has not been examined. We demonstrate that repeated administration of C2C12 cells with low staurosporine (STS) doses causes senescence characterized by G1 cell cycle arrest, enlarged cell and nuclei size, increased senescence-associated heterochromatic foci (SAHF), increased senescence-associated acid β–galactosidase activity (SA-Bgal), and myogenic differentiation impairment. However, none of these cellular features occurred in cells repeatedly incubated in amino acid and serum free media (HBSS), which massively induced

autophagy. Additionally, while senescent cells were protected from cell death caused by the DNA damaging agent cisplatin, HBSS-treated cells were not. When Atg7-deficient cells were intermittently given low dose STS, senescence did not occur, likely due to the vastly decreased ability to actually survive without functional autophagy. Therefore, Chapter II demonstrates that although autophagic activity is implicated in senescence development, massive sub-lethal autophagy induction itself does not cause senescence.

Next, we wanted to further examine autophagy-induced stress resistance development, as some protection from STS-induced cell death was observed in HBSS-treated cells in Chapter II. To do this, normal and Atg7-deficient cells were intermittently incubated in amino acid free media or rapamycin to induce autophagy, and the sensitivity to cell death caused by STS, cisplatin, or hydrogen peroxide was examined. Results indicated that prior repeated amino acid withdrawal protected cells from STS-induced cell death, and this required Atg7. This effect was likely due to reduced mitochondrial-mediated caspase activation, as caspase-9 activity was significantly lower in amino acid starved cells and administering a chemical inhibitor of caspase-3 could mimic the protective effect. Surprisingly, not only were rapamycin-treated cells not similarly protected, but they displayed increased sensitivity to cell death induced by hydrogen peroxide and cisplatin in an Atg7-independent manner. These cells were additionally characterized by greatly enlarged cell size, altered cell cycle profiles, and completely prevented myogenic differentiation. Therefore, Chapter III demonstrates autophagy's potential as a cellular remodelling mechanism that causes context-dependent stress resistance, and highlights the significant differences between metabolic stimulation of autophagy and that caused by mTOR inhibition.

Lastly, to investigate the relevance of mitophagy and mitochondria-specific mechanisms in mediating this observed autophagy-induced stress resistant phenotype, similar experiments were performed to

compare the effects caused by intermittently incubating cells in HBSS or CCCP. Although CCCP treatments did not protect from STS-induced cell death to the same extent as HBSS, both treatments attenuated calcium-induced mitochondrial membrane depolarization and permeability pore formation. In fact, this protection was abrogated in Atg7-deficient cells, demonstrating that autophagy is required for this adaptation. Further examination into mitochondrial function showed that previous intermittent amino acid starvation increased maximal ADP-stimulated cellular oxygen consumption when provided with complex-I and/or complex-II substrates. Additionally, not only was mitochondrial respiration significantly impaired in Atg7-deficient cells, but amino acid starvation did not increase oxygen consumption without Atg7. By generating Bnip3-deficient cells with CRISPR/Cas9, it was also shown that Bnip3 is dispensable for repeated amino acid starvation to cause resistance to STS-induced cell death and to increase maximal mitochondrial respiration. Therefore, Chapter IV demonstrates that specific amino acid starvation-induced autophagy causes mitochondrial remodelling resulting in increased stress resistance and function, and furthermore that Bnip3 may have a redundant role in this regard.

Acknowledgements

First, I want to thank my supervisor Dr Joe Quadrilatero for being my mentor and teacher throughout this process, and my committee members Dr Russ Tupling and Dr Paul Spagnuolo for your time and thoughtful recommendations in conceiving the Projects which comprise this dissertation.

The design and execution of this thesis could not have been accomplished without the invaluable assistance of Elliott and Mitch. Not only did the scientific theory and hypotheses behind these studies stem from our numerous conversations and thought experiments, but your contributions made to protocol development, actual collection of data, my psyche, and real life were indispensable and irreplaceable. Thank you for learning to fail and failing to learn with me. My fellow MBCDL members, including Brittany, Troy, Moe, Tina, and Boonstra, were also vital to numerous aspects of this thesis and my life, and as such I'd like to thank you for: being smarter than me and helping/forcing me to understand the scientific intricacies involved here (Brittany), making me exercise (Troy and Brittany), assisting with lab work (everyone), drinking beer with me (everyone except Brittany), allowing me to ignore your project (Moe and Boonstra), physically getting me out of BMH (everyone), finding Waldo (Tina), keeping me grounded (everyone), making sweet jokes (Troy and Tina), letting me call you funny names (Moe, Tina, B-Dawg, Boomstick, Trade Man), and of course, being a friend (everyone). Thank you also to everyone else in the department, including but not limited to Eric, Chris, Dan Ian, Val, Katie, Ryan, Crystal, and Aaron who helped teach, learn, and problem solve with me. Lastly, thanks to everyone mentioned and unmentioned (you know who you are) for the absolutely necessary fun and relaxing times we've had outside the lab, particularly to Jen and Lana for keeping me fed and lending me your husbands: these have really been the good ol' days.

Emily, thank you for your consistent motivation and support when things got tough both inside and outside the lab, and for having such a positive attitude about everything; I wouldn't have made it out alive without you bae. You are a generous, hard-working, amazing person and meeting you is undeniably the best thing to result from being here.

Finally, thank you to my family for your lifetime of support. Mom and Dad, your sacrifices gave me the opportunity to pursue this and the lessons you taught have allowed me to succeed in doing so. Jamie and Dan, you guys are great brothers; thank you for being there when I needed you and for letting me bore you with science. Although Dad had a lot of sayings, the two I most often consider when working and thinking about my future are "love what you do" and "you can be successful doing anything as long as you're good at it". Dad always emphasized the value of work and said he didn't care what we did, as long as it wasn't what he did. I would dedicate this thing to you if I actually believed that having a PhD guarantees that I won't become a drywaller someday, but I suppose that wouldn't be the worst thing in the world anyways: it seemed to work out pretty good for you.

Table of Contents

List of Figures

APPENDIX B

List of Abbreviations

3MA, 3-methyladenine
AIF, apoptosis inducing factor
Ambra1, autophagy and beclin 1 regulator 1
Akt, protein kinase B
AMPK, AMP-activated protein kinase
ANT, adenine nucleotide translocase
APAF1, apoptotic protease activating factor 1
ARC, apoptosis repressor with caspase recruitment domain
Atg, autophagy related
Bad, Bcl2-associated death promoter
BAG3, Bcl2 associated athanogene 3
Bak, Bcl2 homologous antagonist killer
Bax, Bcl2-associated X protein
Bcl2, B-cell lymphoma 2
BH, Bcl2 homology
Bid, BH3 interacting-domain death agonist
Bnip3, Bcl2/adenovirus E1B 19 kDa protein-interacting protein 3
Ca^{2+} , Calcium
CCCP, carbonyl cyanide 3-chlorophenylhydrazone
CDK, cyclin dependent kinase
CisPL, cisplatin
Cq, chloroquine
DISC, death-induced signaling complex
DD, death domain
DDR, DNA damage response
DMEM, Dulbecco's modified Eagle's medium
DRAM1, DNA-damage regulated autophagy modulator 1
Drp1, dynamin-related protein 1
ECL, enhanced chemiluminescence
ER, endoplasmic reticulum
FADD, Fas-associated protein with death domain
FBS, fetal bovine serum
FUNDC1, FUN14 domain containing 1
GABARAP, GABA type A receptor-associated protein
GAP, GTPase activating protein
GFP, green fluorescent protein
GM, growth media
H_2O_2, hydrogen peroxide
HB/HBSS, Hank's balanced/buffered salt/saline solution
HB+F, HBSS with 1% FBS
HRP, horse radish peroxidase
Hsp27, heat shock protein 27
Hsp70, 70 kDa heat shock protein
IAP, inhibitor of apoptosis protein
ICAD, inhibitor of caspase-activated DNase
IR, ischemia reperfusion

IRE1, serine/threonine-protein kinase/endoribonuclease inositol-requiring enzyme 1
JNK, c-Jun N-terminal kinases
LAMP, lysosomal associated membrane protein
LC3, microtubule-associated light chain 3-beta
Leu, leupeptin
LIR, LC3 interacting region
MAPK, mitogen-activated protein kinase
MAVS, mitochondrial anti-viral signaling
MEKK, mitogen activated protein kinase kinase kinase
Mfn, mitofusin
Miro, mitochondrial Rho GTPase 1
mLST8, MTOR Associated Protein, LST8 Homolog
MnSOD, manganese-dependent superoxide dismutase
MOMP, mitochondrial outer membrane permeabilization
mPTP, mitochondrial permeability transition pore
MST1, mammalian sterile 20-like kinase 1
mTOR, mechanistic target of rapamycin
mTORC1, mechanistic target of rapamycin complex 1
NAC, N-acetyl-L-cysteine
NBR1, autophagy cargo receptor
NDP52, nuclear dot protein 52 kDa
OMM, outer mitochondrial membrane
Opa1, optic atrophy 1
OPN, optineurin
PARP, poly ADP ribose polymerase
PARL, presenilin-associated rhomboid-like proteind
PBS, phosphate buffered saline
PDK1, phosphoinositide dependent kinase 1
PE, phosphatidyl ethanolamine
PERK, eukaryotic translation initiation factor 2-alpha kinase 3
PGC1a, peroxisome proliferator-activated receptor gamma co-activator 1-alpha
PI, propidium iodide
PI3K, phosphatidylinositol 3-kinase
PI3P, phosphatidylinositol 3-phosphate
PINK1, PTEN-induced kinase 1
PKC, protein kinase C
PRAS40, proline-rich Akt substrate of 40 kDa
PTEN, presenilin and tensin homolog
PUMA, p53-upregulated mediator of apoptosis
PVDF, poly-vinyl difluoride
Raf1, Raf-1 proto-oncogene, serine/threonine kinase
Rb, retinoblastoma protein
RCD, regulated cell death
RFP, red fluorescent protein
Rheb, Ras homologue enriched in brain
ROS, reactive oxygen species
SA-βGal, senescence-associated beta-galactosidase activity
SAHF, senescence-associated heterochromatic foci

SDS-PAGE, sodium dodecyl sulphate poly-acrylamide gel electrophoresis
Smac, second mitochondrial activator of caspases
STS, staurosporine
TAX1BP1, Tax1 binding protein 1
TBK1, TANK-binding kinase 1
TNF, tumor necrosis factor
TOM, translocase of the outer membrane
TRADD, tumor necrosis factor receptor type 1-associated death domain
TRAF2, TNF receptor-associated factor 2
TRAIL, TNF-related apoptosis inducing ligand
TRX1, thioreductase 1
TSC1, tuberous signaling complex 1
UBA, ubiquitin-associated domain
ULK1, unc-51 like autophagy activating kinase 1
UPR, unfolded protein response
UPS, ubiquitin proteasome system
VDAC, voltage dependent anion channel
XIAP, x-linked inhibitor of apoptosis protein

CHAPTER I: Introduction, review of the literature, and overall purpose

Overview

Cells deal with and respond to stressors in a variety of ways. Depending on a cell's current functional status, stress signal integration will direct response mechanisms ultimately leading to survival or death. A commonly investigated method of cell death is apoptosis, where cells mediate their own destruction upon reaching a critical level of damage. Currently attributed with both pro-survival and pro-death functions, autophagy is a mechanism of intracellular protein degradation which is activated in response to various stimuli. Importantly, many human disease states are associated with or caused by dysregulation of these two fundamental biological processes. Autophagic degradation is currently characterized with seemingly opposing roles. On one hand, research has demonstrated that autophagy contributes to detrimental cellular breakdown. On the other, autophagy has displayed cyto-protective functions as cells are more sensitive to death-inducing insults when it is inhibited. Importantly, it is known that several stressors, including damaging pharmacological agents (staurosporine, doxorubicin, cisplatin), pathophysiological conditions (ischemia reperfusion, infection/inflammation), and even exercise, induce autophagy before or while cell death processes are activated. While initial assessments of these observations concluded that autophagy was contributing to cellular demolition and elimination, subsequent experiments indicate that autophagy occurs in an attempt to mitigate the encountered stress. Although autophagy appears to be generally benevolent, as with other biological phenomena the most likely answer is that an optimal level of autophagy exists, and that specific conditions of overactive and underactive autophagy can be pathological. However, an interesting concept can be taken from these studies: if a properly-regulated induction of autophagy is considered a front-line defence mechanism, it is possible that intermittent autophagic degradation functions to remove hazardous cellular contents, thereby improving the cellular environment over time. Taken one step further, if autophagy *specifically* is induced, that is, not in the context of mediating dysfunction/damage, it may

serve as a pro-active mechanism of stress resistance. In this way, autophagy may constitute a mechanism through which cell composition and function can be improved.

This literature review provides an overview of the biochemical and physiological signals responsible for initiating and regulating both cell death and autophagy. Specifically, an emphasis will be placed on the autophagic removal of mitochondria, an occurrence termed mitophagy, due to the important role these organelles play in energy production and cell death. Furthermore, the interaction between the molecular signals regulating these degradative systems and their importance in maintaining tissue function and organ health will be considered.

Cell Death Functions and Processes

Apoptosis is a physiologically regulated cell death (RCD) mechanism responsible for eliminating abnormal, damaged, and/or unnecessary cells (1-3). Its activation results in cell removal by intracellular demolition stemming from protein cleavage, nuclei condensation, and directed packaging of cellular material. During development, specific cells undergo cell death in a genetically planned manner, thus regulating tissue shape and adult organ function (3). In adult organisms, apoptosis is responsible for removing cells which have lost specific functional abilities due to extra/intracellular damage or genetic disruption (2,3). Apoptosis represents a relatively clean method of cell death by limiting the exposure of potentially dangerous cellular contents to surrounding cells. In comparison, the cell death processes of necrosis and necroptosis elicit an immune response, which may lead to additional unwarranted tissue damage (4). Therefore, apoptosis allows cell removal while providing protection for the tissue and organism as a whole. Due to this important role, several disease states are associated with its dysregulation (3). For example, cancerous cells typically develop alterations which remove apoptosis-activating sensors or result in an apoptotic-resistant phenotype (2,3). On the other hand, overactive

apoptosis is implicated in the development of several autoimmune disorders as well as in the tissue loss contributing to neurodegeneration and heart failure (2,3). The primary executioners of apoptotic cell death are a family of enzymes known as caspases which cleave substrates between cysteine and aspartic acid residues (2,3,5). Caspases are generally separated into two broad categories: initiator and effector. Both exist as inactive procaspases and are activated by proteolytic cleavage, removing their pro-domain and leaving a truncated, active form. Initiator caspases, such as caspases-8 and -9, are activated on large, enzyme-specific, multi-subunit scaffold platforms. Effector caspases, such as caspases-3, -6, and -7, are activated by initiator caspases and are responsible for the cleavage of >400 cellular proteins (6). Cleavage of these numerous substrates results in cellular degradation, DNA fragmentation, and blebbing typical of cell death. The array of targeted proteins is large and includes: cytosolic and nuclear structural proteins such as actin and lamin; the DNArepair enzyme PARP, and the DNA-fragmenting enzyme ICAD; pro-death kinases MEKK and PKC; and additional pro-apoptotic effectors such as Bid (7).

Cell death can be initiated by several extra- and intra-cellular mechanisms. The extracellular/extrinsic pathway involves activation of a formal death-receptor from the tumor necrosis factor (TNF) super-family by the respective ligand (ie. TNF-a, Fas-L, TRAIL) (8). These receptors contain death-domains (DD), and their activation stimulates assembly of protein scaffolds such as the death-inducing signalling complex (DISC) through interaction of regulatory molecules including TRADD/FADD and procaspase-8 (8). This results in caspase-8 activation leading to cleavage-induced activation of caspase-3 (9). Intracellularly, cell death is induced by stressors sensed by the mitochondria and endoplasmic reticulum. Mitochondrial-mediated mechanisms are activated by toxic stimulants, growth-factor exhaustion, DNA damage, and/or reactive oxygen species (ROS) (1-3). These stimuli disrupt electron transport and ATP

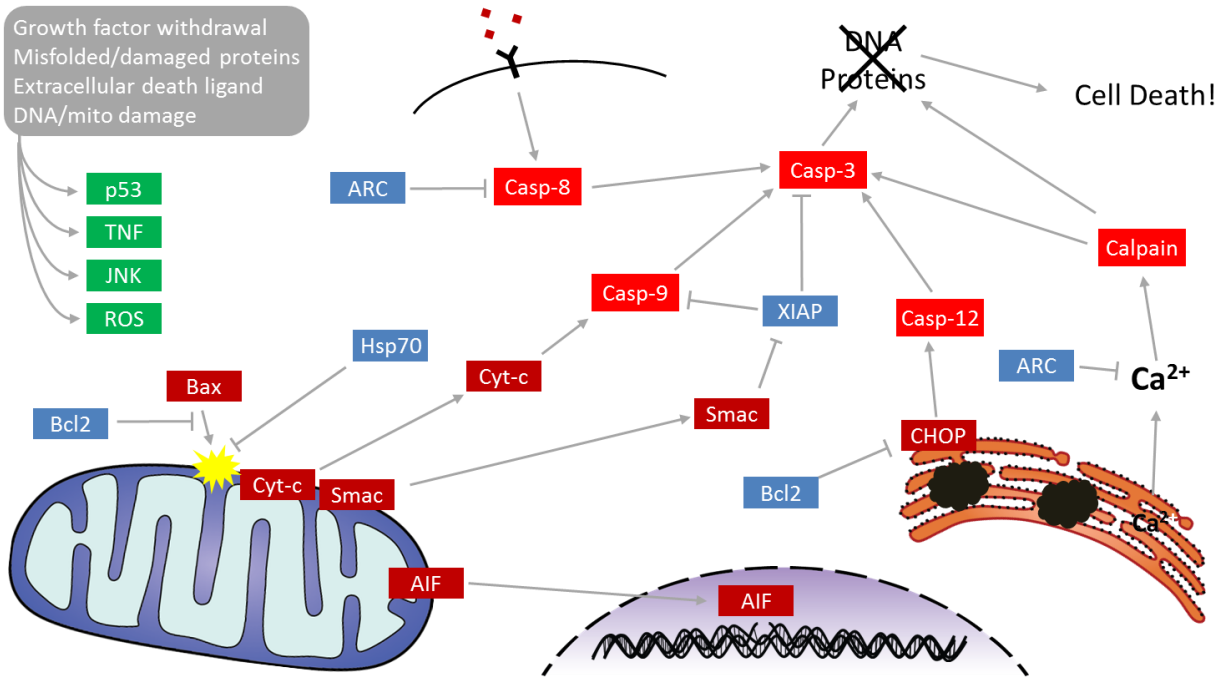

Fig. 1. Overview of downstream apoptotic cell death signaling pathways. This figure illustrates the molecular signaling pathways of important apoptotic cell death molecular effector proteins. In response to various extra/intra-cellular stimuli (grey box, upper left), several signaling families (TNF, JNK) integrate information and activate death-associated transcription factors (p53) and effector signaling mechanisms (ROS) (green boxes). Cells use mitochondria as central mediators of cell death: as their function greatly impacts cells' ability to produce engery and therefore live, the presence of mitochondrial-located proteins in the cytosol (indicating damage) act as strong proxy signals for the progression of cell death execution. Here, pro-death proteins (burgundy boxes) such as Bax participate in the permeabilization of mitochondria, causing them to release Cyt-c, Smac, and AIF, among others. Once release, these proteins directly damage DNA (AIF) and contribute to caspase activation (cyt-c, Smac). Caspases (red boxes) are proteolytic enzymes with numerous cellular targets whose activation ultimately leads to directed cellular demolition: these enzymes participate in amplification loops where their activities become unstoppable upon reaching a certain threshold. The binding of extracellular ligands at so-called death receptors is typically associated with caspase-8 activation through production of a series of highly ordered protein scaffolds. At the endoplasmic reticulum, accumulated misfolded proteins (brown clouds) and improper calcium handling can activate unique effectors such as CHOP, which promotes many aspects of cell death, and an additional family of proteolytic enzymes known as calpains. These pro-death signaling mechanisms are resisted by several proteins with anti-cell death functions (blue boxes), which provide an additional level of control. Note that significant cyclical redundancy exists with respect to these relationships: for example, although AIF cleaves DNA, DNA damage itself may initiate a similar chain of events (ie. activate p53) leading to caspase activation; similarly, caspase-dependent degradation of specifc targets, such as DNA or mitochondrial proteins, functions to amplify this response. TNF, tumor necrosis factor; JNK, c-jun N-terminal kinases; ROS, reactive oxygen species; casp-, caspase-; cyt-c, cytochrome c; Smac, second mitochondrial activator of caspases; AIF, apoptosis inducing factor; ARC, apoptosis repressor with caspase recruitment domain; XIAP, x-linked inhibitor of apoptosis protein; CHOP, C/EBP homologous protein; Ca^{2+}, calcium.

production, alter mitochondrial membrane potential, and cause release of proteins such as cytochrome c, second mitochondrial activator of caspases (Smac), apoptosis-inducing factor (AIF), and endonuclease G (EndoG) (2,3). In the cytosol, cytochrome *c* joins with apoptotic protease activating factor (Apaf-1) and procaspase-9, forming a molecular structure known as the apoptosome (10). The apoptosome cleavage-activates caspase-9, which in turn activates effector caspases (10). Smac release also leads to caspase activation by reducing the caspase-inhibiting potential of cytosolic proteins known as inhibitors of apoptosis (IAPs), which act on caspases-9 and -3 (11,12). AIF and EndoG, once released, can translocate to nuclei and cause DNA fragmentation independent of caspase activation (13,14).

These processes are regulated by many accessory proteins which provide various levels of control. Apoptosis repressor with caspase recruitment domain (ARC) inhibits apoptosis by preventing DISC assembly and the association of proteins which cause mitochondrial release of pro-apoptotic factors (15,16). Heat shock protein 70 (Hsp70) directly inhibits caspase-9 and can bind AIF in the cytosol, thus impairing its nuclear translocation (17,18). An important cell death-regulating group of proteins are those belonging to the Bcl2 family. The Bcl2 family consists of both activators and inhibitors of cell death and mediate the release of pro-apoptotic factors from the mitochondria (1,2,13,19). These proteins share specific Bcl2 homology (BH) domains, the number of which determines their apoptotic role. The inhibitors (Bcl2, Bcl-xL) contain four BH domains, while the pro-apoptotic members are either missing the fourth BH domain (Bax, Bak) or contain only the BH3 domain (PUMA, Bid, Bad, Bnip3) (1,2). The BH3-only proteins exist under extensive transcriptional and post-translational control. For example, PUMA transcription is initiated by p53 (20), Bid becomes pro-apoptotic after proteolytic cleavage by caspase-8 and caspase-2 (21,22), Bad is activated by dephosphorylation during growth factor deprivation (23), and Bnip3 is hypoxia-inducible (24). Upon their activation, BH3-only proteins promote the cell death promoting roles of Bax and Bak by binding anti-apoptotic Bcl2 proteins, thus relieving

their inhibitory associations with Bax/Bak, and by directly interacting with Bax/Bak (1-3). Ultimately, Bax activation leads to a conformation change, causing its mitochondrial translocation where it oligomerizes in the outer mitochondrial membrane (1,2). At the mitochondria, Bax and Bak participate in the opening of channels in the outer mitochondrial membrane (OMM), which results in the loss of membrane potential and release of soluble proteins from the intermembrane space such as cytochrome c (1,2). Additionally, Bax and Bak may contribute to the development of mitochondrial permeability transition pores (mPTP). These mPMP, which are formed by reconfiguration of the F-ATP synthase and perhaps the additional interactions of cyclophilin D (CypD), translocator protein (TSPO), voltage dependent anion channel (VDAC), phosphate carrier (PiC), and adenine nucleotide transporters (ANT) allow the outflow of material from the mitochondria (25). The loss in membrane polarization and resulting osmotic imbalance causes swelling of the inner mitochondrial membrane (IMM), mitochondrial outer membrane permeablization (MOMP), and subsequent release of cell death activating factors into the cytosol (1,2). Mitochondrial permeablization, therefore, is a critical point in cell death regulation, as the loss of membrane potential additionally decreases the ATP generating capacity which, in itself, induces apoptosis (2,26).

An important regulator of cell death is p53, which operates through direct protein-protein interactions and by acting as a transcription factor. Many cell-death inducing signals including DNA damage, elevated ROS, and various stress/mitogen activated protein kinases converge and depend on p53 to execute their apoptotic functions (2,3). As mentioned previously, p53 upregulates transcription of several pro-apoptotic proteins including PUMA, Bax, and Bad, while simultaneously repressing transcription of Bcl2 and ARC (20,27-29). In addition, mitochondrial p53 localization contributes to MOMP by interacting with Bad, Bax, Bak, Bcl2, and/or Bcl-xL, (28,30-33). Finally, p53 is able to reduce mitochondrial membrane potential by stimulating ROS production (34), and shuttling Fas receptor to the cell surface (35). Despite

the multitude of pathways through which p53 induces cell death, it also plays a primary role in regulating autophagy (36).

In addition to the mitochondria, sufficient stress to the endoplasmic reticulum (ER) can activate cell death-promoting mechanisms (37). ER stress is induced by improper folding and/or the accumulation of misfolded proteins, resulting in activation of the unfolded protein response (UPR) (37). Here, a build-up of damaged proteins in the ER induces the oligomerization of eukaryotic translation initiation factor 2-alpha kinase 3 (PERK), leading to translation inhibition in an attempt to limit the ER functional load (37,38). If the stress persists, continued PERK activation will stimulate the transcription factor C/EBP homologous protein (CHOP), thereby causing Bcl2 downregulation and translocation of Bax to the mitochondria (39-41). Another UPR-related factor, IRE1, will activate c-Jun N-terminal kinases (JNKs) as well as recruit TNF receptor-associated factor 2 (TRAF2), each of which promotes apoptosis-inducing cell signalling mechanisms (42,43). Furthermore, sufficient ER stress will lead to impaired Ca^{2+} homeostasis. Elevated cytosolic calcium can activate caspase-12 as well as a class of apoptosis-associated Ca^{2+}-induced proteases known as calpains (43-45).

Regulation of Autophagy

Autophagy is a degradative process responsible for breaking down various subcellular content (46-49). Unlike the other major proteolytic pathway, the ubiquitin-proteasome system (UPS), which targets individual substrates based on specific ligase-substrate identification, autophagy is thought to degrade large portions of cytoplasm in addition to entire organelles. Briefly, autophagy operates by generating double-membrane organelles known as autophagosomes, filling them with cellular cargo, and fusing these structures with lysosomes where their contents are degraded and recycled back into the cytosol (46,48,49). The execution of autophagy involves a highly conserved molecular signalling pathway that

can be induced by numerous stimuli (46-49). The primary function of autophagy seems to be the provision of energetic substrates during periods of starvation, thus sacrificing cellular material to enable adequate ATP production. In fact, systemic deletion of many autophagy-related genes is embryonically lethal in mice, largely due to autophagy's ability to regulate and maintain the dramatic metabolic alterations which occur during development and the subsequent transition from *in utero* feeding (50-55). Autophagy is additionally involved in defense, remodelling, and the removal of damaged and long-lived proteins and organelles. Due to these functions, autophagy is considered cyto-protective, serving to prolong proper cellular functioning (46-49). However, the importance of proper autophagic regulation is emphasized during conditions of its overactivation, which can promote unnecessary degradation and even cell death (46,49). This is highlighted in the observation that dysfunctional autophagy is implicated in the pathogenesis of several diseases including cancer, neurodegeneration, and heart disease (46,49). Several classifications of autophagy exist; these are typically categorized based on the mechanism of lysosomal targeting (48,49). Autophagic degradation characterized by autophagosome-lysosome fusion is termed macroautophagy, but will be referred to simply as autophagy here.

Autophagic degradation is carried out using well characterized molecular signalling machinery. Initially described in yeast, novel genes regulating autophagy were identified and termed autophagy-related (Atg) (46,48,49). However, many homologues have been identified in mammals and given names separate from their yeast "Atg" counterpart (46,48,49); the mammalian forms will be used here. Autophagy begins with the production of a double membrane structure known as the isolation membrane (yeast: phagophore). Development of the isolation membrane is controlled by two multi-subunit kinase complexes (46,48). One such complex contains, among others, the proteins ULK1/2, Atg13, and FIP200, and will be referred to as the ULK complex (46-48). Under nutrient/growth factor-rich conditions, the mechanistic target of rapamycin (mTOR) complex 1 (mTORC1) is active and exists in

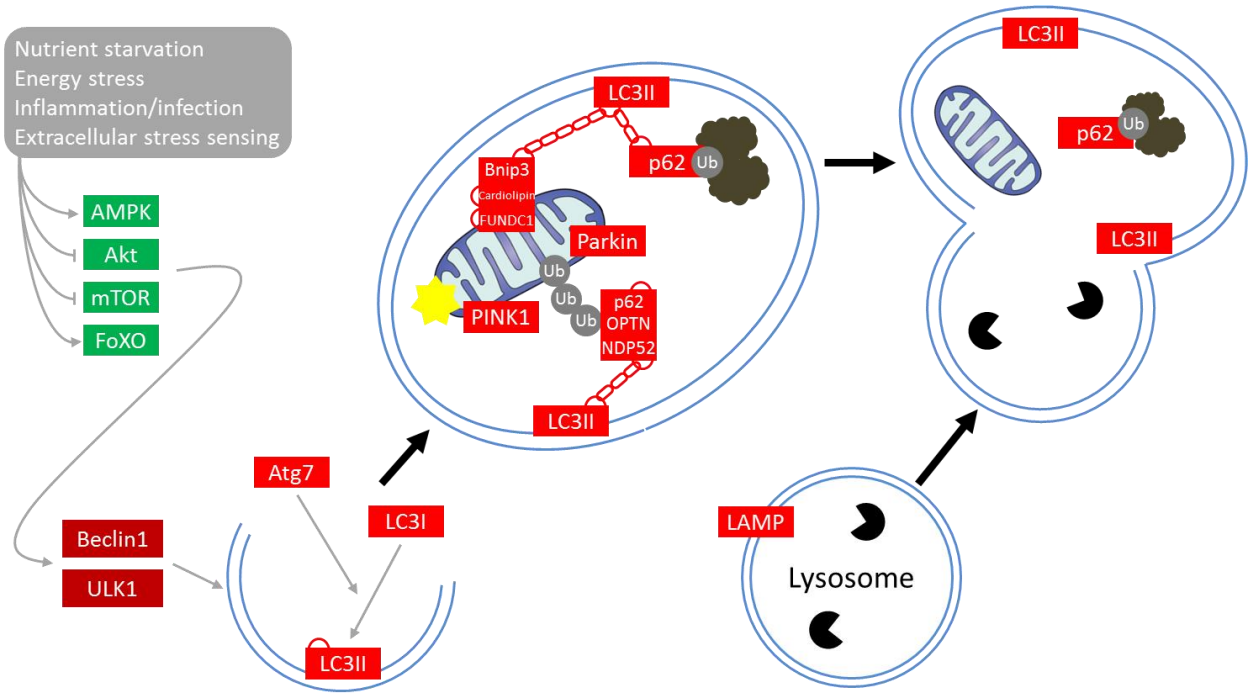

Fig 2: Overview of downsteam autophagy signaling pathways. Although autophagy is acutely sensitive to energy/nutrient status, numerous other stimuli affect the execution of autophagic flux (grey box, upper left). These stimuli typically function by activating (AMPK, FoXO) and/or inhibiting (Akt, mTOR) cellular stress and energy/nutrient sensing molecular signaling mechanisms (green boxes). Autophagy involves de-novo production of an organelle called the autophagosome, principally mediated by the Beclin and ULK signaling complexes which modulate downstream autophagy-related (Atg) protein function. An important member of this developing organelle is LC3, the activated form of which (LC3II) is responsible for identifying appropriate targets for autophagic degradation. These potential substrates are identified by several means: p62 binds to aggregated and misfoled proteins (brown clouds) with ubiquitin tags, while mitochondria are identified by unique ubiquitin binding and complex kinase-dependent activation of Parkin and PINK1, which accumulates on dysfunctional mitochondria. Additional proteins such as Bnip3, Nix, and FUNDC1 as well as cardiolipin are also capable of interacting with LC3 and therefore identifying mitochondria to be degraded. Upon their complete formation, autophagosomes bind to lysosomes with the help of adaptor proteins such as LAMP, after which all autophagosomal contents (including the inner membranes) are degraded by proteolytic lysosomal enzymes (Pac-men shapes). The resulting peptides/amino acids are then released into the cytosol for recycling, or perhaps used for subsequent immunomodulation purposes. LAMP, lysosome associated membrane protein; LC3, microtubule associated protein light chain 3; PINK1, PTEN-induced putative kinase 1; Ub, ubiquitin.

close association with the ULK complex (47,56). In this state, mTORC1 maintains a level of ULK1/2 and Atg13 hyperphosphorylation thereby inhibiting their activation (56,57). mTOR inhibition results in dissociation of the ULK complex from mTORC1 leading to ULK1/2 hypophosphorylation (56,57). This

activates ULK1/2, promoting its autophosphorylation and phosphorylation of distinct residues on other ULK complex members Atg13 and FIP200 (58). These phosphorylation events induce ULK complex activation and translocation to the site of pre-autophagosome production, leading to isolation membrane production as well as activation of other autophagy-related cellular machinery (56,58,59). Although the exact downstream targets of the active ULK complex are just being characterized (60), there is evidence that, in addition to stimulating phagophore production, it interacts with other regulators of isolation membrane development (47,61,62). The main protein members of this second kinase platform are Beclin1, Vps34, and Ambra1, and will be referred to as the Beclin1 complex (46,48). This complex functions as a class-III phosphatidylinositol 3-kinase (PI3K), and is responsible for the production of phosphatidylinositol 3-phosphate (PI3P) (63). The phosphatidylinositol for this reaction is sourced from other cellular membranes such as that of the plasma membrane (64), ER (65,66), or mitochondria (67), indicating that existing double membranes are required for autophagosome biosynthesis. In fact, it's been demonstrated that ER-mitochondria contact sites, known as mitochondria-associated ER membranes (MAM), are the likely source of elongation membrane formation, as upstream autophagy-related proteins such as Beclin1 converge here during autophagy induction and whose dysfunction impairs autophagosome formation (68,69). Like ULK, the Beclin1 complex is controlled by several mechanisms ensuring it is only activated when necessary. Primarily, due to the BH3 domain of Beclin1, the activity of this complex is reduced by direct binding of the anti-apoptotic Bcl2 family members Bcl2 and Bcl-xL to Beclin1 (70). In addition, ULK-mediated Ambra1 phosphorylation also contributes to Beclin1 complex activation (71). This event appears necessary to release the Beclin1 complex from a dynein light chain, thereby allowing its translocation to sites of membrane production (71). This, therefore, may represent a mechanism through which ULK signalling may aid in the sourcing of initial phagophore membrane products (71,72). Ultimately, the production of

PI3P induces autophagosome development by recruiting a number of adaptor proteins responsible for double membrane production (73,74).

The pre-autophagosomal membrane produced by active ULK and Beclin1 complexes is elongated with the help of two ubiquitin-like conjugation systems. The first involves the assembly of a protein complex composed of Atg12, Atg5, and Atg16 (75,76). Here, Atg12 is activated by Atg7 in an E1-like manner and is ligated by the E2-like carrier Atg10 to Atg5, thus forming an Atg5-Atg12 heterodimer (77). This is joined by Atg16, forming the active Atg5-Atg12-Atg16 conjugated protein, which then translocates to the developing isolation membrane (46,48). The second ubiquitin-like conjugation system is responsible for activating a very important protein member of autophagosome membranes, microtubule-associated light chain 3 (LC3). LC3 is a cytosolic protein whose autophagic role is initiated by Atg4-dependent cleavage, leaving a product known as LC3I (78,79). LC3I, like Atg12, is activated by Atg7 in an E1-like manner and is subsequently conjugated to phosphatidylethanolamine (PE) by the E2-like carrier Atg3 (80). The LC3I-PE conjugate, termed LC3II, is recruited by the Atg5-Atg12-Atg16 complex to the developing isolation membrane. Once the proper molecular machinery has been recruited, the ULK and Beclin1 complexes guide autophagosome elongation in association with Atg5-Atg12-Atg16, making LC3II a major membrane component (78,80). Here, in addition to basic structure, LC3II provides important functional roles. Upon completion of the autophagosome, the Atg5-Atg12-Atg16 conjugate dissociates, leaving LC3II embedded in the membrane. This is followed by autophagosome-lysosome fusion, dependent on the function of lysosomal associated membrane proteins (LAMPs), forming a structure known as the autolysosome (81). Finally, lysosomal hydrolases and cathepsins break down the autophagic cargo as well as the inner autophagosome membrane, including LC3II (46,48). Degraded material is released into the cytosol, where it is used for energy metabolism, protein synthesis, and various other tasks (46,48,49).

Because the biochemical products of autophagic degradation are used in a variety of cellular functions, and as overactive autophagy would be unnecessarily catabolic, its execution is precisely regulated. The mTORC1 is perhaps the most important control point for autophagy induction which, as previously mentioned, responds to cellular nutrient and energy status and affects ULK complex function (46-48). mTORC1 integrates information from several signalling pathways to regulate mRNA translation, subsequently impacting various cellular functions including cell cycle, differentiation, and cytoskeletal organization in addition to autophagy (46,47). mTORC1, composed of the subunits mTOR, raptor, mLST8, and PRAS40, is canonically inhibited with rapamycin, which stabilizes mTOR-raptor association thereby reducing the complex kinase activity (46). Active mTOR phosphorylates specific targets resulting in promotion of protein synthesis and prevention of autophagy; its inhibition therefore reduces mRNA translation and induces autophagy (46). The typical method of autophagy induction is nutrient deprivation, and many signals related to this phenomenon modulate mTOR function (46,47). Insulin and growth factor signalling inhibit autophagy through an Akt-mTOR axis. Insulin receptor activation stimulates phosphorylation of insulin receptor substrates (IRS), recruitment of class 1 PI3Ks, and production of phosphatidylinositol triphosphate (PIP_3). PIP_3 activates phosphoinositide dependent kinase 1 (PDK1) which subsequently phosphorylates and activates Akt. Activated Akt promotes phosphorylation of tuberous sclerosis complex components (TCS1, TSC2), thus preventing TSC2 interaction with TSC1 and blocking formation of the TSC1/2 complex (82). TSC1/2 is the GTPase activating protein (GAP) for the GTP-binding protein Rheb, and its inhibition causes Rheb to exist in its active GTP-bound state, allowing it to directly bind and activate mTORC1 (83,84). During periods of amino acid availability, mTORC1 is maintained in its active, protein synthesis promoting form via the interaction between raptor and the Rag family of small GTPases (85,86). Reduced cellular amino acid concentrations caused by starvation therefore remove the Rag/Rheb-mediated sensitisation of mTOR to nutrient availability, releasing the brake on autophagy induction (87). Finally, nutrient unavailability

increases the AMP:ATP ratio, resulting in AMPK activation. AMPK inhibits mTORC1 by phosphorylating TSC2 in a manner similar to Akt (but on different residues), as well as downstream of TSC1/2 by directly phosphorylating the mTORC1 component raptor (88,89). Furthermore, AMPK can activate autophagy by directly phosphorylating ULK1 (90,91).

Many of the autophagy-regulating mechanisms just described are additionally controlled by stress-sensitive systems like ROS as well as elaborate kinase signalling pathways involving JNKs, mitogen-activated protein kinases (MAPKs), and extracellular-signal regulated kinases (ERKs) (36,46,49). Although elevated ROS impact autophagy by causing cellular damage that autophagy attempts to mitigate, ROS additionally play direct roles regulating autophagy induction and execution (36,46,49). In fact, antioxidant administration actually depresses the level of starvation- (92) and ROS- (93,94) induced autophagy. Specifically, oxidation of Atg4 is partially required for autophagosome production (92), and ROS-induced inhibition of mTOR is dependent on AMPK (95). In this latter paper, autophagy activation in response to ROS also required the DNA damage sensor ataxia-telangiectasia mutated (ATM), and rescuing autophagy in ATM-deficient mice by administration of rapamycin reversed ROS-induced lymphomagenesis (95). Typically, autophagy protects from ROS-induced apoptosis (36,46). However, in specific cell types, suppression of autophagy-related genes actually ameliorated ROS-induced cell death (96), demonstrating the complexity of this relationship. Several stress-related kinases also impact autophagy in both mTOR-dependent and independent ways. JNK1-dependent phosphorylation of Bcl2 decreases its inhibition of Beclin1, thereby permitting autophagy induction during starvation (97). JNK signalling also contributes to mitophagy specifically by inducing FoxO3a-dependent transcription of Bnip3 (98). Growth-factor dependent activation of Ras signalling inhibits autophagy through MAPK-dependent activation of Akt (99). Furthermore, an amino-acid sensitive MAPK, Raf-1, impairs activation of downstream MAPKs MEK1/2 and ERK1/2 thereby inhibiting autophagy during nutrient excess

conditions (100). Likely, the integration of information processed by these complex signalling pathways allows cells to fine-tune their autophagic responses.

As mentioned, autophagy is capable of degrading non-specific portions of sequestered cytoplasm as well as specific cellular targets, including whole organelles. One way in which specific substrates are identified is through the interaction of LC3II with p62 (46,48). P62 is a multifunctional adaptor protein commonly found in clusters of protein aggregates. Damaged and misfolded proteins can be tagged for UPS degradation with the small regulatory factor ubiquitin. In addition to the proteasome, p62 can identify mono- and poly-ubiquitinated proteins and directly bind to them via its ubiquitin-associated domain (UBA) (101,102). P62 can subsequently bind to LC3 via its LC3-interacting region (LIR), thus directing specific substrates for autophagic degradation (101,102). This function is vital not only for the clearance of accumulated proteins but for basal autophagy, and therefore p62 is commonly analyzed as an indicator of autophagic flux (103). A similar protein, NBR1, also contains UBA and LIR, and functions similar to p62 (104). NBR1 can also directly bind to p62, where together they act as receptors for autophagic degradation of ubiquitinated substrates. Another method of aggresome degradation involves the recruitment of heat-shock proteins and the E3-ligase CHIP along with the co-chaperone BAG3 (105,106). Here, misfolded and ubiquitinated targets are sequestered by heat-shock complexes and shuttled to developing autophagosomes through the interaction between BAG3, p62, and LC3 (105,106). Lastly, several proteins participate in the identification of entire organelles for autophagic degradation. While autophagy appears capable of sequestering ribosomes, peroxisomes, and endoplasmic reticulum, the targeting of mitochondria is of particular interest given their role in energy production and apoptosis.

Mitophagy as Targeted Autophagic Degradation

Autophagy of mitochondrial (mitophagy) is a precisely controlled process, often regulated independently of the nutrient/energy/stress signals that govern basal autophagy (107). Mitophagy is important for the maintenance of mitochondrial morphology and function. Specifically, it appears that mitophagy primarily operates as a quality control mechanism, targeting and degrading dysfunctional mitochondria that may otherwise contribute to the activation of apoptotic signalling (107). Additionally, mitophagy is responsible for eliminating healthy mitochondria during the differentiation of several cell types (108-110). While the stimuli for induction and targeting may differ between mitophagy and "non-specific" autophagic degradation, mitochondria are thought to be degraded by full autophagosome sequestration and subsequent lysosomal fusion. In this sense, mitochondria are simply treated as very large autophagic substrates, thereby requiring activation of the molecular machinery responsible for phagophore production and substrate recognition (ie. Beclin1, ULK, LC3, etc.) (107). However, due to the size and complexity of mitochondrial networks, specific biological events related to mitochondrial identification and sequestration during mitophagy do exist.

Execution of mitophagy actually involves unique/additional substrate identification mechanisms. Notably, this typically includes the proteins Parkin and PINK1. Parkin, a cytosolic E3-ubiquitin ligase, and the mitochondrial phosphatase PTEN-induced kinase 1 (PINK1), were initially described due to their association with recessive form of parkinsonism (111,112). Specifically, this form of Parkinson's is associated with PINK1/Parkin dysfunction stemming from their genetic mutation. Normally, PINK1 is constitutively transported into mitochondria, cleaved by the protease presenilin-associated rhomboid-like protein (PARL), and subsequently degraded by mitochondrial proteases (113,114). When mitochondria become dysfunctional, PINK1 degradation by PARL is restricted and PINK1 becomes stabilized on the outer mitochondrial membrane (114-116). Specifically, it appears that PARL function is

dependent on proper mitochondrial membrane polarity, and dissipation of membrane potential reduces its activity resulting in PINK1 accumulation (114,117). In response, Parkin translocates to sites of mitochondrial damage denoted by PINK1 presence (114-116,118). Despite this widely accepted mechanism of mitophagy targeting and autophagic sequestration, it is unknown how exactly accumulation of PINK1 on mitochondrial membranes triggers Parkin recruitment (107). It is currently thought that mitochondrial proteins phosphorylated by PINK1 serve as Parkin docking sites or that direct phosphorylation of Parkin stimulates its translocation (107,119). More recently, the phosphorylation of ubiquitin by PINK1 and formation of specific poly-ubiquitin chains has been shown to regulate Parkin recruitment (120). Here, through an apparent feed-forward mechanism, mitochondrial depolarization and ubiquitination of mitochondrial outer membrane proteins allows PINK1-dependent phosphorylation of polyubiquitin as well as Parkin, both enhancing mitochondrial tethering of Parkin thereby causing further ubiquitination (121,122). In addition, one study has shown that the constitutively produced PINK1 cleavage fragment travels to the cytosol and impairs Parkin recruitment (123). Regardless, Parkin ubiquitinates several outer mitochondrial membrane proteins following its translocation, resulting in the isolation of mitochondrial fragments from the healthy population (124,125). Subsequently, these mitochondria are identified by ubiquitin-p62-LC3 autophagosome targeting and degraded following lysosomal fusion (117,118,126). However, it is important to note that several reports have indicated p62 is required for mitochondrial clustering/fragmentation during mitophagy, but not in their degradation specifically (117,127,128).

Several mitochondrial proteins have been identified as Parkin substrates which appear to be important for mitochondrial fragmentation and targeting, as well as autophagic identification. This includes the outer membrane fusion proteins mitofusins 1 and 2 (Mfn1/2), the translocases of the outer membrane (TOMs), voltage dependent anion channels (VDACs), and Miro (124,129-131). Parkin-mediated Mfn

ubiquitination stimulates its proteasomal degradation, and it is thought this occurs to prevent defective mitochondria from fusing back into the mitochondrial network (124,132). However, although Mfn degradation is necessary for mitophagy, this does not trigger mitophagy itself, as PINK1 and Parkin can initiate mitophagy in cells lacking Mfns (124,132). It was recently demonstrated that PINK1-dependent phosphorylation of Mfn2 was required for ubiquitination by Parkin, perhaps providing a mechanism for PINK1-dependent mitochondrial Parkin recruitment (133). Mfn elimination highlights the requirement for correct mitochondrial segregation during mitophagy. Importantly, excessive fusion, caused by overexpression of optic atrophy 1 (Opa1) or dominant-negative dynamin related protein 1 (Drp1), inhibits autophagic degradation of mitochondria (134). In fact, rounds of fission may be necessary or even responsible for causing mitochondrial fragments with phenotypes appropriate for autophagic degradation (ie. depolarized membranes) (134). Thus, functioning mitochondrial fission/fusion machinery, particularly the fission-regulating protein Drp1, should be considered prerequisite for proper mitophagy. During mitophagy, PINK1 and Parkin also become associated with Miro, a protein that anchors a kinesin/microtubule motor complex to mitochondria (131). Similar to Mfn, phosphorylation by PINK1 and ubiquitination by Parkin stimulates proteasomal degradation of Miro, releasing mitochondria from the kinesin complex and reducing mitochondrial motility, perhaps providing an additional mitochondrial quarantine measure (131). VDACs are also required for efficient Parkin recruitment, and their Parkin-dependent ubiquitination is necessary for mitophagy (118,130). However, in this study, as long as cells expressed one of the three VDACs present in mammals, mitophagy occurred seemingly unimpaired (130), supporting the findings of others who concluded VDAC ubiquitination was dispensable for mitophagy (117). Finally, Parkin ubiquitination of several TOM isoforms during membrane depolarization stimulates their proteasomal degradation (129). Although the specific role this has on mitophagy is unclear, PINK1 associates with TOM on mitochondria with polarized

membranes, therefore depolarization-induced PINK1 accumulation may affect TOM degradation and subsequent import of PINK1 (135).

Proper autophagic sequestration of mitochondria is aided by several adaptor molecules which function alongside and independently of PINK1 and Parkin. In yeast, the protein Atg32 functions alone in mitochondrial tagging, fragmentation, and identification of damaged mitochondria by autophagic machinery (136,137). A mammalian structural homologue, Bcl2-L-13, was recently demonstrated to be required for mitochondrial fragmentation and mitophagic degradation in HEK293 cells, and was additionally shown to mimic Atg32 in yeast (138). Here, this protein was shown to be capable of causing mitochondrial fragmentation independent of Drp1 through its BH domains, binding to LC3 using its LIR domains, and incorporation of mitochondrial fragments into lysosomes and depletion of mitochondrial proteins (indicating mitophagy) in the absence of Parkin. However, due to their relative complexity, previous research in mammalian cells has characterized a growing list of proteins which regulate mitophagy during various conditions (139). Two other Bcl2 family members possess autophagy promoting capabilities independent of their pro-apoptotic functions associated with being BH3-only proteins (140). Bnip3 (Bcl2/adenovirus E1B 19-kDa interacting protein 3) and its homologue Nix (Bnip3L) are implicated in several means of autophagy induction (141-144). Bnip3 and Nix induce autophagy by competitively binding to and displacing Bcl2/Bcl-xL from Beclin1, and perhaps by their ability to depolarize mitochondria (145). Furthermore, both interact directly with LC3 via LIR domains, and are therefore important for autophagosome-mitochondria targeting (142,146-148). The existence of LIR domains and binding of Bnip3/Nix with LC3 is the mechanism through which these proteins are thought to induce mitophagy independent of PINK1/Parkin. Alternatively, although PINK1- or Parkin-mediated exposure of Bnip3/Nix LIR domains is enticing, thus far evidence of such interactions is limited. However, it has been demonstrated that Bnip3 affects PINK1 function by suppressing its proteolytic cleavage thus

enabling PINK1-dependent mitophagy during hypoxia, and that Bnip3 overexpression suppresses muscle degeneration caused by PINK1 deactivation (149). In separate studies performed in cardiomyocytes, Bnip3 and Nix were able to trigger the translocation of Drp1 to mitochondria resulting in mitochondrial fission, followed by Parkin-dependent mitophagy (126,150). Another mitophagy targeting protein, FUNDC1, has been identified as an outer mitochondrial membrane protein involved in mitophagy (151). FUNDC1, similar to Bnip3/Nix, functions as an autophagosome receptor and mediates mitochondrial selective autophagy by interacting with LC3 through a LIR-like motif (151). Interestingly, ULK1 was recently shown to phosphorylate FUNDC1, enhancing its ability to bind LC3 (152). In this study, FUNDC1 reciprocally participated in mitochondrial recruitment of ULK1. The essential mitochondrial membrane phospholipid cardiolipin was also observed to signal mitochondria for autophagic degradation (153). In response to several autophagy inducers, cardiolipin externalization occurs and is subsequently bound to by specific LC3 residues (153). The protein optineurin, dysfunction of which is associated with amyotrophic lateral sclerosis (ALS) (mutation of optineurin on its own actually causes symptoms of ALS), also interacts with Parkin-dependent ubiquitinated mitochondria and LC3 using its LIR (154). In fact, despite the array of mitophagy-related adaptors, two recent studies have identified optineurin and the xenophagy-related protein NDP52 as the *de facto* receptor proteins required for mitophagy (128,155). These researchers suggest these two receptors function partly redundantly to link phosphorylated polyubiquitin to LC3 and subsequent Parkin-dependent enhancement of mitochondrial membrane protein ubiquitination (128). Here, PINK1-dependent phosphorylation of ubiquitin is vital to activating ubiquitin, optineurin, and NDP52 irrespective of Parkin presence. Importantly, fully Parkin-independent execution of mitophagy has been described (156). These researchers observed that the ULK-complex member Ambra1 promoted mitochondrial sequestration and mitophagy in Parkin-expressing cells. Additionally, in the absence of Parkin and p62, Ambra1 relocated to depolarized mitochondria and recruited LC3, a function dependent on its LIR (156). Similar observations of Parkin- (138,157-159) and

PINK1-independent (160) mitophagy have also been made by others, observations typically ascribed to the function of alternate mitochondrial targeting mechanisms. The existence of multiple and redundant mitochondrial targeting mechanisms underscores the importance of accurate substrate identification in mitophagic degradation.

Notably, the mechanisms of mitophagy induction outlined above all relate to mitochondrial segregation and identification by autophagosomes. Assuming that mitophagy requires autophagosome sequestration, an important question is: how does mitochondrial dysfunction induce autophagosome membrane production? In fact, recent work has demonstrated some interaction between the mitophagy machinery and upstream autophagy kinase complexes. First, Beclin1 has been shown to be involved with mitochondrial translocation of Parkin and subsequent Parkin-induced mitophagy (161). Importantly, following mitophagic stimuli, PINK1, Beclin1, and Parkin localize to MAM (162). Here, PINK1 aids in recruiting Beclin1 to MAM independently of Parkin, and this interaction was required for proper MAM-associated autophagosome biogenesis (162). The Beclin1 complex component Ambra1 is also recruited to depolarized mitochondria and promotes isolation membrane production and mitochondrial clearance (156,163). Next, full-length PINK1, which would only accumulate during mitochondrial depolarization, interacts with Beclin1 to promote autophagy (164). Finally, recent evidence shows that phosphorylation of the mitophagy receptors NDP52 and optineurin can activate the upstream autophagy regulating protines ULK1, DFCP1, and WIPI1 (128). Therefore, the ultimate result of these interactions is that during normal cellular functioning mitochondria prepped for mitophagy are degraded alongside other autophagy substrates, and that this occurs to a greater extent when markers of dysfunction (PINK1, Parkin, ubiquitin, Bnip3, p62, etc.) are present. One consideration to make is that these molecular descriptions of mitophagy execution were performed after an induction of mitochondrial dysfunction, an experimental necessity as mitophagy occurs relatively infrequently in

healthy mammalian cells (107). Typically, this involved chemical interruption of membrane polarization, photo-irradiation of mitochondria, or specific genetic manipulation (107). While pharmacological mitochondrial depolarization definitely activates mitophagy, other, physiological mechanisms of mitophagy induction are less well characterized. Perhaps the most commonly examined biological stimulator is ROS. Of note, Bnip3 is hypoxia-inducible and has been implicated in the regulation of mitophagy during ischemia-reperfusion (IR) in the heart (140,141,143,145).

Autophagy in Skeletal Muscle

In skeletal muscle, autophagy has demonstrated divergent functions. First, autophagy participates in the degradation of energetic substrates in skeletal muscle tissues during nutrient deprivation (165-168). This function is likely vital for converting and mobilizing skeletal muscle's large protein and glycogen stores into fuel for use by other tissues. In fact, it was recently shown that mice lacking skeletal muscle AMPK displayed hypoglycemia during fasting, a finding attributed to their inability to supply the liver with alanine for gluconeogenesis resulting from depressed skeletal muscle autophagy (169). However, this catabolic response must be properly regulated, and therefore autophagy may unnecessarily contribute to atrophy during specific circumstances (165). Elevated skeletal muscle autophagic activity has been observed in response to denervation (166,170,171), fasting (166,168,172), oxidative stress (173,174), chemotherapy (175), inflammation (176), glucocorticoid administration (176,177), and disuse (178,179). Although relatively fewer examinations regarding the specific activation of mitophagy in skeletal muscle have been performed, fasting has been shown to cause elevations in Bnip3 and Parkin levels (180,181), while indirect measurements have suggested increased mitophagy during fasting and denervation (170,171,180). Additionally, one study demonstrated that Parkin-deficient mice displayed delayed atrophy and decreased UPS activation during denervation compared to their wild-type counterparts

(171). Despite increased autophagic activity in skeletal muscle during these atrophic conditions, it is unclear whether this response contributes pathologically.

Importantly, the lack of autophagy also produces a number of detrimental effects. Owing to its important role as a cyto-protective mechanism in post-mitotic tissues, autophagy is required for maintenance of adult skeletal muscle, and dysfunctions in autophagy are associated with several pathological conditions, including aging, chronic disease, specific myopathies, and muscular dystrophies (165,182-186). In fact, simply inhibiting autophagy in skeletal muscle of adult mice through genetic deletion of Atg7 or Atg5 results in structural and functional abnormalities (182,184). Additionally, mice with skeletal muscle Atg7 deficiency since birth actually display increased atrophy during denervation (182). Reductions in mitophagy-related factors have also been observed during aging (187). Due to the energy demands and stress incurred, autophagy is unsurprisingly induced in skeletal muscle during and after exercise (188-190). It was previously demonstrated that autophagy contributes to the provision of metabolic substrates during prolonged acute exercise, and mice that are unable to induce autophagy during exercise have decreased running capacity (189). However, others have reported no detriment in exercise capacity in autophagy-deficient mice (191,192). Importantly, repeated autophagy induction is thought to be partially responsible for the beneficial effects of exercise training (190). This stems from the idea that skeletal muscle undergoes dramatic remodelling in response to chronic exercise, and that these changes require the turnover/transformation of cellular proteins and structures (190). The occurrence of mitophagy has also been noted after a bout of exercise, albeit indirectly (193), a response which theoretically has implications regarding training-induced mitochondrial biogenesis (110). Clearly then, autophagy serves a number of important roles in maintaining adult skeletal muscle structure and function. Finally, autophagy also appears to be important for skeletal muscle formation, where it

contributes to energy provision (194), protects from apoptotic signalling (183), and participates in mitochondrial remodelling (110).

In fact, investigations of autophagy's physiological relevance are normally performed to examine its cyto-protective role during various conditions. Specifically, without mitophagy, accumulation of dysfunctional mitochondria will theoretically lead to promotion of mitochondrial-mediated apoptotic signaling (107). Unsurprisingly then, significant cooperation exists between mitophagy and apoptosis mediators.

Interplay Between Autophagy and Cell Death: Molecular Signalling and Relevance

Several molecular components with apoptosis- and autophagy-specific roles have been shown to regulate both mechanisms. These functions provide a further level of pathway complexity that translates into a greater ability to fine-tune a stress response. The molecular interactions between apoptosis and autophagy are characterized by proteins with directly overlapping functions, the blunting of apoptotic proteolysis during elevated autophagic activity, and a tendency for autophagy inhibition during apoptosis.

As previously mentioned, the Bcl2 family of proteins are responsible for mediating apoptosis primarily through their roles related to mitochondrial permeablization. With respect to autophagy, the anti-apoptotic Bcl2 members (Bcl2, Bcl-xL) inhibit Beclin1 complex PI3K activity by directly binding to Beclin1's BH3 domain (70,195). Therefore, inhibiting Bcl2 through competitive binding by BH3-only proteins (ie. Bad, among others) and BH3 mimetics will increase Beclin1 complex activity and subsequently promote autophagy (195). Furthermore and as already cited, in addition to functioning as mitophagy receptors by interacting with LC3 (146,147), the BH3-only proteins Bnip3 and Nix interrupt

Beclin1-Bcl2 binding (145). Although their ability to induce apoptosis versus autophagy is not clear, the mitochondrial localization of Bax/Bak and BH3-only proteins may contribute to mitochondrial membrane depolarization and autophagosome membrane production at low activation levels, thereby only promoting apoptosis during prolonged/high intensity stresses. The apoptosis regulator p53 has also been shown to inhibit autophagy (196). Cytosolic localization of p53 protein allows its direct interaction with and inhibition of FIP200 (197) and Parkin (198), thereby reducing Beclin1 complex activity and preventing mitochondrial autophagic clearance. However, during situations of induced autophagy, p53 is responsible for activating transcription of TSC and AMPK components, two platforms with mTOR inhibiting, and therefore autophagy promoting, functions (199). Another p53 transcriptional target, DNA-damage regulated autophagy modulator 1 (DRAM1) is additionally responsible for executing p53-dependent autophagy during DNA damage and inhibition of mitochondrial respiration (200,201). As mentioned above, mitochondrial externalization of cardiolipin is required for mitochondrial targeting by LC3 and sequestration by autophagosomes (153). This essential membrane phospholipid also possesses several functions related to apoptosis. Oxidation of cardiolipin is known to be a major mechanism contributing to the mitochondrial release of cytochrome c (202), cardiolipin provides an activating platform for caspase-8 (203), and its oxidation also promotes OMM pore formation by tBid (204). A number of additional proteins display overlapping but less well examined roles. Death associated protein kinases (DAPKs) phosphorylate Beclin1 thereby relieving binding by Bcl-xL (205), JNK-dependent phosphorylation of Bcl2 similarly decreases inhibition of Beclin1 (97), and Akt inhibits autophagy and apoptosis by phosphorylating Beclin1 and Bad, respectively (206,207).

Several stressors have been shown to sequentially induce autophagy and apoptosis. Likely, this allows cells to mediate damage through elevated autophagic degradation before reaching a level obliging death (107). In fact, a recent analysis indicated that not only did cells induce autophagy and apoptosis

consecutively in response to several stressors, but those which mounted the most robust autophagic response displayed the greatest apoptotic resistance (208). This potential cyto-protective function of autophagy is commonly observed and is highlighted by the numerous observations that cell death increases when autophagy is inhibited (46,48,49) or that cell death can be attenuated by increasing autophagy (209,210). A quick internet/PubMed search for "autophagy and cell death" demonstrates the *huge* number and variety of situations in which this relationship is observed. Importantly, many of these effects are due to autophagic clearance of defective mitochondria whose continual dysfunction would lead to the activation of typical mitochondrial-mediated cell death mechanisms. Mitophagy was shown to attenuate heat-shock induced apoptosis, and chemical inhibition of the Beclin1 complex with 3-MA decreased mitophagy while increasing cytochrome c release and caspase-3 activity (211). Reducing Parkin protein levels sensitized neural cells to apoptotic cell death (212), and its overexpression protected cardiomyocytes during hypoxia (213). Finally, Bnip3-meidated mitophagy has also been shown to limit the mitochondrial amplification of apoptosis by reducing cytochrome c release capability (214). In addition to tempering the damage caused by dysfunctional mitochondria, other actions associated with mitophagy induction prevent apoptosis activation. Upon mitochondrial depolarization, PINK1 stabilizes the anti-apoptotic abilities of Bcl-xL by phosphorylating and preventing its cleavage (215). Although cytosolic p53 can bind to and inhibit mitochondrial Parkin translocation, Parkin has been shown to prevent p53-induced caspase-3 activation by acting as a transcriptional repressor of p53 (216). Additionally, specific targeting and degradation of caspase-8 during autophagy induction has been observed (217). In another interesting study, the proteins Bcl2 and FKBP38 were shown to selectively escape mitophagic degradation, and this contributed to apoptotic resistance (218). Clearly, autophagy and mitophagy not only serve as a first line of defence but also actively obstruct cell death associated processes.

When cellular stress and damage reaches a critical level however, apoptotic signalling mechanisms will overcome autophagy's protective capabilities and induce cell death. In fact, part of this response involves caspase-dependent cleavage and inactivation of autophagy executing proteins. The Beclin1 complex again constitutes a major site of this regulatory action. Caspase-3 can cleave Beclin1 itself during apoptosis induced by Bax, subsequently causing autophagy inhibition (219). Interestingly, the C-terminal fragment of Beclin1 resulting from caspase cleavage was shown to translocate to mitochondria where it promoted the release of pro-apoptotic factors (219,220) Ambra1 is a substrate for both caspase- and calpain-mediated cleavage during staurosporine induced apoptosis, subsequently contributing to inhibition of autophagy (221). Similarly, the Beclin1 complex member Atg3 also undergoes caspase-dependent cleavage during apoptotic stress (222). Substrates for apoptosis-induced inactivation of autophagy apart from the Beclin1 complex have also been identified. Of note, calpain-mediated Atg5 cleavage sensitized tumour cells to apoptotic stress, presumably due to inhibition of autophagic flux (223). Additionally, in several non-cancer cell lines, calpain activation produces an Atg5 cleavage product which undergoes mitochondrial translocation, leading to cytochrome c release and caspase activation (223). Similarly, the product of caspase-dependent cleavage of Atg4 has apoptosis-promoting effects (224). Finally, caspases cleave and inactivate Parkin, preventing the degradation of dysfunctional mitochondria and promoting a feed-forward cycle of cellular damage (225). Non caspase-dependent cleavage mechanisms also occur. The pro-apoptotic kinase mammalian sterile 20-like kinase 1 (Mst1) phosphorylates Beclin1, enhancing Beclin1 interaction with Bcl2/Bcl-xL, thus inhibiting autophagy and enhancing apoptosis (226). Furthermore, JNK phosphorylation of Mfns lead to their degradation during apoptosis and restricts Parkin-mediated mitophagy (227). Therefore, cells possess multiple redundant mechanisms which, during adequate apoptotic signalling, ensure autophagy inhibition and reinforce the commitment to cell death.

Although cells normally induce autophagy to protect themselves from further damage, there are a few examples of autophagy-promoted cell death. Of course, unrestrained autophagy and mitophagy would be unnecessarily catabolic and theoretically lead to cellular mitochondrial depletion. While these are not commonly observed methods of cell death in mammalian cells, some autophagy machinery is involved in cell death execution and the induced cell death of some specific cancer cell types is known to involve autophagy (36). Although caspase-8 activation typically occurs on a plasma membrane-bound complex called the DISC, a similar platform forms on autophagosomes and is required for complete enzyme activation (228). Atg12 has also been shown to promote apoptosis by binding to and inhibiting Bcl2, a function required for full cytochrome c release during staurosporine induced apoptosis (229). Furthermore, autophagy inhibition prevented cell death induced by falcarindiol in breast cancer cells (230), by MG-2477 in neuroblastoma cells (231), and by sunitinib in prostate cancer cells (232). In a more general setting, an interesting study demonstrated that inhibiting mitophagy resulted in less cell loss during starvation (233). Here, mitochondrial fusion increased during nutrient withdrawal, generating mitochondria that were too big to fit into autophagosomes. While starvation stimulated autophagy, the impact of specific mitophagy inhibition was maintenance of ATP generating capacity. When fission, and therefore mitophagy, was increased, starvation resulted in more cell death (233). Therefore, proper regulation of mitophagy and apoptosis is clearly necessary to appropriately respond to a variety of stresses.

Pathophysiological Implications of Autophagy

Until this point, autophagy and cell death have mostly been considered with respect to their context on a molecular and/or cellular level. Importantly, these molecular and cellular consequences of autophagy's impact on cellular stress resistance and function are relevant to numerous pathological conditions. Due to overlapping regulatory mechanisms, defective autophagy and mitophagy contribute

to unnecessary cell death and tissue loss, and the development of cellular pro-apoptotic environments can decrease the limit of survivable stress (46,48,49).

An obvious example of this is cancer development. Although apparently paradoxical, as autophagy is typically a pro-survival process, decreased autophagic activity is suggested to contribute to tumourigenesis (49,234). Mechanistically, several genetic alterations, such as p53 mutations, Bcl2 upregulation, and Beclin1 inactivation, are commonly observed in human cancers and cause cell death avoidance and alter cell cycle regulatory processes while additionally impairing autophagy (49,235,236). With respect to tumour development then, two hypotheses are generally agreed upon occurring (49,234,236). First, chronic/accumulated cellular stress, including that associated with oncogenesis, leads to genomic instability and oncogene activation in the absence of the damage-controlling relief of autophagy (a process that is likely mediated through p62 accumulation-induced NRF2 activation (237-239)); and similarly, without autophagy the stress associated with tumour development causes cell death through less immunologically-silent mechanisms and promotes an inflammatory environment, thereby leading to cancer progression (240). However, it is also well established that enhanced autophagy promotes the growth of established cancers and definitely contributes to therapy resistance (234). Therefore, cells that arise with increased ability to activate autophagy will thereby resist the ischemic and metabolic stresses associated with cancer progression and drive tumour growth. Although much is known regarding how this increased level of autophagy keeps cancer cell alive (for example by maintaining mitochondrial function, limiting ROS production, providing energetic substrates, resisting acute stresses, etc.), it appears relatively unknown how and why cells with augmented autophagic abilities arise at the onset of oncogenesis, particularly given that the genetic links briefly listed above (p53, Bcl2, Beclin1) cause autophagy impairment. It would additionally be interesting to identify specific cellular targets degraded by autophagy that promote tumour growth.

Insufficient mitophagy is directly related to the development of certain forms of Parkinson's (111,112). As outlined above, specific mutations in PINK1 and Parkin lead to the accumulation of protein aggregates and defective mitochondria thereby resulting in cell damage caused by impaired mitophagic flux (111,112,241,242). In fact, Parkin deficiency directly contributes to the accumulation of amyloid beta, a known protein aggregate associated with several neurodegenerative conditions including Alzheimer's (241,243). Additionally, mutations in PINK1 lead to dopaminergic cell loss typically observed during neurodegenerative diseases due to mitochondrial calcium stress (242,243). Mitophagy has also been shown to attenuate neuronal cell loss during ischemia (157), ischemia-reperfusion (244), and in response to staurosporine (245). Therefore, mediation of mitochondrial-related stresses by mitophagy is evidently necessary for preserving neural cell number and function. Importantly, a decrease in neuron mitophagy additionally contributes to aging-related neurodegeneration (243). These studies demonstrate that ways to maintain or increase mitophagy may alleviate cognitive decline during various conditions.

Mitophagy also plays a protective role in the heart. After myocardial infarction (MI), mitophagy and Parkin protein levels increase in the infarct border area (213). Not only do *Park2*$^{-/-}$ (Parkin) knockout mice display larger infarct areas, suggesting mitophagy prevents cell loss, they additionally show decreased survival (213). On the other hand, elevating mitophagy by decreasing p53 expression is associated with increased cardiac resistance to ischemic stress (198,246). Importantly, this was observed to occur through Bnip3-dependent mitophagy and not Parkin (246), demonstrating that mitophagy in general is protective. Although *Park2*$^{-/-}$ mice display normal cardiac and mitochondrial function at 12 months of age (213), mitophagy is impaired in the hearts of aged mice (198). In fact, mice overexpressing Parkin were resistant to the age-related decline in cardiac function, and this was

associated with elevated mitochondrial activity, decreased ROS production, and reduced inflammation (198).

In skeletal muscle, autophagy both and contributes to protects from specific pathological conditions (165). Autophagy participates in the degradation of energetic substrates in skeletal muscle tissues during nutrient deprivation (165-168). This function is likely vital for converting and mobilizing skeletal muscle's large protein and glycogen stores into fuel for use by other tissues. In fact, it was recently shown that mice lacking skeletal muscle AMPK displayed hypoglycemia during fasting, a finding attributed to their inability to supply the liver with alanine for gluconeogenesis resulting from depressed skeletal muscle autophagy (169). However, this catabolic response must be properly regulated, and therefore autophagy may unnecessarily contribute to atrophy during specific circumstances (165). Elevated skeletal muscle autophagic activity has been observed in response to denervation (166,170,171), fasting (166,168,172), oxidative stress (173,174), chemotherapy (175), inflammation (176), glucocorticoid administration (176,177), and disuse (178,179). Although relatively fewer examinations regarding the specific activation of mitophagy in skeletal muscle have been performed, fasting has been shown to cause elevations in Bnip3 and Parkin levels (180,181), while indirect measurements have suggested increased mitophagy during fasting and denervation (170,171,180). Additionally, one study demonstrated that Parkin-deficient mice displayed delayed atrophy and decreased UPS activation during denervation compared to their wild-type counterparts (171). Despite increased autophagic activity in skeletal muscle during these atrophic conditions, it is unclear whether this response contributes pathologically. On the other hand, inadequate clearance of autophagic cargo is observed in a number of lysosomal myopathies (185). Danon's disease, classically known as a glycogen storage disease, occurs primarily due to LAMP2 deficiency, resulting in the accumulation of autophagic vacuoles due to impaired autophagosome-lysosome fusion (185,247). Another glycogen storage disease,

Pompe's, is due to deficiency in alpha-1,4-glucosidase and is also characterized by autophagic build-up in the core of myofibers (185,248). Here, in a mouse model of Pompe's, the additional genetic inhibition of autophagy exacerbates the disease phenotype, suggesting autophagy is activated as a protective measure (248). Additionally, several studies have shown that impaired autophagic flux is a shared characteristic between several models of muscular dystrophy (249-251). Notably, when autophagic flux was promoted by feeding *mdx* mice a low protein diet, they displayed reversal in multiple skeletal muscle functional and structural abnormalities (250). Likewise, using the *Col4-/-* mouse model of muscular dystrophy, researchers showed that activation of autophagy by administration of a low protein diet or rapamycin, but not exercise training, dramatically decreased the level of several apoptotic markers and improved functional parameters (188,249). However, emphasizing the dual nature of autophagy, it was observed that inhibiting autophagy improved clinical symptoms of muscular dystrophy in a mouse model of MDC1A (laminin α2 chain deficiency) (251). Finally, it was recently demonstrated that skeletal muscle stem cells (satellite cells) from aged/geriatric mice displayed poorer functional capabilities compared to their younger counterparts and that this was related to the loss of basal autophagy (252). Remarkably, forced autophagy induction with rapamycin was able to restore the regenerative potential of these aged satellite cells (252).

Various other tissues also show examples of altered mitophagy impacting their pathophysiology. Pancreatic beta cells display reduced mitophagy during type 1 and type 2 diabetic conditions (253). When mitophagy was increased with Parkin overexpression, $p53^{-/-}$, or chemical p53 inhibition, beta cell function, marked by insulin secretion and whole-body glucose uptake, was maintained (253). In addition, Mst1, mentioned above to inhibit autophagy, was recently identified to be an important inducer of beta cell apoptosis during diabetic conditions (254). Mitophagy in kidney proximal tubule cells is responsible for maintaining mitochondrial function during metabolic acidosis (255), and, as in other

tissue types, impaired mitophagy contributes to cell damage, such as that which occurs during diabetic nephropathy (256). The extent of kidney injury during acute ischemia was additionally shown to be reduced by Bnip3-dependent mitophagy (257). Hepatitis B virus (HBV) can also affect liver cell death by modulating mitophagy (258). Here, instead of mitophagy impairment leading to increased apoptosis, HBV infection induced mitophagy thereby reducing hepatic cell apoptosis and allowing infection persistence (258).

Cellular Senescence

Another important phenomenon with connections to pathophysiological changes as well as aging that is intimately linked with cell death and autophagy is the development of cellular senescence. Senescence was originally described as the inability for normal proliferative cells to continue dividing when explanted for cell culture, now famously known as the "Hayflick limit" (259,260). Despite these cells maintaining viability and metabolic activity, they were observed to have undergone irreversible cell cycle arrest after a specific number of replications. From a disease pathogenesis perspective, senescence is thought to be tumor suppressive, in that its occurrence may restrict the growth and propagation of genomically-damaged cancer cells (261,262). On the other hand, the replacement of normally operating cells with senescent ones is also theorized to contribute to the declining regenerative capacity and tissue function associated with aging (262,263). Senescence is currently viewed as a perplexing and ill-defined occurrence, as despite efforts reconcile these seemingly opposing functions, fundamental information such as the triggers and prevalence of senescent cells *in vivo* is not presently known (264).

The gaps in knowledge regarding senescence exist for two reasons: 1) it was originally defined using cell culture, and it is unclear whether these *in vitro* observations translate *in vivo*, and 2) although several markers for senescence exist, it is generally a qualitative description that cells have stopped

proliferating, as the biochemical indicators are not universally found (264). Although Hayflick's initial experiments demonstrated that senescence naturally occurred after cells had divided a certain number of times (259,260), an occurrence suggested to be due to telomere shortening (265), studies performed since then have shown that senescence can be induced by numerous means (262,264,266). This includes oncogene activation/tumor suppressor loss, DNA damage, oxidative damage, overactive mitogen signaling, epigenetic changes (such as chromatin remodelling), and others (262,264,266). Experimentally, senescence stimuli are typically investigated by administering noxious chemicals or transcription-modifying factors to proliferative cells in culture and characterizing the molecular manner in which senescence develops (262,264,266). Usually, these various stressors activate the DNA damage response (DDR), a highly structured sequence of molecular events induced to repair double strand breaks which involves activating senescence-causing downstream signaling mechanisms (267). Broadly, these are divided into two major signaling pathways: those initially involving p53-mediated induction of the CDK inhibitor p21, and those involving activation of the CDK inhibitor p16 (266). Subsequent inactivation of retinoblastoma protein (Rb) by both signaling platforms reinforces cell cycle inhibition.

In addition to cell cycle arrest, the feature which best identifies senescence cells and characterizes the relevance of their existence is their production of unique endocrine/paracrine signals, termed the senescence-associated secretory phenotype (SASP) (262,264,266). These secreted proteins most often include TNFα,, TGFβ, IGF binding proteins (IGFBPs), IL6, IL8, matrix metalloproteinases (MMPs), monocyte chemoattractant protein 1 (MCP1) and others (262,264,266), and are primarily driven by NFκB related signaling in senescent cells (268). While these factors have numerous effects on neighbouring cells, it has been demonstrated that the SASP recruits immune cells, causes inflammatory responses in non-immune cells, reduces replication, promotes wound healing, remodels tissue structure, increases stem-ness, damages DNA, and actually induces senescence (269-273). Other typical

markers of senescence include increased number of genomic herterochromatic foci at non-telomeric sites (SAHF) which mark sites of DNA damage that generate molecular signals to impair cell cycle progression, and the development of acidic β–galactosidase activity (SA-βgal) which, despite its widespread use as a senescence marker, does not appear to have a senescence-relevant function and whose appearance is actually dispensable for senescence development (262,264,266).

A central conundrum regarding senescence development is that it is often utilized as a cell culture surrogate for "aging" (274). Although the link between replicative senescence and "senescence causes aging" seems apparent, there are a number of caveats in addition to the obvious apprehension required to give physiological relevance to cell culture findings. Notable among them is the difference in telomere biology between mice and humans. Despite their significantly reduced lifespans, mice telomeres are 5-10 times longer than humans, they display increased telomerase activity in most cell types (only stem cells in humans possess such activity), and telomerase knockout mice do not display a dramatic early aging phenotype (275). Additionally, most senescence-associated markers, including SASP, SA-βgal, p16 expression, and telomere shortening are observed in diverse biological situations such as during embryonic development, wound healing, professional immune cells, HIV infection, and cancer (264,276-280). Despite this, senescent cells do in fact increase in number during *in vivo* aging and two landmark studies demonstrate this. These researchers engineered mice to inducibly eliminate cells that expressed p16, thus preventing senescence development (281,282). Not only did this prevent aging-associated phenotypes in the adipose tissue, skeletal muscle, and eyes of a rapidly-aging mouse model, but it extended the lifespan of normally-aging male and female mice from two different genetic backgrounds (281,282).

Given its role mediating cellular stress responses, many connections have been made between autophagy and senescence. Unsurprisingly, the relationship between autophagy and senescence is complex (283). While studies have concluded autophagic activity can promote senescence or that a positive association between their induction exists (284-286), an equal body of evidence suggests autophagy prevents senescence or that they are negatively correlated (287-291). Single-cell analyses showed that autophagy inhibition triggered cell death and decreased senescence induced by DNA damage, suggesting that autophagy promotes senescence by suppressing death signaling (292). It was recently demonstrated that during oxidative stress-induced senescence in mouse 3T3 fibroblasts, autophagy inhibition was crucial for senescence development, autophagic flux was impaired in senescent cells, and restoration of autophagy was able to attenuate senescence (293). Meanwhile, another large study showed that senescent cells display increased "general" autophagy and that autophagy inhibition also caused senescence (294). Here, irradiation-induced senescence of human lung fibroblasts was suppressed by selective autophagic degradation of the transcription factor GATA4, activation of which promoted Nf-KB activity and the SASP, while general autophagy supported senescence transition by making substrates available for the SASP (294). Additionally, GATA4 protein accumulation was proposed to be caused by decreased association of p62 with GATA4. Notably, this observation provides mechanistic explanation for the cancer versus senescence consequence of DNA damage: p62 accumulation can activate NRF2 thereby contributing to oncogenesis (237-239), while decreased p62 may contribute to senescence (294). As p62's autophagic targeting functions depend on ubiquitination, these researchers also suggested altered activity of ubiquitin ligases or deubiquitinating enzymes for GATA4 may mediate its protein stability (294), although the factors which determine its expression after DNA damage are unknown. However, despite numerous examples of autophagy positively and negatively regulating senescence development in response to diverse stimuli, an

experiment testing whether autophagy induction through the strongest and most physiologically-relevant stimuli, amino acid starvation, occurs, has not been performed.

Cellular Hormesis, Preconditioning, and Autophagy

The concept of hormesis suggests that exposure to stressors at low doses results in generally beneficial changes, while high doses of similar stressors have negative effects (295). In biology, this is typically demonstrated by showing that administration of toxins in low doses conditions cells to be relatively resistance to damage subsequently caused by those toxins, a corollary similar to but distinct from the acquisition of senescence *in vitro* (296,297). This notion of adaptive preconditioning is an important protective measure in the heart and brain (298). In these tissues, intermittent periods of ischemia (ischemia-reperfusion, IR) is classically known to stimulate resistance to tissue damage and cell death caused by subsequent larger doses (299,300). Although IR-related protection is an accepted adaptive process for cardiomyocytes and neurons, examples of preconditioning involving other stressors and cell types exist. Previous hypoxia exposure was shown to contribute to cancer-associated resistance to cell death caused by doxorubicin and etoposide (301). Administrating relatively low doses of hydrogen peroxide (H_2O_2) to endothelial cells protected them from apoptosis caused by serum depletion, effects that were partially dependent on ROS-induced activation of the redox regulating enzyme thioreductase-1 (Trx-1) (302). Arsenite preconditioning reduced cell death and caspase-3/9 activity induced by ultraviolet radiation in corneal endothelial cells through activation of heat shock protein 27 (Hsp27) (303). It was demonstrated that 1 hour of heat shock treatment prevented H_2O_2-induced cell death in primary cardiomyocytes and C2C12 cells by attenuating mitochondrial Smac release and caspase-3/9 activation (304). Heat shock pre-treatment was also shown to protect HeLa cells from various apoptotic signaling including activation of caspases-3/9, mitochondrial Bax translocation, and p53 transcriptional activity caused by H_2O_2 (305). In this study, thermotolerant HeLa cells displayed several antioxidant

adaptations including increased expression and activity of MnSOD and catalase, while inhibiting glutathione production during heat exposure prevented the development of cell death resistance (305). Finally, exposing primary neurons to sub-lethal concentrations of ceramide provided protection against cell death triggered by oxygen/glucose deprivation (306), a finding partly explained by the observation that ceramide administration increased Bcl2 and Bcl-xL protein expression in neural tissue *in vivo* (307).

Despite these observations in cell culture models, the physiological relevance of hormesis is debated due to the complexity of biological organisms, the toxic side-effects associated with exposure to damaging stimuli, and the lack of specific adaptive mechanisms (295). However, on a cellular level, autophagy may represent an adaptive mechanism that contributes to preconditioning given its roles in defense and remodelling (296,297). In fact, autophagy's role in mediating the effects of ischemic preconditioning (IPC) is beginning to receive attention, where it is known to be a mediator of the protective effects of IPC in several tissues. Numerous modes of autophagy and/or mitophagy inhibition during the reperfusion phase prevented IPC-induced protection during middle cerebral artery occlusion or oxygen deprivation of cultured cortical neurons (244). Autophagy inhibition also prevented IPC-induced protection from subsequent liver ischemia in mice and rats (308). Similarly, the protective effects IPC are attenuated when autophagy is inhibited in neurons (309,310). Additionally, autophagy is implicated in contributing to the beneficial effects of caloric restriction and regular exercise, which can also be considered hormetic responses (296,311). In skeletal muscle, exercise training-induced mitochondrial biogenesis and running endurance were attenuated in *beclin1*-haploinsuffucient mice (191). Mice incapable of exercise-induced autophagy were also not protected from high fat diet-induced metabolic dysfunction applied after an exercise training regimen compared to their wild-type couterparts (189).

Finally, various modes of caloric restriction are known to induce longevity in model organisms (312). The potential involvement of autophagy in this context is clear and under intense investigation. In fact, studies have demonstrated that long-term administration of rapamycin increases longevity in species from yeast (311,313) to mice (311,314-317). Importantly, autophagy is required for the longevity inducing effects of caloric restriction and administration of various small molecules in yeast, worms, flies, and fish (311). However, the translation of these findings to non-human primates has been met with controversy, largely owing to the definition of what represents a "healthy" adult control (318-321) (This Sohal and Forster paper is interesting). Regardless, despite our vast knowledge of autophagy's molecular regulatory mechanisms, significantly less is known regarding the implications of its induction.

Conclusion

This literature review highlights that the balance between cell survival and death is determined not only by the type and intensity of stress but also a cell's ability to appropriately respond. Typically, surviving mild stresses is necessary for maintaining tissue function and is additionally associated with the development of advantageous cellular adaptations. Equally as important, however, is the efficient removal of mutated cells and those beyond repair as their accumulation is similarly dysfunctional. The proper interaction between stress processes is particularly salient in neural and muscle tissues, as cells lost here are difficult to replace and significantly contribute to their pathology. Fortunately, autophagy acts not only as a first or second line of defense during acute stressors, it also allows chronic stimuli to be sensed and responded to appropriately. This responsive remodelling function has demonstrated importance in such diverse cellular events as preventing cancer progression, transforming cells during differentiation, and mediating the exercise-induced benefits to skeletal muscle. Importantly, as progress is made towards conducting a human trial investigating the effects of rapamycin administration on aging (322), it is noteworthy that rapamycin is widely used as an immunosuppressant which also causes insulin

resistance, glucose intolerance, testicular degeneration, and cataracts (311). Therefore, it is likely that if a drug whose purpose is to activate autophagy is ever approved for human use, it will have to target autophagy in a more direct way.

Overall Purpose

Although the molecular mechanisms of cell death, autophagy, and mitophagy regulation are becoming well-characterized, many questions remain regarding their importance and relevance in specific physiological conditions. Amongst these are the general effects resulting from repetitive autophagy induction. Given its role as a cellular remodelling mechanism and potential involvement mediating the protective effects of preconditioning, it is possible that exclusive autophagy induction could mimic the effects of preconditioning without experiencing the associated toxic effects. Particularly, the abundance of specific targeting interactions suggests autophagy displays high level control, and is perhaps capable of avoiding non-discriminate degradation. Therefore, autophagy may affect cell composition by degrading cellular material, such as mitochondria, in a "worst is first" manner, particularly if an acute stress (like ischemia) is absent. However, this has yet to be shown experimentally. Therefore, the overall objectives of this thesis were to examine:

1) if autophagy induction itself leads to senescence development,

2) whether autophagy and/or mitophagy function as mechanisms of cyto-protective remodelling, and

3) what specific mechanisms of stress-resistance are affected by autophagy.

These objectives were examined using cell culture of C2C12 cells. These are murine/mouse skeletal muscle myoblasts (stem cell-like cells that spontaneously undergo characteristic skeletal muscle differentiation/development in culture) that is considered immortalized: current cell lines are derived

from a clone isolated in the 1980's from a line of cells originally obtained in the 1970's. These cells were chosen to conduct the experiments for this Thesis for several reasons: 1) the Muscle Biology and Cell Death Laboratory has extensive experience using this cell line and possesses robust protocols for culturing and analyzing them, 2) the hypothesis that autophagy generally mediates forms of cellular adaptation suggests this relationship should be observed regardless of the cell type used (ie. as long as it has autophagy, this relationship would exist in every biological system), and 3) given (2), mature skeletal muscle possesses a remarkable ability to adapt to stress, and some of these mechanisms might be conserved in myoblasts and therefore be relevant to observing the effects hypothesized here. In general, to examine the consquences of deliberate autophagy induction and/or the roles of its parallel activation on cell composition and function, the experiments contained herein were performed by treating/incubating/growing C2C12 cells in/with various modes of stressful stimuli. Using cell culture provides numerous advantages in this regard, as 1) cells can be administered an almost infinite array of interrogative stimuli for examining numerous specific biological phenomena, 2) genetic manipulation is relatively simple, and 3) cultured cells can be relevantly analyzed by varied and purposeful biological research techniques. Essentially, examining the effects of autophagy-dependent cellular remodelling in cultured mammalian cells allows the inspection of specific molecular and cellular mechanisms driving these relationships in an environment close to the genetic/physiological make-up of cells *in vivo*. Details regarding the general methological performance of these studies are outlined below.

Methodological Considerations for Study Design

A significant number of pilot experiments were performed to identify and optimize cell culture protocols that would appropriately answer the questions posed in this Thesis. As outlined, this primarily involved determining experimental treatment conditions that differentiated between specific autophagy induction and toxic stress-associated autophagy induction. Regarding the first treatment condtion, this

meant finding a stimulus capable of strongly inducing autophagy but avoiding the activation of cell death processes. This is an important consideration, as cultured cells are well known to become stress-resistant after "rounds" of stress (likely through repeated death of the inherently weaker cells combined with repetitive exposure to a specific stress), and since *physiologically-relevant cellular preconditioning is likely counterproductive if cells are lost in the process*. Of course, autophagy is very sensitive to cellular nutrient and energy status and therefore various forms of starvation such as growth factor, amino acid, vitamin and other macromolecule withdrawal are commonly used alone or together to investigate autophagy in cell culture. With respect to proliferating C2C12 cells, it was previously observed that incubation in Earle's Balanced Salt Solution (EBSS – an ionic solution (calcium chloride, magnesium sulphate, potassium chloride, sodium chloride, sodium phosphate, sodium bicarbonate) similar in osmolarity, pH, and glucose concentration to regular cell culture media), caused expected starvation-related changes to LC3I and LC3II levels, maximal caspase-3 activation after 4 hours, DNA fragementation beginning at 16 hours, and increased annexin binding also beginning at 16 hours (464). Here, while roughly 70% of cells remained metabolically viable (possessed caclein AM activity) after 48 hours in EBSS, a similar number of total cells displayed positive annexin binding. Based on these observations, I investigated the autophagy and cell death responses to a similar "starvation" media, Hank's Balanced Salt Solution (HBSS), which is similar in composition to EBSS (same osmolarity, HBSS contains 15% of the sodium bicarbonate of EBSS and adds roughly 0.5 mM magnesium chloride and potassium dibasic). Effectively, incubating cells in HBSS represents amino acid and growth factor withdrawal. Alongside this, I additionally examined the autophagic response to several stress-inducing laboratory chemicals. The results of these tests are outlined in Appendix B Figure 1. Notably, HBSS consistently reduced p62, LC3I, and LC3II protein levels and increased Bnip3 while relatively high concentration staurosporine (STS) reduced p62, LC3I, and Bnip3 protein. These observations indicated that although HBSS and STS both induce autophagy, these responses are phenotypically different. As the

activation of cell death during EBSS incubation was previously observed to increase with time, I assessed autophagy induction during shorter time periods of HBSS incubation. Remarkably, HBSS-induced autophagic flux analyses proved to be almost impossible due to the strength of the autophagic response. This assay is performed by incubating cells with/without the selected treatment with/without an inhibitor of autophagy and then measuring p62/LC3 with immunoblotting; however, extremely high concentrations of lysosomal inhibiting compounds were required to prevent HBSS-induced LC3II and p62 degradation and this was only possible at relatively short time points (Appendix B Fig. 3). Importantly, it was frequently found that incubating C2C12 cells in HBSS up to 5-6 hours did not significantly induce cell death, as indicated by caspase-3 activity and pH2AX protein expression (Chapter II Fig. 1, Chapter IV Fig. 2, Appendix B Fig. 9). Based on these observations, I concluded that HBSS treatments up to 6 hours satisfied a treatment condition characterized by "autophagy induction without cell death". Because autophagy also appeared to be induced by STS, traditionally an apoptosis-causing stimulus, it was examined for its suitability as a "toxic sress-associated autophagy" treatment. We typically use STS to induce cell death at concentrations between 1-2 μM for 3-4 hours, which constitutes a severe stress (>50% cell death). To decrease the stress level and allow more cell survival (again, the intention is to examine how cells respond to different stresses, therefore I don't necessarily want them to be eliminated), lower concentrations of STS were examined that would be time-synchronized with HBSS treaments. The results of these tests are largely presented in Chapter II Figures 1 & 2. However, the initial test in this experiment is not presented. To begin, proliferative C2C12 cells were separately incubated with 12 different concentrations of STS for 6 hours and visually examined 24 hours later. Of these concentrations, two were used for subsequent analyses: a relatively low dose which did not affect cell numbers but did give them an abnormal appearance, and a very low dose in which cells appeared normal the following day. Including two concentration groups was intended to further explore the relationship between stress, autophagy, cell death, and cellular adaptation by altering the stress dosage.

A similar search for mitophagy-inducing stimuli was conducted alongside these pilot experiments. Initial research outlining the functional relationship between PINK1, Parkin, and mitophagy performed in the Youle laboratory utilized FCCP/CCCP (cyanide) to cause mitochondrial depolarization, which was discovered to cause widespread autophagy-dependent degradation of mitochondria in Parkin-expressing cells (114-117). More recent studies involve combinations of oligomycin and antimycin a (122, 128, 155) to examine molecular mitophagy machinery. In fact, CCCP was previously shown to qualitatively increase overlap of LC3-GFP punta with mitochondria in C2C12 cells using fluorescent microscopy (439). In-house testing with CCCP exposure indicated that our C2C12 cells did not display significant cell death with concentrations up to 30 μM for 4-6 hours (Appendix B Fig. 8 & 9; Chapter IV Fig. 2). Similar to the previous studies, CCCP administration induced LC3II formation, puncate mitochondrial morphology, and degradation of mitochondria-specific proteins in my C2C12 cells (Appendix B Fig. 2, 3, 4, & 7; Chapter IV Fig. 1). Not shown in Appendix Figures are experiments involving oligomycin/antimycin a administration: the mitophagic response to these chemicals in C2C12 cells was less robust compared to CCCP, likey for the reasons explained in the following paragraph. Regardless, as with HBSS-induced autophagy, I found that incubating C2C12 cells in growth media with 30 μM CCCP for 4-6 hours induced mitophagy and did not significantly activate cell death processes. A final important step was determining a protocol for intermittently treating cells with these various autophagy and/or cell death inducing stimuli to examine the potential adaptations and mechanisms caused by their repeated administration. Importantly, as C2C12 cells will spontaneously differentiate into myotubes upon reaching confluence in culture (and as this process is associated with a myriad of cellular changes) it was paramount for cells in different treatment groups to be of similar confluence at the end of the treatment protocol. It can be seen in pilot experiments that some groups experienced such unintentional premature differentiation (Appendix B Fig. 10). Therefore, throughout the expeirments in

this Thesis, each specific intermittent treatment protocol was always performed to ensure equal cell confluence after 3 days of treatments (Appendix B Figs. 8, 10, & 11).

Another methodological consideration was selecting the specific targets of genetic manipulation used herein. Due to its complexity and importance, a myriad of cellular actors are known to impact autophagy. Although many of these roles are somewhat accessory and therefore deemed redundant in various situations, even so-called “autophagy-genes” (Atg’s) have been shown to be unnecessary for actual execution of autophagy. In effect, due to their downstream and relatively specific-to-autophagy actions, two Atg’s are typically manipulated in order to generate models of “autophagy deficiency”: Atg5, which helps construct autophagosome membranes, or Atg7, which activates LC3 and Atg5-12 (103). For the experiments in this Thesis, C2C12 cells with negligible Atg7 protein content were created and examined. Importantly, the incorporation of these autophagy-deficient cells allows the impacts of the models of autophagy induction just described to be attributed to autophagy *specifically*. Again, although amino acid and serum starvation is a strong stimulus for autophagy activation, this stress alters many cellular processes: examining the differences observed between Atg7-possessing and Atg7-lacking cells allows these findings to be specifically credited to autophagic degradation. In separate experiments, C2C12 cells with CRISPR-mediated knockout of Bnip3 are also investigated. Preliminary experiments suggested mitophagy can be induced in C2C12 cells using oft-cited chemical perturbations (outlined above), and that these manipulations significantly alter Bnip3 expression. As Bnip3 is implicated with autophagy and specific mitophagy regulation, additional studies were conducted in Chapter IV to investigate such a role in C2C12 cells.

A final aspect of deliberate study design in which additional troubleshooting expeirments were performed was selecting modes of cell death induction. Chapters III and IV focus on the effect of forced

intermittent autophagy on stress resistance development. In these studies, cell death was induced by administering one of three compounds: staurosporine (STS), cisplatin (CisPL), or hydrogen peroxide (H_2O_2). These three chemicals were chosen due to the different effector mechanisms through which each executes cell death. In our hands, STS causes classic apoptotic cell death characterized by phosphatidyl serine exposure, cell permeablization, DNA damage, robust caspase-9 and -3 activation, and release of several mitochondrial pro-death factors (369, 388). CisPL (or other platinum-containing compounds) is a frequently-used chemotherapeutic that functions by binding and therefore interfering with DNA replication, causing widespread DNA damage thereby targeting quickly-dividing cells. C2C12 cells given CisPL are characterized by strong upregulation of p53, dramatically decreased Bcl2, activation of caspases and significant DNA damage (357). Finally, H_2O_2 administration is an oxidative stress that causes cell permeabilization, DNA damage, and release of mitochondrial AIF (388). Including these various forms of cell death activation was intended to examine potential specific phenotypes and thereby cellular aspects of stress mediation that are impacted by autophagy.

CHAPTER II: Autophagy induction through intermittent amino acid starvation does not cause senescence in vitro

Project Rationale and Hypotheses

Although cellular senescence was initially observed *in vitro* (and even considered an artifact of it), it is currently acknowledged that senescent cells in fact exist *in vivo* and that they increase in number throughout human lifespan. These cells are characterized by lacking tissue-specific functions, significantly reduced or arrested cell cycle progression, and altered paracrine/endocrine signaling. While the physiological purpose of these cells is debated and under extensive examination, their biological/genetic induction is suggested to be anti-oncogenic and their accumulation is thought to contribute to aging. Because their first observation was described in the context of exhaustive replication, some theorize that aging itself is the primary (and perhaps only) driver of senescence development. However, several cellular stressors induce a senescence-like phenotype in cell culture, and the most widely-held theory is that chronic/additive damaging stresses interact with the changing cellular environment which occurs during normal aging that leads to senescence *in vivo*. Given its role in stress response adaptation and cell death, autophagy's role in senescence development is frequently investigated. Typically, this involves determining: 1) whether autophagy is altered during senescence caused by "intervention X", and 2) if this response facilitates or functions to attenuate senescence. Importantly, this relationship remains cloudy partly because whether autophagy induction itself affects senescence is relatively unexplored.

Another growing body of literature aims to give scientific credence to the adage "what doesn't kill you makes you stronger", specifically by testing the hypothesis that autophagy mediates the health and longevity benefits of relative/intermittent caloric restriction and regular exercise. Although, despite strong evidence that autophagy provides such a role in model organisms (yeast, flies, worms, and fish) and extensive epidemiological evidence that healthy diets and exercise are beneficial to human health, translating the "autophagy induction promotes health and longevity" theory to mammals and non-

human primates has yet to occur. Despite this, significant effort is being directed towards using or designing a drug for human use that would benefit health by systemically inducing autophagy. Importantly, despite robust understanding of the molecular control and execution of autophagy, some fundamental effects of autophagy induction remain relatively unexplored. Notably, it is unknown if chronic/repeated autophagy induction through the strongest and most physiologically relevant autophagic stimulus, starvation, causes senescence.

Therefore, the purpose of Chapter II was to investigate precisely this: does starvation-induced autophagy cause senescence *in vitro*? This was tested by repeatedly culturing C2C12 cells in amino acid- and serum-free media and examining several phenotypic alterations consistent with senescence development. This was compared to toxic stress-induced senescence, and the mechanisms which differentiate or are shared by these conditions were investigated. Finally, the contribution of autophagy to toxic stress-induced senescence was determined by examining senescence development in autophagy-deficient cells by knocking down Atg7 expression.

The hypotheses for this Project were:

1. Repeated autophagy induction through amino acid starvation will not cause senescence.
2. Toxic stress-induced senescence will be greater in the absence of autophagy.

Summary Statement

These experiments contribute to our knowledge of autophagy and senescence by demonstrating that although robust autophagy induction through amino acid and serum withdrawal does not cause senescence, toxic stress-induced senescence is attenuated in autophagy-deficient cells.

Abbreviations

CisPL, cisplatin; HBSS, Hank's Balanced/Buffered Saline/Salt solution; NAC, N-acetyl-L-cysteine; pH2AX, phosphorylated histone H2AX; SA-Bgal, senescence-associated β–galactosidase activity; SAHF, senescence-associated heterochromatic foci; SASP, senescence-associated secretory phenotype; STS, staurosporine.

Abstract

Cellular adaptation to survivable stressors has wide-ranging outcomes from the acquirement of beneficial stress-resistance to senescence and cancer. The mechanisms that regulate these responses are complex. In this study, we investigated the effects of repeated amino acid and serum withdrawal (HBSS) on the development of senescence *in vitro* and compared these to the effects caused by repeated toxic stress (staurosporine, STS). We found that intermittent STS administration caused cell cycle arrest, development of enlarged and misshapen cells/nuclei, increased senescence-associated heterochromatic foci and senescence-associated β–galactosidase activity, and prevented myogenic differentiation in C2C12 cells. These features were not observed in HBSS-treated cells. While STS-treated cells displayed less DNA damage (pH2AX content) and caspase activity when administered cisplatin, amino acid starved cells were protected from STS. Additionally, STS-induced senescence was attenuated in Atg7-deficient cells. These results demonstrate that repeated nutrient withdrawal did not cause senescence, although autophagy was required for senescence caused by toxic stress.

Introduction

Upon sensing a critical threshold of damage, cells can remove themselves by activating cell death processes such as apoptosis and programmed necrosis (2-4). Cellular elimination functions to remove potential sources of damage and allow their replacement; however, it is equally important to avoid the unnecessary removal of cells which could survive and continue functioning normally. In fact, neural and muscle tissues do not regenerate by simply replacing lost cells; maintenance of them depends on preventing and removing damage which could lead to cell death and tissue loss (36,49). Correspondingly, numerous pathological conditions are associated with cell death in these tissues, including: neurodegenerative diseases (323-330), stroke (331), myocardial infarction (332-335), dilated cardiomyopathy (336,337), and skeletal muscle myopathies (338-340). In fact, the degree of tissue loss is an important clinical consideration and therapeutic benefit is often observed with cell death inhibition (327,329,330,332,334,337,340). An important stress resistance mechanism in neural tissues and cardiac muscle is ischemic preconditioning (298). Here, intermittent ischemia induces resistance to tissue damage and cell death caused by subsequent ischemia, suggesting these cells possess an inherent ability to beneficially adapt to stress (300,341). This has been shown to involve autophagy, which is thought to be required to attenuate stress and allow cellular remodelling (244,342-344).

However, cells do not always adapt to stress in physiologically advantageous ways. Although initially described as a state of permanent cell cycle arrest directly related to cellular divisions and telomere length (260,265), senescence occurs during several disturbances including oncogene or tumour suppressor loss, DNA damage, oxidative damage, overactive mitogen signaling and others (264,266,345). These stressors commonly invoke senescence through shared molecular pathways including the DNA damage response (DDR) and subsequent p53-mediated induction of p21 and/or p16 activation along with retinoblastoma protein inactivation (264,266,345). Regardless, senescence cells are characterized

by significantly reduced replicative capacity, the secretion of specific paracrine signals, and resistance to cell death (264,266,345). The result is the appearance of cells which lack tissue-relevant function, like cancerous cells, but don't divide or die while maintaining the ability to respond to and regulate their environment. The biological purpose for this response is unclear, but the acquisition of damage-induced senescence is considered anti-oncogenic (264,266,345). Despite this, the number of senescent cells increases with age and is thought to contribute to tissue dysfunction and perhaps even aging itself (266,281,282).

Many questions regarding the mechanisms and relevance of senescence development remain. Unsurprisingly, the interaction between autophagy and senescence is complex (283,293,294). In specific situations, it's been demonstrated that autophagy promotes senescence, (284-286,292), prevents senescence (287-291,293), or both (294). These conclusions are typically explained by autophagy's modulation of cell death signaling, as senescence occurs when the incurred stress is strong enough to cause oxidative stress and activate the DDR and p53, but not strong enough to cause complete cell death. Additionally, targeted degradation of specific senescence-regulating factors and the generation of amino acids required for maintaining cell viability and secretory factor production are also suggested to be autophagy-dependent mechanisms related to senescence development (294).

Previous studies examining the relationship between senescence and autophagy have typically involved assessing whether autophagic degradation mediates senescence development caused by known stimuli or how chemical autophagy modifiers affect this response. Importantly, very limited evidence exists regarding senescence development caused by the strongest and most physiologically-relevant mode of autophagy induction: relative starvation. Therefore, the purpose of this study was to investigate the effect of repeated amino acid withdrawal on senescence development *in vitro*. We compared these

changes to those associated with repeated toxic stress, a known senescence-inducing insult. In doing so, we attempted to gain insight regarding the differences between adaptations caused by starvation and those typically associated with dysfunction.

Results

Short term amino acid and serum withdrawal induces massive autophagy and low concentration STS slightly activates cell death signaling in C2C12 cells

Importantly, our intention was to compare the effects of *non-lethal* nutrient withdrawal to those caused by repeated toxic stress, as prolonged starvation would be unnecessarily stressful. We began by determining the cell death and autophagy response to Hank's Buffered/Balanced Salt/Saline Solution (HBSS) which contains no amino acids or added serum, as well as low doses (15 nM and 125 nM) of staurosporine (STS) in regular growth media (GM). Incubation in HBSS for up to 8 hours only modestly increased ($p<0.05$) caspase-3 activity (Fig. 1A) and did not change protein expression of phosphorylated histone H2AX (pH2AX) (Fig. 1C & 1D) compared to cells in GM, indicating that cell death mechanisms were not highly activated in this context. However, 15 nM and 125 nM STS elevated ($p<0.05$) caspase-3 activity by 3.9-fold and 6.2 fold and pH2AX expression by 3.0-fold and 5.5-fold, respectively, after 8 hours (Fig. 1A, 1C & 1D). 125 nM STS exposure also increased ($p<0.05$) caspase-3 activity by 3.4-fold and pH2AX content by 4.2-fold at the 4 hour time point. These magnitudes were far less than those triggered by 3 hours of 2.0 μM STS, which caused 15- and 11-fold elevations ($p<0.05$) in caspase-3 and pH2AX levels, respectively (Fig. 1A, 1C & 1D). As expected, HBSS caused time-dependent reductions ($p<0.05$) in p62 and LC3II protein levels compared to GM (Fig. 1E, 1F & 1G). Low concentration STS treatment also reduced ($p<0.05$) p62 protein levels, although to a lesser degree than HBSS, and altered LC3 expression (Fig. 1E, 1F, & 1G). Although consistent changes to Beclin1 and Atg7 did not occur, Bnip3 protein content was elevated ($p<0.05$) in HBSS-treated cells and reduced ($p<0.05$) in STS-treated cells after 8 hours.

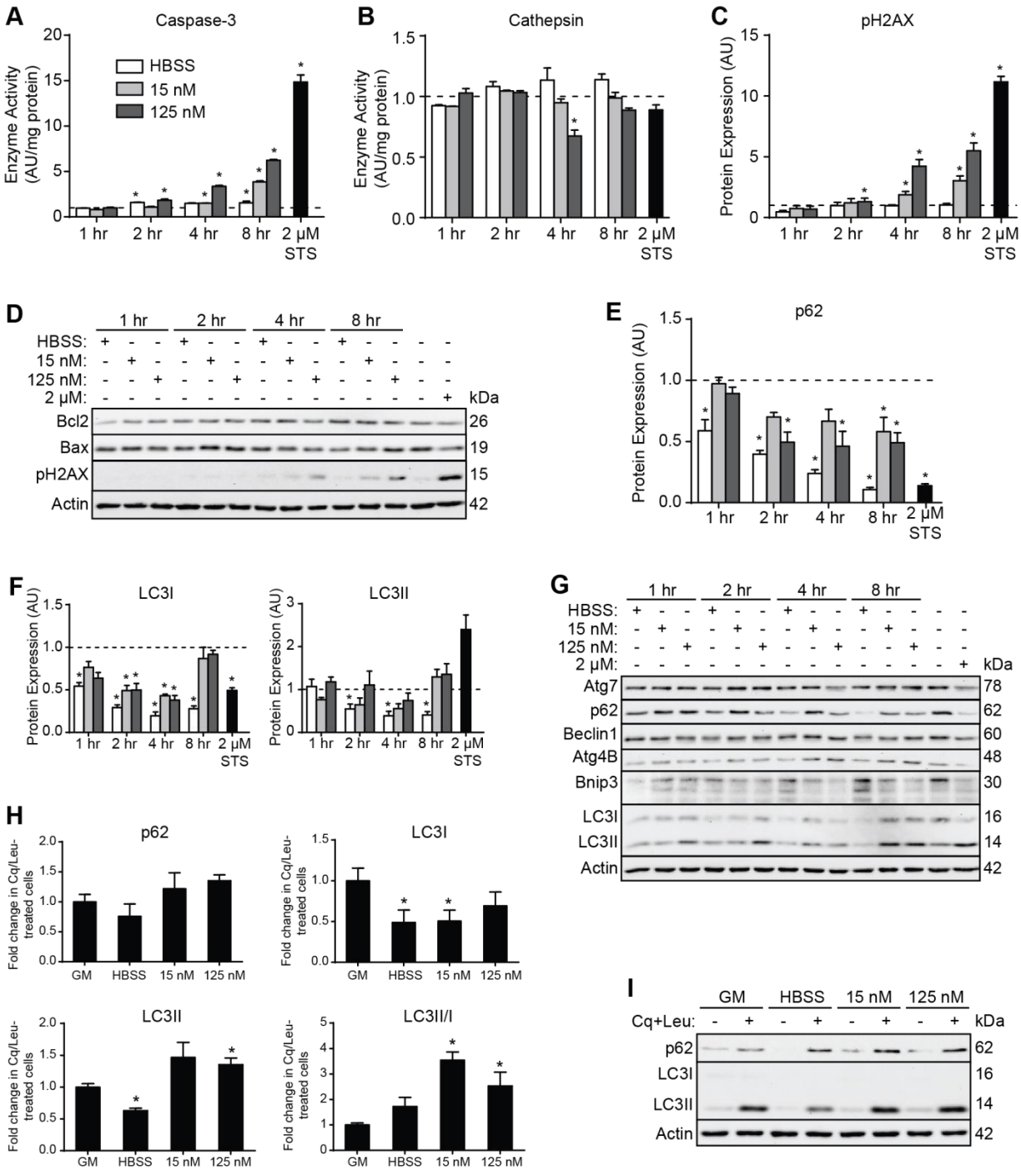

Fig. 1. Cell death and autophagy induced by starvation (HBSS) and low-concentration toxic stress (STS). (A-G) C2C12 cells were incubated in HBSS or culture media containing 15/125 nM STS for 1-8 hours and assessed for changes to caspase-3 (A) and cathepsin (B) activity or Bcl2, Bax, pH2AX (C & D), Atg7, p62, Beclin1, Atg4B, Bnip3, and LC3 protein content (E, F & G). (H & I) LC3 and p62 protein expression in cells treated as indicated for 4 hours with or without a combination of chloroquine and leupeptin (Cq+Leu). Actin is shown as a loading control. In all graphs, dashed line represents cells which remained in GM, arbitrarily given a value of 1.0 for comparison purposes. Significant differences from GM-receiving cells as calculated using T-tests are indicated with asterisks (*), where $p<0.05$ and $n=3$.

To measure autophagic flux, cells were treated for 4 hours with or without the addition of 50 μM chloroquine (Cq) and 250 μM leupeptin (Leu) (Fig. 1H & 1I). 15 nM and 125 nM STS increased ($p<0.05$) the LC3II/I ratio 3.5-fold and 2.5-fold more, respectively, than cells which remained in GM when administered Cq/Leu, demonstrating increased autophagic flux (Fig. 1 H, lower right panel). Notably, it appears that HBSS-induced autophagy was not fully inhibited by Cq+Leu, as p62 and LC3II protein levels are lower in HBSS/Cq+Leu cells compared to CTRL/Cq+Leu cells (Fig. 1H & 1I). This is likely due to the massive autophagy induction caused by HBSS and the extended time of the assay (103).

Next, we characterized recovery from HBSS/STS treatments by replacing fresh GM after 4 hour treatment (Fig. 2). Caspase-3 activity (Fig. 2A) and pH2AX protein expression (Fig. 2C & 2E) were not increased in HBSS-treated cells during the recovery period. In cells given 15 nM STS, these two markers were highest ($p<0.05$) after 3 hours of recovery but dropped after 6 hours (Fig. 2A, 2C & 2E). Cells given 125 nM STS did not recover, as caspase-3 and pH2AX remained elevated ($p<0.05$) during the recovery period (Fig. 2A, 2C & 2E). As p62 and LC3I protein levels in HBSS and 15 nM STS treated cells were not different ($p>0.05$) from untreated cells after 6 hours of recovery, this indicates recovery of autophagic activity (Fig. 2D & 2E). However, the sustained decrease ($p<0.05$) in p62 protein content in cells given 125 nM STS suggests these cells were unable to fully recover (Fig. 2D & 2F).

Repeated STS administration, but not HBSS, causes a senescence-like phenotype

Next, the effect of repeated amino acid and serum withdrawal or toxic stress on senescence was evaluated by incubating C2C12 cells in HBSS, 15 nM STS in GM, or 125 nM STS in GM for 4 hours per day for 3 consecutive days. Additional cells were left in GM and served as controls (CTRL). 20 hours following the final treatment, cells were analyzed for changes to cell morphology, cell cycle, differentiation, and typical senescence-associated markers (Fig. 3 & Fig. 4). HBSS treatments did not affect cell or nuclear

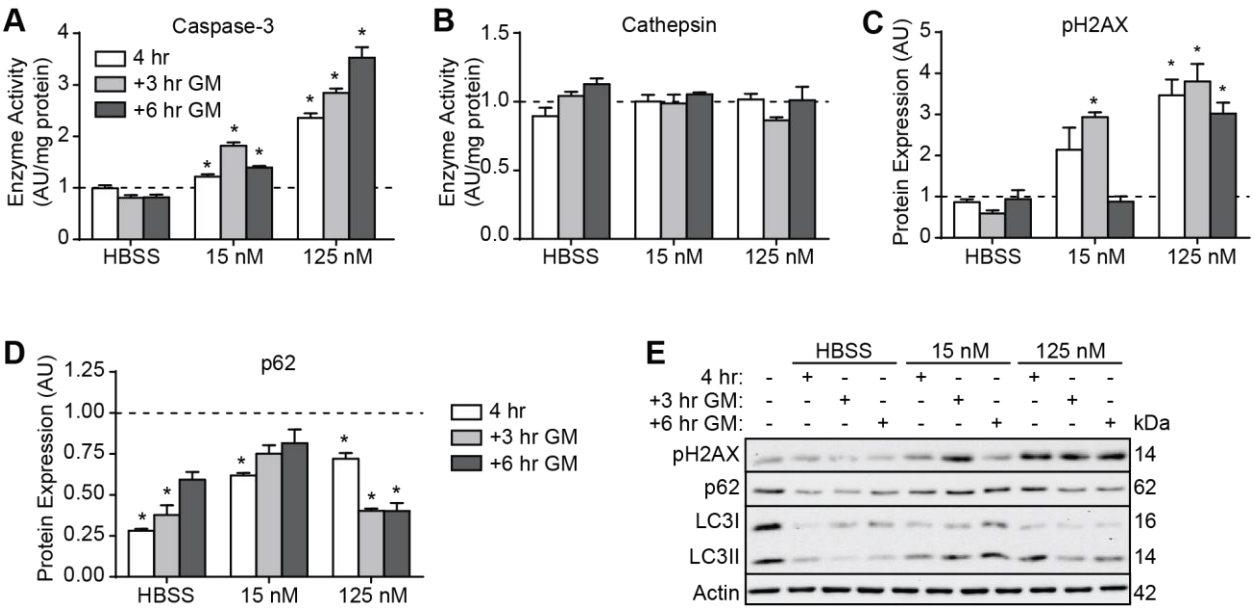

Fig. 2. Recovery from HBSS and STS treatments. C2C12 cells were incubated in HBSS, 15 nM STS, or 125 nM STS for 4 hours and allowed to recovery in fresh GM for 3 or 6 hours. (A) Caspase-3 and (B) cathepsin activity. (C) pH2AX, (D) p62, and (E) LC3 protein levels. (F) Representative immunoblots. Actin is shown as a loading control. Dashed line represents cells which remained in GM, arbitrarily given a value of 1.0 for comparison purposes. Significant differences from GM-receiving cells as calculated using T-tests are indicated with asterisks (*), where $p<0.05$ and $n=3$.

size or shape, as measured on cells immunostained for actin and DAPI (Fig. 3A – 3E). However, STS caused concentration-dependent increases ($p<0.05$) in cell and nuclear size (Fig. 3A & 3B), as well as altered nuclear shape (Fig. 3D). Importantly, these morphological indicators are consistent with the development of senescence *in vitro* (264). Additionally, there was no difference between CTRL and those given HBSS on cell cycle, as 60% of cells in both groups appeared in G_0/G1, 20% in M/G2, and 20% in S phase (Fig. 3E). However, cell cycle was arrested in cells repeatedly administered STS, as significantly more ($p<0.05$) cells existed in G_0/G1 (90%) and less ($p<0.05$) in M/G2 (7%) and S (3%) phases compared to both control and HBSS groups (Fig. 3E).

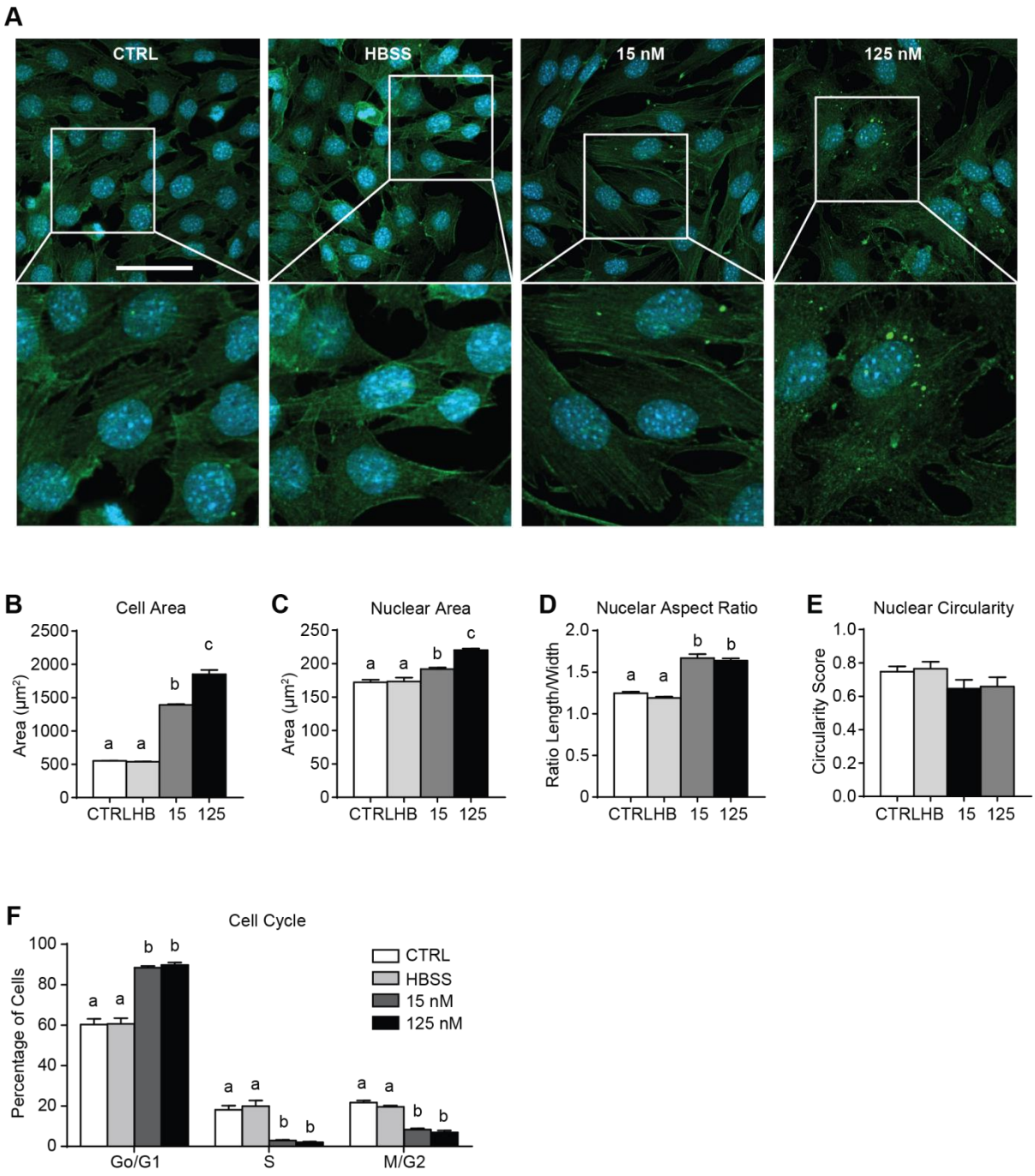

Fig. 3. Repeated STS exposure, but not HBSS treatment, alters cell morphology and causes growth arrest. Cells were incubated in HBSS or culture media with 15 or 125 nM STS for 4 hours per day for 3 consecutive days. (A) Cells were then immunolabelled with an anti-actin antibody (green) and counterstained with DAPI (blue) and analyzed for total cell area (B), nuclear area (C), nuclear length to width aspect ratio (D), and nuclear circularity (E). (F) Cell cycle analyses on similarly treated cells. For morphological measurements, n=3 where at least 100 cells were analyzed per group per experiment. For cell cycle analysis, n=5. Groups were compared with 1-way ANOVAs and significant differences ($p<0.05$) are indicated with lower case letters, where bars with different letters are significantly different than each other. Scale bar represents 50 µm.

Giemsa staining was also performed to assess cell morphology. Intermittent STS dramatically altered cell morphology, growth pattern characteristics, and apparent organelle shape (Fig. 4A). STS-treated cells also demonstrated increased ($p<0.05$) number of nuclear foci per cell (SAHF) as measured on Giemsa-stained images compared to CTRL and HBSS (Fig. 4B). HBSS caused no obvious morphological changes (Fig. 4A) or affected the number of nuclear foci compared to CTRL (Fig. 4B). Analysis of another typical senescence-associated phenomenon, the acquisition of β–galactosidase activity at pH 6.0 (SA-Bgal) (263), was also conducted; only STS-treated cells displayed strong X-gal staining (Fig. 4C). Lastly, as C2C12s are capable of myogenic differentiation, additional cells were induced to differentiate by placing them in low-serum media for 4 days. While HBSS-treated cells differentiated similar to CTRL as demonstrated by similar myosin induction and transient myogenin expression, neither STS-treated group produced detectable levels of myosin and both displayed very low myogenin content (Fig. 4D). Both STS groups also displayed altered Pax7 and p21 protein expression (Fig. 4D & 4E). Therefore, it appears that repeated low concentration STS administration induced a senescence-like state in C2C12 cells.

Intermittent nutrient withdrawal and STS exposure uniquely alter cell death induction

We next compared the effects of repeated nutrient withdrawal or senescence on subsequent cell death resistance. Cells were intermittently administered HBSS or STS for 4 hours per day for 3 consecutive days as done previously and given either 0.5 μM STS for 4 hours, 50 μM cisplatin (CisPL) for 18 hours, or nothing (vehicle, Veh) the day following the third treatment. In CTRL, STS caused a 25.7% drop in the number of healthy cells, compared to a 38.8% drop ($p>0.05$) in cells given 15 nM STS and a 43.0% decrease ($p<0.05$) in cells given 125 nM STS (Fig. 5A). HBSS-treated cells experienced a 16.4% decrease in the number of healthy cells, although this was not statistically different from CTRL (Fig. 5A). Similar trends were observed in early (Fig. 5B) and late (Fig. 5C) apoptotic cell counts after STS administration.

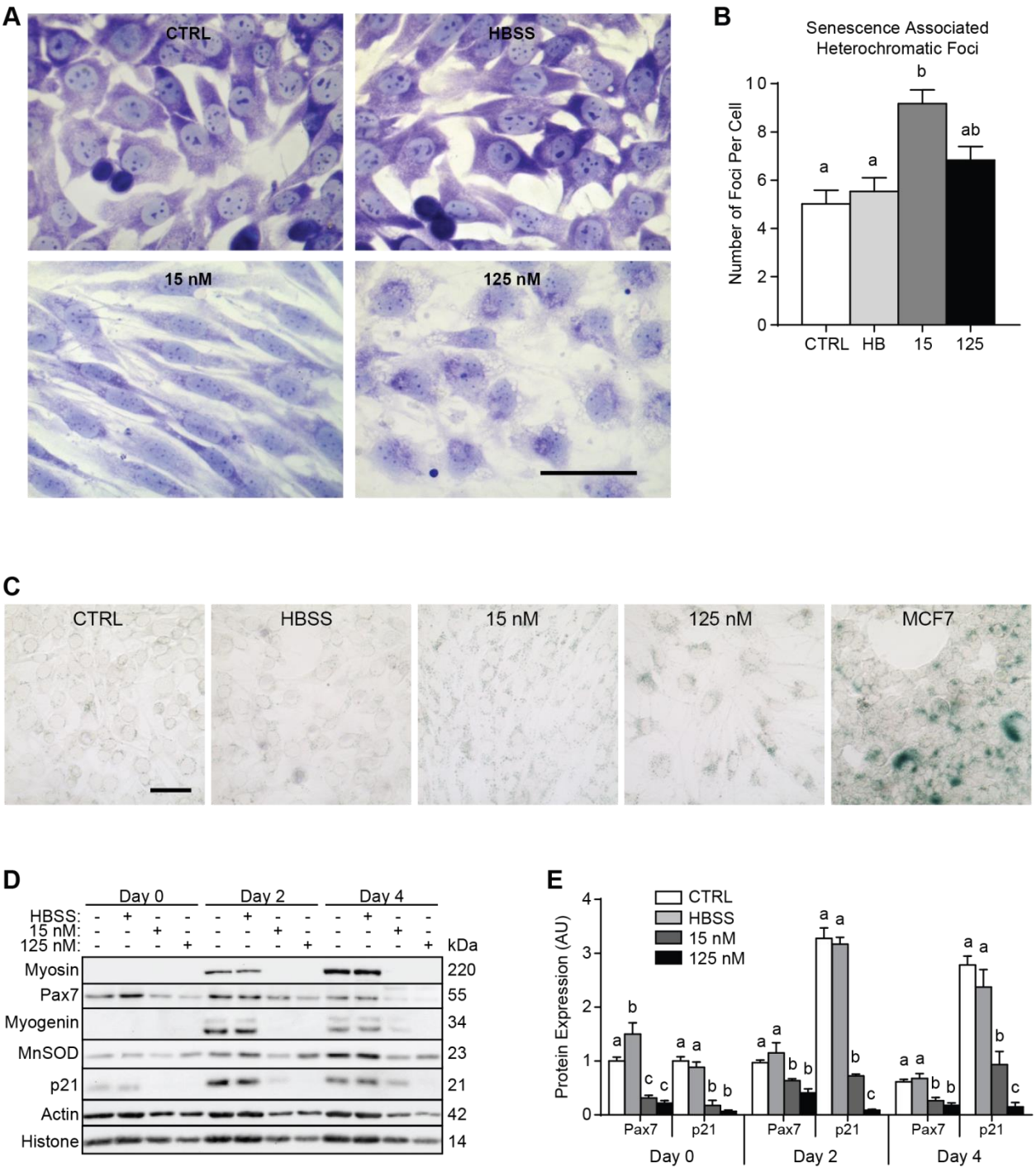

Fig. 4. Repeated STS exposure, but not HBSS treatment, induces features of senescence and prevents myogenic differentiation of C2C12 cells. Cells were incubated in HBSS or culture media with 15 or 125 nM STS for 4 hours per day for 3 consecutive days. (A & B) Giemsa staining was used to analyze the number of nuclear foci number per cell. (C) β-galactosidase activity staining at pH 6.0. MCF7 cells are included as a positive control. (D & E) Separate cells were differentiated by switching to low serum media and collected after the indicated number of days; Day 0 refers the time other cells were first given differentiation media. (E) Pax7 and p21 protein content. Actin and histone are shown as loading

controls. Groups were compared with 1-way ANOVAs and significant differences ($p<0.05$) are indicated with lower case letters, where bars with different letters are significantly different than each other. For foci counting n=3 where at least 100 cells were analyzed per group per experiment, for immunoblotting n=4. Scale bars represent 20 µm.

In response to CisPL, no effect of previous HBSS incubation was observed, as the number of healthy and dying cells was not different ($p>0.05$) compared to CTRL (Fig. 5). However, while CisPL caused a 45.6% reduction in healthy cells (Fig. 5A) and a 26.6% increase in early-apoptotic cells (Fig. 5B) in CTRL, the number of healthy cells decreased by 7.4% (Fig. 5A) and the number of early apoptotic cells only increased by 4.6% (Fig. 5B) in the group repeatedly given 15 nM STS.

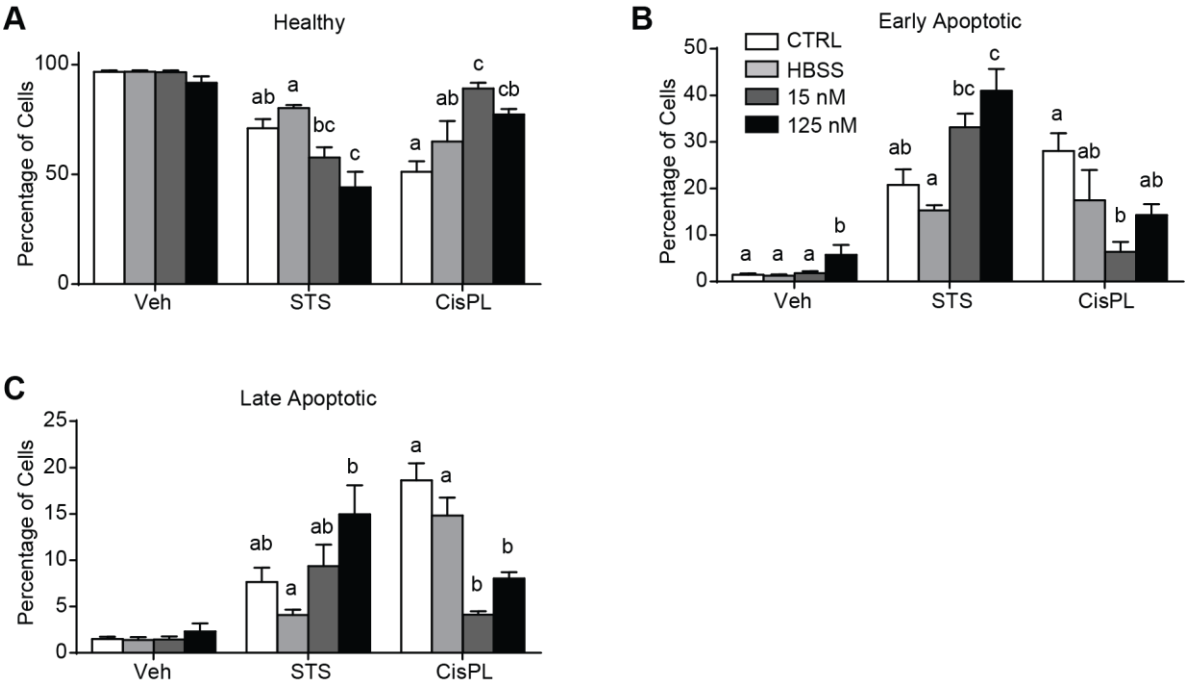

Fig. 5. Intermittent HBSS and STS exposure causes unique responses to cell death induction. After repeated treatments, cells were given 0.5 µM STS for 4 hours or 50 µM cisplatin (CisPL) for 18 hours to induce cell death or did not receive a death-inducing insult (vehicle, Veh). (A) Number of healthy cells demonstrating negative staining for both annexin and PI. (B) Number of cells undergoing early stages of cell death that are positive for annexin but negative for PI. (C) Number of cells in late stages of cell death which are positive for both annexin and PI. Groups were compared with 1-way ANOVAs and significant differences ($p<0.05$) are indicated with lower case letters, where bars with different letters are significantly different than each other. N=5.

Unique mechanisms of cell death are altered by previous intermittent HBSS and STS treatment

To examine the mechanisms of STS- and CisPL-induced cell death modulated by prior starvation and toxic stress, enzyme activities and protein expressions were assessed. First, measuring the DNA fragmentation marker pH2AX closely mirrored annexin/PI data: repeated HBSS reduced ($p<0.05$) pH2AX expression compared to CTRL during STS-mediated death and senescent cells displayed dramatically lower ($p<0.05$) pH2AX expression compared to CTRL and HBSS cells after CisPL administration (Fig. 6A). Additionally, repeated HBSS treatments decreased ($p<0.05$) caspase-3 (Fig. 6B) and caspase-9 (Fig. 6C) activities by 44% and 33%, respectively, compared to CTRL after 0.5 µM STS administration. To support this, protein expression of cleaved caspase-3 in cells given 0.5 µM STS was also 55% lower ($p<0.05$) in HBSS-treated cells compared to CTRL (Fig 6D). While HBSS did not reduce ($p>0.05$) caspase activity in response to CisPL, senescent cells displayed a complete lack of caspase activation (Fig. 6B & 6C) and cleaved caspase-3 expression (Fig. 6D) from CisPL. Both STS-treated groups also displayed significantly reduced ($p<0.05$) Bax:Bcl2 ratios compared to CTRL and HBSS-treated cells with or without cell death triggers (Fig. 6G). In fact, Bcl2 was 50% higher ($p<0.05$) in cells given 15 nM STS compared to CTRL without being intentionally killed, and 1.9-fold higher after cell death induction with CisPL (Fig. 6F).

Autophagy is altered during senescence

P62 protein content in STS-treated cells was noticeably reduced ($p<0.05$) 90-95% compared to CTRL and HBSS (Fig. 7A). However, when expressed as a percentage change, senescent cells did experience *relative* p62 accumulation when administered Cq+Leu and p62 degradation during HBSS at levels similar to CTRL and HBSS cells (Fig. 7B) (although the *absolute* amount of p62 accumulation or degradation was

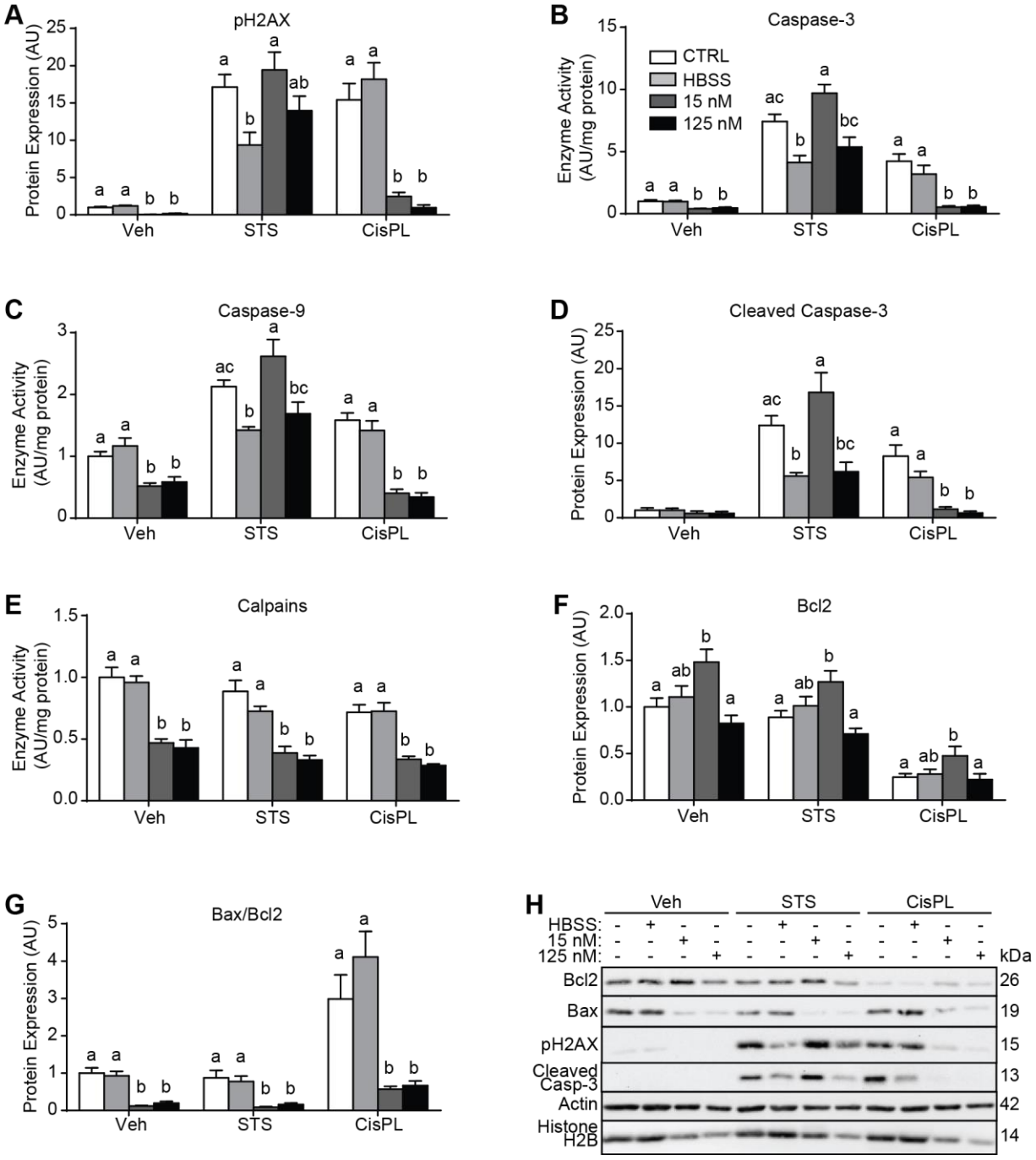

Fig. 6. Mechanisms of cell death execution are altered by intermittent HBSS and STS administration. After repeated treatments, cells were given 0.5 µM STS for 4 hours or 50 µM cisplatin (CisPL) for 18 hours to induce cell death, or did not receive a death-inducing insult (vehicle, Veh). (A) pH2AX, (D) cleaved caspase-3, and (F) Bcl2 protein contents with Bax/Bcl2 ratio (G). (B) Caspase-3, (C) caspase-9, and (E) and calpains enzyme activity. (H) Representative immunoblots. Results are presented relative to Veh CTRL, arbitrarily given a value of 1.0. Actin and histone are shown as loading controls. Groups were compared with 1-way ANOVAs and significant differences ($p<0.05$) are indicated with lower case letters, where bars with different letters are significantly different than each other. N=5-6.

far greater in CTRL and HBSS). There was additionally no difference ($p>0.05$) in p62 levels during the flux assay between CTRL and HBSS-treated cells (Fig. 7A & 7B). Despite the large change in p62 content, LC3 protein levels in senescent cells were much closer to CTRL; although LC3I content was lower ($p<0.05$) in both STS groups (Fig. 7C). Similar to p62, the relative change in LC3II protein levels was similar between groups during the autophagic flux assay (Fig. 7D).

STS-induced senescence is partly mediated by oxidative stress

As oxidative stress is known to cause senescence, the contribution of reactive oxygen species (ROS) to STS-induced senescence was examined (Fig. 8). 15 and 125 nM STS increased ($p<0.05$) ROS production to a greater extent than untreated and HBSS-treated cells as measured by detecting DCF fluorescence (Fig. 8A). Additionally, the antioxidants N-acetyl-L-cysteine (NAC) and 4,5-dihydroxy-1,3-benzenedisulfonic acid (tiron) each reduced ($p<0.05$) STS-induced ROS when administered with STS at specific concentrations (Fig. 8A). Next, cells were treated with 15 nM STS for 4 hours per day for 3 consecutive days with or without 20 μM NAC and several senescence markers were analyzed. Co-treatment with NAC slightly prevented STS-induced cell cycle arrest as fewer ($p<0.05$) cells were present in G_0/G1 compared to STS alone (Fig. 8B). NAC administration also attenuated STS-induced alterations to nuclear shape (Fig. 8C & 8D) and SAHF number (Fig. 8E & 8F). Importantly, NAC also prevented SA-βgal caused by repeated STS exposure (Fig. 8G).

Loss of Atg7 attenuates STS-induced senescence

Finally, to determine if increased autophagy (Fig. 1H) was relevant to STS-induced senescence, C2C12 cells with stable Atg7 knockdown were generated (Fig. 9A). Similar to previous experiments, control (SCR) and Atg7-deficient (shAtg7, clone #1) cells were administered 15 or 125 nM STS for 4 hours per day for 3 consecutive days and analyzed for senescence markers. While STS caused cell cycle arrest in SCR as indicated by increased ($p<0.05$) cells in Go/G1 and decreased ($p<0.05$) cells in M/G2 compared to

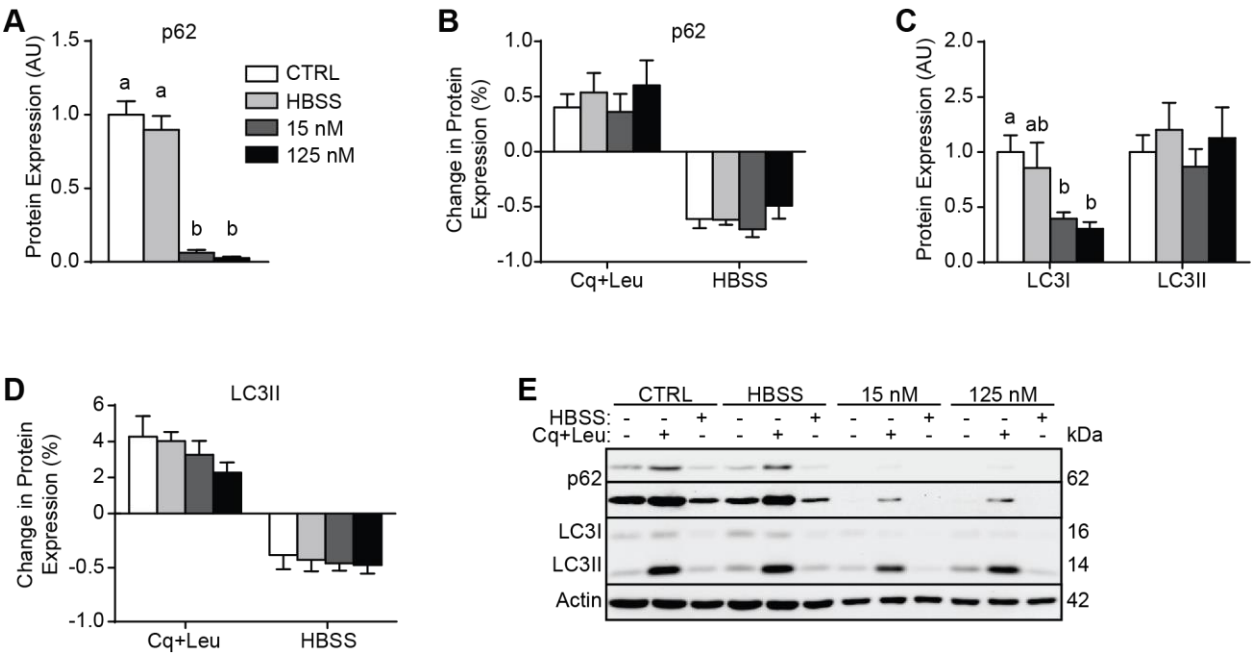

Fig 7. Autophagic flux is altered in senescent cells. Autophagic flux assay performed on cells intermittently treated with HBSS, 15 nM STS, or 125 nM STS. (A) p62 protein expression in GM flux cells. (B) Change in p62 induced by Cq+Leu and HBSS. (C) LC3 protein expression in GM flux cells. (D) Change in LC3II induced by Cq+Leu and HBSS. (E) Representative immunoblots, where p62 is shown at low (top) and high (bottom) exposures. Groups were compared with 1-way ANOVAs and significant differences ($p<0.05$) are indicated with lower case letters, where bars with different letters are significantly different than each other. N=4-5.

CTRL, the number of STS-treated shAtg7 in each cell cycle phase was not different ($p>0.05$) from CTRL or SCR CTRL (Fig. 9B). Notably, shAtg7 treated with 125 nM STS are absent in these analyses: in fact, regardless of how many cells were seeded, no shAtg7 remained after 3 days of receiving 125 nM STS. SCR demonstrated similar senescence-associated changes to cell morphology as unmodified C2C12 cells in previous experiments (Fig. 3 & Fig. 4), as intermittent STS increased ($p<0.05$) SAHF, nuclear size, and nuclear aspect ratio compared to CTRL (Fig. 9C – 9G). However, shAtg7 did not display ($p>0.05$) increased SAHF, nuclear size, or nuclear aspect ratio in response to repeated STS (Fig. 9C – 9G). These observations suggest autophagy is required for and contributes to senescence. However, as shAtg7

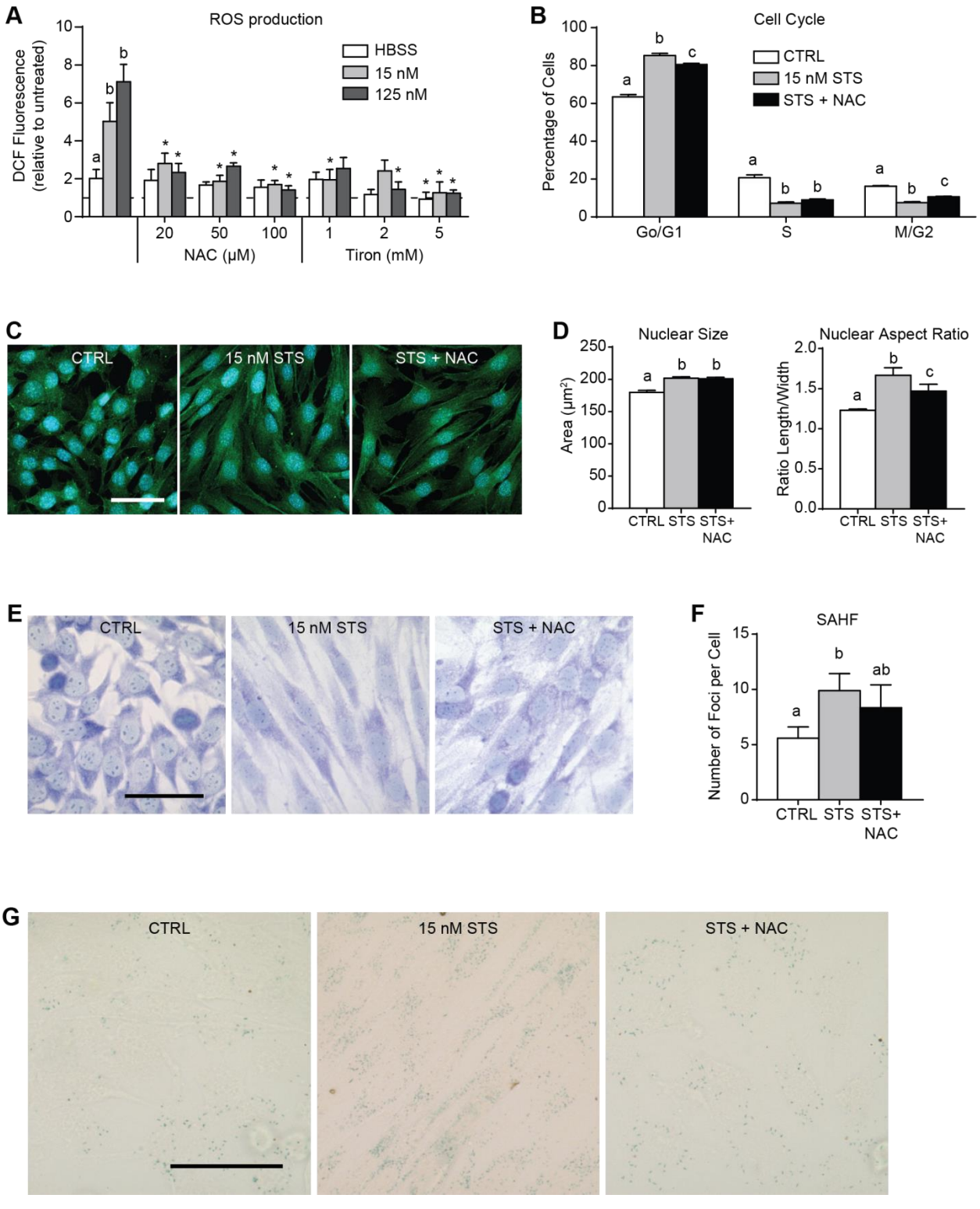

Fig. 8. STS-induced senescence is partly mediated by oxidative stress. (A) ROS production in cells treated with HBSS, 15 nM STS, or 125 nM STS with or without NAC or Tiron for 4 hours. Dashed line represents cells in GM, arbitrarily given a value of 1.0. (B-G) Cells were administered 15 nM STS with or without 20 μM NAC for 4 hours per day for 3 consecutive days. (B) Cell cycle analyses. (C & D) Nuclei size and shape

assessed on actin- and DAPI-labelled cells. (E & F) Cells stained with Giemsa solution were analyzed for the number of nuclear foci per cell. (G) SA-Bgal staining. Groups were compared with 1-way ANOVAs and significant differences ($p<0.05$) are indicated with lower case letters, where bars with different letters are significantly different than each other. In (A), asterisk (*) represents difference ($p<0.05$) from treatment-specific groups that did not receive antioxidant calculated with T-tests. For cell cycle and ROS analyses n=4. For morphological and foci counting measurements, n=3 where at least 100 cells were analyzed per group per experiment. Scale bars represent 50 μm.

displayed significantly reduced ($p<0.05$) cell counts 24 hours following a single STS treatment (Fig. 9H), this conclusion is complicated by the increased sensitivity of shAtg7 to STS-induced cell death.

Discussion

These results demonstrate some mechanisms that differentiate cellular remodelling caused by repeated nutrient withdrawal versus toxic stress in proliferative C2C12 cells. Although initially appearing paradoxical, stress-induced stress resistance is an exceptionally important physiological phenomenon. This induced resistance to stress is most commonly observed after ischemia/reperfusion (IR) of neural and cardiac tissues (298,300,341), although this process also occurs in skeletal muscle (346) and has shown potential clinical relevance during liver, kidney, lung, and stem cell transplants (347,348). Classically, IR causes significant resistance to subsequent ischemic insults 1-2 hours following IR administration and delayed protection for 1-4 days (341). The mechanisms which mediate tissue protection are diverse, but those most often implicated are related to MAPK/ERK signaling pathways, activation of Akt and protein kinase C, Hif-1a and oxidative defence, heat shock proteins, and anti-cell death factors (298,300,341). The search for mimetics of IR-induced preconditioning has demonstrated that preconditioning mechanisms are observed with other types of stressors. Perhaps the most often examined is oxidative stress; notably, ROS signaling is required for cardiac IR preconditioning (349) and antioxidant administration attenuates the metabolic enhancements caused by exercise training in skeletal muscle (350). However, various stimuli produce preconditioning-like responses in other tissues,

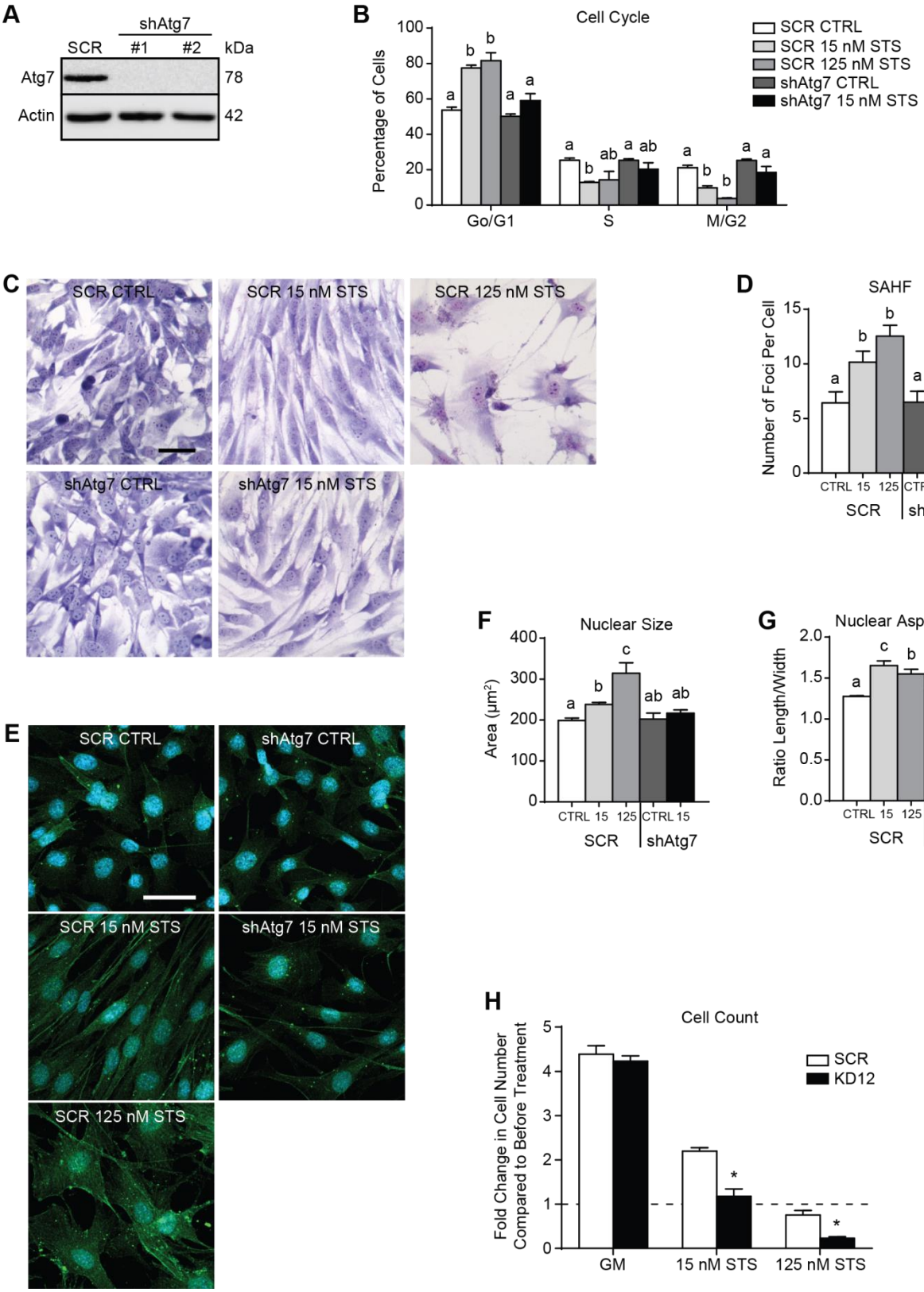
A
shAtg7
SCR
#1
#2
kDa
Atg7
78
Actin
42
B
Cell Cycle
SCR CTRL
SCR 15 nM STS
SCR 125 nM STS
shAtg7 CTRL
shAtg7 15 nM STS
Percentage of Cells
Go/G1
S
M/G2
C
SCR CTRL
SCR 15 nM STS
SCR 125 nM STS
shAtg7 CTRL
shAtg7 15 nM STS
D
SAHF
Number of Foci Per Cell
CTRL 15 125 CTRL 15
SCR
shAtg7
E
SCR CTRL
shAtg7 CTRL
SCR 15 nM STS
shAtg7 15 nM STS
SCR 125 nM STS
F
Nuclear Size
Area (μm²)
CTRL 15 125 CTRL 15
SCR
shAtg7
G
Nuclear Aspect Ratio
Ratio Length/Width
CTRL 15 125 CTRL 15
SCR
shAtg7
H
Cell Count
SCR
KD12
Fold Change in Cell Number Compared to Before Treatment
GM
15 nM STS
125 nM STS

Fig. 9. Loss of Atg7 attenuates STS-induced senescence. (A) Immunoblot demonstrating Atg7 expression in control (SCR) and Atg7-deficient (shAtg7) C2C12 cells. Subsequent experiments were conducted on knockdown clone #1. (B-G) SCR and shAtg7 were administered 15 nM or 125 nM STS for 4 hours per day for 3 consecutive days. (B) Cell cycle analyses. (C & D) Cells stained with Giemsa solution were analyzed for the number of nuclear foci per cell. (E-G) Nuclei size and shape assessed on actin- and DAPI-labelled cells. (H) Cell counts conducted 24 hours after treating SCR and shAtg7 with 15 nM or 125 nM STS for 4 hours or left in GM. Counts are expressed relative to the number of cells in culture wells prior to treatments, arbitrarily given a value of 1.0 and represented by dashed line. Groups were compared with 1-way ANOVAs and significant differences ($p<0.05$) are indicated with lower case letters, where bars with different letters are significantly different than each other. In (H), asterisk (*) represents significant difference ($p<0.05$) between SCR and shAtg7 compared using a T-test. For cell cycle analyses n=4, for morphological and foci counting measurements, n=3 where at least 100 cells were analyzed per group per experiment. In (C), scale bar represents 20 μm; in (E) scale bar represents 50 μm.

and experiments have shown that: hydrogen peroxide-induced preconditioning was partly mediated by the antioxidant enzyme thioredoxin-1 (302); arsenite-induced preconditioning was mediated by Hsp27 (303); heat shock-induced preconditioning involved Hsp70, reduced release of mitochondrial pro-death factors (304,305), and the antioxidants MnSOD and catalase (305); and hypoxia-induced preconditioning was mediated by Hif-1a (301), Bcl2 and erythropoietin (347), Hif-1a and erythropoietin (351), and p38/MAPK (352). These studies demonstrate that a wide variety of stresses can cause protective cellular phenotypes and suggest that a common set of cellular mechanisms may mediate this response. Evidently, these systems respond to a diverse array of stimuli and their shared activation appears essential to providing proactive cellular protection.

Increasing evidence shows that forms of caloric restriction have beneficial effects on health and/or longevity. Like the preconditioning stimuli just mentioned, the mild stress associated with relative or intermittent starvation is thought to produce cellular adaptations that cause the development of stress resistance and subsequent health benefits (353,354). However, it is unclear whether caloric restriction can be considered a hormetic stress or if it is a separate phenomenon with distinct biological mediators (354). Interestingly, the cellular response to stress is highly variable: while preconditioning represents a

physiologically beneficial adaptation, cancer and/or senescence development represent pathological outcomes. Notably, the cellular mechanisms that differentiate these responses are complex and unknown. In fact, despite the accepted longevity/health benefits of mild caloric restriction, the actual cellular consequences induced by relative nutrient deficiency are highly tissue dependent (355). The results of this study showed that repeated amino acid and serum withdrawal caused stress resistance that was phenotypically different than that caused by repeated toxic stress in C2C12 cells. While cells intermittently incubated in HBSS displayed resistance to cell death caused by STS, cells repeatedly administered nanomolar STS were resistant to CisPL-induced death. We also found that protection from STS-induced death caused by repeated nutrient withdrawal was mediated by reduced caspase activation. A number of mechanisms can explain these observations as amino acid starvation can alter a variety of cellular processes (355). Although this could be an exhaustive list, those related to beneficial cellular adaptations include insulin/Akt and mTOR signaling, which are nutrient-sensitive; AMPK and sirtuins, which are energy-sensitive; and antioxidants, which are ROS-sensitive (353-356). Importantly, these signaling platforms are implicated during many models of increased longevity, and are thought to function partly through their shared induction of relative stress resistance. Of course, autophagy is an essential cellular remodelling mechanism implicated in longevity which is induced by nutrient withdrawal (311). Experiments in model organisms have shown that functional autophagy is required to observe the longevity-inducing effects of various interventions (311). As a result, it is enticing to hypothesize that autophagy mediates the beneficial effects of caloric restriction by acting as a cellular recycling mechanism through its targeting of damaged/dysfunctional proteins and organelles. However, data precisely showing the improvement of specific cellular contents or modulation of particular signaling mechanisms by autophagy is lacking. It is also possible that forced nutrient withdrawal promotes the expression of protective cellular proteins. However, HBSS-treated cells did not possess increased protein content of Bcl2 (Fig. 6F) or the antioxidant MnSOD (Fig. 4D) and did not display altered

autophagic activity (Fig. 7) compared to controls. Potentially, nutrient withdrawal may target and thereby modulate upstream signaling platforms responsible for sensing and integrating stress signals. Although nanomolar STS treatments were expected to cause resistance to STS-induced death in a hormesis-like manner, analyses indicated these cells were actually more sensitive to STS-induced death and were protected from CisPL (Fig. 5). CisPL is a common chemotherapeutic because it directly causes DNA damage, making quickly proliferating cells more sensitive to it. As STS-treated cells were growth arrested (Fig. 3), it is not surprising that they were relatively resistant to CisPL. These cells also displayed increased Bcl2 protein content, which likely contributed to CisPL resistance given the massive reduction in Bcl2 that CisPL causes (357).

Staurosporine functions as a non-specific kinase inhibitor by competing for ATP-binding sites of enzymes (358). Its use has been instrumental in determining the mechanisms of programmed cell death execution (19,359-362). The cellular response to STS is characterized by increased ROS production (363,364), elevated cytosolic calcium (363,364), release of mitochondrial pro-death factors (19,361), caspase activation (359,362,363,365), and DNA damage (359,360,362). Importantly, many of these features are similar to known causes of senescence including telomere attrition, which induces replicative senescence, as well as forms of stress-induced senescence such as oxidative stress and oncogene activation (264,266,345). Despite some differences in signaling mechanisms, it appears that DNA damage and the resultant activation of the DNA damage response (DDR) is the most integral component of senescence induction (264,266,345). Because STS exposure causes these effects, its administration has previously been shown to cause senescence (366). In the present study, nanomolar concentrations of STS elevated caspase-3 activity and caused DNA damage, indicated by pH2AX content (Fig. 1 & 2). After repeated treatments with STS, cells and their nuclei appeared large and mis-shapen, proliferation was halted, cells displayed increased senescent-associated heterochromatic foci (SAHF)

and senescence-associated b–galactosidase activity (SA-Bgal), and myogenic differentiation was completely prevented (Fig. 3 & 4). Notably, we did not detect p16 protein expression in any treatment condition. Although the current unavailability of the most commonly used p16 antibody (252,367,368) hindered our ability to assess this marker, the lack of molecular data questions whether the cellular phenotype we observed can be considered “senescence”. The growing complexity of senescence biomarkers and confusion regarding their interpretation further affirms that additional research on senescence is warranted (264,266). Regardless, the senescence-associated changes to cell morphology observed in STS-treated cells were absent in intermittently starved cells. Therefore, despite the repeated stress of nutrient deficiency, these cells appeared to function normally.

The relationship between autophagy and senescence is complex (283). While studies have concluded autophagic activity can promote senescence or that a positive association between their induction exists (284-286), an equal body of evidence suggests autophagy prevents senescence or that they are negatively correlated (287-291). Single-cell analyses showed that autophagy inhibition triggered cell death and decreased senescence induced by DNA damage, suggesting that autophagy promotes senescence by suppressing death signaling (292). It was recently demonstrated that during oxidative stress-induced senescence in mouse 3T3 fibroblasts, autophagy inhibition was crucial for senescence development, autophagic flux was impaired in senescent cells, and restoration of autophagy was able to attenuate senescence (293). Meanwhile, another large study showed that senescent cells display increased “general” autophagy and that autophagy inhibition also caused senescence (294). Here, irradiation-induced senescence of human lung fibroblasts was suppressed by selective autophagic degradation of the transcription factor GATA4, activation of which promoted Nf-KB activity and the SASP, while general autophagy supported senescence transition by making substrates available for the SASP (294). Of relevance to the present study is that GATA4 protein accumulation was proposed to be

caused by decreased association of p62 with GATA4; therefore, our observed reduction in p62 protein content associated with repeated STS administration (Fig. 7A) provides additional explanation for STS-induced senescence. As p62's autophagic targeting functions depend on ubiquitination, these researchers also suggested altered activity of ubiquitin ligases or deubiquitinating enzymes for GATA4 may mediate its protein stability (294). Several observations in this study contribute to our knowledge regarding the relationship between autophagy and senescence: 1) repeated nutrient withdrawal, which induces massive autophagy, did not cause morphological and functional features of senescence; 2) levels of p62 and LC3 were altered in STS-treated cells, although the relative change in protein content was similar during an evaluation of flux; 3) nanomolar STS concentrations induced autophagy, thereby implicating autophagic activity in regulating senescence development; 4) senescence was attenuated in Atg7-deficient cells, although this is likely due to their decreased ability to survive STS treatments; and 5) while both nutrient withdrawal and nanomolar STS administration activated autophagy, senescence was associated with repeated STS-induced cell death signaling.

The physiological purpose of senescence is incompletely understood. The most widely acknowledged theory for its continued presence in humans is its role as a "less bad" response to DNA damage compared to cancer (264,266,345). It is also suggested that the cellular acquisition of senescence is not genetically regulated and exists as an unintentional response to stress, the increased accumulation of which contributes to tissue dysfunction during aging and even aging itself (264,266,345). This is likely due to the replacement of healthy/functioning cells with senescent ones and the inflammatory impact of SASP-related molecules (264,266,345). Either way, an important feature of senescent cells is their relative resistance to cell death induction leading to their prolonged existence. This permanence amplifies their effects and as a result strategies to remove senescent cells have been investigated to study their impact on aging. In fact, it's been demonstrated that selective elimination of p16-positive

cells in mice attenuates the aging phenotypes of several tissues and may even increase longevity (281,282). In this sense, the development of stress resistance in senescent cells could be considered pathological. This contrasts the typical link made between cellular stress resistance and aging, where increased stress resistance is shared between several models of increased longevity (353,354). In fact, the mechanisms that cause senescence-associated stress resistance are likely different than those which mediate the forms of stress resistance associated with reduced tissue dysfunction and aging. The results here show that different stresses produce different adaptations: not only did the form of stress resistance depend on the type of incurred stress, but the mechanisms behind these stress-resistance profiles were specific. Although it would be conjecture to comment on the physiological implications of being resistant to staurosporine versus cisplatin, these chemicals do simulate the insults cells regularly deal with. Even more complex is the relationship between autophagy and senescence. While we observed reduced senescence development in Atg7-deficient cells, thereby suggesting that autophagy contributes to senescence, this came at the expense of increased cell death and division. Importantly, this raises the question whether it is physiologically/functionally preferable for a tissue's cells to display increased sensitivity to stress, die, and have to be replaced, or for those cells to continue functioning and perhaps become senescent. Although the answer to this question is highly complex and likely depends on numerous contextual factors, recent evidence suggests the accumulation of senescent cells is pathological in some tissues (281). Interestingly, forced autophagy induction through starvation was not associated with senescence, but it did cause resistance to STS-induced cell death signaling mechanisms. Regardless, it is notable that these findings resulted from an *in vitro* experiment lasting only a few days, further emphasizing cellular capacity for remodelling and how easily this can be manipulated, particularly given the relatively slow rate that senescence develops and aging occurs. These observations highlight the potential for directed cellular adaptation.

This study demonstrates the similarities and differences between the mechanisms of cellular adaptation caused by intermittent nutrient withdrawal or toxic stress in proliferative C2C12 cells. Notably, these results show that repeated and robust autophagy induction through amino acid and serum withdrawal did not lead to senescence development. Furthermore, although repeated starvation caused a cyto-protective response, the specific changes implicated in this adaptation are unknown. Understanding the molecular regulators that respond to and mediate these changes could be relevant to the fields of caloric restriction, exercise, and aging. Importantly, this includes the specific involvement of autophagy and/or mitophagy as inducible mechanisms of beneficial cellular remodelling. Finally, while autophagy deficiency attenuated the senescence phenotype observed in these experiments, the physiological implications regarding this relationship are complex and warrant further study. As our understanding of senescence grows, it will also be important to define and differentiate the morphological features and molecular factors therein related, which may lead to the identification of currently overlooked cellular phenotypes.

Materials and Methods

Materials

Cells were treated as indicated with: Hank's Balanced Salt Solution (HBSS; Gibco formulation: 140mg/L $CaCl_2$, 100mg/L $MgCl_2$-$6H_2O$, 100mg/L $MgSO_4$-7H2O, 400mg/L KCl, 60mg/L KH_2PO_4, 350mg/L $NaHCO_3$, 8.0g/L NaCl, 48mg/L Na_2HPO_4, 1.0g/L D-glucose, with 1% penicillin/streptomycin), chloroquine (Cq, 30 µM; Sigma-Aldrich), leupeptin (Leu, 250 µM; Sigma Aldrich), staurosporine (STS, 15 nM, 125 nM, 0.5 µM or 2.0 µM; Enzo Life Sciences), cisplatin (CisPL, 25 µM; Enzo Life Sciences), N-acetyl-L-cysteine (NAC, 10, 20, or 50 µM; Sigma Aldrich), tiron (1, 2, or 5 mM; Sigma Aldrich), and 2',7'-dichlorodihydrofluorescein diacetate (DCF, 25 µM; Sigma Aldrich).

Cell Culture

C2C12 mouse skeletal myoblasts (ATCC) were cultured in growth media (GM) consisting of low-glucose Dulbecco's Modified Eagles Medium (DMEM; Hyclone, ThermoFisher) containing 10% fetal bovine serum (FBS; ThermoFisher) and 1% penicillin/streptomycin (ThermoFisher) on polystyrene culture dishes (BD Biosciences), as previously performed (357,369). Differentiation was induced by switching 90% confluent cells to differentiation media (DM) consisting of low-glucose DMEM containing 2% horse serum and 1% penicillin/streptomycin. For microscopy experiments, cells were grown on Cultrex- (R&D Systems) coated glass coverslips. When necessary, cells were isolated via trypsinization after washing in warmed PBS and centrifuged at 1000g. For all cell death experiments culture media and PBS were collected to include non-adhered cells and debris.

Atg7 Knockdown

C2C12 cells grown in 12-well plates were transfected with vectors encoding either an shRNA against Atg7 (Gene ID 74244, Origene TG504956) or a scramble control sequence (Origene TR30013) using Lipofectamine 2000 (ThermoFisher) at a DNA:lipofectamine ratio of 1 μg: 3 μL as previously performed (183). Cells with stable incorporation of each vector were selected using 2 μg/mL puromycin (Sigma). Surviving clones were individually isolated and assessed for Atg7 protein expression using immunoblotting. Two Atg7-deficient cell lines were obtained, termed shAtg7 in Figure 7; clone #1 was used for subsequent experiments.

Immunoblotting

Immunoblotting was performed as previously described (357,369). Whole-cell lysates were generated by adding ice-cold lysis buffer (LB, pH 7.4; 20mM HEPES, 10mM NaCl, 1.5mM $MgCl_2$, 1 mM DTT, 20% glycerol, and 0.1% Triton-X100, Sigma Aldrich) with protease inhibitors (Complete Cocktail; Roche) to

cell pellets followed by sonication for 12 seconds. Protein content was measured using the BCA protein assay method. Briefly, equal amounts of protein were loaded into and separated using 10-12% SDS-PAGE, transferred onto PVDF membranes (Bio-Rad Laboratories), and blocked for 1 hr at room temperature with 5% non-fat dry milk in TBS-T. Membranes were then probed with primary antibodies against Bcl2 (sc-7382, 1:200), Bax (sc-493, 1:1000), p21 (sc-397, 1:1000), phosphorylated histone H2AX (pH2AX, sc-101696, 1:1000; Santa Cruz), Atg7 (8558, 1:1000), Atg4B (5299, 1:1000), Beclin1 (3738, 1:1000), LC3 (2775, 1:1000; Cell Signalling), histone H2B (07-371, 1:2000; Millipore), MnSOD (SOD-110, 1:4000; Enzo Life Sciences), actin (A-2066, 1:2000), Bnip3 (B7931, 1:1000), cleaved caspase-3 (C8487, 1:1000; Sigma Aldrich), myosin (MF-20, 1:2000), myogenin (F5D, 1:200), Pax7 (PAX7, 1:200; Developmental Studies Hybridoma Bank), or p62 (PM045, 1:2000; MBL) overnight at 4^{o}C. Membranes were then incubated with the appropriate horseradish peroxidase- (HRP) conjugated secondary antibody (anti-rabbit: sc-2004, anti-mouse: sc-2005; Santa Cruz), and bands visualized using ECL immunoblotting substrates (BioVision) or Clarity ECL substrates (Bio-Rad) and the ChemiGenius 2 Bio-Imaging System (Syngene). The approximate molecular weight for each protein was estimated using Precision Plus Protein WesternC Standards and Precision Protein Strep-Tactin HRP Conjugate (Bio-Rad Laboratories).

Proteolytic Enzyme Activity

Enzymatic activity of caspases-3 and caspase-9 was determined using the substrates Ac-DEVD-AFC and Ac-LEHD-AMC (Enzo Life Sciences), respectively, as previously performed (357,369). Calpain activity was determined similarly, using the substrate Suc-LLVY-AMC. To account for proteasomal cleavage of this substrate, each sample was also analyzed with 25 μM of the calpain inhibitor Z-LL-CHO and the difference in fluorescence was taken as calpain activity. Cell lysates were prepared using lysis buffer

without addition of protease inhibitors and incubated in duplicate with 20 µM of the appropriate fluorogenic substrate in assay buffer (20 mM HEPES, 10 mM DTT, and 10% glycerol).

Lysosomal enzyme activity was measured using the substrate z-FR-AFC (Enzo Life Sciences), generally considered to indicate the activities of cathepsins L and B (357,369). Cell lysates were prepared similar to caspase/calpain assays and analyzed in duplicate with 25 µM of z-FR-AFC in a buffer containing 50 mM sodium acetate, 8 mM DTT, 4 mM EDTA, and 1 mM Pefabloc at pH 5.0. For all enzyme activities, fluorescence was measured at 30^{o}C using a Synergy H1 microplate reader (BioTek) with excitation and emission wavelengths of 360 nm and 440 nm for AMC substrates, and 400 nm and 505 nm for AFC substrates, respectively. All enzyme activities are presented normalized to total protein content and expressed as fluorescence intensity in arbitrary units (AU) per milligram protein.

Flow Cytometry

Cell Death

Annexin-V/PI staining was performed to assess the degree and type of cell death occurring after various stressors. For these measurements, culture media and one PBS wash were collected along with the adherent cells in order to include dying/detached cells. After treatment, cells were removed from culture dishes and suspended in Annexin Binding Buffer (10 mM HEPES/NaOH, 150 mM NaCl, 1.8 mM $CaCl_2$, pH 7.4) and incubated with 1 µL of Annexin V-FITC (Life Technologies) and 1 µL of 500 µg/mL propidium iodide (PI). Cells were incubated for 20 min at room temperature, after which they were washed and suspended in HBSS.

Cell Cycle

After collection, cells were fixed by slowly suspending them in ice-cold 70% ethanol in PBS. Following at least 24 hr fixation, cells were washed with PBS and suspended in PI staining solution containing 40

μg/mL PI, 0.1% Triton-X, and 20 μg/mL RNAse in PBS for 30 minutes at room temperature. All flow cytometry analyses were performed on a BD FACSCalibur flow cytometer equipped with Cell Quest Pro software (BD Bioscience).

Microscopy

Giemsa

Cell morphology was visualized using Giemsa staining, as previously performed (357). Briefly, after fixing in ice-cold methanol for 10 min and air-drying, cells were incubated with 1:20 dilution of 0.45 μm filtered Giemsa staining solution (Sigma Aldrich) in PBS (pH 6.0) for 45 min at room temperature. Cells were then washed with distilled water and mounted with Permount (ThermoFisher).

Immunofluorescence

Cell and nuclear morphology was also determined using immunofluorescent identification of actin and DAPI. After fixing in 4% formaldehyde and permeabilizing in 0.5% Triton-X 100 in PBS, cells were blocked in 5% goat serum for 1 hr and incubated with an anti-actin antibody (A-2066, 1:200; Sigma Aldrich) overnight at room temperature. Cells were then incubated with anti-rabbit AlexaFluor 488 secondary antibody for 1 hr, counterstained in 300 nM DAPI (ThermoFisher), and mounted with Prolong Gold (ThermoFisher). ImageJ was used to analyze cell and nuclear shape parameters. After masking nuclei by colour threshold, Area and Shape Descriptors measurements were performed. Calculations of these measurements can be found under the Analyze heading of the ImageJ user guide.

β-galactosidase Staining

Senescence-associated β-galactosidase activity staining (SA-Bgal) was performed as previously indicated by others (263). After washing with PBS, cells were fixed in 2% formaldehyde for 5 min at room

temperature, washed again with PBS, and then incubated at 37^{o}C for 48 hours in the staining solution consisting of PBS with 1 mg/mL X-gal, 40 mM citric acid, 5 mM potassium ferrocyanide, 5 mM potassium ferricyanide, 150 mM NaCl, and 2 mM $MgCl_2$ at pH 6.0. For all microscopy experiments, cells were grown on Cultrex- (R&D Systems) coated glass coverslips. Fluorescent microscopy was performed using a Zeiss Laser Scanning Microscope (LSM) 780. Brightfield images were acquired with a Nikon microscope equipped with a PixeLink digital camera.

ROS Measurement

ROS production was assessed by measuring DCF fluorescence. 20,000 cells were plated in each well of a black-walled 96-well plate and 24 hours later cells were pre-loaded with dye by incubating them in HBSS with 25 µM H_2DCFDA (ThermoFisher) for 45 minutes at 37^{o}C/5% CO_2. Cells were then washed twice with warmed PBS and treated as indicated for 4 hours. After washing again in PBS, HBSS was added to all wells and fluorescence was measured at 37^{o}C using a Synergy H1 microplate reader (BioTek) with excitation and emission wavelengths of 395 nm and 528 nm, respectively. Data is reported as arbitrary fluorescence and corrected for background fluorescence.

Cell Counting

A Beckman-Coulter Z2 particle analyzer was used to assess cell numbers. Events from 12-23 µm were counted as cells.

Statistics

Results are presented as means ± SEM, where n=3-6 independent experiments. Time- and/or concentration-dependent single treatment effects were determined with T-tests (performed using Microsoft Excel) by comparing individual treatment conditions to untreated cells or to those which

remained in growth media. Effects between intermittently HBSS- or STS-treated groups were determined with 1-way ANOVA analyses and Tukey post-hoc tests and calculated using GraphPad Prism. Statistical significance is indicated when $p<0.05$.

Competing Interests

No competing interests declared.

Author Contributions

Conceived of and designed study (DB and JQ), performed experiments and analyzed data (DB), interpreted data and wrote manuscript (DB and JQ).

Funding

This work was funded by a Natural Sciences and Engineering Research Council of Canada grant to JQ and a University of Waterloo Network for Aging Research Catalyst Grant to JQ and DB. DB is the recipient of a Natural Sciences and Engineering Research Council of Canada Postgraduate Scholarship.

CHAPTER III: Autophagy mediates stress resistance development caused by repeated amino acid starvation

Project Rationale and Hypotheses

In Chapter II, it was found that C2C12 cells repeatedly grown in amino acid and serum free media were protected from subsequent cell death induction by staurosporine, suggesting that autophagy caused cellular remodelling that led to stress resistance. While autophagy is widely thought of as an on-demand mechanism of mediating stress and preventing cell death, relatively less is known regarding its role as a remodelling mechanism in the absence of additional stress. In neural and cardiac tissues, ischemic preconditioning (IPC) is well established as a protective measure that reduces the damaging impact of subsequent ischemic insults. Interestingly, some have reported that autophagy is required for the beneficial effects of preconditioning. Importantly, this involves actual execution of autophagic flux, implying that IPC doesn't simply *prime* autophagic signaling (as is the case with our understanding of classical preconditioning), but that its degradative activity is necessary for this response. Additionally, autophagy is required for the dramatic cellular remodelling that occurs during skeletal muscle, adipocyte, and red blood cell differentiation, and demonstrates importance during the adaptations that occur in skeletal muscle during exercise training. Despite this, the general effects resulting from specific autophagy induction are relatively unknown.

Therefore, the purpose of this Project was to examine the importance of autophagy in mediating the development of stress resistance caused by repeated amino acid withdrawal observed in Chapter II. This was performed by intermittently incubating unmodified and Atg7-deficient cells in amino acid-free media (HBSS) and subsequently determining the sensitivity to cell death induced by staurosporine, hydrogen peroxide, or cisplatin. Additionally, this effect was compared to repeated rapamycin administration, which induces autophagy by inhibiting mTOR.

The hypotheses for Chapter III were:

1. Repeated autophagy induction would prevent cell death caused by various stressors

2. Rapamycin would cause stress resistance similar to amino acid starvation

3. Without Atg7, the protective effect of intermittent autophagy induction would be lost

Abstract

Autophagy is an important stress response mechanism that mediates cellular remodelling, adaptation, and death. Despite regulatory links to numerous stimuli, the consequences of specific autophagy induction are relatively unknown. In this study, we tested the hypothesis that repeated autophagy would cause stress resistance *in vitro*. Intermittent amino acid withdrawal protected unmodified, but not Atg7-deficient, cells from subsequent cell death induced with staurosporine (STS) and this was characterized by reduced DNA damage and caspase-3 and -9 activation. Adenoviral recovery of Atg7 content restored the amino acid starvation-induced protection from STS. However, previous repeated rapamycin administration increased sensitivity to cell death induced by hydrogen peroxide and cisplatin regardless of Atg7 content. Additionally, rapamycin treatments altered cell cycle parameters, greatly increased cell and nuclear size, and prevented myogenic differentiation of C2C12 cells. These results show that resistance to specific stressors can be achieved through metabolic autophagy induction, but the autophagy-independent effects of rapamycin increased cell death sensitivity and impaired growth and differentiation patterns.

Introduction

The cellular response to stress is highly complex, but the ultimate consequence is whether to live or die. Several programmed cell death (PCD) pathways, such as apoptosis, necroptosis, and necrosis, ensure that cells beyond repair are removed, allowing their replacement accordingly (2,4,36,370). However,

numerous tissues display reduced self-regenerative abilities and their healthy operation therefore depends on maintaining the proper function of existing cells.

The degradation mechanism autophagy is suggested to play such a role. Autophagy is best characterized as a starvation-induced response that turns cellular structures into energetically-useful material during times of nutrient deficiency (36,49). Despite its degradative nature, autophagy involves sophisticated substrate identification machinery that can selectively target damaged proteins and organelles (36,49). Consequently, the induction of autophagy during stress is normally considered a defensive measure used to mitigate cellular dysfunction (36,46,49). This cyto-protective function of autophagy is commonly observed in experiments where cell death caused by various means is blocked by its induction (36,46,49,157,209,210,371-374) or promoted by its inhibition (36,46,49,375-379). Apart from these numerous pharmacological stressors, autophagy displays protective roles during physiologically-regulated cell death (380), such as during the differentiation and development of neural tissues (381), skeletal muscle (183), adipocytes (382), lymphocytes (383), and erythroid cells (384). These studies highlight autophagy's function as a cellular remodeller, where it allows the removal and replacement of proteins and structures as cells evolve. Importantly, autophagy likely provides similar functions during less dramatic forms of transformation.

In fact, autophagy mediates the protective effects of ischemic preconditioning (IPC) in neural and cardiac tissues (244,342,385). Numerous modes of autophagy and/or mitophagy inhibition during the reperfusion phase prevented IPC-induced protection during middle cerebral artery occlusion or oxygen deprivation of cultured cortical neurons (244). In another study, autophagy inhibition with bafilomycin or 3-MA reduced infarct volume, while rapamycin pre-treatment mimicked the protective effects of IPC during permanent focal ischemia (342). In the heart, autophagy and mitophagy inhibition similarly

prevented the protective effects of IPC (343,344), and this effect could be mimicked with rapamycin (386). Autophagy-dependent IPC has also been observed during hepatic ischemia (308). Additionally, autophagy is required for the cellular remodelling responsible for the beneficial effects of exercise training on skeletal muscle (189,191). Here, autophagy-deficient mice did not experience functional adaptations (191) or were protected from subsequent metabolic stress (189) compared to their wild-type counterparts. In fact, autophagy is thought to mediate the health effects of caloric restriction and regular exercise through the development of general stress resistance (296,311). Importantly, studies have demonstrated that long-term administration of rapamycin increases longevity in species from yeast to mice (311,314,315,317). Therefore, in addition to providing protective functions during stressful conditions, autophagy is likely a vital mediator required by cells to adapt and acquire resistance to stress.

Despite the well accepted acute anti-stress functions of autophagy, the specific mechanisms and targets which mediate autophagy's protective effects are relatively unknown. Furthermore, knowledge is limited regarding its role as a pro-active mechanism of stress-resistance, such as during its induction in response to stimuli which are not specifically toxic or lethal. Therefore, the purpose of this study was to investigate the remodelling effects of repeated autophagy induction and to examine the potential impact on subsequent stress resistance. This was performed by intermittently inducing autophagy in proliferative C2C12 cells and testing whether the sensitivity to cell death induced by several means was altered.

Results

Starvation-and rapamycin-induced autophagy in C2C12 cells

Autophagy-deficient C2C12 cells were obtained by transfecting vectors coding for shRNA against Atg7 or a scramble control sequence (SCR) and selecting puromycin-resistant colonies as previously performed (183). Cell lines with 97% (shAtg7 #1), 96% (shAtg7 #2), and 98% (shAtg7 #3) lower protein expression of Atg7 compared to unmodified C2C12 and SCR were achieved (Fig. 1A). In Chapter II, amino acid and serum withdrawal using Hank's Balanced/Buffered Salt/Saline Solution (HBSS) caused massive autophagy that was detectable in 1 hour but did not increase caspase-3 activity or cause DNA damage up to 8 hours in C2C12 cells (Chapter II Fig. 1). Unsurprisingly, shAtg7 #1 and #2 displayed significantly more ($p<0.05$) caspase-3 activity during 4 hour HBSS than C2C12 cells and SCR (Fig. 1B). To avoid cell loss, media formulations were tested that induced autophagy but not cell death (Fig. 1B). It was found that 1.5 hours in HBSS supplemented with 1% FBS (HB+F) induced autophagy in SCR and limited caspase-3 activation in shAtg7 #1 and #2 (Fig. 1B & 1C). To examine how cells recovered from this treatment condition, HB+F was replaced with GM and cells were collected 3 and 6 hours later (Fig. 1D – 1H). This recovery experiment indicated: 1) Atg7 and p62 protein levels displayed temporary post-treatment increases ($p<0.05$) in SCR, 2) shAtg7 were unable to induce LC3II formation ($p>0.05$) or p62 degradation ($p>0.05$), 3) autophagy-related protein contents in SCR were normalized after 6 hours in regular culture media, and 4) HB+F did not increase caspase-3 activity in SCR but temporarily increased ($p<0.05$) it by 30% in shAtg7, although this amount was dramatically less than that caused by 2.0 μM STS for 3 hours (Fig. 1D – 1G).

We also wanted to examine the effects of rapamycin- (Rap) induced autophagy. Rap-induced autophagic flux was assessed by administering 0.5 – 10 μM Rap in GM to C2C12 cells with or without the lysosomal inhibitor chloroquine (Cq) (Fig. 2A, 2B, & 2C). While Rap concentrations were generally related to LC3II

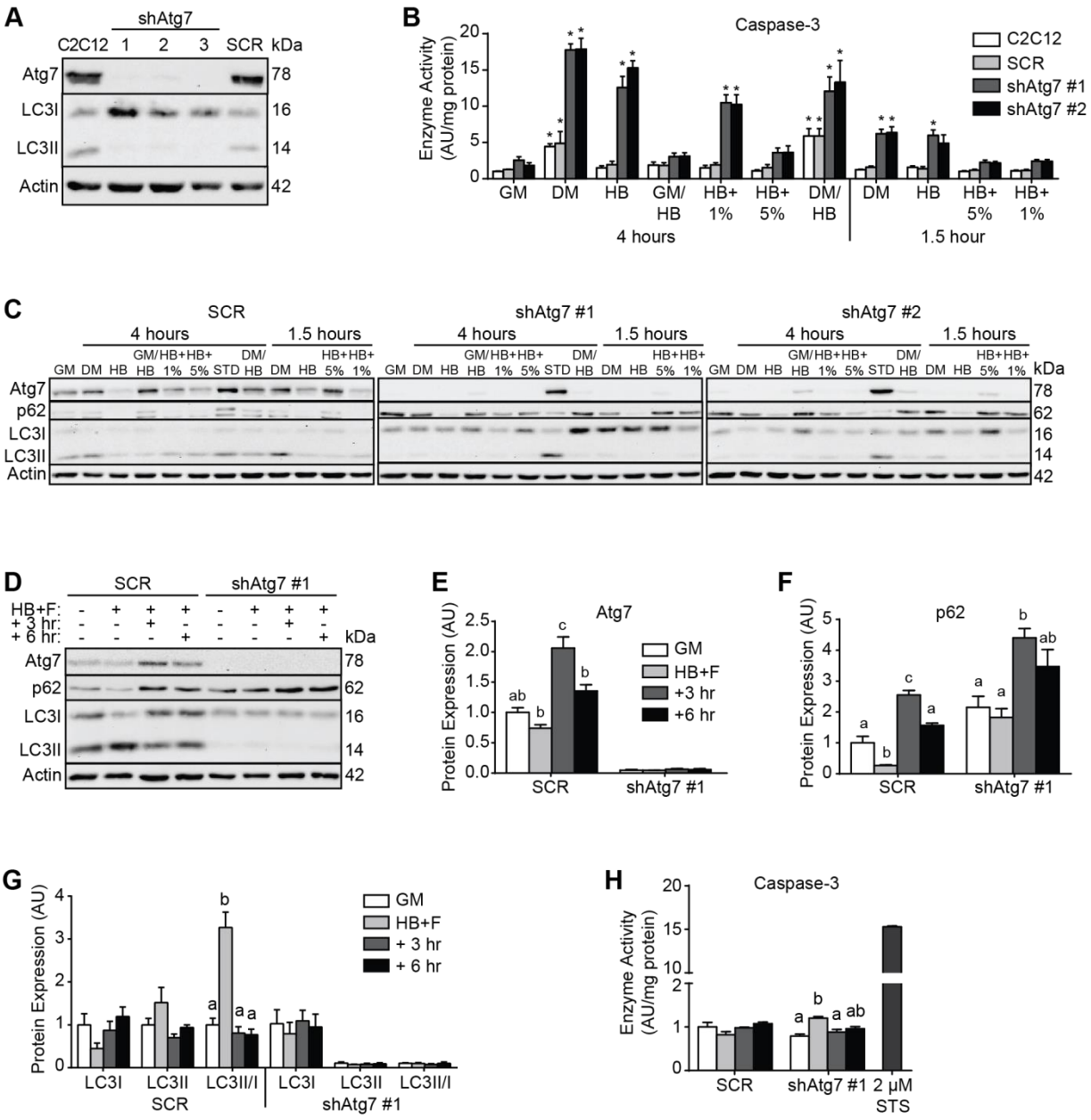

Fig. 1. Inducing autophagy with amino acid and serum withdrawal in Atg7-deficient C2C12 cells. (A) Atg7 and LC3 protein content in C2C12, 3 shAtg7 clones, and SCR cells. (B & C) Cells were incubated in the indicated media formulations and assessed for caspase-3 activity (B) and LC3 and p62 protein content (C). GM = growth media, DM = DMEM, HB = HBSS, GM/HB = 1:1 mixture of GM and HBSS, DM/HB = 1:1 mixture of DMEM and HBSS, 1/5% refers to FBS concentration. STD represents a loading standard. (D - H) Cells were left untreated (GM) or incubated in HBSS with 1% FBS (HB+F) for 1.5 hours and collected immediately or after spending 3 (+3 hr) or 6 (+6 hr) hours in GM. Assessment of Atg7 (E), p62 (F) and LC3 (G) immunoblotting. (H) Caspase-3 activity, with C2C12 cells administered 2.0 µM STS for 3 hours included for comparison. In (B), "*" denotes significant difference ($p<0.05$) from clone-specific GM calculated using a T-test. In (E-H), groups were compared with 1-way ANOVAs and significant differences ($p<0.05$) are indicated with lower case letters, where bars with different letters are significantly different than each other. N=3-4.

formation, 1.0 μM was the lowest concentration that consistently increased ($p<0.05$) the LC3II/I ratio compared to cells given Cq alone (Fig. 2B & 2C). Therefore, all subsequent experiments involving Rap were performed with 1.0 μM. The potential toxicity of this dose was tested by measuring caspase-3 activity in SCR and shAtg7 after 2 hr, 4 hr, and 8 hr incubations; caspase-3 activity was lower ($p<0.05$) at the 2 hr and 4 hr time points compared to untreated cells in both groups (Fig. 2D). Importantly, Cq-induced p62 accumulation is significantly lower ($p<0.05$) in shAtg7 #1 and #2 compared to SCR (Fig. 2E), and Rap-induced LC3 lipidation is severely restricted ($p<0.05$) in both knockdown lines (Fig. 2F), demonstrating that Atg7 deficiency reduces autophagic flux and rapamycin-induced LC3II formation.

Repeated autophagy induction by amino acid starvation or rapamycin causes diverse responses to cell death

To examine the effect of previous autophagy induction on stress-resistance, SCR and shAtg7 #1 were incubated in HB+F for 1.5 hours twice per day (cells spent 6 hours in GM between treatments) or administered 1.0 μM Rap in GM for 8 hours per day for 3 consecutive days or remained in GM (CTRL). 20 hours following the final treatment, cell death was induced using staurosporine (STS, 0.5 μM for 3 hours), hydrogen peroxide (H_2O_2, 2.5 mM for 5 hours), or cisplatin (CisPL, 25 μM for 18 hours). Additional cells not administered a death-inducing chemical (vehicle/Veh) were also analyzed. shAtg7 displayed significantly less ($p<0.05$) healthy cells and significantly more ($p<0.05$) dead/dying cells when administered STS (Fig. 3D – 3F) or CisPL (Fig. 3J – 3L). Additionally, Rap treatments increased sensitivity to H_2O_2- and CisPL-induced cell death, where Rap-receiving groups displayed less ($p<0.05$) healthy and more ($p<0.05$) late-apoptotic cells with both death-inducing chemicals regardless of Atg7 expression (Fig. 3G – 3L). To demonstrate and compare the potential autophagy-dependent effects of repeated HB+F and Rap, the "healthy" data is also presented as a change from CTRL (Fig. 3M – 3O). Although there was no difference ($p>0.05$) in the change of the percent of healthy cells between SCR and shAtg7

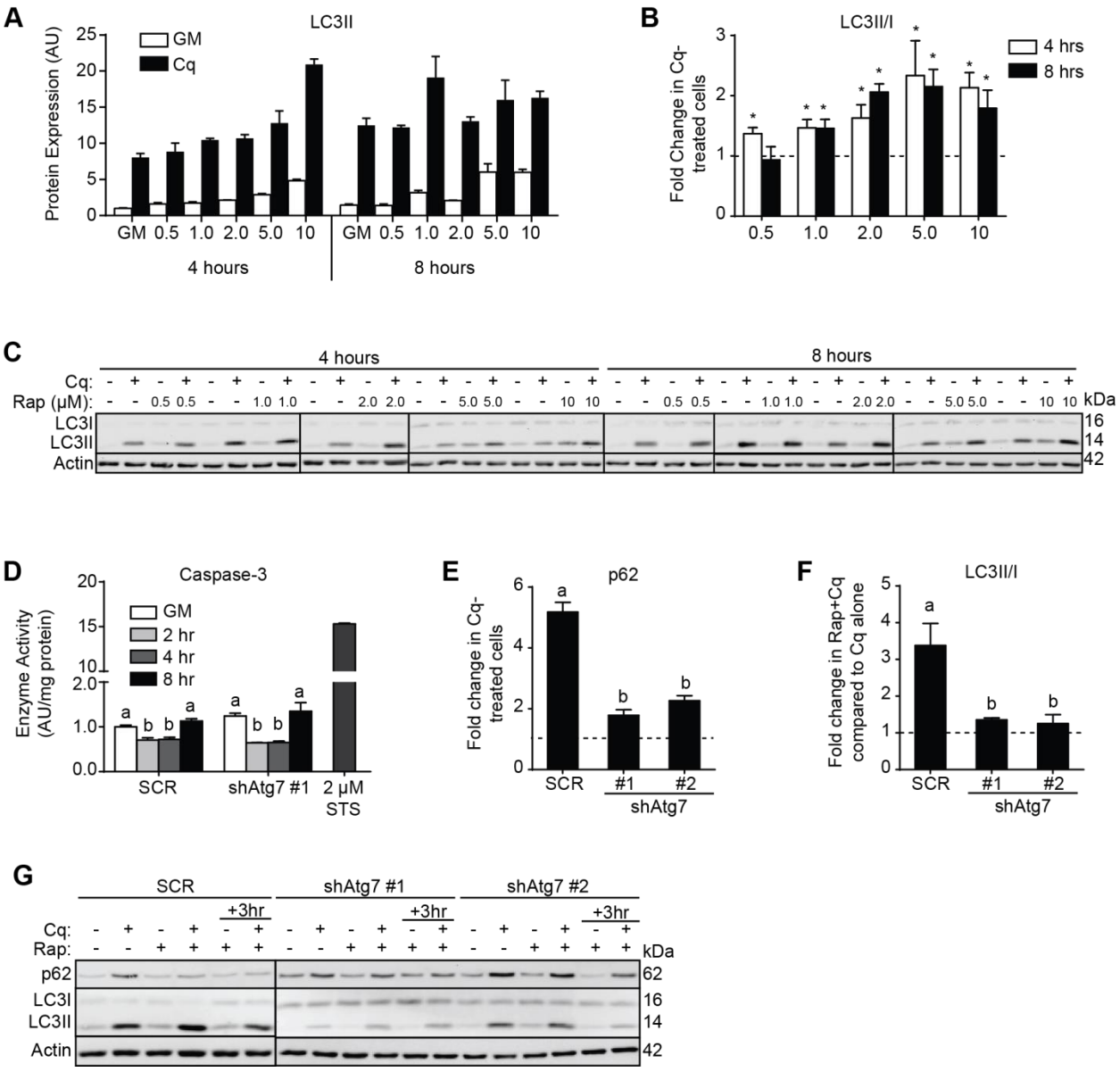

Fig. 2. Inducing autophagy with rapamycin in C2C12 cells and effect of Atg7 knockdown. (A-C) C2C12 cells were treated with the indicated concentrations of rapamycin (Rap) and/or chloroquine (Cq) and immunoblotted for LC3. In (B), 1.0 μM was the lowest concentration that consistently increased the LC3II/I ratio compared to untreated (GM + Cq) cells (dotted line). (D) Caspase-3 activity in SCR and shAtg7 #1 treated with 1.0 μM Rap for the indicated time periods or left in GM. (E-G) SCR and 2 shAtg7 clones were treated as indicated with/without Cq and 1.0 μM Rap for 8 hours and immunoblotted for p62 and LC3. In (G), +3hr indicates cells administered Rap and switched to GM containing Cq for 3 subsequent hours. In (B), "*" denotes significant difference ($p<0.05$) from untreated (GM + Cq) calculated using a T-test. In (D-F), groups were compared with 1-way ANOVAs and significant differences ($p<0.05$) are indicated with lower case letters, where bars with different letters are significantly different than each other. N=3-4.

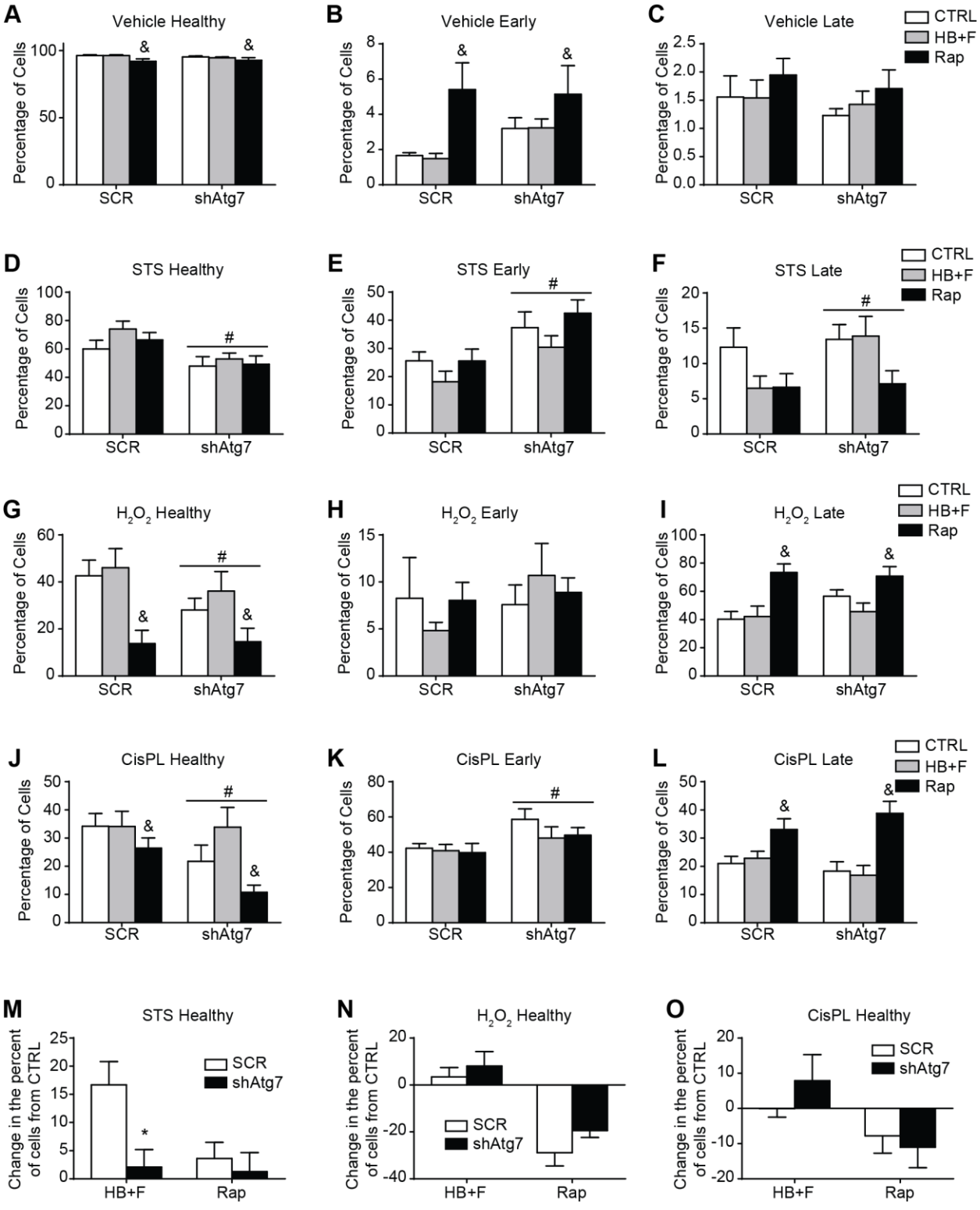

Fig. 3. Repeated autophagy induction by starvation or rapamycin causes diverse responses to cell death. SCR and shAtg7 #1 were intermittently incubated in HB+F or administered 1.0 μM Rap for 3 consecutive days or remained in GM (CTRL) and 20 hours following the final treatment cell death was induced. (A-C) Cells not administered a cell death-inducer. (D-F) Cells administered 0.5 μM STS for 3 hours. (G-I) Cells

administered 2.5 mM H_2O_2 for 5 hours. (J-L) Cells administered 25 μM CisPL for 18 hours. (M-O) Change in the percent of healthy cells compared to CTRL groups. In (A-L), groups were compared using 2-way ANOVAs: pound signs (#) denote a significant ($p<0.05$) main effect difference between SCR and shAtg7, and ampersands (&) indicate a significant ($p<0.05$) main effect of Rap compared to CTRL and HB+F. In (M-O), SCR and shAtg7 were compared at individual treatment conditions and significance ($p<0.05$) indicated with asterisks (*). N=5-6.

when death was induced by H_2O_2 or CisPL (Fig. 3N & 3O), HB+F treatments resulted in 17% more healthy SCR cells with STS administration and this was significantly more ($p<0.05$) than the number of additional healthy shAtg7 cells, demonstrating that Atg7 was required for this protective effect (Fig. 3M).

Repeated autophagy induction reduces caspase activity and DNA damage associated with subsequent cell death induction by STS

Similarly-treated cells were evaluated for changes to death-related enzyme activities and protein contents to examine the mechanisms of cell death execution assessed in Fig. 3. In agreement with annexin/PI data, shAtg7 displayed higher ($p<0.05$) caspase-3 activity compared to SCR when cell death was induced with STS or CisPL (Fig. 4A), and higher ($p<0.05$) caspase-9 activity when cell death was induced with STS (Fig. 4C). Rap treatments reduced ($p<0.05$) the activities of both enzymes during STS- and CisPL-mediated cell death while HB+F reduced ($p<0.05$) both enzyme activities during STS-induced cell death regardless of Atg7 content (Fig. 4A & 4C). However, activities of both enzymes were lower ($p<0.05$) in Rap-treated Veh groups compared to CTRL (Fig. 3A & 3C), suggesting Rap altered the basal capacity/content of these two caspases. When expressed as a change from CTRL, HB+F and Rap treatments reduced STS-associated caspase-3 (Fig. 4B) and caspase-9 (Fig. 4D) activities to a larger extent ($p<0.05$) in SCR compared to shAtg7, indicating that autophagic degradation specifically is required for the observed reduction in caspase activity.

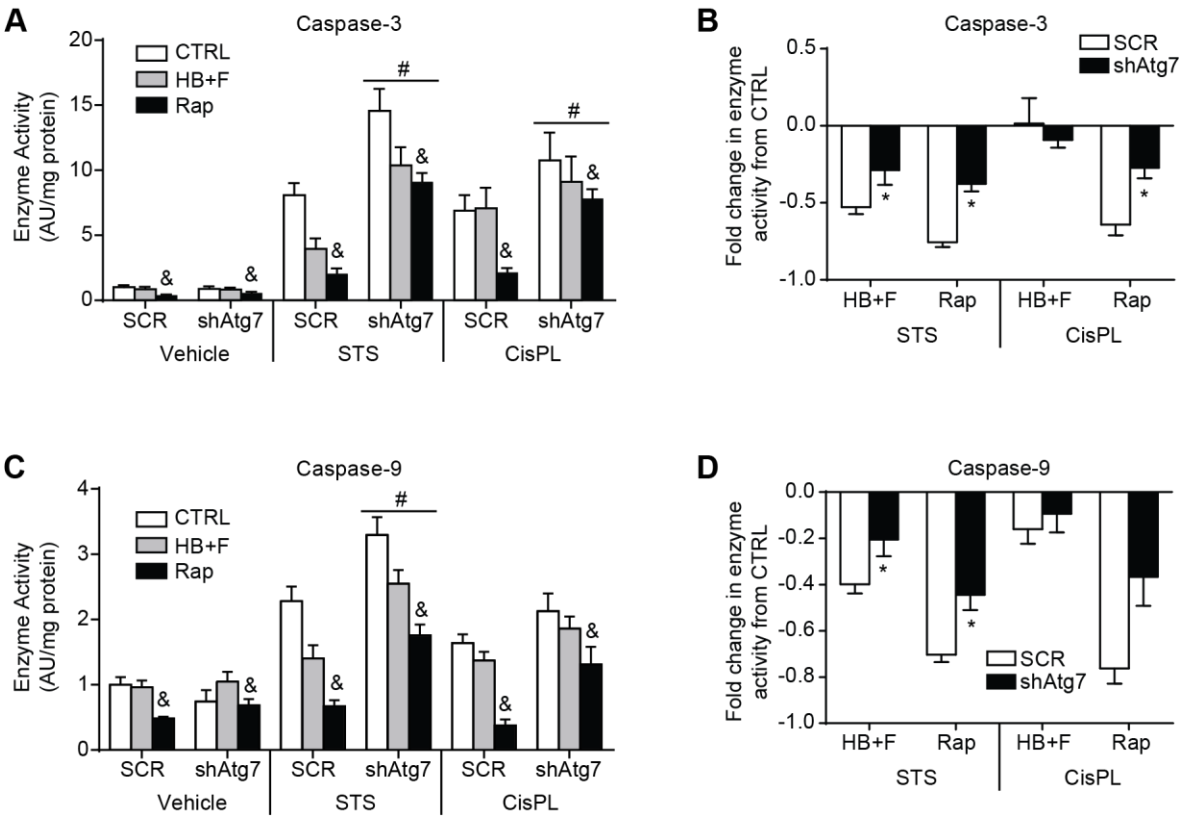

Fig. 4. Intermittent starvation- and rapamycin-induced autophagy reduces caspase activity associated with STS and CisPL exposure. Cells were administered 0.5 µM STS or 25 µM CisPL after 3 days of repeated HB+F or Rap treatments and assessed for caspase-3 (A & B) and caspase-9 (C &D) activities. In (A & C), data is presented relative to SCR CTRL Veh, arbitrarily given a value of 1.0. In (A & C), individual cell death groups were compared using 2-way ANOVAs: pound signs (#) denote a significant ($p<0.05$) main effect difference between SCR and shAtg7, and ampersands (&) indicate a significant ($p<0.05$) main effect of Rap compared to CTRL and HB+F. In (B & D), SCR and shAtg7 were compared at individual treatment conditions with T-tests and significance ($p<0.05$) indicated with asterisks (*). N=5-6.

As another measure of cell death, the DNA damage marker pH2AX was examined. Although treatment- and Atg7-dependent effects were not observed in H_2O_2- and CisPL-killed cells, shAtg7 displayed increased ($p<0.05$) pH2AX content compared to SCR during STS administration regardless of treatment condition (Fig. 5A – 5C). When expressed as a change from CTRL, the reduction in pH2AX content caused by previous HB+F treatments was significantly greater ($p<0.05$) in SCR compared to shAtg7 (Fig. 5G), similar to annexin/PI (Fig. 3) and caspase activity (Fig. 4) data. Select cell death-related proteins were

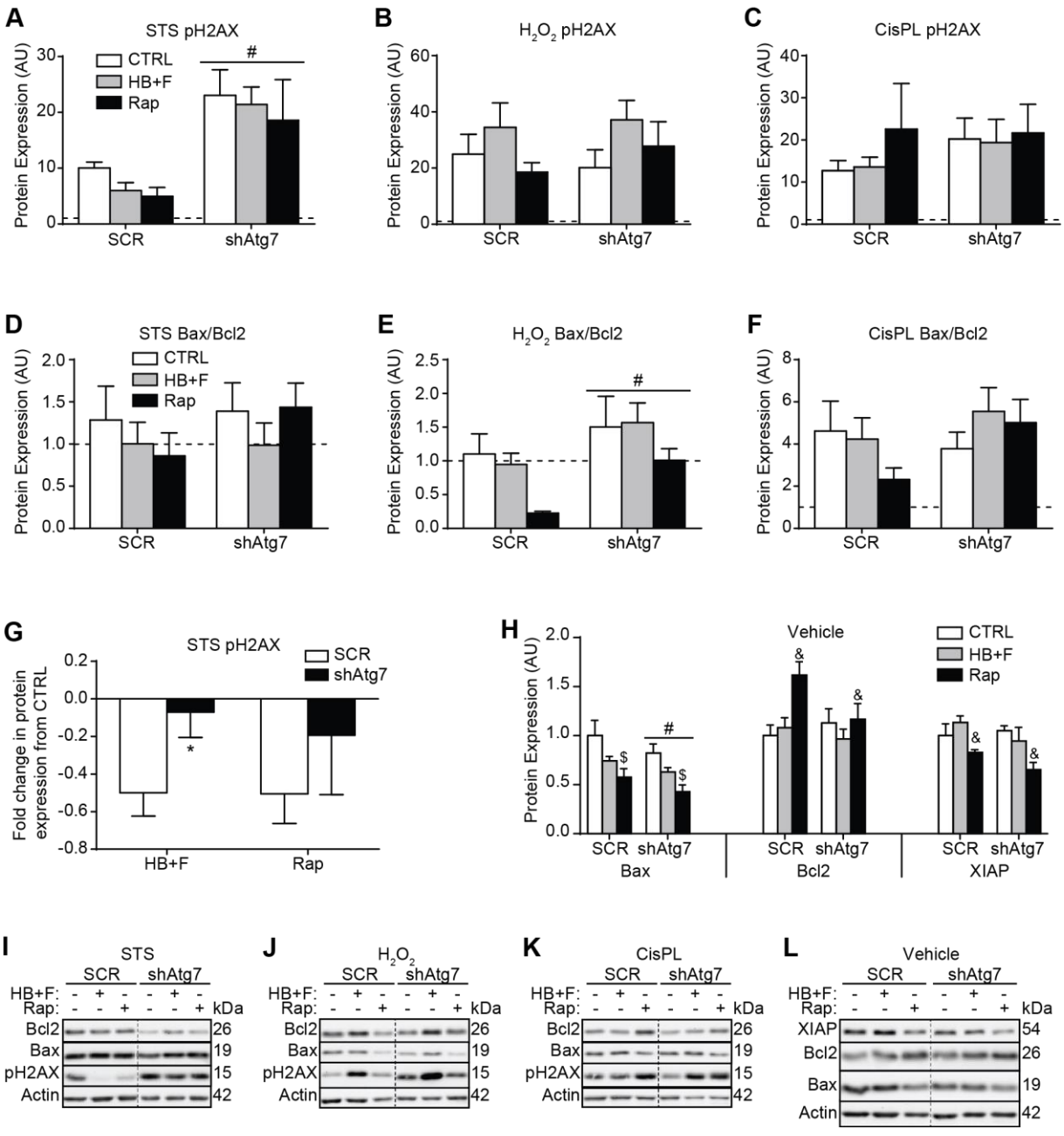

Fig. 5. Cell death related signaling is altered by previous autophagy induction. SCR and shAtg7 cells were administered 0.5 µM STS, 2.5 mM H_2O_2, or 25 µM CisPL after 3 days of repeated HB+F or Rap treatments and immunoblotted for pH2AX (A-C), Bax, and Bcl2 (D-F). (H) Assessment of Bax, Bcl2, and XIAP immunoblotting of cells not administered a death-inducing chemical. (I-L) Representative immunoblots. In (A-F & H), data is presented relative to SCR CTRL Veh, arbitrarily given a value of 1.0 and represented by a dotted line in (A-F). In (A-F & H), groups were compared using 2-way ANOVAs: pound signs (#) denote a significant ($p<0.05$) main effect difference between SCR and shAtg7, and ampersands (&) indicate a significant ($p<0.05$) main effect of Rap compared to CTRL and HB+F and dollar signs ($) indicate a significant ($p<0.05$) main effect of Rap compared to CTRL. In (G), SCR and shAtg7 were compared at individual treatment conditions with T-tests and significance ($p<0.05$) indicated with asterisks (*). N=5-6.

also quantitatively analyzed. No Atg7- or HB+F-dependent differences in the Bax:Bcl2 ratios in killed cells (Fig. 5D – 5F) or changes to Bax, Bcl2, and XIAP levels in Veh cells (Fig. 5H) were observed. However, Rap treatments decreased ($p<0.05$) Bax and XIAP and increased ($p<0.05$) Bcl2 protein levels compared to CTRL and HB+F in vehicle cells regardless of Atg7 expression (Fig. 5H).

Recovering Atg7 expression restores amino acid starvation-induced protection from STS-mediated cell death

To further confirm these findings, adenovirus encoding human Atg7 protein (adAtg7) was used to restore Atg7 expression in shAtg7. Appropriate titrations of two adAtg7 batches correctly re-established Atg7 and LC3II proteins in shAtg7 to the levels observed in SCR, while a control adGFP construct had no effect (Fig. 6A). SCR and shAtg7 with adGFP or adAtg7 were then treated with HB+F twice per day for three consecutive days and then given STS as in previous experiments. While HB+F treatments decreased ($p<0.05$) STS-induced caspase-3 activity in SCR and had no effects in shAtg7 infected with adGFP, adAtg7 recovered the HB+F-mediated caspase-3 lowering ($p<0.05$) effect in shAtg7 (Fig. 6B). This finding was echoed by pH2AX content analysis (Fig. 6C). These observations provide strong evidence that HB+F-mediated protection from STS-induced cell death is autophagy-dependent. Additionally, the dependence of HB+F-induced protection from STS-induced cell death on prevention of caspase activation was determined by administering the broad-spectrum caspase inhibitor z-FAD-FMK to CTRL SCR during STS (Fig. 6E & 6F). Here, STS-induced pH2AX expression could be decreased ($p<0.05$) with caspase inhibition, mimicking the reduced cell death observed in HB+F-treated cells (Fig. 6E & 6F).

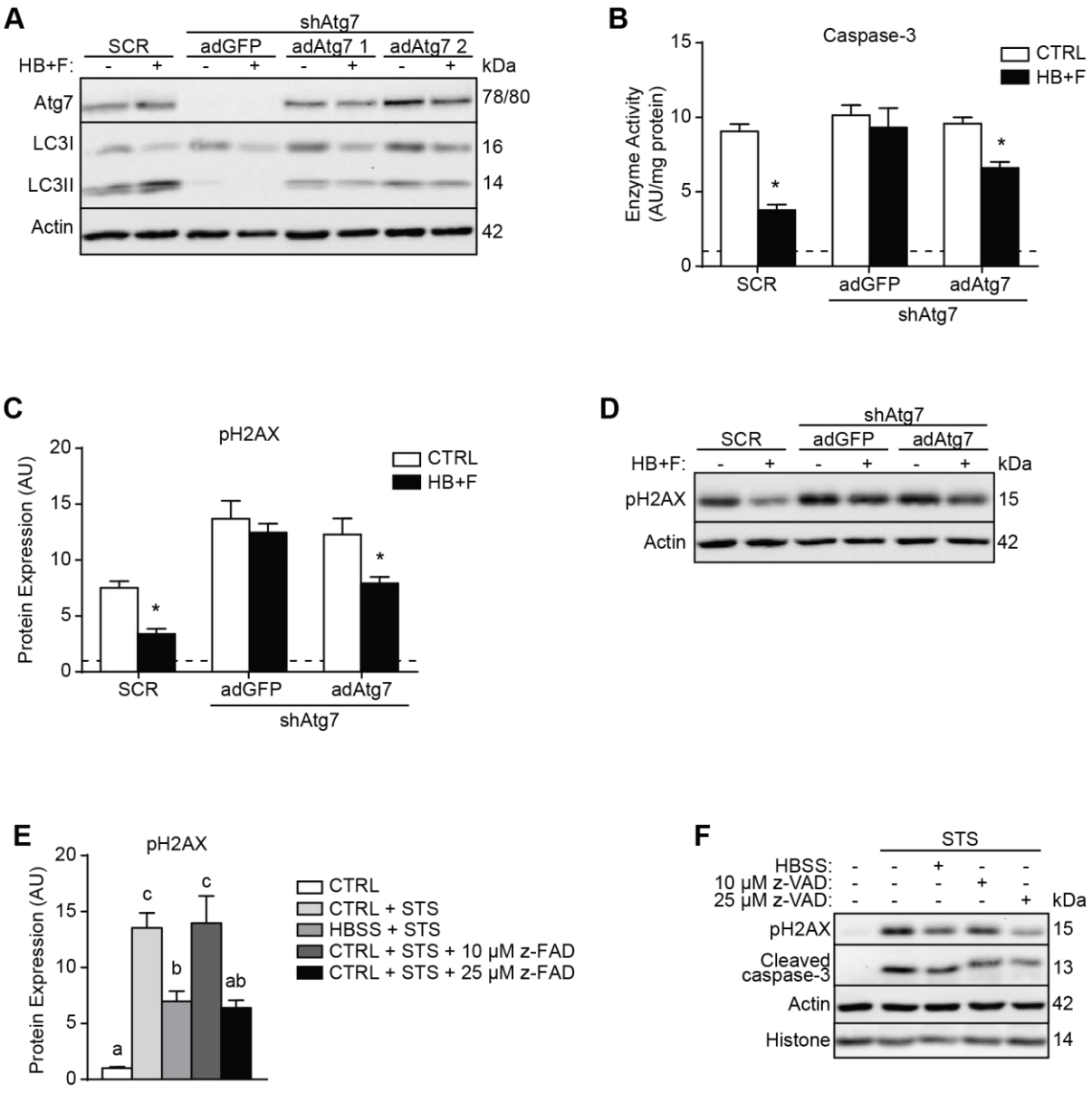

Fig. 6. Recovering Atg7 expression restores autophagy-induced protection from STS mediated cell death. (A) Immunoblotting of LC3 and p62 in cells administered adGFP or separate adAtg7 batches. (B-D) SCR, shAtg7 with adGFP, and shAtg7 with adAtg7 were intermittently incubated in HB+F for 3 consecutive days and subsequently administered STS. (B) Caspase-3 activity and (C) pH2AX protein content expressed relative to Veh arbitrarily given a value of 1.0 and represented by the dotted line. (E-F) SCR repeatedly given HB+F or remained in GM were administered 0.5 µM STS for 3 hours with or without Z-FAD-FMK and immunoblotted for pH2AX. Asterisks (*) denote significant difference between SCR and shAtg7 ($p<0.05$) calculated using a T-test. In (E), groups were compared with 1-way ANOVAs and significant differences ($p<0.05$) are indicated with lower case letters, where bars with different letters are significantly different than each other. N=4.

Repeated rapamycin exposure alters cell cycle and morphology and impairs C2C12 myogenic differentiation

In addition to the diverse observations regarding intermittent Rap and stress-resistance (more cell death as measured using annexin/PI, less caspase activity, altered stress-related protein contents), it was apparent that Rap treatments were affecting cell morphology. Cell cycle assessment using flow cytometry showed that repeated Rap increased ($p<0.05$) the number of cells in S phase and decreased ($p<0.05$) the number of cells in M/G2 compared to CTRL and HB-F in both SCR and shAtg7 (Fig. 7A). Morphological measurements performed on cells immunofluorescently-labelled with an anti-actin antibody and stained with DAPI demonstrated that shAtg7 were larger ($p<0.05$) than SCR and that Rap dramatically increased ($p<0.05$) cell area compared to CTRL and HB+F regardless of Atg7 content (Fig. 7B & 7D). Nuclear area of Rap-treated cells was also larger ($p<0.05$) compared to CTRL and HB+F (Fig. 7C). Rap-treated cells also possessed highly-developed actin structures, as ordered assembly of fibers/filaments is very apparent (Fig. 7D). Qualitative morphological observations of Giemsa-stained cells indicate general similarities between SCR and shAtg7 in CTRL and HB+F conditions, increased cell and nuclear size with Rap, and accumulation of vacuole-like structures in shAtg7 given Rap (Fig. 7E).

We previously reported that senescent C2C12 cells are incapable of myogenic differentiation and that repeated incubation in HBSS does not affect this process. Given the alterations to cell cycle and morphology in Rap-treated cells, we also examined the effects on differentiation. Unexpectedly, Rap treatments completely prevented myogenesis as cells possessed undetectable levels of myosin protein after 4 days of differentiation (Fig. 8A). While normal C2C12 differentiation is characterized by temporarily increased myogenin and p21 (both of which occurred in SCR CTRL and HB+F groups), Rap-treated cells displayed reduced ($p<0.05$) myogenin and p21 protein contents during both differentiation time points compared to SCR and HB+F (Fig. 8B & 8C). Interestingly, Pax7 levels were not different

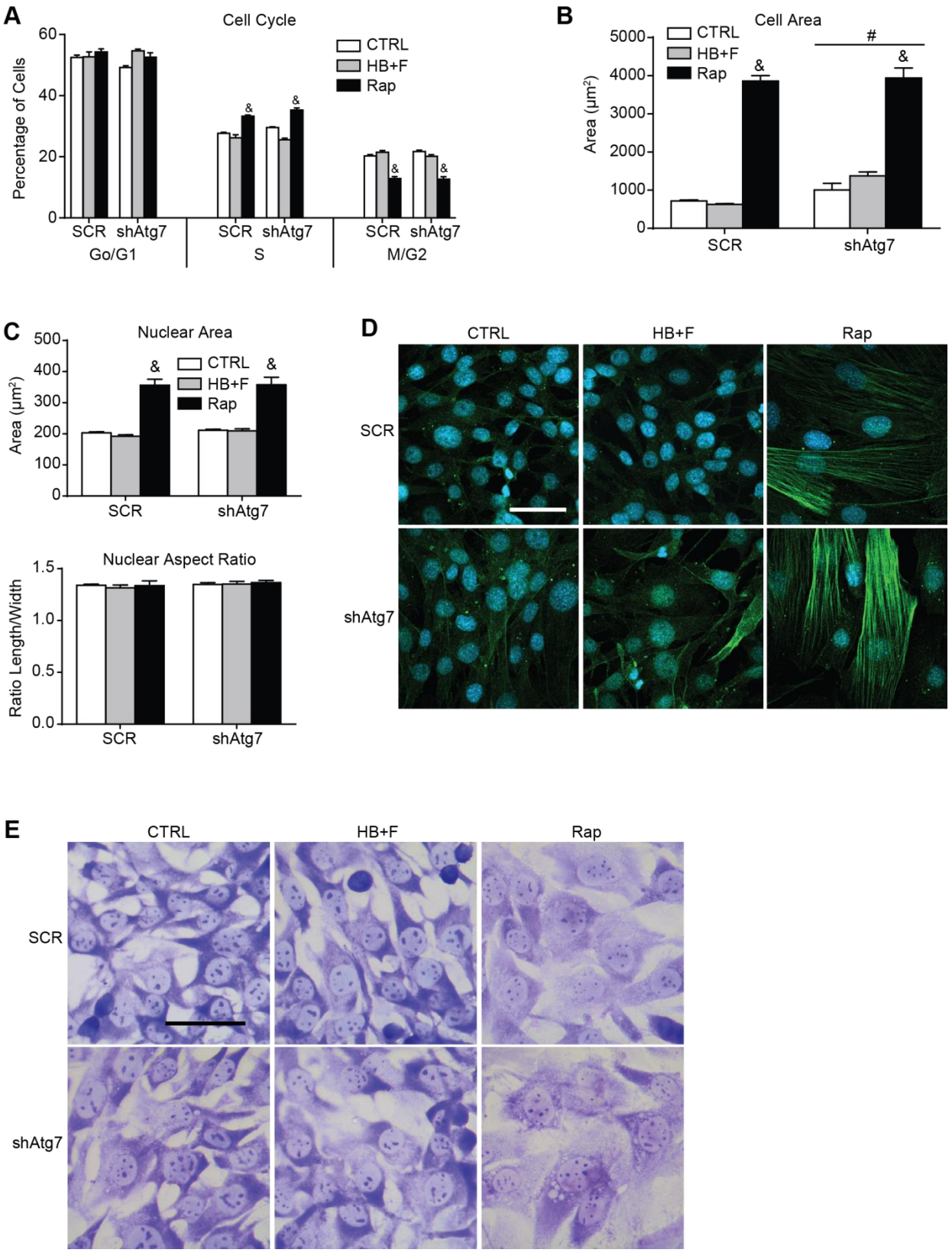
A
Cell Cycle
Percentage of Cells
CTRL
HB+F
Rap
SCR shAtg7 SCR shAtg7 SCR shAtg7
Go/G1
S
M/G2
B
Cell Area
Area (µm²)
CTRL
HB+F
Rap
#
SCR
shAtg7
C
Nuclear Area
Area (µm²)
Nuclear Aspect Ratio
Ratio Length/Width
SCR
shAtg7
D
CTRL
HB+F
Rap
SCR
shAtg7
E
CTRL
HB+F
Rap
SCR
shAtg7

Fig. 7. Changes to cell cycle and morphology with Atg7 deficiency and repeated autophagy induction. SCR and shAtg7 were intermittently treated with HB+F or Rap for 3 consecutive days. (A) Assessment of cell cycle using flow cytometry detection of PI fluorescence. (B-D) Morphological analyses of cell area (B) and nuclear shape parameters (C) on cells immunolabelled with an anti-actin antibody (green) and counterstained with DAPI (blue) (D). (E) Representative images of Giemsa-stained cells. Groups were compared using 2-way ANOVAs: pound signs (#) denote a significant ($p<0.05$) main effect difference between SCR and shAtg7, and ampersands (&) indicate a significant ($p<0.05$) main effect of Rap compared to CTRL and HB+F. In (D), scale bar represents 50 µm. In (E), scale bar represents 50 µm. In (A) n=4, in (B & C) n=3.

($p>0.05$) between groups on day 2 of differentiation but were significantly higher ($p<0.05$) in Rap-treated cells on day 4, perhaps identifying a location for the observed differentiation obstruction (Fig. 8D). Although shAtg7 were included in this experiment, we previously demonstrated that autophagy is required for C2C12 differentiation (183), and as a result statistical comparisons between SCR and shAtg7 were not performed here. Despite this, it is clear that differentiation is prevented or delayed in shAtg7 compared to SCR, and the use of completely different cell clones in the present experiment confirms the findings of our previous study.

Discussion

These findings demonstrate the diverse cellular adaptations caused by two different autophagy inducing stimuli. While amino acid starvation increased resistance to cell death caused by STS, repeated rapamycin treatments actually increased sensitivity to cell death caused by oxidative stress and DNA damage. Additionally, rapamycin induced a cellular phenotype characterized by altered cell cycle, greatly enlarged cell size, and differentiation impairment.

Autophagy primarily functions to provide cells with energetic substrates during times of nutrient deficiency. However, due to numerous specific targeting interactions, autophagy additionally regulates development and differentiation, immunity and inflammation, and is typically activated as an on-

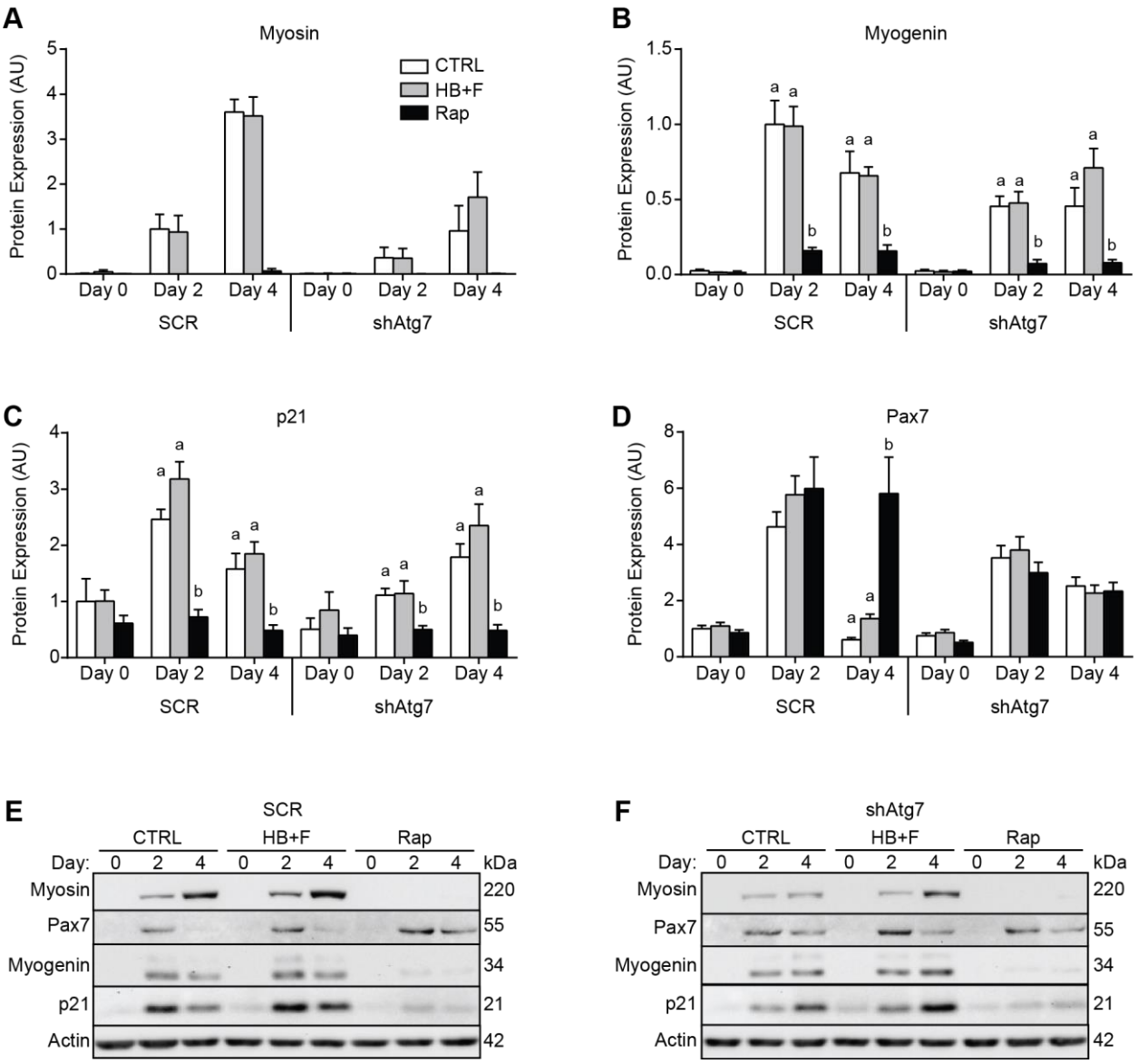

Fig. 8. Myogenic differentiation is prevented by previous rapamycin exposure. After 3 days of intermittent HB+F or Rap treatments, differentiation was induced and cells collected at various time points during the differentiation process. Quantification of myosin (A), myogenin (B), p21 (C) and Pax7 (D) immunoblotting analyses. (E & F) Representative immunoblots of SCR (E) and shAtg7 (F). Groups were compared with 1-way ANOVAs at individual time points and significant differences ($p<0.05$) are indicated with lower case letters, where bars with different letters are significantly different than each other. N=4.

demand mechanism of stress resistance (49,380,387). Because of this, dysregulated autophagy is implicated in the development of numerous diseases including cancer, neurodegeneration, and skeletal and cardiac muscle myopathies (49). In fact, autophagy is so essential that individual genetic deletion of numerous autophagy-associated genes is lethal in mice and induced deficiency of autophagy in adulthood causes dysfunction in several tissues. Furthermore, it is suggested that autophagy induction throughout life may have beneficial health effects through intermittent "recycling" of cellular material, and is a mechanism through which regular exercise and proper nutrition affect human health (49,311). However, relative caloric restriction and exercise impact innumerable processes that contribute to cellular adaptation (such as antioxidant defence) and although a link between these and autophagy is beginning to be established, specific autophagy-dependent effects remain largely unknown. Considering our first observation, that repeated amino acid starvation protected from subsequent STS-induced DNA damage and cell death, several findings can help explain this response.

Notably, caspase-3 and -9 activities were significantly reduced in HB+F-treated cells, and this reduction was partially abrogated with Atg7-deficiency (Fig. 4). Given the role these proteolytic enzymes provide in executing cell death through protein and DNA cleavage, their reduced activities likely explain the protective effect of repeated autophagy induction. In fact, protection from STS-induced DNA damage could be mimicked with a chemical caspase-3 inhibitor (Fig. 6). Specifically, these observations suggest that STS-induced mitochondrial-mediated cell death signaling was attenuated. Of course, mitochondria are essential regulators of cell death execution (2). We previously demonstrated that a modest increase in mitochondrial content protected from cell death induced by STS and this was also associated with decreased caspase-3 activity (388). Forced/overexpression of PGC1α is also well-known to protect cells from oxidative stress-induced cell death, suggesting that mitochondria can adapt to become stress resistant (389,390). Specifically preventing STS-induced cell death, and not that caused by hydrogen

peroxide or cisplatin, further supports our conclusion that autophagy induction caused stress-resistance by attenuating mitochondrial-mediated caspase activation. Cisplatin is a widely-used chemotherapeutic because it damages DNA thereby preferentially causing cell death in quickly dividing cells (391); in C2C12s it induces p53, dramatically reduces Bcl2 levels, and increases caspase-3 activity (357). While oxidative stress causes cell death through a variety of mechanisms, in our hands hydrogen peroxide does not activate caspases (which is why such data is absent from Fig. 4), but causes mitochondrial AIF release and DNA damage (Fig. 5, 388). Therefore, it appears that repeated autophagy induction affected a specific aspect of STS-induced cell death activation. Importantly, we did not detect HB+F-induced changes to Bcl2 or XIAP protein expression, indicating that neither of these cell death inhibiting proteins were likely involved with the observed protective phenotype. We therefore suggest that protection from STS occurred by maintaining mitochondrial integrity. However, as numerous cellular pathways affect cell death execution, it is possible that an unidentified factor is involved here. It is also noteworthy that Atg7-deficiency had independent effects on cell death sensitivity. In response to all three toxic chemicals investigated, less healthy shAtg7 compared to SCR cells were observed (Fig. 3), while STS and CisPL also increased caspase activity significantly more in shAtg7 than SCR cells (Fig. 4). This supports autophagy's role as an on-demand mediator of stress resistance or indicates the development of a relatively stress-sensitive environment in the absence of autophagy. Given the aforementioned potential adaptations relevant to stress-resistance, the question is how does forced autophagy induction cause these changes? Importantly, although the specific cellular aspects targeted by autophagy are relatively unknown and highly context-dependent, some autophagy-related interactions can explain these adaptations.

Notably, autophagy preferentially targets dysfunctional and damaged proteins and organelles. Due to interactions between ubiquitin and the LC3 receptors p62 and NBR1, abundance of direct cargo

receptors, and existence of autophagy-specific chaperone mechanisms, misfolded and aggregated proteins are preferentially degraded by autophagy (101,104,105,392-394). Autophagy similarly targets depolarized and ROS-producing mitochondria as well as endoplasmic reticulum with accumulated misfolded proteins and dysregulated calcium signaling (134,395-397). In fact, this ability for autophagy to selectivity target damaged cellular material drove our hypothesis that its forced induction would pro-actively "clean" cells thereby reducing their basal stress levels and increasing their resistance to cell death. In addition to these impacts on immediate sources of cellular damage, autophagy degrades other specific targets that potentially influence stress resistance. A direct example of such targets is caspase-8, which has been shown to be degraded by autophagy thereby attenuating TRAIL- and hydrogen peroxide-induced cell death (217,398). P62 accumulation itself can also lead to cellular dysfunction by affecting ROS and NRF2 signaling (237,239,291,399). Additionally, selective autophagic degradation of diverse proteins such as Notch1 (400), AIM2 (401), NLRP3, pro-caspase-1 (402), Chk1 (403), and IKKβ (404) suggests its induction may modulate complex cellular signaling pathways. Furthermore, NFkB transcriptionally promotes Beclin1, Atg5, and LC3 expression (405,406), and HBSS-induced NFkB activation requires Atg5 and Atg7 (407). This possibly explains an adaptable feedback mechanism leading to increased stress resistance through elevated autophagy activation in response to subsequent stress. In fact, this explanation that resistance to cell death from STS is due to starvation-induced "priming" of autophagy, is supported by the numerous post-translational means through which autophagy is regulated (408). Cumulatively, it is clear that autophagy's ability to turn unnecessary/dysfunctional and specific un-damaged proteins into cellular building blocks emphasizes its potential role as an inducible cellular remodelling mechanism, and our observation that repeated autophagy induction protected cells from STS-mediated cell death highlights this function.

Interestingly, not only did rapamycin treatments not similarly protect cells from STS, but rapamycin-treated cells were actually sensitized to cell death caused by hydrogen peroxide and cisplatin, regardless of Atg7 content (Fig. 3). As healthy cell counts were similarly reduced in SCR and Atg7-deficient cells when administered these death inducing chemicals (Fig 3N & 3O) and HB+F treatments did not alter sensitivity to H_2O_2 or CisPL-induced cell death (Fig. 3), the autophagy-independent actions of rapamycin likely caused these effects. Although rapamycin's ability to activate autophagy is intensely researched, its main use is as a non-steroidal immunosuppressant widely administered during organ transplants and synthetic material implamts. This is due to its ability to potently arrest cell cycle at G1 by inhibiting TOR1/TOR2 in yeast and mTOR in mammalian cells (409-411) thereby significantly impairing T-cell expansion (411,412). Importantly, mTOR regulates numerous cellular processes which are still being fully unravelled. Interestingly, although we observe G_0/G1 arrest in C2C12 cells upon differentiation induction (Boonstra et al, accepted August 2017) and senescence (Bloemberg and Quadrilatero, unpublished), repeated rapamycin treatments arrested cells in S phase here (Fig. 7) and actively mitotic cells were qualitatively very rare during microscopy analyses. We also found that *prior* rapamycin treatments completely prevented subsequent myogenic differentiation (Fig. 8). It is established that rapamycin prevents myogenic differentiation when administered in differentiation-promoting culture media to C2C12 and other myogenic cell types (413-418). In these experiments, rapamycin prevented p21 induction (416,418) similar to our observations (Fig. 8). However, the specific mTOR effectors implicated are complex, as these studies demonstrated that rapamycin's effects: are mTOR dependent (417), involve PI3K and S6K activity (416), are mTORC2 dependent (413), do not require mTOR's kinase activity (417), do require mTOR's kinase activity (414), and are NFkB dependent (415). These observations suggest mTOR is intricately regulated during muscle differentiation. However, in our experimental protocol cells did not receive rapamycin during differentiation, suggesting its repeated effects pre-emptively induced an anti-differentiation state. Notably, we report sustained Pax7

expression in rapamycin-treated cells compared to those grown in GM alone or those intermittently starved of amino acids, not only implying that these cells were capable of entering the initial myogenic stages, but also indicating a mechanistic location for differentiation obstruction (Fig. 8C). Interestingly, treating isolated aged mouse satellite cells with rapamycin restored their proliferation defects, reduced senescence markers, and rescued their regenerative potential when transplanted after injury; effects that were abrogated by Atg7-deficiency (252). Rapamycin furthermore reduced mitochondrial ROS production, removed protein aggregates, and reverted the senescent phenotype in aged human satellite cells (252). Perhaps, differences between C2C12 cells and primary muscle/satellite cells account for these discrepant findings. It is also important to note the difference between the cellular phenotype we observed here with rapamycin treatments and that of toxic stress-induced senescence (Bloemberg and Quadrilatero, unpublished). We previously showed that senescent C2C12 cells are arrested in G1 and display resistance to CisPL (Bloemberg and Quadrilatero, unpublished). Despite the significantly enlarged and flattened appearance of rapamycin-treated C2C12 cells and their differentiation impairment, they were arrested in S phase and were not resistant to CisPL, suggesting this phenotype is separate from senescence. Additionally, although we chose 1.0 μM rapamycin based on measurements of autophagy induction, this is 10 times more concentrated than that used to restore the regenerative abilities of aged satellite cells (252). However, rapamycin typically demonstrates proliferation obstruction and myogenic differentiation impairment between 10-100 nM (411-414,416-418).

Although the reason for increased sensitivity to cell death by oxidative stress and DNA damage after repeated rapamycin treatments is unknown, interestingly, CisPL reduced the number of healthy cells by 60% in untreated Atg7-expressing cells and by 85% in rapamycin-treated Atg7-deficient cells (Fig. 3A & 3J). Therefore, the dual insults of autophagy deficiency and previous rapamycin administration greatly increased the sensitivity to cell death caused by this chemotherapeutic. Similarly, hydrogen peroxide

exposure resulted in 30% less healthy cells in rapamycin-treated shAtg7 compared to SCR controls (Fig. 3A & 3G). This suggests chronic rapamycin exposure actually increases the cellular sensitivity to specific stressors, an effect amplified by autophagy-deficiency. Whether *this* finding (rapamycin-induced cell death sensitivity) could partly explain its effects on healthy aging and longevity is unknown; however, it would be interesting to demonstrate this phenomenon in other/human cell lines and test this hypothesis *in vivo*. Particularly, given the observation that transplant recipients receiving rapamycin show decreased cancer risk (419) and the use of rapamycin/mTOR inhibitors in several combination chemotherapy regimens (420,421), it is likely that its effects on cell death sensitivity are involved and perhaps unrelated to autophagy. Regardless, these findings suggest that several exceptions and caveats exist regarding the "autophagy protects cells" theory, particularly autophagy induced by rapamycin. At the very least, it is clear that more-specific chemical modifiers of autophagy are required to answer and potentially solve these complicated physiological and clinical questions (422,423).

We report here that repeated autophagy induction by amino acid starvation pro-actively increased stress resistance *in vitro*, as demonstrated by protection from staurosporine-induced cell death. While this possibility is often hypothesized to be responsible for the beneficial health and longevity effects of relative caloric restriction and exercise, it is seldomly demonstrated explicitly. We additionally show this is likely due to decreased mitochondrial-mediate caspase activation. Unexpectedly, similar experiments performed with rapamycin administration instead of amino acid starvation showed that rapamycin increased the sensitivity to cell death induced by oxidative stress and DNA damage. Repeated rapamycin treatments also greatly increased cell size, altered cell cycle, and prevented myogenic differentiation. These findings validate the ability of autophagy to function as an inducible mechanism of cellular remodelling and suggest further investigation into the physiological effects of chronic rapamycin exposure is warranted.

Materials and Methods

Cell Culture

C2C12 mouse skeletal myoblasts (ATCC) and HEK 293A cells were cultured in growth media (GM) consisting of low-glucose Dulbecco's Modified Eagles Medium (DMEM; Hyclone, ThermoFisher) containing 10% fetal bovine serum (FBS; ThermoFisher) and 1% penicillin/streptomycin (ThermoFisher) on polystyrene culture dishes (BD Biosciences), as previously performed (357,369). C2C12 differentiation was induced by switching 90% confluent cells to differentiation media (DM) consisting of low-glucose DMEM containing 2% horse serum and 1% penicillin/streptomycin. For microscopy experiments, cells were grown on Cultrex- (R&D Systems) coated glass coverslips. When necessary, cells were isolated via trypsinization after washing in warmed PBS and centrifuged at 1000g. Note that for all cell death experiments culture media and PBS were collected to include non-adhered cells and debris.

Materials

Cells were treated as indicated with various chemicals/solutions to induce or measure cell stress. These include: Hank's Balanced Salt Solution (HBSS; Gibco formulation: 140mg/L $CaCl_2$, 100mg/L $MgCl_2$-$6H_2O$, 100mg/L $MgSO_4$-7H2O, 400mg/L KCl, 60mg/L KH_2PO_4, 350mg/L $NaHCO_3$, 8.0g/L NaCl, 48mg/L Na_2HPO_4, 1.0g/L D-glucose, with 1% penicillin/streptomycin), HBSS with 1% FBS and 1% penicillin/streptomycin (HB+F), rapamycin (Rap, 0.5 – 10.0 μM; Enzo Life Sciences), chloroquine (Cq, 50 μM; Sigma-Aldrich), staurosporine (STS, 0.5 μM or 2.0 μM; Enzo Life Sciences), cisplatin (CisPL, 25 μM; Enzo Life Sciences), hydrogen peroxide (H2O2, 2.5 mM; Sigma Aldrich), and the caspase inhibitor z-VAD-FMK (10 or 25 M μM; Enzo Life Sciences).

Atg7 Knockdown

C2C12 cells grown in 12-well plates were transfected with vectors encoding either an shRNA against Atg7 (Gene ID 74244, Origene TG504956) or a scramble control sequence (Origene TR30013) using Lipofectamine 2000 (ThermoFisher) as previously performed (183). Cells with stable incorporation of each vector were selected using 2 µg/mL puromycin (Sigma). Surviving clones were individually isolated and assessed for Atg7 protein expression using immunoblotting. When not otherwise indicated, experiments were performed with Atg7-deficient cell clone (shAtg7) number 1.

Adenoviral Atg7 Expression

Adenovirus coding for human Atg7 protein (adAtg7) was generously provided by Dr. Gokhan S. Hotamisligil, Department of Genetics and Complex Diseases, T.H. Chan School of Public Health, Harvard (424). An adenoviral construct encoding GFP (adAVH6/adGFP) was a generous gift from Dr. Robin Parks, Ottawa Hospital Research Institute (425). Virus were amplified using HEK 293A cells (generously provided by Dr. Robin Duncan, Department of Kinesiology, University of Waterloo) and viral particles were isolated/concentrated through repeated freeze-thaw cycles as indicated in the ViraPower Adenoviral Expression System protocol (Life Technologies). AdAtg7 stock volumes were titred to recover Atg7 protein content in Atg7-deficient cells to the levels observed in control/SCR cells.

Immunoblotting

Immunoblotting was performed as previously described (357,369). Whole-cell lysates were generated by adding ice-cold lysis buffer (LB, pH 7.4; 20mM HEPES, 10mM NaCl, 1.5mM $MgCl_2$, 1 mM DTT, 20% glycerol, and 0.1% Triton-X100, Sigma Aldrich) with protease inhibitors (Complete Cocktail; Roche) to cell pellets followed by sonication for 12 seconds. Protein content was measured using the BCA protein assay method. Briefly, equal amounts of protein were loaded into and separated using 10-12% SDS-

PAGE, transferred onto PVDF membranes (Bio-Rad Laboratories), and blocked for 1 hr at room temperature with 5% non-fat dry milk in TBS-T. Membranes were then probed with primary antibodies against Bcl2 (sc-7382, 1:200), Bax (sc-493, 1:1000), p21 (sc-397, 1:1000), phosphorylated histone H2AX (pH2AX, sc-101696, 1:1000; Santa Cruz), Atg7 (8558, 1:1000), LC3 (2775, 1:1000; Cell Signalling), actin (A-2066, 1:2000), myosin (MF-20, 1:2000), myogenin (F5D, 1:200), Pax7 (PAX7, 1:200; Developmental Studies Hybridoma Bank), p62 (PM045, 1:2000; MBL), or XIAP (ADI-AAM-050, 1:1000; Enzo Life Sciences) overnight at 4^{o}C. Membranes were then incubated with the appropriate horseradish peroxidase-(HRP) conjugated secondary antibody (anti-rabbit: sc-2004, anti-mouse: sc-2005; Santa Cruz), and bands visualized using ECL immunoblotting substrates (BioVision) or Clarity ECL substrates (Bio-Rad) and the ChemiGenius 2 Bio-Imaging System (Syngene). The approximate molecular weight for each protein was estimated using Precision Plus Protein WesternC Standards and Precision Protein Strep-Tactin HRP Conjugate (Bio-Rad Laboratories).

Proteolytic Enzyme Activity

Enzymatic activity of caspases-3 and -9 was determined using the substrates Ac-DEVD-AFC and Ac-LEHD-AMC (Enzo Life Sciences), respectively, as previously performed (357,369). Cell lysates were prepared using lysis buffer without addition of protease inhibitors and incubated in duplicate with 20 µM of the appropriate fluorogenic substrate. Caspase activity measurements were performed in an assay buffer of 20 mM HEPES, 10 mM DTT, and 10% glycerol. For all activities, fluorescence was measured at 30^{o}C using a Synergy H1 microplate reader (BioTek) with excitation and emission wavelengths of 360 nm and 440 nm for AMC substrates, and 400 nm and 505 nm for AFC substrates, respectively. All enzyme activities are presented normalized to total protein content measured using BCA and expressed as fluorescence intensity in arbitrary units (AU) per milligram protein.

Flow Cytometry

Cell Death

Annexin-V/PI staining was performed to assess the degree and type of cell death occurring after various stressors. For these measurements, culture media and one PBS wash were collected along with the adherent cells in order to include dying/detached cells. After treatment, cells were removed from culture dishes and suspended in Annexin Binding Buffer (10 mM HEPES/NaOH, 150 mM NaCl, 1.8 mM $CaCl_2$, pH 7.4) and incubated with 1 µL of Annexin V-FITC (Life Technologies) and 1 µL of 500 µg/mL propidium iodide (PI). Cells were incubated for 20 min at room temperature, after which they were washed and suspended in HBSS. Cells negative for both annexin and PI were classified as healthy, those positive for annexin and negative for PI were considered to be in early stages of cell death, and those positive for both annexin and PI were considered to be in late stages of cell death.

Cell Cycle

After collection, cells were fixed by slowly suspending them in ice-cold 70% ethanol in PBS. Following at least 24 hr fixation, cells were washed with PBS and suspended in PI staining solution containing 40 µg/mL PI, 0.1% Triton-X, and 20 µg/mL RNAse in PBS for 30 minutes at room temperature. All flow cytometry analyses were performed on a BD FACSCalibur flow cytometer equipped with Cell Quest Pro software (BD Bioscience).

Microscopy

Giemsa

Cell morphology was visualized using Giemsa staining, as previously performed (357). Briefly, after fixing in ice-cold methanol for 10 min and air-drying, cells were incubated with 1:20 dilution of 0.45 µm

filtered Giemsa staining solution (Sigma Aldrich) in PBS (pH 6.0) for 45 min at room temperature. Cells were then washed with distilled water and mounted with Permount (ThermoFisher).

Immunofluorescence

Cell and nuclear morphology was also determined using immunofluorescent identification of actin and DAPI. After fixing in 4% formaldehyde and permeabilizing in 0.5% Triton-X 100 in PBS, cells were blocked in 5% goat serum for 1 hr and incubated with an anti-actin antibody (A-2066, 1:200; Sigma Aldrich) overnight at room temperature. Cells were then incubated with anti-rabbit AlexaFluor 488 secondary antibody for 1 hr, counterstained in 300 nM DAPI (ThermoFisher), and mounted with Prolong Gold (ThermoFisher). ImageJ was used to analyze cell and nuclear shape parameters, with at least 100 cells measured per trial. After masking nuclei by colour threshold, Area and Shape Descriptors measurements were performed. Calculations of these measurements can be found under the Analyze heading of the ImageJ user guide. All fluorescent microscopy was performed using a Zeiss Laser Scanning Microscope (LSM) 780. All light microscope images were acquired with a Nikon microscope equipped with a PixeLink digital camera.

Statistics

Results are presented as means ± SEM, where n=3-6 independent experiments. GraphPad Prism was used to perform 1- and 2-way ANOVA analyses and Tukey post-hoc tests where appropriate with significance indicated when $p<0.05$. Microsoft Excel was used to perform T-tests with significance indicated when $p<0.05$. Specifics regarding the statistical comparisons made can be found in figure captions. In figures, 1-way ANOVA significant differences are denoted with lowercase “a, b, c” characters and 2-way ANOVA main effect differences are denoted with pound signs (#) and ampersands (&). T-test significance is denoted with asterisks (*).

CHAPTER IV: Autophagy and mitophagy as inducible regulators of mitochondrial stress resistance and function

Project Rationale and Hypotheses

Despite the well accepted anti-stress functions of autophagy, relatively less is known regarding autophagy and mitophagy's roles as *pro-active* mechanisms of stress-resistance. Additionally, although it contributes to attenuated-aging phenotypes in model organisms, the specific mechanisms through which autophagy remodels cells as well as the aspects of the cellular environment that autophagy potentially changes are not known. Therefore, the purpose of this study was to examine the mitochondrial mechanisms involved in mediating the protective effects of repeated autophagy and mitophagy induction.

This was performed by investigating the specific mitochondrial changes and mechanisms involved in autophagy- and mitophagy-mediated development of stress resistance in proliferative C2C12 cells by measuring factors which facilitate cell death, as well as by testing the stress-resistance of these systems. The dependence of these changes on autophagy specifically were illustrated by performing experiments in Atg7-deficient cells. Finally, a specific mitophagy regulating protein, Bnip3, was examined for its role in mediating Parkin-independent mitophagy and the adaptive effects of autophagy induction, as preliminary observations have indicated it may be important for autophagy/mitophagy in C2C12 cells.

The hypotheses for Chapter IV were:

1. Repeated mitophagy induction causes general cellular stress resistance.

2. Repeated autophagy or mitophagy induction increases the specific stress resistance of mitochondria, and this does not occur in the absence of Atg7.

3. Repeated autophagy or mitophagy induction increases mitochondrial content and function, and this does not occur in the absence of Atg7.

4. Bnip3 is required for proper autophagy and mitophagy induced by amino acid and serum withdrawal and mitochondrial membrane depolarization, respectively, in C2C12 cells.

5. Autophagy/mitophagy-induced stress resistance development requires Bnip3.

6. Autophagy/mitophagy-induced mitochondrial functional increases require Bnip3.

Abstract

Autophagy and mitophagy are important regulators of diverse cellular functions, but relatively limited data exists regarding the effects of their exclusive induction or the specific cellular components involved. In this study, we examined the impact of previous autophagy or mitophagy induction on stress resistance development and mitochondrial function. Intermittent mitophagy, induced with CCCP, and autophagy, induced with amino acid starvation (HBSS), protected C2C12 cells from death caused by staurosporine (STS). Of the mechanisms investigated, this involved decreased caspase-9 activation. Mitochondrial stress resistance, tested with flow cytometry detection of calcein and JC-1, was specifically increased in CCCP- and HBSS-treated cells and this effect was abolished in Atg7-deficient cells. Repeated amino acid starvation also increased maximal mitochondrial oxygen consumption, while Atg7-deficient cells demonstrated severe impairments in mitochondrial respiration and did not display starvation-induced adaptations. As C2C12 cells possessed undetectable levels of Parkin protein, we also investigated the importance of Bnip3 in these findings. Although HBSS and CCCP differentially altered Bnip3 content, HBSS-induced stress resistance development and mitochondrial functional increases occurred in Bnip3-CRISPR cells. These results demonstrate the independent roles of autophagy and mitophagy in cellular remodelling, emphasizing their importance during situations of altered activity.

Introduction

Cells possess numerous mechanisms through which to resist acute stress. Existing proteins such as antioxidants absorb damaging stimuli like reactive oxygen species (ROS), post-translational modifications activate other protective proteins (Hsp's, IAPs, sirtuins) and alter stress signalling mechanisms (ERK, MAPK, Akt), and ubiquitin and molecular chaperones identify and promote degradation of damage sources (298). However, unsurvivable stressors cause cells to remove themselves by activating cell death mechanisms such as apoptosis and/or programmed necrosis (2-4).

Although these two cell death processes occur for distinct reasons and are regulated by specific and differing mechanisms, they are linked through their mutual involvement of mitochondrial dysfunction and/or signaling (2-4).

In addition to their roles in energy production and transfer, mitochondria are important sensors, resistors, and mediators of stress- and death-related signaling (2). Proper execution of these functions is so essential that mitochondrial dysfunction is generally thought to contribute to disease pathogenesis and aging (426). These abilities are facilitated through numerous mechanisms, including: 1) physiologically-regulated signal transduction by mediators such as mitochondrial anti-viral signaling (MAVS) (427), 2) intra-cellular stress indicators and effectors like ROS and mtDNA (427), 3) storage and maintenance of cellular Ca^{2+} concentrations (428), 4) release of pro-death factors such as cytochrome c, Smac, AIF, and EndoG (10,11,13,14), and 5) the extra-cellular effects of mitochondrial damage associated molecular patterns (DAMPs) (429). Unsurprisingly then, the biological status of mitochondria greatly impacts the cellular response to stressors (2). In fact, a modest elevation in mitochondrial content was shown to protect cultured L6 cells from caspase-dependent and independent cell death (388). Furthermore, the physiological relevance of mitochondrial health is commonly demonstrated by the adaptive effects of exercise training on skeletal muscle (338), a phenomenon that induces several mitochondrial adaptations.

Another important mediator of the cellular stress response is autophagy. Although autophagy primarily functions as a catabolic means of energy provision, it is sensitive to numerous stimuli and in most scenarios contributes to preventing unnecessary cell removal (36,46,49). This cyto-protective role is typically observed in experiments where cell death is prevented by inducing autophagy (157,209,210,371,372), or where the sensitivity to cell death is increased by inhibiting autophagy

(36,49,183,245,372,430-433). Autophagy's protective functions occur partly because it involves sophisticated substrate identification machinery that can selectively target damaged cellular material (36,46,49). Although microautophagy, chaperone-mediated autophagy, and chaperone-assisted selective autophagy (CASA) are known as substrate-specific responses, it is becoming increasingly apparent that degradation through macroautophagy-related mechanisms is also highly targeted. Importantly, this includes the specific degradation of mitochondria, an occurrence termed mitophagy (107). Research indicates that mitophagy targets metabolically impaired mitochondria (434,435) and those with decreased membrane potential (134), suggesting a preference for the removal of dysfunctional mitochondrial fragments/proteins (436). Biochemically, this process is primarily mediated by the proteins PINK1 and Parkin, which participate with mitochondrial fission machinery to segregate appropriate mitochondrial fragments and mark them for elimination (115,116). However, the Atg8-like autophagosome structural proteins LC3 and/or GABARAP identify a growing list of proteins including p62, NBR1, Bnip3, Nix, FUNDC1, cardiolipin, Bcl2-L-13, TAX1BP1, NDP52, optineurin, TBK1, and FKBP8 which help mark damaged cellular cargo for elimination (104,128,138,142,147,151,153,155,159,392), demonstrating significant redundancy in mitophagic cargo selection. Due to the important cellular roles mitochondria play, mitophagy is a mechanism through which autophagy influences stress resistance (2,36,46,49). Cumulatively, these specific targeting interactions suggest autophagy displays high level control, and is perhaps capable of avoiding non-discriminate degradation. In this way, mitophagy specifically has important implications regarding cellular defense and remodelling.

Therefore, autophagy may affect cell composition by degrading cellular material, such as mitochondria, in a "worst is first" manner. In fact, autophagy and mitophagy have been shown to contribute to the protective preconditioning effects of ischemia-reperfusion (IR) in the brain (244,342) and heart (343,437,438). However, the specific cellular aspects targeted by autophagy are largely unknown. We

previously demonstrated that autophagy is required for the development of stress resistance caused by repeated amino acid withdrawal. In this study, data is presented demonstrating that repeated autophagy or mitophagy induction causes resistance to specific stresses, particularly those related to mitochondrial damage, and that repeated autophagy induction increases mitochondrial functional capacity.

Results

CCCP, but not HBSS, induces mitophagy in C2C12 cells

It was previously demonstrated that CCCP administration qualitatively increased the number of mitochondria colocalized with LC3 puncta in C2C12 cells (439). To more specifically investigate this process, the autophagic and mitophagic response to 30 μM CCCP was assessed and compared to that caused by amino acid and serum withdrawal (HBSS) (Fig. 1). Immunoblotting analyses indicated that CCCP: 1) increased LC3II in whole cell fractions, 2) decreased Bnip3 in whole cell fractions, 3) decreased LC3I in cytosolic subcellular fractions, 4) increased LC3II dramatically in mitochondrial-enriched subcellular fractions, and 5) increased PINK1 in mitochondrial-enriched subcellular fractions (Fig. 1A & 1B). To determine whether CCCP affects general autophagic flux, C2C12 cells were treated with CCCP or HBSS with/without 50 μM chloroquine (Cq) for 6 hours (Fig. 1C & 1D). CCCP alone did not reduce p62 protein levels but did increase ($p<0.05$) the LC3II/I ratio compared to GM and CCCP+Cq elevated ($p<0.05$) the LC3II/I ratio above that caused by Cq alone (Fig. 1C & 1D). These results alone suggest CCCP induces the beginning biochemical features of autophagy (such as LC3 lipidation), but may not increase autophagic flux activity (degradation of target material). However, the contents of several mitochondrial proteins were 20-30% lower ($p<0.05$) in cells administered CCCP for 6 hours compared to those which remained in GM (Fig. 1E & 1F). Therefore, it appears that CCCP in fact specifically causes mitophagy in C2C12 cells, while HBSS causes autophagy that is not specific to mitochondria.

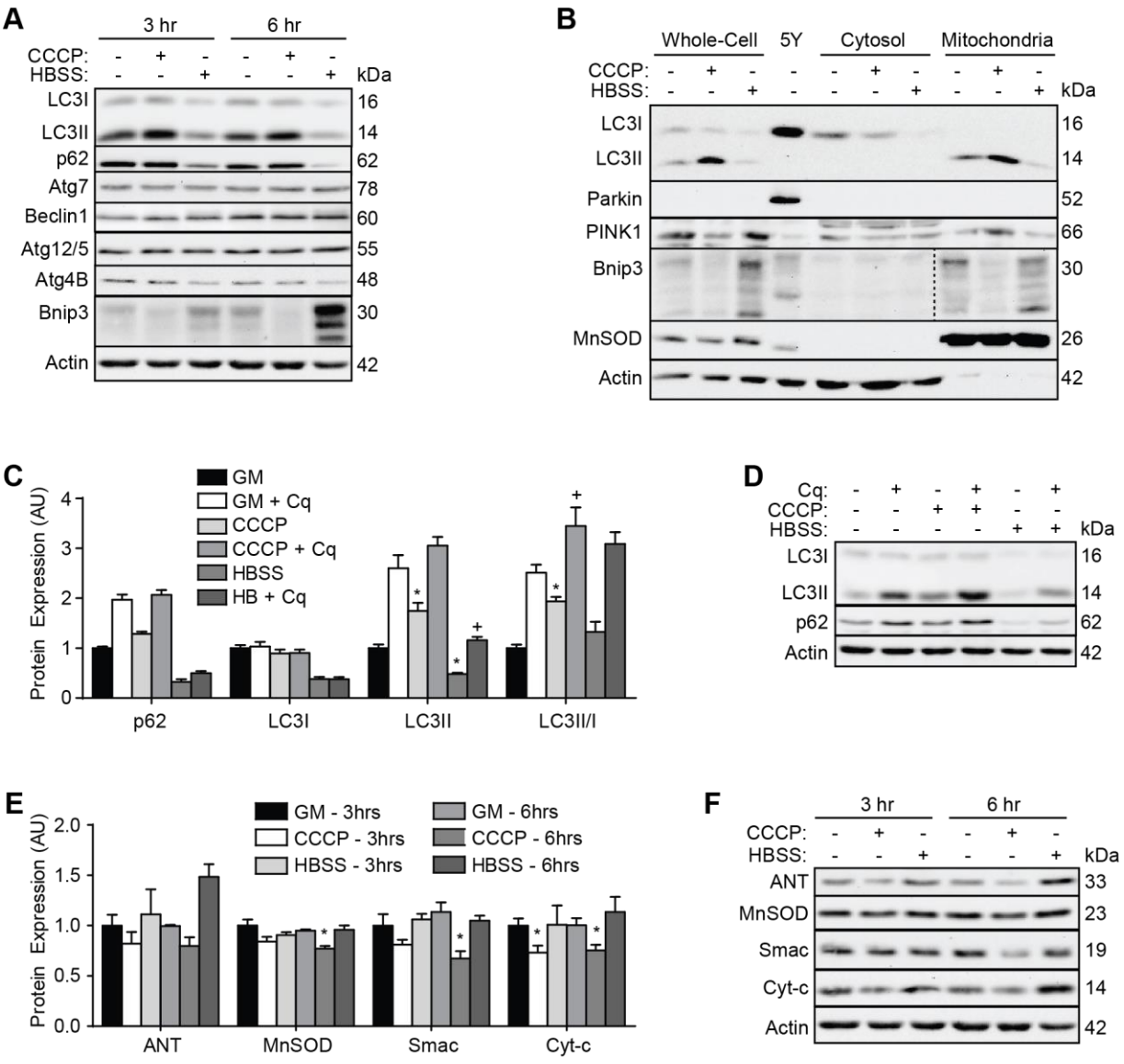

Fig. 1. CCCP, but not HBSS, Induces mitophagy in C2C12 cells. (A) Cells incubated in HBSS or 30 µM CCCP in GM for 3 or 6 hours were immunoblotted for autophagy markers. (B) Immunoblotting of autophagy markers in cells treated for 6 hours and separated into subcellular fractions; 5Y represents SH-SY5Y lysate, included as Parkin positive control. (C & D) Assessment of p62 and LC3 immunoblotting in cells treated for 6 hours with or without 50 µM Cq. (E & F) Assessment of mitochondria-specific protein contents in whole cell lysates. Asterisks (*) indicate difference ($p<0.05$) from GM and plus-signs (+) indicate difference ($p<0.05$) from GM+Cq calculated using T-tests. N=4-6.

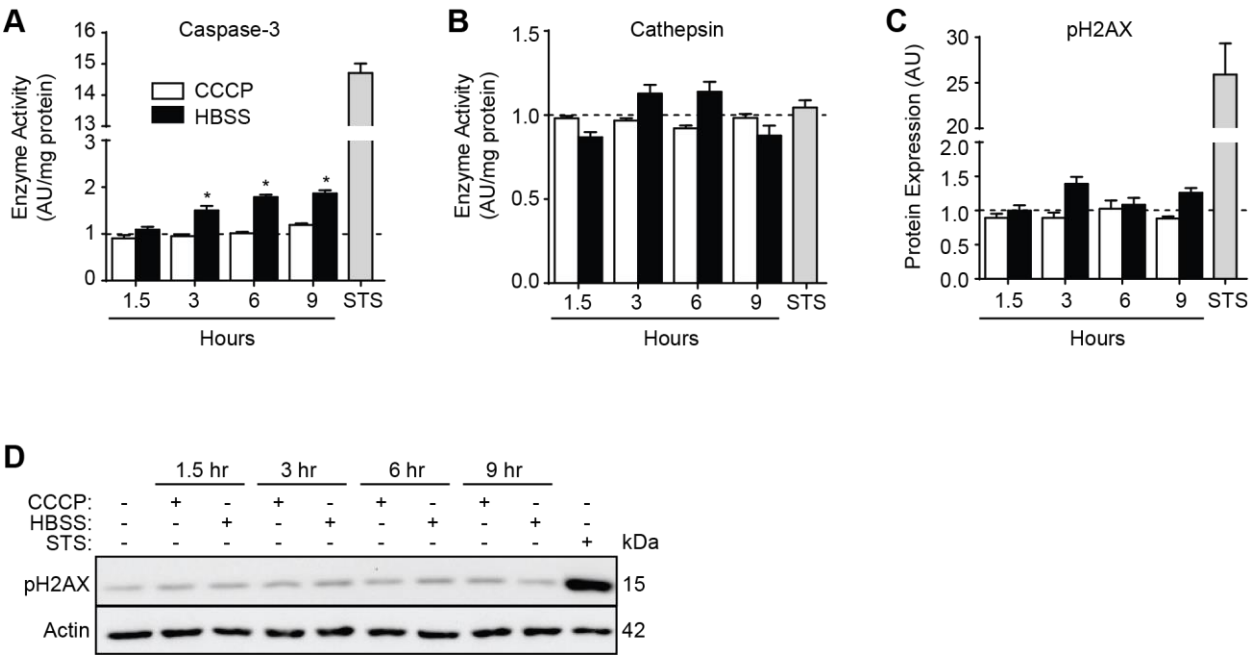

Fig. 2. Cell death signaling during mitophagy- and autophagy-inducing treatments. C2C12 cells incubated in HBSS or 30 µM CCCP in GM were assessed for caspase-3 activity (A), cathepsin activity (B), and pH2AX protein expression (C & D). Data is expressed relative to cells which remained in GM, arbitrarily assigned a value of 1.0 and represented by the dotted line. Asterisks (*) indicate significant statistical difference from GM cells ($p<0.05$), calculated using T-tests. N=3.

To examine if these autophagy/mitophagy induction modes affected cell death, C2C12 cells were incubated in HBSS or given 30 µM CCCP in GM and evaluated for caspase-3 activity and DNA damage (Fig. 2). While HBSS increased ($p<0.05$) capsase-3 activity by almost 2-fold at longer time points, this was far less than that caused by 2.0 µM STS (Fig. 2A), and this level of caspase activation did not cause DNA damage as indicated by pH2AX protein content (Fig. 2C). Additionally, CCCP did not elevate ($p>0.05$) caspase-3 activity or pH2AX expression above the levels observed in cells which remained in GM.

Recovery from CCCP and HBSS is characterized by dramatic p62 and PGC1α induction

As we were interested if removing CCCP would allow progression of autophagic flux, additional cells were incubated in HBSS or 30 µM CCCP in GM or for 6 hours, given GM, and collected 3 or 6 hours later

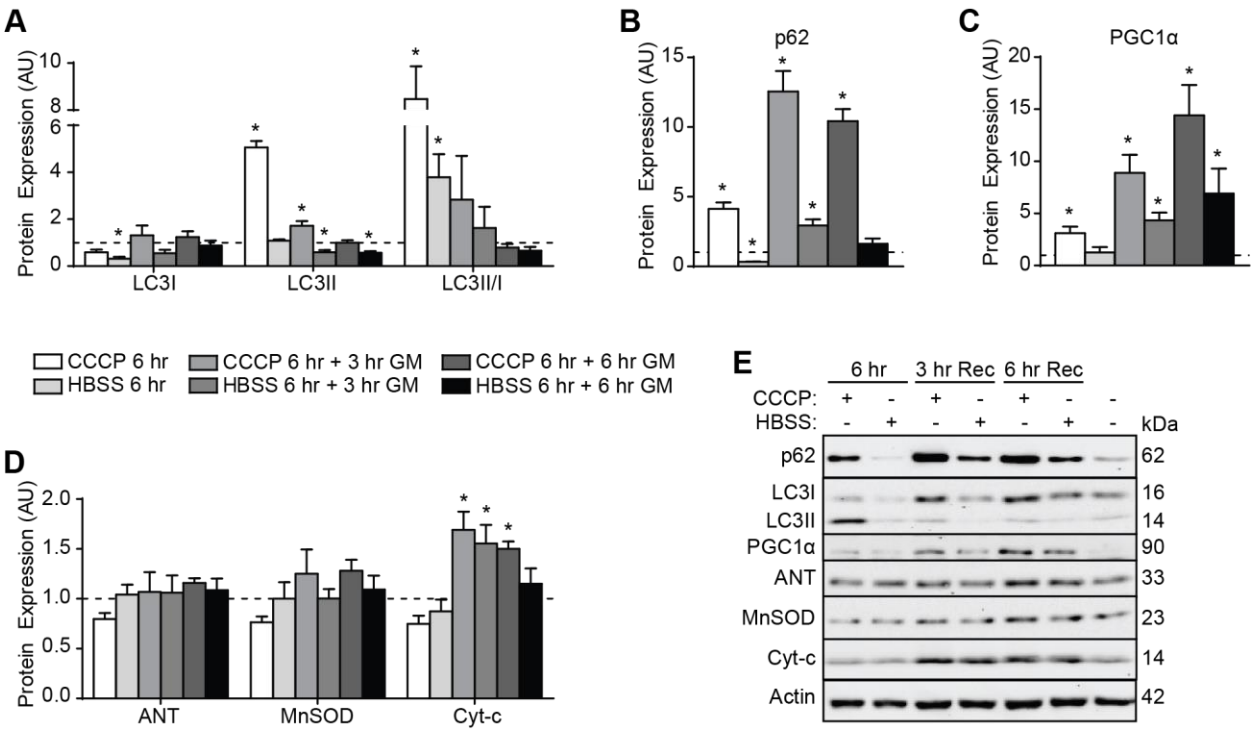

Fig. 3. Recovery from CCCP and HBSS is characterized by dramatic p62 and PGC1a induction. C2C12 cells incubated in HBSS or 30 µM CCCP in GM for 6 hours were washed in PBS and collected after spending an additional 3 or 6 hours in GM. Assessment of LC3 (A), p62 (B), PGC1α (C), and mitochondria-specific protein (D) immunoblotting. (E) Representative immunoblots. Data is expressed relative to cells which remained in GM, arbitrarily assigned a value of 1.0 and represented by the dotted line. Asterisks (*) indicate significant statistical difference from GM cells ($p<0.05$), calculated using a T-test. N=4.

(Fig. 3). After 6 hours in GM, the CCCP- and HBSS-induced changes to LC3 had recovered, as LC3I content and the LC3II/I ratio were not different ($p>0.05$) from cells which remained in GM (Fig. 3A). However, p62 protein levels were elevated ($p<0.05$) during recovery; this was particularly dramatic in CCCP-treated cells where p62 was 13-fold higher ($p<0.05$) at the 3 hour recovery time point compared to GM (Fig. 3B). CCCP and HBSS also increased ($p<0.05$) PGC1α protein levels 15- and 7-fold, respectively, at the 6 hour recovery time point (Fig. 3C). This was accompanied by 70% and 55% increased ($p<0.05$) cytochrome-c protein content in CCCP- and HBSS-treated cells, respectively, after 3 hours (Fig. 3D).

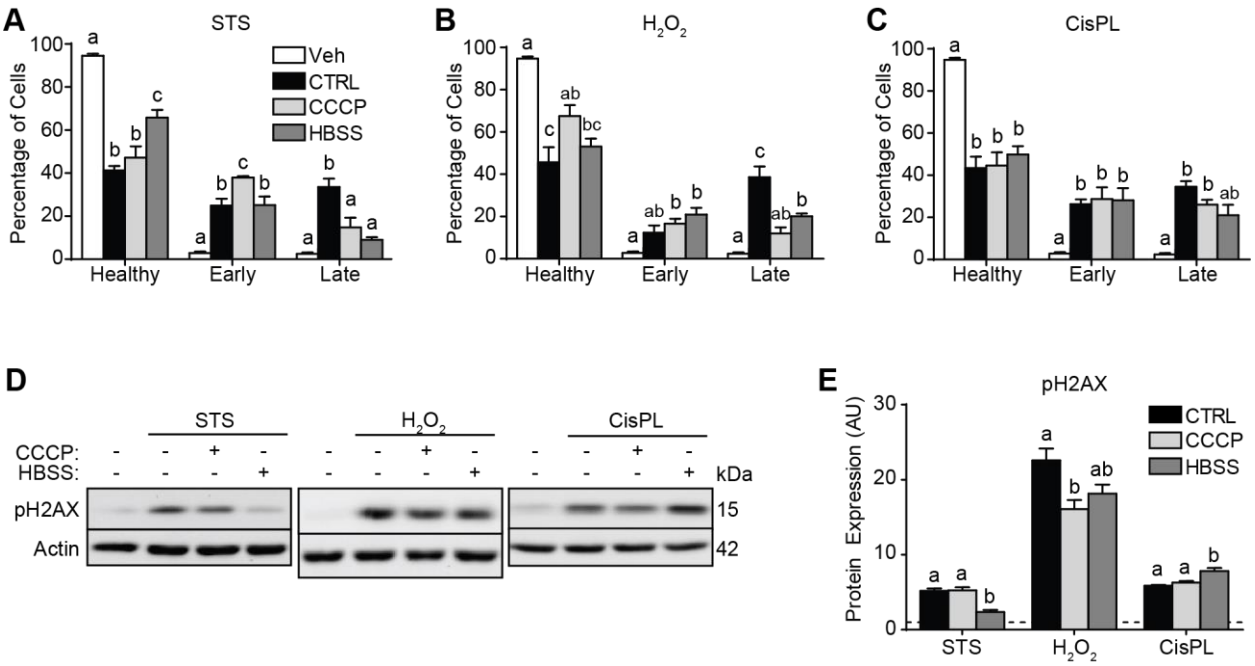

Fig. 4. Repeated CCCP affects subsequent cell death induction differently than HBSS. C2C12 cells were incubated in HBSS or 30 µM CCCP in GM for 6 hours per day for 3 consecutive days or remained in GM (CTRL), and given 0.5 µM staurosporine (STS), 2.5 mM hydrogen peroxide (H_2O_2), 25 µM cisplatin (CisPL). Cells which remained in GM and not administered a death inducing chemical are included as negative/healthy controls (vehicle, Veh). Flow cytometry assessment of annexin/PI staining was used to classify cells given STS (A), H2O2 (B), and CisPL (C) into specific cell death stages. (D & E) Similarly-treated cells were immunoblotted for pH2AX. In (E), data is expressed relative to Veh, arbitrarily assigned a value of 1.0 and represented by the dotted line. Groups were compared using 1-way ANOVAs and statistically significant differences are denoted with lowercase letters, where groups with different letters are significantly different ($p<0.05$) than each other. N=4.

Repeated CCCP affects subsequent cell death induction differently than repeated HBSS

The effect of prior CCCP or HBSS on cell death sensitivity was then tested by incubating cells in HBSS, 30 µM CCCP in GM, or GM alone (CTRL) for 6 hours per day for 3 consecutive days. 20 hours following the third treatment, cell death was induced by administering 0.5 µM staurosporine (STS) for 3 hours, 2.5 mM hydrogen peroxide (H_2O_2) for 5 hours, or 25 µM cisplatin (CisPL) for 18 hours. Cells which remained in GM and not administered a cell death inducing chemical served as negative/healthy controls, denoted

as vehicle (Veh) or depicted as dotted lines in Figures 4-6. Flow cytometry analysis of annexin/PI staining indicated that there were significantly more ($p<0.05$) healthy and less ($p<0.05$) late-apoptotic cells in HBSS-treated cells compared to CTRL (Fig. 4A). Previous CCCP administration similarly increased ($p<0.05$) the number of healthy cells and decreased ($p<0.05$) the number of late stage cells during H_2O_2 exposure (Fig. 4B). However, neither intermittent autophagy nor mitophagy affected subsequent cell death induced by CisPL (Fig 4C). pH2AX immunoblotting mirrored the annexin/PI data: intermittent HBSS treatments decreased ($p<0.05$) DNA damage caused by STS, and previous CCCP treatments decreased ($p<0.05$) DNA damage caused by H_2O_2.

Intermittent HBSS-induced protection from STS is characterized by decreased caspase activation

Additional cells were similarly incubated in HBSS or CCCP for 3 days, administered death-inducing stimuli, and analyzed for cell death related enzyme activities and protein contents (Fig. 5 & Fig. 6). HBSS treatments dramatically decreased ($p<0.05$) caspase-3 and -9 activities during STS-induced cell death compared to CTRL (Fig. 5A). These observations are supported by significantly reduced ($p<0.05$) protein levels of cleaved caspase-3 and a lower ($p<0.05$) cleaved :full-length PARP ratio in HBSS-treated cells compared to CTRL (Fig. 5D & 5G). Previous HBSS had similar but modest effects on these markers during CisPL-induced cell death (Fig. 5C, 5F & 5G). The effects of previous CCCP treatments were not as consistent, although cleaved caspase-3 protein content was lower ($p<0.05$) than CTRL during STS exposure (Fig. 5D). Interestingly, H_2O_2–mediated cell death did not involve caspase activation.

The contents of several other cell death-related proteins were also analyzed to identify potential mechanisms which mediated autophagy-induced stress resistance development (Fig. 6). Only two parameters were statistically significant: 1) previous HBSS and CCCP treatments decreased ($p<0.05$) the

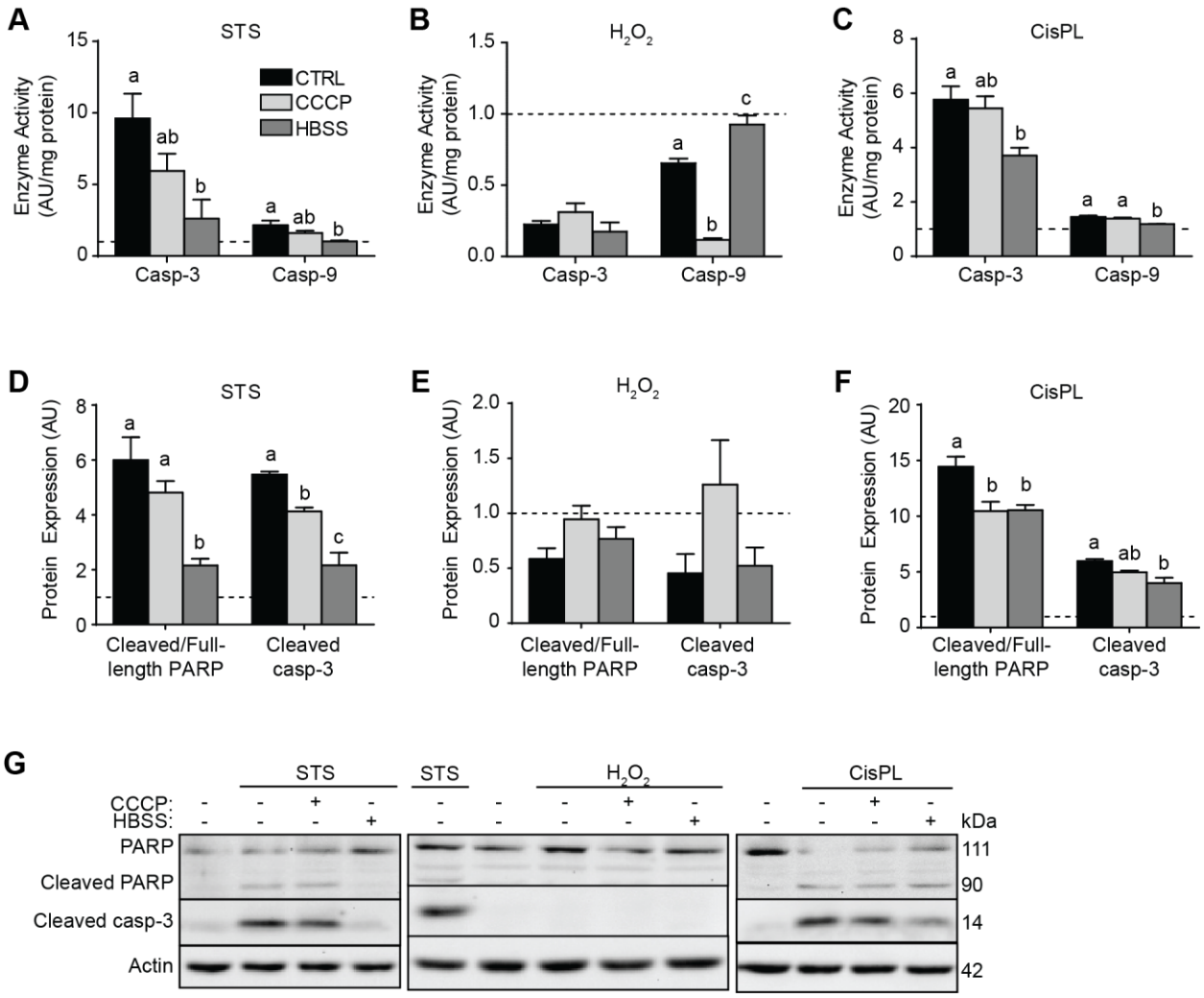

Fig. 5. Intermittent autophagy-induced protection from STS is characterized by decreased caspase activation. After repeated HBSS or CCCP treatments, cells were administered STS, H_2O_2, or CisPL. (A – C) Caspase-3 and caspase-9 activities. (D – F) Immunoblotting of PARP cleavage and cleaved caspase-3. (G) Representative immunoblots. Data is expressed relative to cells which remained in GM and not given a death inducing chemical, arbitrarily assigned a value of 1.0 and represented by the dotted line. Groups were compared using 1-way ANOVAs and statistically significant differences are denoted with lowercase letters, where groups with different letters are significantly different ($p<0.05$) than each other. N=4.

Bax:Bcl2 ratio compared to CTRL during STS-induced cell death (Fig. 6A & 6B), and 2) p53 content was lower ($p<0.05$) in HBSS-treated cells compared to CTRL during CisPL-induced cell death (Fig. 6E & 6F).

Repeated autophagy and mitophagy cause mitochondrial-specific stress resistance

We have consistently observed that previous HBSS treatments attenuate STS-induced cell death, and that this is characterized by decreased caspase-9 activity (Fig. 5A). To test mitochondria stress resistance specifically, we performed flow cytometry analyses of calcein and JC-1 fluorescence, which indicate mitochondrial permeability transition pore (mPTP) formation and mitochondrial membrane potential, respectively, after inducing calcium (Ca^{2+}) stress with the calcium ionophore A23187. Similar to previous experiments, C2C12 cells were intermittently incubated in HBSS or 30 µM CCCP or remained in GM (CTRL). Subsequently incubating cells for 30 minutes in A23187 led to progressive drops in calcein fluorescence (Fig. 7A) and the JC-1 red:green fluorescence ratio (Fig. 7B), indicating mPTP formation and membrane depolarization, respectively. Previous HBSS and CCCP treatments attenuated ($p<0.05$) the reduction in calcein fluorescence at specific A23187 concentrations compared to CTRL (Fig. 7A), suggesting increased resistance to Ca^{2+} stress. Similarly, cells given HBSS and CCCP experienced a smaller ($p<0.05$) decrease in the JC-1 red:green fluorescence ratio when incubated with 5 µM A23187 compared to CTRL (Fig. 7B). Performing a similar experiment Atg7-deficient (shAtg7) and control (SCR) cells showed that previous incubation in HB+F and CCCP decreased ($p<0.05$) the reduction in calcein fluorescence caused by 5 µM A23187 in SCR, but not shAtg7 (Fig. 7C). When presented as a change from CTRL, it is apparent that both HB+F and CCCP decreased the reduction in calcein fluorescence by 40% in SCR, and this was significantly more ($p<0.05$) than in shAtg7.

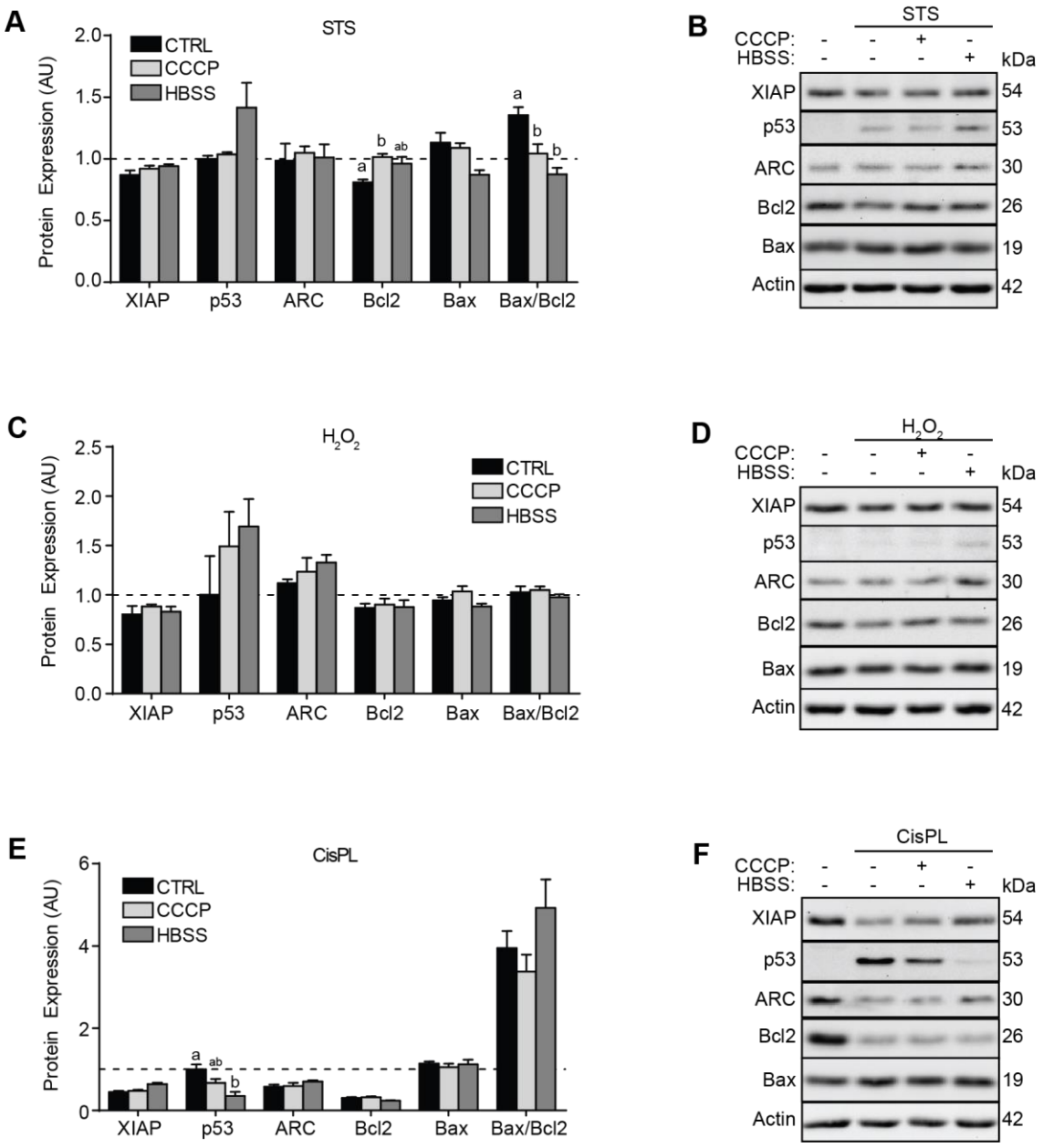

Fig. 6. Cell death signaling proteins are largely unaltered by previous repeated CCCP or HBSS. After repeated HBSS or CCCP treatments, cells were administered STS, H_2O_2, or CisPL. (A & B) Assessment of cell death related protein contents in cells administered STS. (C & D) Assessment of cell death related protein contents in cells administered H_2O_2. (E & F) Assessment of cell death related protein contents in cells administered CisPL. Data is expressed relative to negative/healthy control cells which remained in GM and were not administered a death inducing chemical, arbitrarily assigned a value of 1.0 and represented by the dotted line. Groups were compared using 1-way ANOVAs and statistically significant differences are denoted with lowercase letters, where groups with different letters are significantly different ($p<0.05$) than each other. N=4.

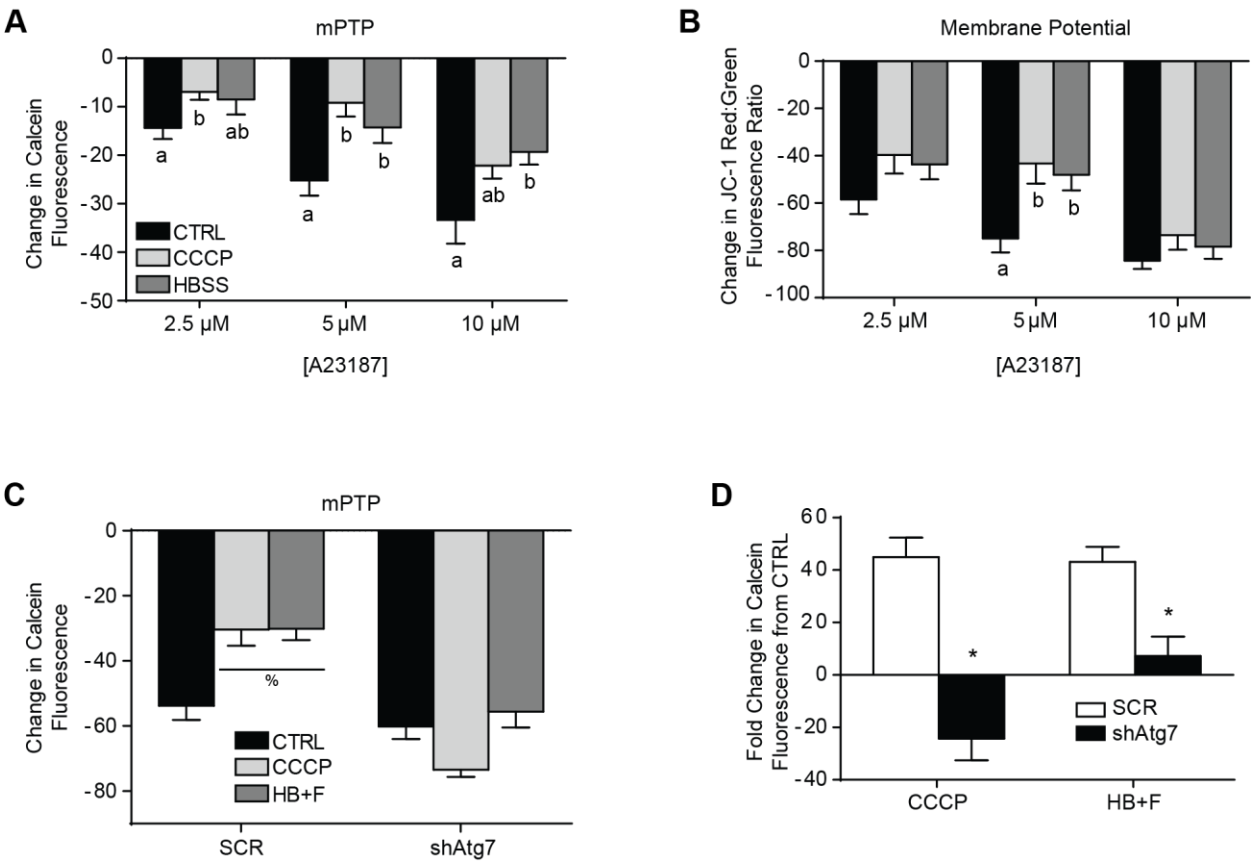

Fig. 7. Repeated autophagy and mitophagy increase mitochondrial stress resistance. (A & B) After repeated HBSS or CCCP treatments, C2C12 cells were assessed for calcium-induced mitochondrial permeability transition pore (mPTP) formation (A) or membrane depolarization (B). (C & D) Atg7-deficient (shAtg7) and control (SCR) cells were intermittently incubated in HB+F or 30 µM CCCP in GM and similarly assessed for calcium-induced mPTP formation caused by 5 µM A23187. Data in (A – C) is expressed as a change from cells which did not receive A23187. In (A & B), groups at individual A23187 concentrations were compared using 1-way ANOVAs and statistically significant differences denoted with lowercase letters, where groups with different letters are significantly different ($p<0.05$) than each other. In (C), data was compared by 2-way ANOVA: this revealed a main effect of shAtg7 compared to SCR, a main effect of HB+F compared to CTRL, and interaction effects where CCCP and HB+F are lower than CTRL in SCR (%) and CCCP is higher than CTRL in shAtg7. In (D), T-tests were used to compare between SCR and shAtg7 and asterisks (*) denote a statistically significant difference ($p<0.05$). N=4-5.

Repeated amino acid and serum withdrawal increases mitochondrial respiration and this requires Atg7

Next, to examine if mitochondrial stress resistance was associated with altered mitochondrial function, SCR and shAtg7 cells were repeatedly incubated in HB+F or 30 μM CCCP for 3 consecutive days, after which high-resolution respirometry (using the O2k by Oroboros) was used to measure several oxygen consumption metrics (Fig. 8). In general, shAtg7 displayed dramatically decreased oxygen consumption rates (OCR) in various conditions and HB+F treatments increased OCR only in SCR. Specifically, we first determined the sensitivity and maximal response to complex I-supported ADP-stimulated respiration by performing an ADP titration (Fig. 8A). Here, both Vmax and EC50 were significantly ($p<0.05$) lower in shAtg7 compared to SCR, and HB+F increased ($p<0.05$) Vmax by 28% compared to CTRL only in SCR (Fig. 8B & 8C). Maximal (at 1.0 mM ADP) complex I+II-supported OCR was similarly increased ($p<0.05$) by previous HB+F and was notably lower ($p<0.05$) in shAtg7 compared to SCR (Fig. 8D). To confirm integrity of the mitochondrial membrane during experimental preparations, cytochrome c (cyt-c) is added at the end of the protocol. While this increased OCR 5-10% in SCR, shAtg7 experienced a significantly greater ($p<0.05$) 2.5-3.5-fold increase in OCR (Fig. 8E). To determine if shAtg7 possessed altered mitochondrial content and if HB+F caused mitochondrial biogenesis in SCR, immunoblotting of mitochondria specific proteins was also performed. Although HB+F did not generally increase these in SCR, CCCP increased ($p<0.05$) MnSOD and cyt-c protein content in shAtg7 compared to CTRL (Fig. 8F & 8G).

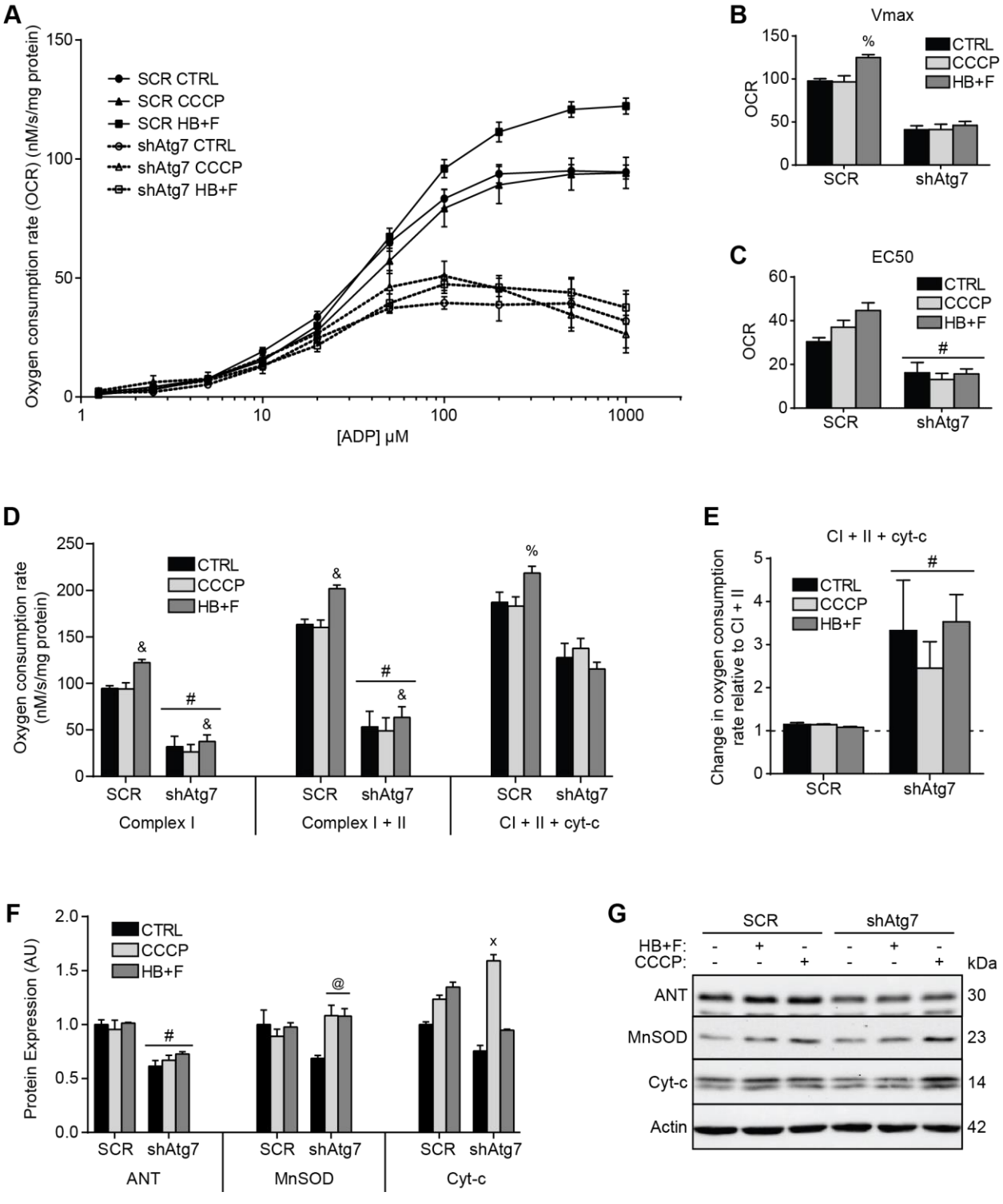

Fig. 8. Repeated amino acid and serum withdrawal increases mitochondrial respiration and this requires Atg7. SCR and shAtg7 intermittently incubated in HB+F, CCCP in GM, or GM alone (CTRL) were assessed for mitochondrial respiration kinetics. (A – C) Complex I-supported ADP-stimulated oxygen consumption rate (OCR). (A) Average of titration curves with calculation of Vmax (B) and EC50 (C) values. (D) Maximal

OCR (at 1.0 mM ADP) with complex I substrates, complex I and II substrates, and cytochrome c (cyt-c). (E) Change in OCR caused by cyt-c. (F & G) Assessment of mitochondria-specific protein contents. Groups were compared using 2-way ANOVAs: pound signs (#) denote significant ($p<0.05$) main effect differences between SCR and shAtg7, ampersands (&) indicate significant ($p<0.05$) main effect of HB+F compared to CTRL and CCCP, percentage sign (%) represents interaction effect where HB+F is different ($p<0.05$) than CTRL only in SCR, (@) denotes interaction where HB+F and CCCP are different ($p<0.05$) than CTRL only in shAtg7, and (x) represents interaction effect where CCCP is different ($p<0.05$) than CTRL only in shAtg7. N=4-5.

Role of Bnip3 in autophagy and mitophagy induction

Individual CCCP and HBSS treatments significantly decreased and increased Bnip3 protein content, respectively, in C2C12 cells (Fig. 1A). Additionally, C2C12 cells were found to possess undetectable levels of Parkin protein (Fig. 1B). Therefore, we next examined the importance of Bnip3 in HBSS-induced autophagy and CCCP-induced mitophagy as well as the stress resistant phenotype and mitochondrial functional increases caused by HBSS. CRISPR/Cas9 was used to generate C2C12 cells deficient in Bnip3; a vector containing a non-targeting scramble gRNA sequence was used to generate control cells (SCR) (Fig. 9A). SCR and Bnip3-KO were then incubated in HB+F or 30 μM CCCP and assessed for autophagy and mitophagy markers, with some allowed to recover in GM for 6 hours after a 6 hour treatment (Rec). Unlike Atg7-deficient cells, caspase-3 activity was slightly lower in Bnip3-KO during HB+F and CCCP treatments compared to SCR (Fig. 9B). No differences ($p>0.05$) were observed in p62 or LC3 protein levels between SCR and Bnip3-KO with HB+F (Fig. 9C & 9E). During CCCP administration, p62 levels were also not different ($p>0.05$) between groups, although Bnip3-KO did experience significantly increased ($p<0.05$) LC3II/I ratios (Fig. 9D & 9F). Additionally, mitochondrial protein contents were similarly decreased ($p>0.05$) between SCR and Bnip3-KO during 6 hour CCCP; ANT is quantitatively shown as a representative (Fig. 9G & 9H). However, PCG1α protein content was significantly reduced ($p<0.05$) in Bnip3-KO compared to SCR during both HB+F and CCCP recovery periods.

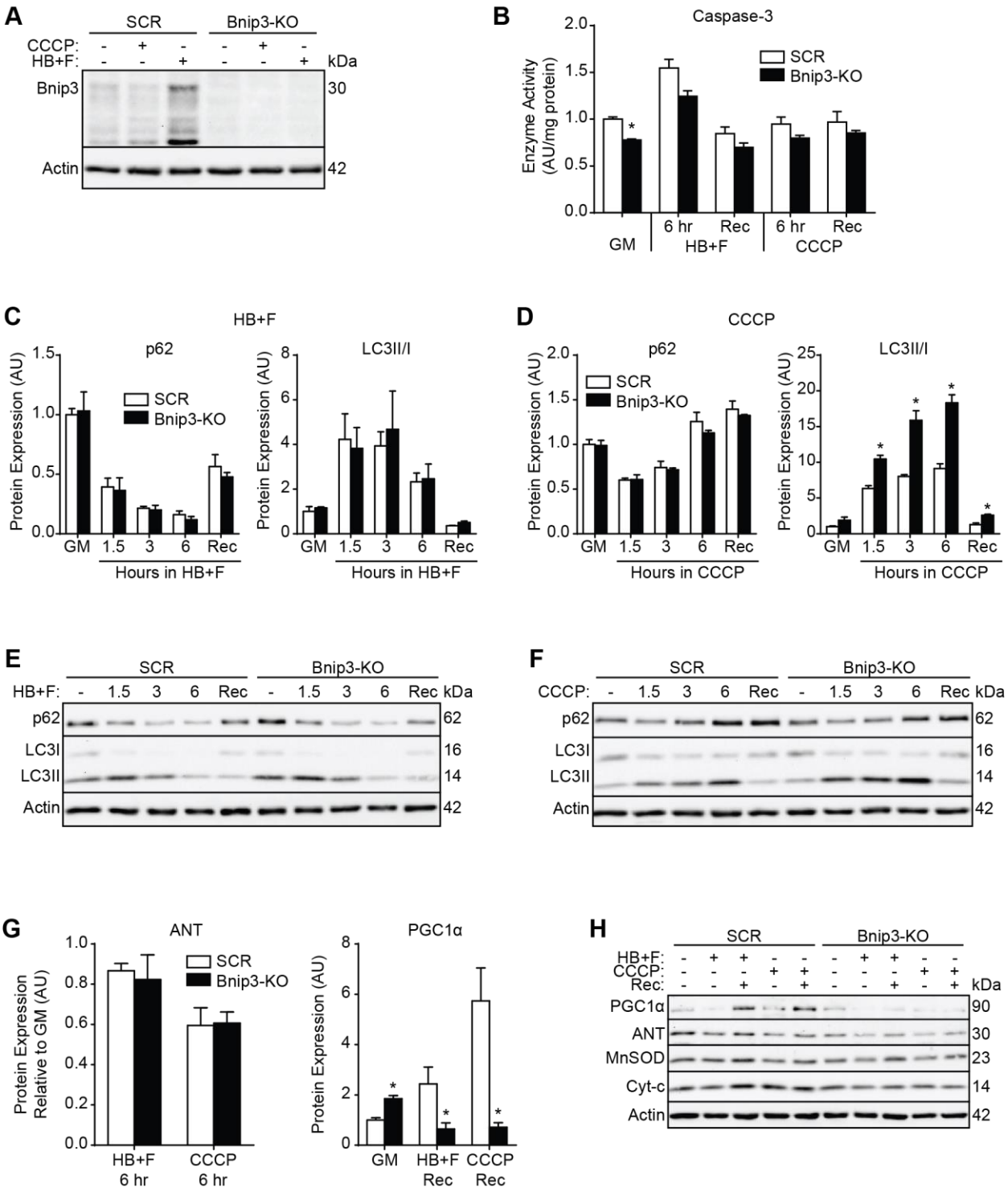

Fig. 9. Role of Bnip3 in autophagy and mitophagy induction. (A) Bnip3 protein content in control (SCR) and Bnip3-CRISPR (Bnip3-KO) C2C12 cells. Assessment of caspase-3 activity (B) and p62 and LC3 immunoblotting (C & D) in cells incubated in HB+F or CCCP. Recovery (Rec) represents cells treated for 6 hours and collected after spending 6 additional hours in GM. (E & F) Representative immunoblots. (G & H) Mitochondria-related protein content. T-tests were used to compare between SCR and Bnip3-KO and asterisks (*) denote a statistically significant difference ($p<0.05$). N=3.

Autophagy-induced protection from STS is not altered by Bnip3 deficiency

To determine if Bnip3 contributed to autophagy-induced resistance to STS-mediated cell death, SCR and Bnip3-KO were incubated in HB+F, 30 μM CCCP in GM, or GM alone (CTRL) for 6 hours per day for 3 consecutive days before being administered 0.5 μM STS as previously performed. Similar to previous findings, intermittent HB+F decreased ($p<0.05$) caspase-3 activity during subsequent STS exposure (Fig. 10A). However, this reduction was not different ($p>0.05$) between SCR and Bnip3-KO. Similarly, previous HB+F and CCCP treatments decreased ($p<0.05$) pH2AX protein contents compared to CTRL during STS-induced cell death (Fig. 10C); although this effect was not affected by Bnip3 deficiency (Fig. 10D).

Bnip3-deficient cells display decreased maximal mitochondrial respiration but previous intermittent amino acid starvation still increases oxygen consumption

Finally, we tested whether Bnip3 was required for HBSS-induced elevations in mitochondrial respiration (Fig. 8). Although maximal (at 1.0 mM ADP) complex I-supported, complex I+II-supported, and complex I+II+cyt-c-supported OCR was lower ($p<0.05$) in Bnip3-KO compared to SCR (Fig. 11A), HB+F treatments increased OCR similarly ($p>0.05$) between groups (Fig. 11B), suggested Bnip3 is not involved in this effect.

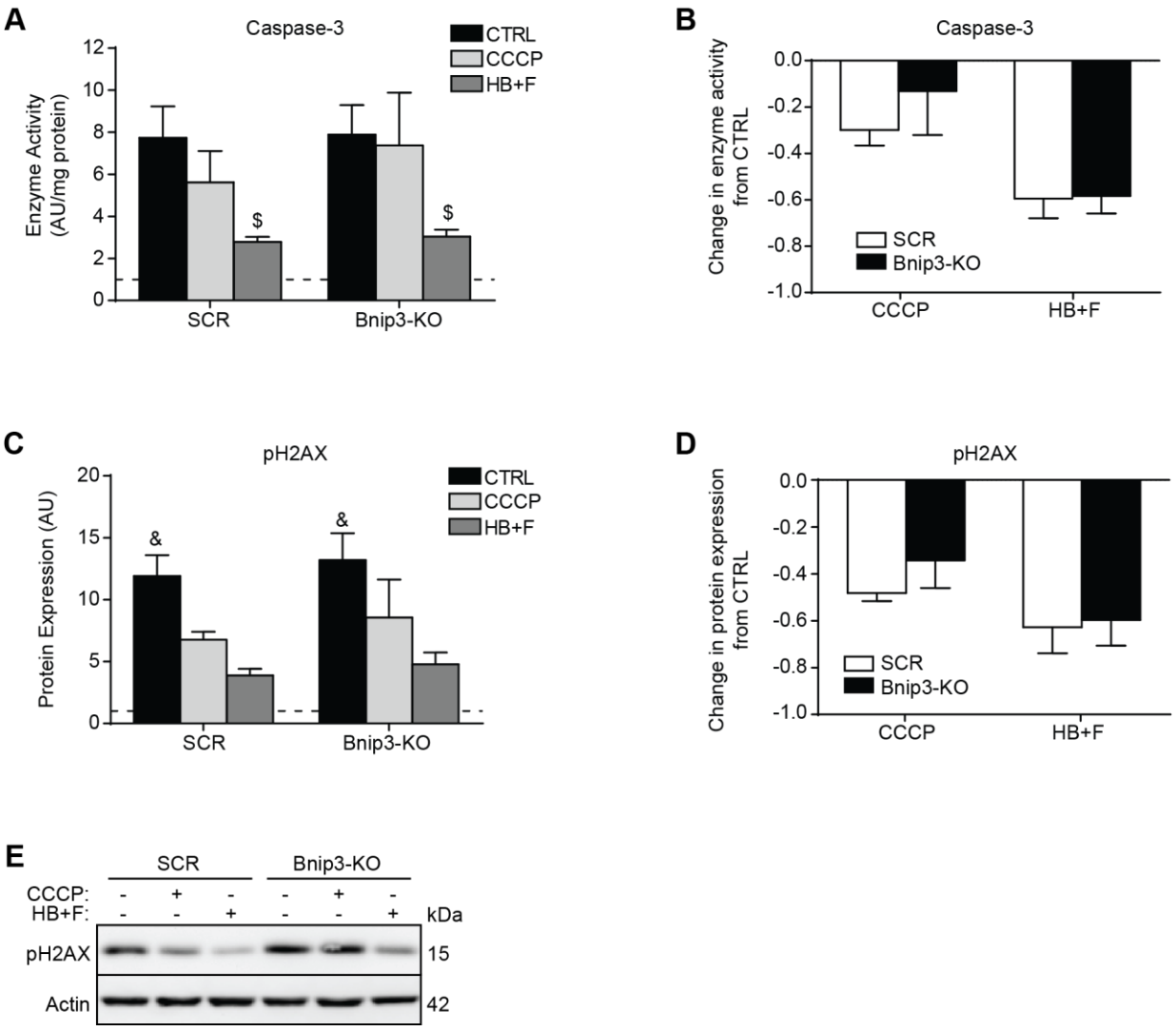

Fig. 10. Autophagy-induced protection from STS is not altered by Bnip3 deficiency. SCR and Bnip3-KO cells were intermittently incubated in HBSS or 30 µM CCCP in GM, or GM alone (CTRL) and administered STS. (A & B) Caspase-3 activity. (C - E) Assessment of pH2AX immunoblotting. In (A & C), data is expressed relative to cells which remained in GM and not administered STS, arbitrarily assigned a value of 1.0 and represented by the dotted line. In (A & C), groups were compared using 2-way ANOVAs: ampersands (&) indicate significant ($p<0.05$) main effect compared to all other groups and dollar signs ($) indicate significant ($p<0.05$) main effect of HB+F compared to CTRL. In (B & D), T-tests were used to compare between SCR and Bnip3-KO and asterisks (*) denote a statistically significant difference ($p<0.05$). N=4.

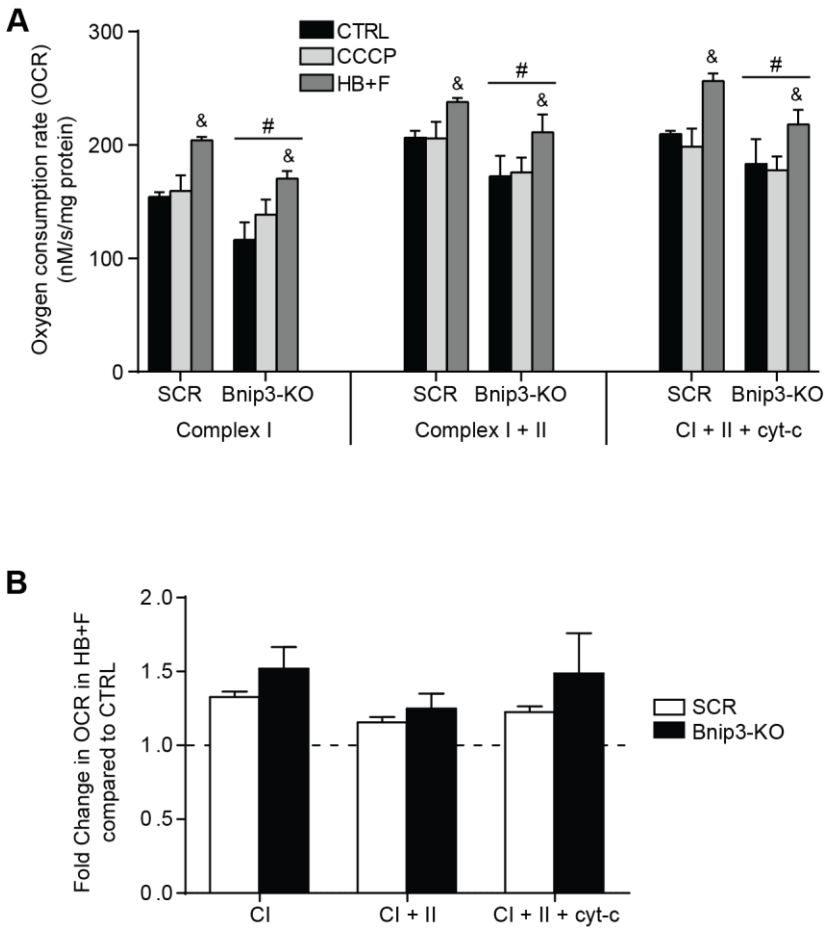

Fig. 11. Bnip3-deficient cells display decreased maximal mitochondrial respiration but previous intermittent starvation still increases oxygen consumption. (A) Maximal (at 1.0 mM ADP) oxygen consumption (OCR) with complex I substrates, complex I and II substrates, and cytochrome c (cyt-c) in cells repeatedly incubated in HBSS, CCCP, or GM alone (CTRL). (B) Change in OCR caused by repeated HB+F treatments expressed relative to CTRL. In (A), groups were compared using 2-way ANOVAs: pound signs (#) denote significant ($p<0.05$) main effect differences between SCR and shAtg7 and ampersands (&) indicate significant ($p<0.05$) main effect of HB+F compared to CTRL and CCCP. Groups in (B) were compared with T-tests but no statistically significant effects were detected. N=4.

Discussion

We previously demonstrated that prior repeated amino acid withdrawal partially protected cells from staurosporine (STS)-induced cell death and that this required Atg7. In that study, we observed less STS-induced caspase-9 activity in cells intermittently starved of amino acids compared to those grown in regular culture media. Here, we empirically tested the hypothesis that these findings were due to mitochondrial remodelling specifically by repeatedly inducing mitophagy and subsequently evaluating cellular stress resistance. While intermittent CCCP did not protect cells from STS to the same extent as HBSS, mitochondrial resistance to calcium stress was similarly increased by both treatments and was not observed in Atg7-deficient cells. However, as increased maximal mitochondrial respiration kinetics were only observed after HB+F and not CCCP treatments, this further suggests the effects of amino acid starvation are phenotypically separate from and may be unrelated to mitochondrial autophagy.

Notably, we were interested in examining the mitophagy-specific effects of our previous experiments involving intermittent amino acid starvation by conducting additional experiments with CCCP. While CCCP-induced mitochondrial fragmentation and overlap of mitoDsRed with LC3 has been previously observed in C2C12 cells (439), we expand on this finding by demonstrating CCCP-induced conversion of LC3I to LC3II, enrichment of LC3II in mitochondrial subcellular fractions, and 20-25% decrease in mitochondria-specific protein contents (Fig. 1). However, similar mitophagy-specific biochemical changes were not observed with amino acid starvation (HBSS), suggesting this does not actually induce mitophagy in C2C12 cells. Previously, HBSS reduced mitochondria-specific protein contents in MEFs (440) and increased mitoDsRed and LC3-GFP overlap in HeLa cells (441), thereby implying mitophagy induction. However, others have shown that HBSS does not deplete mitochondria-specific proteins in MEFs (442) or cause overlap of mitochondrial structures with LC3 in rat kidney cells (67). Furthermore, engulfment of mitochondria into autophagosomes did not occur with various starvation modes but did

with typical mitophagy activators (67), HBSS-induced overlap of mitoDsRed and LC3-GFP was less than that caused by rotenone (441), and HBSS incubation for 5 hours reduced mitochondria-specific protein contents only in cells incapable of mitochondrial fusion (233). In fact, several studies have demonstrated that various cell types hyperfuse their mitochondria upon starvation (including HBSS/amino acid withdrawal) theoretically to preserve mitochondria mass, energy production and therefore survival (233,441,442). Here, we do not observe induction of mitophagy-specific cellular signaling and resultant mitochondria-specific protein depletion with amino acid starvation using HBSS in C2C12 cells. Interestingly, HeLa cells do not express Parkin, and this finding was initially exploited to determine its relevance to the molecular regulation of mitophagy (116,117,119,127,132,241). In these experiments, CCCP administration depleted most Parkin-positive cells of mitochondria in 48 hours (115). Therefore, the specific expression pattern of autophagy- and mitophagy-related genes and receptor proteins potentially explain the diverse mitophagic response to starvation stimuli. Interestingly, we make the observation that C2C12 cells do not express detectable levels of Parkin protein and that neither CCCP administration, HBSS incubation, nor myogenic differentiation of these cells induces Parkin expression (Fig. 1 & Appendix B Fig. 6). However, one previous study has shown Parkin in differentiated C2C12 cells with stable Hsp72 knockdown (443). Despite this, all other myoblast cell lines we investigated including primary mouse, primary human, and L6 immortalized rat cells possessed low Parkin protein levels in proliferative cells and drastically increased expression during differentiation (Appendix B Fig. 6). As we made the additional novel observation that CCCP administration dramatically reduced while HBSS incubation dramatically increased cellular Bnip3 protein levels (Fig. 1), we also wanted to exploit C2C12's lack of Parkin to investigate the role of Bnip3 in autophagy- and mitophagy-induced cellular remodelling.

Bnip3 is a mitochondrial BH3-containing protein originally described to promote apoptotic cell death by interacting with Bcl2 (444,445). Although not appearing to utilize its BH3 domain for its pro-death functions (446,447), cells overexpressing Bnip3 were also initially characterized to induce mitochondrial autophagy (446). Current understanding indicates Bnip3 regulates autophagy by altering Bcl2-Beclin1 interaction and by binding to LC3 thereby targeting mitochondria for mitophagy (142,145,146,214). As CCCP administration drastically reduced cellular Bnip3 protein levels, we hypothesized that Bnip3 regulates depolarization-induced mitophagy in C2C12 cells given their lack of Parkin and that its reduction represented mitochondrial removal. However, despite observing increased CCCP-induced LC3II formation in Bnip3-CRISPR cells compared to controls, there was no difference in mitochondria-specific protein depletion. This suggests that Bnip3 deficient cells could adapt to maintain functional mitochondria removal during depolarization. Interestingly, one feature of CCCP administration that was affected by Bnip3 deficiency was PGC1α induction. While C2C12 (Fig. 3) and SCR-CRISPR (Fig. 9) cells dramatically increased PGC1α protein levels during CCCP treatment recovery periods, this did not occur in Bnip3-CRISPR cells suggesting it is required for this response. In addition to CCCP-induced Bnip3 depletion, HBSS treatments significantly increased cellular Bnip3 protein content (Fig. 1). Interestingly, Bnip3 was identified in an RNA microarray as a target that was significantly increased in the liver of fasted mice (448), a finding robustly demonstrated at the protein level (449). Although one study has demonstrated autophagy-dependent Bnip3 degradation caused by amino acid starvation (450). Nonetheless, its deficiency here did not affect LC3 conversion or p62 degradation during amino acid withdrawal in C2C12 cells in this study, suggesting it does not affect autophagic flux in this scenario (Fig. 9). Furthermore, HB+F-induced resistance to STS was similarly developed in SCR and Bnip3-CRISPR cells, also indicating that Bnip3 is not involved with this cellular remodelling effect. This is in contrast to Atg7, which we previously demonstrated was required for intermittent amino acid starvation to cause resistance to STS-induced cell death (Bloemberg and Quadrilatero, unpublished). Furthermore, although

Bnip3 has been shown to promote cell death cause by several stressors, we did not detect an independent effect of Bnip3 expression on STS-induced caspase-3 activity and DNA damage, despite observing Bnip3 depletion in STS-treated cells (Appendix B Fig. 1). This also suggests the involvement of an unidentified mechanism. Lastly, Bnip3 deficiency reduced maximal cellular oxygen consumption in various conditions, although it did not affect HB+F-induced elevation in mitochondrial respiration (Fig. 11). Previously, massive Bnip3 overexpression reduced maximal uncoupled cellular oxygen consumption in cultured cells, proposed to be due to degradation of specific mitochondrial proteins involved in oxidative phosphorylation (142,451). Additionally, cells from Bnip3-knockout mice have demonstrated increased maximal uncoupled cellular oxygen use in basal conditions and attenuated hypoxia-(452) and doxorubicin-(451) induced mitochondrial bioenergetic dysfunction. These results suggest a negative impact of Bnip3 on mitochondrial function. However, others have hypothesized that Bnip3 is required to ensure appropriate mitochondrial removal during stress that prevents accumulation of dysfunctional, but still oxygen-using, mitochondria (449). Regardless of Bnip3's involvement, we demonstrate here that repeated autophagy induction increased ADP-stimulated mitochondrial respiration.

Intriguingly, repeated incubation of C2C12 cells in amino acid-free media increased maximal ADP-stimulated cellular oxygen consumption (OCR) when supplied with electron transport chain (ETC) complex-I (pyruvate, malate, glutamate) and complex-II (succinate) substrates (Fig. 8). Furthermore, not only did Atg7-deficient cells display significantly reduced complex-I and complex-II supported OCR, intermittent amino acid starvation did not increase OCR in these cells. Additionally, while adding cytochrome c at the end of the respiration protocol caused a 5-10% increase in OCR in SCR cells, it remarkably elevated OCR in shAtg7 cells by several fold. These findings indicate dramatic mitochondrial functional impairment with Atg7 deficiency, potentially involving compromised mitochondrial permeability and membrane stability, as well as an inability to adapt to autophagy-inducing stimuli.

Interestingly, despite observing relatively larger increases in PGC1α protein levels with CCCP compared to HBSS, repeated CCCP treatments did not affect maximal mitochondrial respiration or sensitivity to ADP-stimulated OCR in SCR or Atg7 deficient cells. This was found despite detecting CCCP-induced elevations in mitochondria-specific protein contents in shAtg7. Cumulatively, these results suggest that damaged and/or dysfunctional mitochondria accumulate in the absence of autophagy and that despite being able to induce mitochondrial biogenesis, mitochondrial functional benefits are not observed without functional autophagy. It is well-known that Atg7-deficiency causes mitochondrial dysfunction in yeast (453) and alters mitochondrial morphology in mouse cardiomyocytes and hepatocytes (50,454). Furthermore, autophagy deficiency also leads to mitochondrial accumulation (384,455-457) while simultaneously decreasing maximal mitochondrial respiration kinetics and OCR in various cell types (458,459). Therefore, our findings support a role for autophagy providing important contributions to maintaining mitochondrial homeostasis. Strangely, these collective results indicate a disconnect between PGC1α and mitochondrial respiration: 1) both HBSS/HB+F and CCCP increased PGC1α, 2) only HBSS/HB+F elevated maximal OCR, 3) PGC1α did not increase with HB+F or CCCP in Bnip3-KO, 4) but Bnip3-KO cells still saw HB+F-induced elevations in OCR. Ultimately, these observations raise the question of why mitochondrial functional changes were not induced by CCCP. Possibly, although 30 μM CCCP induces mitophagy, this may represent too stressful of a condition to be appropriately adapted to in this timeframe, as we typically use CCCP during mitochondrial respirometry protocols to measure maximal uncoupled respiration at only 1-2.5 μM (Bradley et al, unpublished). Therefore, despite observing CCCP-induced PGC1α expression, this may not have affected expression of downstream effectors or mitochondrially-encoded proteins. Notably, constant amino acid starvation for 72 hours was previously shown to elevate OCR in HEK cells while potently increasing mitochondrial protein synthesis without affect mitochondrial content in general (460). Caloric restriction has also been shown to induce PGC1α, Sirt1, eNOS, and select mitochondrial markers in mice *in vivo* (461,462). Therefore, we suggest

that autophagy-dependent recycling of cellular material and promotion of bioenergetically favourable mitochondrial adaptations explain the changes to mitochondrial function observed here.

One important finding common to CCCP and amino acid starvation treatments was the development of autophagy-dependent mitochondria-specific stress resistance. Although this hypothesis is often made to explain the potential longevity-causing effects of various interventions that *involve* autophagy (311,463), explicit demonstration of this occurring is rare. We demonstrate here that not only does intermittent amino acid starvation protect from calcium-induced mitochondrial membrane depolarization and permeability pore formation, but this effect was eliminated by Atg7 deficiency. This result suggests that autophagic degradation specifically is responsible for the HBSS/HB+F- and CCCP-induced development of mitochondrial stress resistance. Therefore, these data represent important novel findings that substantiate autophagy's inducible remodelling effects, specifically that of mitochondria. Furthermore, as other markers related to cell death execution were generally unaltered by repetitive autophagy and mitophagy induction (except perhaps Bcl2, Fig. 6A & 6B), this implicates mitochondria as central mediators, effectors, and targets of autophagy-induced cellular remodelling. Notably, and in agreement with our previous experiments, intermittent amino acid starvation protected from STS-, but not H_2O_2- or CisPL-induced cell death, indicating the impact of these mitochondrial adaptations are context dependent. Although the physiological relevance of these findings is unknown, their observation warrants further examination into the impact of autophagy induction on cellular function and tissue health.

This study complements our previous investigation into autophagy-induced stress resistance by demonstrating specific involvement of mitochondrial adaptations. We show that mitochondrial stress resistance and maximal oxygen consumption are increased following intermittent amino acid starvation,

and that these adaptations require Atg7. Additionally, despite C2C12 cells' lack of Parkin, Bnip3 also appeared unnecessary for autophagy-induced changes to occur. These findings provide insight into autophagy's role as an inducible mechanism of cellular remodelling and have important implications regarding the interaction between autophagy, mitochondria biology, longevity, and aging.

Materials and Methods

Cell culture

C2C12 mouse skeletal myoblasts were cultured in growth media (GM) consisting of low-glucose Dulbecco's Modified Eagles Medium (DMEM; Hyclone, ThermoFisher) containing 10% fetal bovine serum (FBS; ThermoFisher) and 1% penicillin/streptomycin (ThermoFisher) on polystyrene culture dishes (BD Biosciences), as previously performed (369). Cells were appropriately sub-cultured using trypsin (0.25% solution with EDTA, ThermoFisher) to ensure all appropriate treatments and analyses were performed before cells reached confluence to avoid the potential side-effects of spontaneous differentiation. Cells were collected for subsequent experimental analyses via trypsinization and centrifuged at 1000g.

Materials

Cells were treated as indicated with various chemicals/solutions to induce or measure cell stress. These include: Hank's Balanced Salt Solution (HBSS; Gibco formulation: 140mg/L $CaCl_2$, 100mg/L $MgCl_2$-$6H_2O$, 100mg/L $MgSO_4$-7H2O, 400mg/L KCl, 60mg/L KH_2PO_4, 350mg/L $NaHCO_3$, 8.0g/L NaCl, 48mg/L Na_2HPO_4, 1.0g/L D-glucose, with 1% penicillin/streptomycin), HB+F (HBSS with 1% FBS and 1% penicillin/streptomycin), chloroquine (Cq, 50 µM; Sigma-Aldrich C6628), staurosporine (STS, 0.5 or 2.0 µM; Alexis Biochemicals 380-014-C100), cisplatin (CisPL, 25 µM; Enzo Life Sciences 400-40-M250),

hydrogen peroxide (H_2O_2, 2.5 mM; Sigma Aldrich), carbonyl cyanide 3-chlorophenylhydrazone (CCCP, 30 µM; Sigma-Aldrich C2759), and the calcium ionophore A23187 (5, 10, or 15 µM; BioVision 1501).

Bnip3 CRISPR Vector

CRISPR/Cas9 vectors targeting mouse Bnip3 were constructed as follows. The region immediately upstream of the transcription start site was searched for candidate guide RNA (gRNA) targets using several available online tools including: Zhang Lab, MIT (http://crispr.mit.edu/), CCTop (http://crispr.cos.uni-heidelberg.de/), and Off-Spotter (https://cm.jefferson.edu/Off-Spotter/). From these, two common gRNA sequences were identified (PAM in brackets): First: 5'GAGCCACCATGTCGCAGAGC(GGG), and Second: 5'GGAGGAGAACCTGCAGGGTG(AGG). The scramble sequence used in Origene CRISPR products was used as a control: 5'GCACTACCAGAGCTAACTCA. Corresponding oligonucleotides were constructed (Sigma Aldrich) to allow cloning into the CRISPR/Cas9 vector pSpCas9(BB)-2A-Puro (PX459) V2.0 (Addgene #62988), which uses a single gRNA. Correct gRNA cloning was confirmed by sequencing constructed vectors (The Center for Applied Genomics, Hospital for Sick Kids, Toronto, Ontario, Canada).

Transfections and Gene Knockdown

C2C12 cells were transfected using Lipofectamine 2000 (Life Technologies), optimized according to the manufacturer's instructions, as previously performed (183,369). Briefly, appropriate vector DNA and Lipofectamine was diluted in 100 µL Opti-MEM (Gibco) at a ratio of 1µg: 3µL, and incubated for 5 min at room temperature. This mixture was added to 50-60% confluent cells with media containing 5% FBS in Opti-MEM and incubated for 6 hours, after which cells were washed with PBS and regular growth media was added.

For generating C2C12 cells with stable knockdown of Atg7, cells grown in 12-well plates were transfected with vectors encoding either an shRNA against Atg7 (Origene TG504956) or a scramble control sequence (Origene TR30013) using Lipofectamine 2000 (ThermoFisher) as previously performed (183). 24 hours later, cells were transferred to 10 cm culture plates and those with stable incorporation of each vector were selected by growing cells in GM with 2 μg/mL puromycin (Sigma Aldrich). Surviving clones were individually isolated and assessed for Atg7 protein expression using immunoblotting.

For generating Bnip3 knockout C2C12s, cells grown in 12-well plates were transfected either with the aforementioned Bnip3 CRISPR or scramble control vector. 24 hours later, cells were transferred to 10 cm culture plates and those with incorporation of each vector were selected by growing cells in GM with 2 μg/mL puromycin (Sigma Aldrich). Surviving clones were individually isolated and assessed for Bnip3 protein expression using immunoblotting.

Subcellular Fractionation

After collection via trypsinization, cells were incubated in digitonin buffer (PBS with 250 mM sucrose, 80 mM KCl, and 50 μg/mL digitonin, Sigma Aldrich D141) for 5 min on ice. Cells were centrifuged at 1000g for 10 min, the supernatant was collected and centrifuged at 16,000g for 10 minutes to pellet any mitochondrial contamination, and the supernatant from this spin kept as the cytosolic-enriched fraction. The pellet (P1) remaining from the 1000g spin was suspended in PBS, centrifuged at 1000g for 5 min, the pellet suspended in lysis buffer (LB, pH 7.4; 20mM HEPES, 10mM NaCl, 1.5mM $MgCl_2$, 1 mM DTT, 20% glycerol, and 0.1% Triton-X100), and allowed to sit on ice for 5 min. This was then centrifuged at 1000g for 5 min, resulting in a pellet (P2) containing nuclei, and a supernatant (S2) containing mitochondria. S2 was centrifuged at 1000g for 10 min to pellet nuclear contamination, with the resulting supernatant kept as the mitochondrial-enriched fraction. The P2 pellet was suspended in LB, centrifuged at 1000g for

10 min, the pellet again suspended in LB, sonicated for 12 seconds on ice, and kept as the nuclear-enriched fraction.

Immunoblotting

Immunoblotting was performed as previously described (357,369). Whole-cell lysates were generated by adding ice-cold lysis buffer with protease inhibitors (Complete Cocktail; Roche) to cell pellets followed by sonication for 12 seconds. Protein content was measured using the BCA protein assay method. Briefly, equal amounts of protein were loaded into and separated using 10-12% SDS-PAGE, transferred onto PVDF membranes (Bio-Rad Laboratories), and blocked for 1 hr at room temperature with 5% non-fat dry milk in TBS-T. Membranes were then probed with primary antibodies against: ANT (sc-9299, 1:100), Bcl2 (sc-7382, 1:200), Bax (sc-493, 1:1000), cytochrome c (sc-13156, 1:2000), parkin (sc-32282, 1:500), PARP (sc-7150, 1:200), PGC1 (sc-13067, 1:200), PINK1 (sc-33796, 1:500), p53 (sc-6243, 1:500), phosphorylated histone H2AX (pH2AX, sc-101696, 1:1000; Santa Cruz), Atg7 (8558, 1:1000), Atg4B (5299, 1:1000), Atg12/5 (4180, 1:1000), Beclin1 (3738, 1:1000), LC3 (2775, 1:1000), MnSOD (SOD-110, 1:4000), Smac (ADI-905-244, 1:2000), XIAP (ADI-AAM-050, 1:1000; Enzo Life Sciences), actin (A-2066, 1:2000), Bnip3 (B7931, 1:1000), cleaved caspase-3 (C8487, 1:1000; Sigma Aldrich), p62 (PM045, 1:2000; MBL) overnight at 4^{o}C. Membranes were then incubated with the appropriate horseradish peroxidase- (HRP) conjugated secondary antibody (anti-rabbit: sc-2004, anti-mouse: sc-2005, anti-goat: sc-2020; Santa Cruz), and bands visualized using ECL immunoblotting substrates (BioVision) or Clarity ECL substrates (Bio-Rad) and the ChemiGenius 2 Bio-Imaging System (Syngene). The approximate molecular weight for each protein was estimated using Precision Plus Protein WesternC Standards and Precision Protein Strep-Tactin HRP Conjugate (Bio-Rad Laboratories).

Proteolytic Enzyme Activity

Enzymatic activity of caspases-3, and -9 was determined using the substrates Ac-DEVD-AFC and Ac-LEHD-AMC (Enzo Life Sciences), respectively, as previously performed (357,369). Cell lysates were prepared using lysis buffer without addition of protease inhibitors and incubated in duplicate with 20 µM of the appropriate fluorogenic substrate. Caspase activity measurements were performed in an assay buffer of 20 mM HEPES, 10 mM DTT, and 10% glycerol.

Lysosomal enzyme activity was measured using the substrate z-FR-AFC (Enzo Life Sciences), generally considered to indicate the activities of cathepsins L and B (357,369). Cell lysates were prepared similar to caspase assays and analyzed in duplicate with 25 µM of z-FR-AFC in a buffer containing 50 mM sodium acetate, 8 mM DTT, 4 mM EDTA, and 1 mM Pefabloc at pH 5.0. For all activities, fluorescence was measured at 30^{o}C using a Synergy H1 microplate reader (BioTek) with excitation and emission wavelengths of 360 nm and 440 nm for AMC substrates, and 400 nm and 505 nm for AFC substrates, respectively. All enzyme activities are presented normalized to total protein content measured using BCA and expressed as fluorescence intensity in arbitrary units (AU) per milligram protein.

Flow Cytometry

Mitochondrial Measurements

Cells were collected as described above and suspended in HBSS. Mitochondrial membrane potential and mitochondrial permeability transition pore formation were measured using JC-1 and calcein, respectively, as previously performed (369). Mitochondrial membrane depolarization can be monitored by changes in the JC-1 red:green fluorescence ratio, where a decreased ratio is indicative of decreased mitochondrial membrane potential. After removing from culture, cells were incubated with 2 µM JC-1 in 100 µL HBSS for 15 min at 37 °C, washed by centrifugation, and suspended in HBSS. Mitochondrial

permeability transition pore (mPTP) formation occurs during mitochondrial-mediated apoptosis prior to mitochondrial apoptotic protein release. The fluorescent dye calcein AM accumulates in intact mitochondria, but is quenched by cobalt if the mitochondrial membrane becomes permeable to cobalt. Thus a decrease in calcein fluorescence indicates mPTP formation. Briefly, cells were incubated with 1 µM calcein AM and 1 mM $CoCl_2$ in 100 µL HBSS for 15 min at 37°C, washed by centrifugation, and resuspended in 500 µl HBSS. Mitochondria-specific resistance to calcium stress was tested by concomitantly incubating cells with 2.5, 5, or 10 µM of the calcium ionophore A23187 along with JC-1/calcein.

Cell Death

In cell culture experiments, Annexin-V/PI staining was performed to assess the degree and type of cell death occurring after various stressors (388). After treatment, cells were removed from culture dishes and suspended in Annexin Binding Buffer (10 mM HEPES/NaOH, 150 mM NaCl, 1.8 mM $CaCl_2$, pH 7.4) and incubated with 1 µL of Annexin V-FITC (BioLegend, 640906) and 1 µL of 500 µg/mL propidium iodide (PI, Sigma Aldrich P-4170). Cells were incubated for 20 min at room temperature, after which they were washed and suspended in HBSS. Cells negative for both annexin and PI were classified as healthy, those positive for annexin and negative for PI were considered to be in early stages of cell death, and those positive for both annexin and PI were considered to be in late stages of cell death. All flow cytometry analyses were performed on a BD FACSCalibur flow cytometer equipped with Cell Quest Pro software (BD Bioscience).

Mitochondrial Respirometry

Analyses of C2C12 mitochondrial bioenergetics were performed using high resolution respirometry measurement of oxygen consumption (O2K, Oroboros Instruments). After collection via trypsinization,

cells were centrifuged at 100g and permeabilized using digitonin buffer (PBS with 250 mM sucrose, 80 mM KCl, and 50 µg/mL digitonin) for 3 min while agitating at room temperature. After centrifuging once more at 200g to remove digitonin, cells were suspended in mitochondrial respiration buffer (Mir06: 0.5 mM EGTA, 3 mM $MgCL_2$-$6H_2O$, 60 mM lactobionic acid, 20 mM taurine, 10 mM KH_2PO_4, 20 mM HEPES, 110 mM sucrose, 1 g/L fatty acid-free BSA, and 100 mg/L catalase; pH 7.1) and transferred into O2K chambers. Respiration was performed in Mir06 at 37^{o}C under hyperoxygenated conditions (350 µM) in the presence of the complex I substrates glutamate (10 mM), pyruvate (5 mM), and malate (2 mM). The sensitivity and maximal response to complex I-supported ADP-stimulated respiration were then measured by conducting an ADP titration with the following concentrations: 1.0 µM, 2.5 µM, 5.0 µM, 10 µM, 20 µM, 50 µM, 100 µM, 200 µM, 500 µM, and 1.0 mM. Succinate was then added in excess (10 mM) to determine maximal complex-II supported respiration. Finally, cytochrome c was added (10 µM) after achieving maximal respiration to test the integrity of the outer mitochondrial membrane. Data is presented normalized to total protein content of the O2K chambers, calculated by aspirating and collecting a portion of the chamber volume upon protocol completion. GraphPad Prism was used to calculate Vmax and EC50 values on ADP titration curves, using the allosteric sigmoidal enzyme kinetics equation: Y=Vmax*X^h/(Khalf^h + X^h).

Statistics

Results are presented as means ± SEM, where n=3-6 independent experiments. GraphPad Prism was used to perform 1-way and 2-way ANOVA analyses with Tukey post-hoc tests where appropriate with significance indicated when $p<0.05$. Microsoft Excel was used to perform T-tests with significance indicated when $p<0.05$.

CHAPTER V: Thesis discussion

Perspectives

This thesis contains several experiments testing the impact of autophagy induction on various cellular functions. Although much has been learned about autophagy's molecular regulation and biological importance from genetic manipulation studies, relatively less is known regarding the consequences of its forced induction. To answer some of these basic biological questions, C2C12 cells were intermittently treated with rapamycin, CCCP, or incubated in amino acid-free media. These stimuli were chosen for their diverse mechanisms of autophagy induction in an attempt to identify common and/or specific resulting phenotypes. The repeated/intermittent nature of these interventions was intentional and is fundamental to understanding the relevance of these studies. Importantly, this was done to partly mimic the ebb and flow that characterizes cellular stress *in vivo*, which is punctuated by recovery periods that allow responsive and potentially long-lasting adaptations to occur. This is particularly relevant to nutritional stresses such as relative and/or short term caloric restriction, given their easily inducible nature and strong connection to autophagy, longevity, and aging. Additionally, performing these experiments in Atg7-deficient cells allows these observations to be attributed to LC3-dependent autophagic degradation specifically, as this enzyme is required for formation of the mature/functional LC3II variant. Furthermore, as Bnip3 was recognized as possibly being involved with CCCP- and HBSS-induced autophagy, experiments were also conducted in Bnip3-deficient cells to better characterize the importance of this autophagy- and mitophagy-regulating protein. In doing so, these Projects contribute several novel discoveries regarding autophagy's role as an inducible mechanism of cellular remodeling.

Notably, the specific experiments contain herein diverge from those initially proposed to be done for this thesis. In the beginning, I wanted to examine the importance of autophagy in mediating the beneficial effects of exercise training on skeletal muscle function and metabolism, made possible as the Quadrilatero Laboratory possesses genetically modified mice capable of inducible- and skeletal muscle-

specific knockdown of Atg7 (Appendix B Fig. 30). In fact, such an experiment would have nicely complemented the data presented here by potentially further demonstrating the cellular remodelling impacts of autophagy induction; some of these experiments have now been performed by others (189,191). With ample foresight, Dr Quadrilatero suggested that some specific cellular aspects of this *in vivo* experiment be investigated, which thus led to the theories and questions tested here *in vitro*. This is relevant for an important reason, because the hypothesis that autophagy does in fact contribute to the *beneficial* effects of exercise training implies several assumptions, primarily that: 1) autophagy is good for cells, 2) what is good for cells is good for the organism, and 3) that "good" means keeping cells alive and functioning. Importantly, these assumptions were generally held while designing the experiments in this this thesis, even though all the results do not necessarily support them. However, whereas keeping cells functioning properly seems like a logical way to preserve tissue function and therefore health, there are a few caveats to this paradigm. First among them is cancer, where keeping cells alive is not good for the organism, thereby violating those second and third assumptions. Similarly, keeping cells alive is not the same as keeping them "healthy" and "functional" as demonstrated during senescence development. Additionally, although examples of autophagy-induced cell death are rare, they do exist and therefore defy the first assumption. Furthermore, it's been shown that the longevity-inducing effects of several interventions, including caloric restriction, are potentially due to increased stress resistance development in post-mitotic tissues such as cardiac muscle, but increased cell turnover and death in tissues such as the liver (355). Based on current understanding, it is possible that autophagy mediates all of these opposing cellular responses, but such information is complex and just beginning to be understood. Therefore, it is likely that different assumptions mentioned above hold true in different manners for each cell type. These are big theoretical biology questions, but essentially it appears that on a cellular level autophagy can promote life and/or death, and that the result of this outcome can be good or bad for health! What this means is that any rational design of a drug that impacts health by

altering autophagy requires deep understanding of the impact of autophagy induction on specific cell types in specific contexts. A number of novel observations regarding the basic biology behind these assumptions are thereby presented in this thesis. The next three pages summarize these findings.

Contributions of Chapter II: Autophagy induction through intermittent amino acid starvation does not cause senescence in vitro

Key findings

- Short-term amino acid and serum withdrawal (HBSS) does not increase caspase-3 activity or cause DNA damage in C2C12 cells
- Low concentration STS administration slightly increases autophagic flux as well as caspase-3 activity and DNA damage
- Repeated low concentration STS administration causes senescence in C2C12 cells as indicated by: enlarged and misshapen cells and nuclei, G1 growth arrest, SAHF, SA-Bgal, and impaired myogenic differentiation
- Repeated HBSS incubation does not cause any of these phenotypic alterations
- Senescent cells, but not those incubated in HBSS, display resistance to cisplatin-induced cell death
- P62 protein content is significantly reduced in senescent cells, which also demonstrate altered basal autophagic flux and starvation-induced autophagy
- ROS partly mediate senescence development induced by low concentration STS
- STS-induced senescence is attenuated in Atg7-deficient cells, likely because they show increased sensitivity to STS-induced cell death

Novelty and relevance of these observations

- Complements recent observations that senescence impairs myogenic potential (252)
- Demonstrates that autophagy is involved with senescence induced by repetitive toxic stress
- Despite numerous prior examples of the previous bullet point, this study is among the first to show that massive autophagy induction itself does not cause senescence

Conclusions

- Sub-lethal autophagy induction through amino acid withdrawal does not cause senescence, demonstrating that this type of stress (which induces massive autophagy) is fundamentally different than those associated with cellular dysfunction
- Senescence was associated with STS-induced DNA damage, implicating the well-characterized DDR in mediating senescence development in this context
- However, despite this, low concentration STS caused *too much* stress that led to cell death in autophagy-null cells and therefore senescence did not occur in the absence of Atg7, suggesting that autophagy promotes senescence caused by specific stressors by keeping cells alive

Contributions of Chapter III: Autophagy mediates stress resistance development caused by repeated amino acid starvation

Key findings

- Atg7-deficient C2C12 cells display significantly increased caspase-3 activity during amino acid and serum starvation compared to control cells
- Shorter time periods of amino acid withdrawal do not decrease p62 protein levels or cause LC3II formation in Atg7-deficient cells
- During the recovery from amino acid starvation, p62 and Atg7 protein contents increase in Atg7-containing cells
- Rapamycin does not increase caspase-3 activity or LC3II formation in the absence of Atg7
- Repeated incubation in amino acid free media partially protects from subsequent STS-induced cell death, and this does not occur in Atg7-deficient cells
- Repeated rapamycin administration increases the subsequent sensitivity to hydrogen peroxide- and cisplatin-induced cell death independent of Atg7
- Protection from STS caused by prior HBSS treatments involves reduced activation of caspase-3 and -9 as well as decreased DNA damage, and this effect can be mimicked with chemical inhibition of caspase-3
- Recovering Atg7 protein levels in Atg7-deficient cells with adenovirus restores the protection from STS-induced caspase-3 activity and DNA damage caused by prior HBSS treatments
- Intermittent rapamycin administration alters cell cycle and massively increases cell and nuclei size
- Intermittent rapamycin administration completely prevents terminal myogenic differentiation, but not induction of Pax7

Novelty and relevance of these observations

- These findings demonstrate that amino acid starvation remodels cells in a way that causes stress resistance, and this depends on autophagy specifically
- Despite previous hypotheses that autophagy might alter cellular composition in such a way, this study is among the first to specifically show that this relationship exists
- This effect was in stark contrast to that of repeated rapamycin treatments: although previous studies have shown that rapamycin can attenuate cell stress/death when administered alongside/during the stress, we found that prior intermittent rapamycin treatments increased sensitivity to death caused by oxidative stress and DNA damage

Conclusions

- In the appropriate context forced autophagy induction serves as a pro-active mechanism of stress resistance development, thus potentially substantiating the cellular-level factors hypothesized to mediate the effects that relative caloric restriction and exercise have on health
- Although it is routinely given to mice and humans, rapamycin has autophagy-independent effects that warrant further investigation
- Additionally, the potential contribution of increased sensitivity to stress caused by rapamycin in specific situations is unexplored

Contributions of Chapter IV: Autophagy and mitophagy as inducible regulators of mitochondrial stress resistance and function

Key findings

- CCCP administration causes mitophagy as indicated by increased LC3II formation, increased LC3II content in mitochondria-enriched subcellular fractions, and reduced mitochondria-specific protein contents
- HBSS incubation does not affect mitochondria-specific protein contents
- CCCP and HBSS dramatically induce PGC1α protein expression
- CCCP does not cause similar protection from STS-induced cell death as HBSS
- Both CCCP and HBSS treatments decrease mitochondrial membrane depolarization and permeability transition pore formation caused by calcium stress
- Protection from calcium-induced mPTP formation caused by CCCP and amino acid starvation requires Atg7
- Repeated amino acid withdrawal increases maximal ADP-stimulated cellular oxygen consumption when provided with mitochondrial ETC complex-I and complex-II substrates
- Atg7-deficient cells display dramatically impaired mitochondrial respiration, and neither amino acid withdrawal or CCCP affects oxygen consumption in these cells
- C2C12 cells do not express Parkin, but L6, primary mouse, and primary human myoblasts do
- CCCP significantly decreases, while HBSS significantly increases Bnip3 protein levels
- Bnip3 is dispensable for starvation-induced p62 degradation and LC3 dynamics as well as CCCP-induced mitochondria-specific protein degradation in C2C12 cells
- Bnip3 is also not required for HBSS-induced protection from cell death caused by STS or increased mitochondrial respiration

Novelty and relevance of these observations

- These findings demonstrate that repeated autophagy induced by amino acid starvation increases mitochondria-specific stress resistance and maximal ADP-stimulated mitochondria respiration
- Despite their lack of Parkin, C2C12 cells are able to execute mitophagy; although apparently to a lower extent than Parkin-expressing cell types
- Although amino acid starvation and CCCP administration alter Bnip3 protein levels, its function in mediating autophagy/mitophagy in C2C12 cells may be redundant

Conclusions

- Autophagy contributes to functional maintenance of mitochondria and is responsible for mitochondrial adaptations to starvation
- Intentional autophagy induction may serve as a mechanism of improving mitochondria composition and function

Autophagy and Mitophagy in C2C12 Cells

A relevant observation made during preliminary/pilot experiments was that Parkin protein content is undetectable in C2C12 cells (Chapter IV Fig. 1 & Appendix B Fig. 6). We initially demonstrated this was not an antibody reactivity issue by showing strong Parkin immunoblotting at the correct molecular weight in ShSY5Y immortalized human neuroblastoma cells (Chapter IV Fig. 1). As Parkin was also detected in differentiated immortalized L6 rat myoblasts and differentiated primary mouse myoblasts (Appendix B Fig. 6), we ruled out species-specific reactivity issues thereby validating that C2C12s are in fact Parkin-deficient. Although this raises a question regarding the mechanism and even the feasibility of depolarization-induced mitophagy in C2C12 cells, many reports of Parkin-independent mitophagy have been made (138,156,158,159). Furthermore, our observation that Bnip3 protein levels were differentially altered by amino acid starvation and CCCP administration suggested it was involved with autophagy and mitophagy regulation in these cells. Although we found that autophagy induced by amino acid starvation and mitophagy induced by mitochondrial depolarization were largely unaltered in Bnip3-CRISPR cells, several explanations can account for these Parkin- and Bnip3-independent responses. Primarily, numerous other mitophagy-regulating proteins that exist were not investigated here and these likely mediate autophagy and mitophagy in the absence of Parkin and Bnip3. This includes Nix/Bnip3L, a structural and functional homologue to Bnip3, as well as various LC3-interacting mitochondrial tagging proteins/factors and proteins which regulate ubiquitination and phosphorylation such as FUNDC1, cardiolipin, Bcl2-L-13, TAX1BP1, NDP52, optineurin, TBK1, and FKBP8. Although assessing the expression pattern of these in C2C12 and other myoblast cell lines would provide interesting mechanistic and functional insight, it is slightly beyond the scope of this thesis. Particularly because the experiments presented here focussed on examining the effects of mitophagy induction, regardless of *how* mitophagy was mechanistically executed. Therefore, our observation that CCCP in fact

caused mitophagy in C2C12 cells satisfied this requirement. Regardless, these experiments do provide some mechanistic insight of Bnip3's role in C2C12 cells.

Autophagy and Cellular Remodelling

Although forms of autophagy such as micro-autophagy, chaperone mediated autophagy (CMA), and chaperone-assisted selective autophagy (CASA) are known to degrade specific cellular targets, macro-autophagy mediated degradation is increasingly characterized as demonstrating cargo selectivity. Because of this, autophagic degradation is becoming viewed as a cellular remodelling mechanism instead of simply a starvation-induced response intended to provide cells with energetic substrates by degrading cellular content *en masse*. Particularly, these molecular interactions frequently suggest that autophagy preferentially targets damaged/dysfunctional proteins and organelles in the same way that the proteasome is used to degrade damaged proteins identified with ubiquitin tags. As such, autophagy is commonly attributed with stress-resistant functions that operate by removing material that might subsequently activate programmed cell death mechanisms. This occurrence is well established during various modes of chemically-induced stress, DNA damage, loss of mitochondrial membrane integrity, accumulated proteins and calcium in ER, and developmentally-encoded stress that occurs during cellular differentiation. Additionally, the degradation of specific proteins involved with stress signaling pathways has also been demonstrated although far less often. Even rarer are investigations into the cellular remodelling associated with autophagy induction in the absence of additional stressors. Although this definition is slightly complicated by two points, namely that cells possess a basal level of autophagic flux and that anything modulating this could therefore be considered a "stress", distinctions can be made regarding the types and effects of various stressors. With respect to autophagy, these differences can be separated by presuming that stresses which activate autophagy may not cause cellular dysfunction and cell death, whereas other "toxic" stressors which do cause dysfunction and death may also induce

autophagy, with the effect of this response highly context dependent. Therefore, fundamental differences likely exist between the types of stresses that activate autophagy but do not cause cellular dysfunction and those that do. Importantly, testing the possibility, mechanisms, and relevance of these relationships was a central focus of this thesis. Notably, repeated autophagy induction by amino acid starvation for periods of time that did not activate cell death signaling was not associated with any type of cellular dysfunction, despite massive levels of autophagy. On the other hand, rapamycin administration caused dramatic changes to cell morphology, increased sensitivity to cell death, and impaired the myogenic capacity of C2C12 cells. Similarly, low-concentration STS increased autophagic flux and senescence development was attenuated in Atg7-deficient cells, indicating that functional autophagy was required for this response.

Autophagy and Senescence

The data presented in this thesis therefore indicates that autophagy is involved with a wide variety of cellular remodelling mechanisms, and the results of its activation mediate diverse responses to stress. In Chapter II, we were specifically interested in two things: 1) whether autophagy induction through nutrient stress would cause senescence, and 2) whether autophagy was involved with senescence caused by toxic stress. Classically, senescence was thought to simply result from telomere shortening, which naturally occurred during replicative exhaustion (259,260,265). However, it is currently understood that a senescence-like phenotype results from numerous cellular stressors, typically those related to oncogene activation, oxidative stress, and essentially DNA damage (262,264,266). Interestingly, whether typical autophagy-inducing stresses themselves, such as nutrient withdrawal, are inherently different with respect to stress-induced senescence is relatively unexplored. The results of Chapter II indicate that repeated amino acid and serum withdrawal does not cause senescence in C2C12 cells. This contrasted the senescence phenotype caused by intermittent administration of low

concentration STS, which led to positive identification of each senescence marker we examined. This finding implies that these two stresses are fundamentally different, as despite inducing massive levels of autophagy, the stress associated with amino acid and growth factor deprivation did not lead to senescence. However, this apparently straight-forward finding does require some explanation and context. Importantly, in these experiments HBSS treatments were performed to maximize autophagy activation, and as such cells were incubated long enough to observe high levels of autophagy but not long enough to cause significant cell death (Chapter II Fig. 1A & 1C; Chapter III Fig. 1B; Chapter IV Fig. 2). Of course, this was intentionally done as prolonged starvation could be stressful enough to activate cell death signaling mechanisms and damage DNA. In C2C12 cells, DNA laddering occurs after continuous incubation in EBSS for 16 hours (464). As the DDR is fundamental to senescence development, it is possible that prolonged amino acid withdrawal enough to damage DNA may cause senescence. Additionally, this "HBSS does not cause senescence" finding could also be considered a consequence of autophagy induction instead of a direct effect resulting from autophagy induction specifically. Although amino acid starvation was selected because autophagy is particularly sensitive to this, it is possible that this nutrient stress induces autophagy so strongly that other starvation-related stress is attenuated. That is, maybe incubation in HBSS and EBSS similarly activate extracellular stress signaling and upstream cell death mechanisms, but HBSS induces extra autophagy that counters these. Similarly, it is possible that low-concentration STS diluted in HBSS instead of GM would promote additional autophagy that would attenutate the senescence-causing effects of STS. Interestingly, this hypothesis not only suggests that other types of starvation or autophagy stressors may have different effects on senescence, but also that inducing autophagy during or alongside toxic stress may prevent senescence. In fact, in Chapter III it was found that rapamycin administration alone caused a cellular phenotype characterized by enlarged cells, altered cell cycle, and impaired myogenic differentiation (Chapter III Fig. 7 & Fig. 8). The decision to not call this senescence was due to the differences between rapamycin- and STS-treated cells with

respect to cell cycle profiles (senescence normally arrests cells in G1: Chapter II Fig. 3F; Chapter III Fig. 7A), sensitivity to CisPL-induced death (Chapter II Fig. 5A; Chapter III Fig. 3J), and lack of significant SA-Bgal activity (not shown). Despite these findings, because rapamycin-dependent effects were similar in SCR and Atg7-deficient cells, we concluded its effects were autophagy-independent regardless. However, evidence for rapamycin-induced senescence has been shown (465).

Separate from the idea that autophagy-associated stressors are fundamentally distinct from those that cause dysfunction and senescence is autophagy's contribution to senescence induced by various stressors. As autophagy functions as an important stress-response mechanism, its potential connection to senescence is clear. As previously mentioned in this Thesis, studies have generally shown that senescence induced by various stressors is attenuated in autophagy-deficient cells or when autophagy is inhibited, while others have also indicated that autophagy inhibition causes senescence (283). Understanding this relationship is complex as autophagy might be activated alongside but independent of senescence, thereby making their correlation meaningless; or, similar to cell death, autophagy may simultaneously mitigate and potentiate senescence-related signaling depending on the situation. However, mechanisms explaining both positive and negative control of senescence by autophagy have been demonstrated. First, autophagy may serve to permit senescence by degrading specific mediators of the senescence program, or by generally increasing cellular stress resistance therefore encouraging senescence instead of cell death (294,466,467). Alternatively, inadequate autophagy may cause accumulation of various cellular insults such as protein aggregates, ER/mitochondria stress, ROS, and DNA damage that subsequently results in senescence (288,293). In addition to these studies of stress-induced senescence, although telomere dysfunction is related to replicative senescence development (265), it's been demonstrated that induced telomere dysfunction stimulates autophagy and that inhibiting autophagy does not significantly affect senescence in this scenario (468). This importantly

questions the relevance of autophagy's impact on senescence *in vivo*. Interestingly, autophagy's impact on senescence has been investigated in other ways where concurrent administration of rapamycin partially prevents H_2O_2-induced senescence in 3T3 cells (293) and p21/p16-induced senescence in (469). Furthermore, rapamycin administration may prevent or revert senescence in skeletal muscle satellite cells (252) and decrease SASP production in senescent fibroblasts, which was demonstrated to suppress the ability of these cells to stimulate prostate tumour growth (470). This Thesis adds to our knowledge of the interaction between autophagy and senescence as In Chapter II it was found that low concentration STS slightly increased autophagic flux and that senescence was abrogated in the absence of Atg7, suggesting that autophagy is required for senescence in this scenario. Additionally, we also demonstrate that senescent C2C12 cells display dramatically reduced p62 protein content (Chapter II Fig. 7), altered basal and starvation-induced autophagic flux (Chapter II Fig. 7), reduced total ubiquitin levels (Appendix B Fig. 27), impaired myogenic differentiation (Chapter II. Fig. 4), resistance to cisplatin-induced cell death (Chapter II Fig. 5 & 6), essentially unaltered sensitivity to staurosporine-induced cell death (Chapter II Fig. 5 & 6), and increased sensitivity to calcium-induced mPTP formation (Appendix B Fig. 27). These findings suggest complex interplay between various autophagy and cell death regulating mechanisms, and function to further characterize the phenotypic alterations present in senescent cells.

Throughout this thesis senescence has been considered an unwanted cellular response with possible pathophysiological implications regarding tissue damage and aging. However, because senescence causes relative stress resistance, autophagy and senescence are also thought to be conserved responses that function to maintain cell viability and prevent death. Importantly, the physiological impact of this effect varies: accumulation of senescent cells would theoretically lead to tissue dysfunction, but senescence is also considered anti-oncogenic. Given this complex relationship, the final decision is likely determined by the type, timing, and duration of stress stimuli and the cell's current stress status.

Although I have a difficult time delineating 1) autophagy generally helps keeps cell alive (which could be senescence) with 2) autophagy targets damaged/damaging material thus keeping cells healthy, it is clear that complicated cellular mechanisms control the stress responses that regulate autophagy thereby deciding between life, death, or senescence.

Autophagy and Stress Resistance

In agreement with extensive literature regarding autophagy and resistance to acute stress, we found that autophagy-deficient cells displayed increased sensitivity to cell death induced by various insults. This includes staurosporine at low (Chapter II Fig. 9) and high (Chapter III Fig. 3) concentrations, hydrogen peroxide, cisplatin (Chapter III Fig. 3), and particularly nutrient starvation (Chapter III Fig. 1). However, the next central focus of this thesis was examining the impact of autophagy on cellular remodelling, specifically whether repeated forced autophagy induction interspersed with recovery periods would allow cellular adaptations that conferred stress resistance. Although autophagy is known to target dysfunctional and damaged proteins and organelles and in doing so is theorized to act as a recycling mechanism that has favourable effects on cellular function, specific demonstration of this occurring is rare. While autophagy is suggested to contribute to the beneficial effects of exercise training on skeletal muscle (189,191) and to ischemic preconditioning in neural and cardiac tissues (244,342-344), the specific cellular changes altered by autophagy which mediate these adaptations are not known. Additionally, the specific contribution of autophagy to these effects is obscured by the complicated nature of physiological stimuli and lack of specific autophagy activation and/or inhibition in various experimental protocols. Here, data is presented in all three Projects regarding the impact of previous repeated autophagy induction on stress resistance. In Chapter II, it was found that intermittent incubation in HBSS decreased subsequent STS-induced caspase activation and DNA damage. In Chapter III we demonstrated that this was autophagy-dependent, where Atg7 knockdown removed the

protective effect and recovering Atg7 expression in these cells restored it. Finally, data in Chapter IV showed that mitochondria-specific stress resistance was increased after multiple treatments with CCCP and HBSS, and furthermore that protection from calcium-induced mPTP formation caused by previous CCCP and HBSS was eliminated with Atg7 deficiency. These experiments strongly demonstrate that autophagy induction through amino acid starvation causes stress resistance, particularly to stress that impacts mitochondria. Notably, we show this protection may be limited to mitochondrial stressors. Initial characterization of this stress-resistance phenotype consistently indicated that cells were partially protected from STS-induced cell death and that this involved reduced caspase-3 and caspase-9 activation (Chapter IV Fig. 5; Appendix B Fig. 8). In fact, the subsequent focus of these studies on mitochondrial-mediated mechanisms was driven by the fact that changes to other cell death regulating factors were generally not observed (Chapter II Fig.6; Chapter III Fig. 5; Chapter IV Fig. 6).

This conclusion is further supported by solely observing protection from STS. In our hands, STS-induced cell death is characterized by mitochondrial cytochrome c release (369), activation and mitochondrial release of AIF (369), caspase-9 activation (388, Chapter III Fig. 4), caspase-3 activation (388, Chapter III Fig. 4), p53 activation (Chapter IV Fig. 6), and DNA fragmentation (Chapter III Fig. 5). This contrasts H_2O_2, which causes AIF release (388) and DNA fragmentation (Chapter III Fig. 5) but does not involve caspases (388, Chapter IV Fig. 5) or p53 (Chapter IV Fig. 5). Lastly, CisPL administration dramatically induces p53, DNA damage, and caspase-3 while significantly reducing XIAP and Bcl2 protein levels (357, Chapter IV Fig. 5). Therefore, it appears that stress resistance caused by previous autophagy induction is specific to the mitochondrial-mediated caspase activation that occurs with STS, and not oxidative stress (H_2O_2) or direct DNA damage (CisPL). However, although pilot experiments were performed to identify optimal doses of these chemicals to cause detectable death-associated changes, it is possible that the concentrations used “overpowered” the protective adaptations and that protective effects may have

been observed with lower doses. Similarly, these effects may be specific to H_2O_2 and CisPL, and that intermittent autophagy may cause resistance to other inducers of oxidative stress or DNA damage.

As previously alluded to in this thesis, the thought that autophagy may serve as an intentionally inducible mechanism of stress resistance shares theoretical similarities to preconditioning and hormesis. Although these terms may in fact describe the same cellular phenomenon, in general they describe situations where previous exposure to stresses causes subsequent resistance to larger doses. As autophagy seems to be sensitive to numerous (and maybe all) cellular stressors, its involvement with these phenomena is logical (296). In fact, it is possible that: 1) autophagy represents a novel mode of hormesis/preconditioning, 2) autophagy contributes to forms of hormesis/preconditioning, or even 3) that hormesis/preconditioning are fundamentally dependent on autophagy and only occur *because* autophagy exists. Although the physiological relevance of hormesis-like effects is debated, there appears to be renewed interest in defining these relationships. Importantly, the findings of this thesis not only suggests that specific autophagy induction itself may represent and produce preconditioning-like effects, but also that adaptations to various stressors (STS-induced senescence, starvation-induced stress resistance, increased starvation-induced mitochondrial respiration) requires functional autophagy.

Interestingly, repeated rapamycin administration caused several unexpected cellular changes. Initially, rapamycin-induced autophagy was conducted to complement experiments involving amino acid starvation, with the hypothesis that these would have generally similar effects. However, in contrast to repeated HBSS incubation, rapamycin exposure did not significantly affect cell death induced by STS and actually increased sensitivity to cell death caused by H_2O_2 and CisPL. As these effects occurred similarly in SCR and Atg7-deficient cells, we concluded that this was independent of its autophagy modulating

capabilities. This again highlights the numerous other cellular signaling mechanisms and functions that mTOR regulates, and justifies further investigation into rapamycin's effects *in vivo*.

Autophagy and Mitochondria

A specific cellular function that was impacted by autophagy deficiency was mitochondrial respiration. In Chapter IV, we saw that maximal cellular oxygen consumption was reduced more than 50% in Atg7-deficient cells when provided with complex I and/or complex II substrates. Furthermore, the addition of cytochrome c significantly increased respiration in these cells, suggesting that existing mitochondria were damaged without autophagy. It is established that Atg7 knockout causes mitochondrial dysfunction in yeast (453) and alters mitochondrial morphology in mouse cardiomyocytes and hepatocytes (50,454). Autophagy deficiency also leads to mitochondrial accumulation (384,455-457) while simultaneously decreasing maximal oxygen consumption in various cell types (458,459). Therefore, our observations in this regard are not surprising. We additionally showed that intermittent amino acid starvation increased OCR only in Atg7 competent cells, indicating autophagy is required for this effect. However, while this demonstrates that autophagy-dependent degradation is required for mitochondrial adaptations in this context, likely through recycling of mitochondrial material, the mechanisms which led to increased mitochondrial function are unknown. Although amino acid starvation dramatically increased PGC1α, CCCP elevated PGC1α to a greater extent (Chapter IV Fig. 3 & Fig. 8) yet OCR did not increase in CCCP-treated cells. Mutual increases in mitochondria-specific protein contents were also not observed in HB+F-treated cells, indicating that elevated respiration is not simply a function of mitochondrial biogenesis. Possibly, starvation-induced PGC1α could impact specific ETC and metabolic enzymes, the expression of which were not measured here, that could account for the mitochondrial adaptations. In fact, it is well-established that "mitochondrial biogenesis" does not necessarily mean increased mitochondrial mass: functional benefits could result from numerous

mechanisms such as increased coupling efficiency (which itself is mediated by several things), increased mitochondrial substrate delivery, increased expression of individual/select enzymes (which could be thought of as increasing the density of functionally-relevant proteins in the mitochondria), or modification of internal mitochondrial degradation mechanisms (which may "clean" mitochondria just as autophagy "cleans" cells). Given these possibilities, we nonetheless demonstrate that this response was specific to amino acid starvation and requires Atg7. Also noteworthy is that OCR did not increase in Atg7-deficient cells despite detecting increased mitochondria-specific protein levels in response to CCCP and HB+F treatments, indicating autophagy is required for generation of new and properly functioning mitochondria or improvement of existing mitochondria.

Similarly, the precise aspects of mitochondrial biology altered by amino acid starvation that contributed to increased stress resistance are also unknown. Although it would be logical to assume that the adaptive mechanisms that conferred respiration benefits may also mediate stress resistance, there are likely some independent factors. This is highlighted in the finding that repeated CCCP administration partially protected mitochondria from calcium stress but did not affect cellular oxygen consumption.

Autophagy-Independent Explanations

As already mentioned, the most prominent autophagy-independent effect observed here was rapamycin-induced cell cycle and morphology alterations and prevention of myogenic differentiation. Although this is confounded somewhat because Atg7-deficient cells already show impaired differentiation, there were generally no differences in rapamycin-dependent effects between SCR and shAtg7 groups. Of course, mTOR affects numerous cellular processes related to general protein synthesis, cell cycle, metabolism, and inflammatory responses through its involvement with NF-κB,

PPAR, S6K, 4E-BP1, FoXO, SREBP1, and other signaling mechanisms (471). Therefore, the fact that rapamycin caused autophagy-independent effects is not that surprising.

Importantly, autophagy induced by amino acid starvation obviously also involves mTOR inhibition, but these treatments had dissimilar effects on cell growth, differentiation, and death patterns. Despite this, autophagy is regulated by numerous mechanisms other than mTOR, which is the sole autophagy-relevant target of rapamycin. Therefore, it is not surprising that differences existed between these two autophagy stimuli. In particular, an economics difference exists between these two interventions. Although rapamycin/mTOR inhibition may stimulate upstream autophagy signaling mechanisms, it does this without a biological purpose for autophagy induction. On the other hand, removing amino acids or damaging mitochondria provides a robust stimuli/reason for autophagy execution. As a result, this likely represents a stronger proxy for actual autophagy induction (ie. degradation of target material) that is biologically warranted, as opposed to the simple activation of autophagy-regulating machinery resulting from mTOR inhibition.

Although these studies focus on autophagy, there are very few situations presented here in which Atg7 deficiency *completely* prevented an effect caused by HBSS, rapamycin, or CCCP. While these interventions were chosen due to their ability to stimulate autophagy/mitophagy, only autophagy and cell death-related mechanisms were measured here and these treatments alter various other cellular processes that regulate stress resistance and mitochondrial metabolism. Among these is antioxidant defence, strongly controlled by Nrf2 signaling (472). However, it has been demonstrated that incubation in HBSS actually does not activate Nrf2 in human lung epithelial cells (473), which is logical given p62's regulation of Nrf2 function (237,239,399). Despite this, amino acid starvation is known to stimulate NF-κB (474), Hif1α (475), and FoXO (476), signaling platforms with numerous impacts outside of autophagy.

Additionally, while HBSS-induced AMPK activation has been shown (477) and thus an experiment involving its inhibition was planned to be conducted here, altered AMPK signaling was not detected in C2C12 cells with CCCP or amino acid starvation (Appendix B Fig. 5).

Relevance to Human Physiology and Health

The relevance that these basic biological mechanisms have on physiology and health has been alluded to throughout this thesis. Primarily, these implications concern how cell death and stress resistance on a cellular level impact tissue function and therefore health in general. These experiments were designed to examine some cellular mechanisms that theories regarding the interaction between autophagy, hormesis, and longevity are based upon.

The benefits of healthy eating and regular exercise have literally been known for thousands of years. Current scientific understanding of these principles significantly implicates autophagy in mediating some of these effects. In fact, relative caloric restriction and/or exercise is widely known to increase longevity of biological research animals and in simpler life forms the effect of nutrient deficiency is abolished with genetic autophagy impairment (311,356). Therefore, it is very likely this highly conserved biological process serves similar functions in human physiology. In fact, a recently published update concluded that “caloric restriction without malnutrition...improves health and survival of rhesus monkeys” (320). Although this effect can be attributed to many physiological factors (ie. weight gain, numerous other biological processes), given autophagy’s sensitivity to nutritional status it is reasonable to assume its contribution is not negligible. The question is, how does increased basal or repeated autophagy make such contributions?

An often made observation is that animal models of longevity generally display increased stress resistance (297,311,354,463). Although the acute interaction between this and autophagy is well-established, most human diseases involve accumulation of stress or damaging stimuli to manifest and become pathological. That is, being able to survive a single insult through increased autophagy may not largely impact physiology over an entire lifetime. Therefore, the stress resistance observed in these longevity models might not be due to increased acute autophagy induction when encountering a stress, but the general development of a stress-resistant phenotype (although whether regular exercise and/or caloric restriction affect acute autophagy induction is possible). Importantly, these ideas align with autophagy's purported cellular recycling abilities, where autophagic machinery preferentially targets damaged and/or dysfunctional proteins and organelles. Hence, its forced induction is theorized to improved cellular composition by decreasing the cell's current stress level or by allowing adaptation and generation of relatively stress-resistance structures. The novel results presented here demonstrate this may in fact be true, as repeated autophagy induction through amino acid starvation increased resistance to cell death caused by staurosporine and mitochondrial permeabilization caused by calcium.

Although this is a nice thought, it is slightly construed by findings that suggest caloric restriction turns on genes related to stress resistance in post-mitotic tissues like cardiac muscle while activating those promoting cell death and turnover in the liver (355). If we assume that relative caloric restriction is always "good" for human physiology and longevity, then this pro-death response should not be considered pathological and therefore has an understandable, evolutionarily-supported reason. In fact, the interaction between autophagy and cell death may explain this dichotomy. Among other things, an obvious effect of exercise/caloric restriction is reduced body mass, functionally decreasing the amount of human being to maintain. If, for example, this means the liver is 25% smaller (ie. is composed of 25% less cells) and can adequately perform its function at this size, it should "age" 25% more slowly.

Imagined another way, this means that 25% more cells can be lost before the liver ages, essentially decreasing the threshold for damage thereby removing cells when they are less dysfunctional than before and potentially improving tissue function. Furthermore, increased autophagy induction in remaining cells might maintain or improve them as well. However, this is a theory, and one that will not be substantiated without research examining more direct mechanisms of autophagy induction. Primarily, while autophagy-induced chemoresistance is thought to be a common characteristic of cancer cells and partly contributes to the administration of the autophagy/lysosome inhibitor chloroquine during therapy (478), the autophagy-inducing chemical rapamycin has well established anti-cancer properties (419,420). Therefore, it is possible these cancer-related effects, as well as those related to longevity, are unrelated to autophagy and/or actually point towards rapamycin-induced sensitivity to cell death. Interestingly, we report here that rapamycin-treated cells showed increased cell death induced by DNA damage and oxidative stress. Regardless, it is apparent that the biological purpose of autophagy on a cellular level is likely to protect cells, and the result of this role is highly tissue and context dependent.

Limitations

These studies tested a number of general hypotheses regarding autophagy. Despite the conserved nature of the assumptions made here, all relevant experiments were performed using C2C12 cells. These cells are commonly used to study the mechanisms of skeletal muscle development as well as general cell biology, but their individual use here questions the widespread relevance of these findings. Although similar results would be expected to occur with other cell lines/types, it is possible that C2C12s possess a unique and inherent ability to adapt to stress, particularly given that adaptation to stress is a fundamental characteristic of mature skeletal muscle.

Another shortcoming is using a single Atg7-deficient cell clone for most autophagy-dependent experiments. Although numerous stable clones were created (Appendix B Fig. 17), only two (Chapter III Fig. 1 & 2, Appendix B Fig. 29) or three (Appendix B Fig. 18 & 19) were tested and compared for subsequent use here. Although shAtg7 #1 and #2 appeared to display similar autophagic and cell death responses to amino acid starvation and rapamycin (Chapter III Fig. 1 & 2), it is possible that the observed effects could be limited to the specific clone (shAtg7 #1) used in following experiments. Additionally, current guidelines suggest performing separate experiments where a biological effect is altered by more than one essential autophagy gene (ie. Atg5 and Atg7) to fully demonstrate autophagy-dependent functions of specific events (103). Given this shortcoming, the observation that adenoviral-mediated recovery of Atg7 protein content in shAtg7 #1 re-established the protective effects observed in Chapter III strongly implies this finding is conserved and not a clone-related artifact.

We generally observed that prior autophagy induction protected cells from STS-induced cell death. As previously mentioned, this may have occurred due to the specific insults and doses employed. For example, it is possible that resistance to oxidative stress may have been detected if lower concentrations of H_2O_2 were applied. Similarly, although we concluded that prior autophagy induction did not protect from subsequent cell death caused by DNA damage, it is possible an effect would have occurred using a chemical other than CisPL.

The measures of cell death utilized here are generally indicators of the apoptotic form of regulated cell death: that involving loss of mitochondrial integrity, caspase activation, DNA fragmentation, and outer membrane phosphatidyl serine exposure. Of course, numerous other modes of cell death occur, both regulated and accidental. Importantly, a central focus in these experiments is that we observed a stress-resistance phenotype, implying cellular protection in general and not protection specific to apoptotic

cell death. In performing the conducted measurements, we thereby assumed any cellular protection would manifest as decreased annexin/PI staining, caspase-3 activity, or DNA damage; however, this potentially ignores additional protection or death from other cellular processes.

Future Directions

A logical next step would be to conduct similar experiments in other cells types, including primary mouse and human cells, to demonstrate the potential general and conserved nature of these findings. It would additionally be interesting to find out if cancerous human cell lines or primary tumour cells display similar responses to repeated autophagy induction, particularly given their subversion of cell death signaling and use of rapamycin in cancer treatments. Other genetic manipulation techniques would also be useful to demonstrate the involvement of autophagy in these results. This could be performed by generating additional knockout cell lines using CRISPR/Cas9 or examining primary cells isolated from genetic knock out animals of essential autophagy genes other than Atg7. As C2C12 are considered muscle precursor cells, the myoblast-specific relevance of these findings could also be investigated by generating induced pluripotent stem cell lines from specific autophagy-knockout mice or diseased human cells and comparing the effects observed after converting these to cardiomyocytes, neurons, myoblasts, etc. Finally, examining the effects of other longevity-associated chemicals (resveratrol, spermidine, urolithin A, NAD) on autophagy-dependent remodelling would also further define these relationships and perhaps point towards a potential nutritional intervention.

A number of *in vivo* experiments could also be useful to demonstrate the physiological relevance of autophagy-mediated cellular remodelling. This includes the skeletal muscle and exercise study initially proposed to be conducted as part of this thesis. Here, to examine if the adaptations associated with exercise training in skeletal muscle are autophagy-dependent, mice with inducible skeletal muscle-

specific knockdown of Atg7 could be exercise trained and examined to see if such adaptations were affected. Although some of these experiments have now been performed, a number of specific parameters such as metabolic enzyme activity, mitochondrial function, contractile ability, and subsequent resistance to stress/atrophy have not been examined.

Another interesting *in vivo* study would be to examine autophagy in the *PolG* mouse model of progeria. These mice lack the function of an important mitochondrial DNA repair enzyme, and therefore quickly accumulate mitochondrial DNA mutations resulting in accelerated aging. Remarkably, forced regular endurance exercise (479), but not caloric restriction (480), dramatically attenuates this phenotype. Although autophagy's role in mediating this effect was postulated by these researchers (479), its contribution has not been demonstrated. Cross-breeding such *PolG* mice with those capable of inducible autophagy knockdown and exercise training the resulting animals would be a direct way to test this hypothesis.

Finally, a particularly interesting idea harnesses a powerful mouse model. In 2005, researchers published a study examining the impact of widespread adipocyte cell death on metabolic syndrome by generating mice that were engineered to produce and then activate a caspase-8 fusion protein in their adipocytes when administered a FK1012-related chemical, which they termed FAT-ATTAC (fat apoptosis through targeted activation of caspase-8) (481). Subsequently, another group of researchers modified these mice to demonstrate the longevity-inducing and health-prolonging effects that selective removal of senescent cells causes by altering them to selectively kill p16-positive cells instead of adipocytes when administered the FK1012-related chemical (281,282). However, instead of *removing* p16-positive cells, it would be interesting to *induce autophagy* in them, which may demonstrate that keeping these cells around *healthily* is better than having them senesce and also better than having them die.

Conclusions

The intention of this Thesis was to examine some relatively unexplored aspects of autophagy's impact on cellular physiology, particularly to further outline and substantiate the thought that all biological phenomena are represented by bell curves where dysfunction in either direction can be pathological. With respect to cell stress and death, there appears to exist an *ideal* hierarchy whereby a very minor insult activates stress signaling to such an extent that their integration deems no response is necessary to continue functioning properly, a slightly stronger insult means that autophagy is activated in defense with the intention of repelling and surviving the damage, a stronger insult then surpasses the protective functions of autophagy and activates regulated cell death mechanisms so as to ensure homeostatic removal of this cell in the tissue/organism, and finally a very strong insult leads to non-regulated cell death destruction which may cause additional tissue damage and would therefore not be evolutionarily selected against. However, as previously mentioned, keeping cells alive is not always good for the organism, as dysfunctional and mutated cells can subvert this paradigm and therapeutic benefit may result from "better of two evils" situations. Another interesting idea potentially connecting basic cell biology to human physiology and health is that autophagy forms a plausible mechanism explaining the idiom "what doesn't kill you makes you stronger"; but, is this expression actually true? The hormesis literature suggests it is always true, but scientific consensus regarding this theory, and even hormesis itself, is far from being reached. If forced to answer, I would say the most likely answer is maybe, but it depends. Although the stress associated with *moderate* exercise and *relative* caloric restriction appear to have universally beneficial effects on human health, other types of stress such as UV radiation or energy-rich diets are responded and adapted to in less than beneficial ways. Perhaps the drastically diverse modulation of autophagy differentiates these types of stresses. In fact, longevity researchers indicate that it might be, and that specific autophagy induction in the absence of additional stress (ie. ischemia) may provide cellular benefits and avoid potential toxic side effects. In this way, autophagy is

imagined as a cellular recycling mechanism instead of a cellular trash disposal mechanism. The experiments contained here clearly suggest that the type of stress greatly impacts cell death and adaptation responses, and that autophagy differentially regulates these in context-dependent manners. In performing such experiments, we attempt to further extend our basic understanding of autophagy, with the intention that these findings will help explain complex physiological questions. Ultimately, "what doesn't kill you..." is likely true for specific stresses when your cells are young and can induce autophagy properly, thereby providing the additional benefit of being able to adapt to these stresses.

Importantly, assuming that every biological process is represented by a bell curve means that 50% of people are worse than average and can therefore be improved. Additionally, although dysfunction in either direction may be pathological, it may also be beneficial. Perhaps sensitivity to autophagy induction was/will be an evolutionarily advantageous change that we can intervene in. However, before progressing past acknowledging the benefits of regular exercise and healthy eating habits to the point of handing out autophagy-inducing drugs, several fundamental aspects of autophagy biology require further examination. This Thesis illustrates some cellular adaptations resulting from autophagy induction, specifically regarding senescence development, stress resistance, and mitochondrial function. These results have implications with respect to our basic understanding of the relationship between autophagy and cell death as well as how these effects impact health and aging.

References

[1] A.B. Gustafsson & R.A. Gottlieb, Bcl-2 family members and apoptosis, taken to heart, Am.J.Physiol.Cell.Physiol. 292 (2007) C45-51.

[2] G. Kroemer, L. Galluzzi & C. Brenner, Mitochondrial membrane permeabilization in cell death, Physiol.Rev. 87 (2007) 99-163.

[3] P. Saikumar, Z. Dong, V. Mikhailov, M. Denton, J.M. Weinberg & M.A. Venkatachalam, Apoptosis: definition, mechanisms, and relevance to disease, Am.J.Med. 107 (1999) 489-506.

[4] P. Vandenabeele, L. Galluzzi, T. Vanden Berghe & G. Kroemer, Molecular mechanisms of necroptosis: an ordered cellular explosion, Nat.Rev.Mol.Cell Biol. 11 (2010) 700-714.

[5] G.M. Cohen, Caspases: the executioners of apoptosis, Biochem.J. 326 (Pt 1) (1997) 1-16.

[6] A.U. Luthi & S.J. Martin, The CASBAH: a searchable database of caspase substrates, Cell Death Differ. 14 (2007) 641-650.

[7] U. Fischer, R.U. Janicke & K. Schulze-Osthoff, Many cuts to ruin: a comprehensive update of caspase substrates, Cell Death Differ. 10 (2003) 76-100.

[8] F.C. Kischkel, S. Hellbardt, I. Behrmann, M. Germer, M. Pawlita, P.H. Krammer & M.E. Peter, Cytotoxicity-dependent APO-1 (Fas/CD95)-associated proteins form a death-inducing signaling complex (DISC) with the receptor, EMBO J. 14 (1995) 5579-5588.

[9] C. Scaffidi, S. Fulda, A. Srinivasan, C. Friesen, F. Li, K.J. Tomaselli, K.M. Debatin, P.H. Krammer, et al, Two CD95 (APO-1/Fas) signaling pathways, EMBO J. 17 (1998) 1675-1687.

[10] P. Li, D. Nijhawan, I. Budihardjo, S.M. Srinivasula, M. Ahmad, E.S. Alnemri & X. Wang, Cytochrome c and dATP-dependent formation of Apaf-1/caspase-9 complex initiates an apoptotic protease cascade, Cell 91 (1997) 479-489.

[11] C. Du, M. Fang, Y. Li, L. Li & X. Wang, Smac, a mitochondrial protein that promotes cytochrome c-dependent caspase activation by eliminating IAP inhibition, Cell 102 (2000) 33-42.

[12] Q.L. Deveraux, N. Roy, H.R. Stennicke, T. Van Arsdale, Q. Zhou, S.M. Srinivasula, E.S. Alnemri, G.S. Salvesen, et al, IAPs block apoptotic events induced by caspase-8 and cytochrome c by direct inhibition of distinct caspases, EMBO J. 17 (1998) 2215-2223.

[13] S.A. Susin, N. Zamzami, M. Castedo, T. Hirsch, P. Marchetti, A. Macho, E. Daugas, M. Geuskens, et al, Bcl-2 inhibits the mitochondrial release of an apoptogenic protease, J.Exp.Med. 184 (1996) 1331-1341.

[14] L.Y. Li, X. Luo & X. Wang, Endonuclease G is an apoptotic DNase when released from mitochondria, Nature 412 (2001) 95-99.

[15] Y.J. Nam, K. Mani, A.W. Ashton, C.F. Peng, B. Krishnamurthy, Y. Hayakawa, P. Lee, S.J. Korsmeyer, et al, Inhibition of both the extrinsic and intrinsic death pathways through nonhomotypic death-fold interactions, Mol.Cell 15 (2004) 901-912.

[16] A.B. Gustafsson, J.G. Tsai, S.E. Logue, M.T. Crow & R.A. Gottlieb, Apoptosis repressor with caspase recruitment domain protects against cell death by interfering with Bax activation, J.Biol.Chem. 279 (2004) 21233-21238.

[17] H.M. Beere, B.B. Wolf, K. Cain, D.D. Mosser, A. Mahboubi, T. Kuwana, P. Tailor, R.I. Morimoto, et al, Heat-shock protein 70 inhibits apoptosis by preventing recruitment of procaspase-9 to the Apaf-1 apoptosome, Nat.Cell Biol. 2 (2000) 469-475.

[18] L. Ravagnan, S. Gurbuxani, S.A. Susin, C. Maisse, E. Daugas, N. Zamzami, T. Mak, M. Jaattela, et al, Heat-shock protein 70 antagonizes apoptosis-inducing factor, Nat.Cell Biol. 3 (2001) 839-843.

[19] R.M. Kluck, E. Bossy-Wetzel, D.R. Green & D.D. Newmeyer, The release of cytochrome c from mitochondria: a primary site for Bcl-2 regulation of apoptosis, Science 275 (1997) 1132-1136.

[20] K. Nakano & K.H. Vousden, PUMA, a novel proapoptotic gene, is induced by p53, Mol.Cell 7 (2001) 683-694.

[21] H. Li, H. Zhu, C.J. Xu & J. Yuan, Cleavage of BID by caspase 8 mediates the mitochondrial damage in the Fas pathway of apoptosis, Cell 94 (1998) 491-501.

[22] C. Bonzon, L. Bouchier-Hayes, L.J. Pagliari, D.R. Green & D.D. Newmeyer, Caspase-2-induced apoptosis requires bid cleavage: a physiological role for bid in heat shock-induced death, Mol.Biol.Cell 17 (2006) 2150-2157.

[23] S.R. Datta, H. Dudek, X. Tao, S. Masters, H. Fu, Y. Gotoh & M.E. Greenberg, Akt phosphorylation of BAD couples survival signals to the cell-intrinsic death machinery, Cell 91 (1997) 231-241.

[24] R.K. Bruick, Expression of the gene encoding the proapoptotic Nip3 protein is induced by hypoxia, Proc.Natl.Acad.Sci.U.S.A. 97 (2000) 9082-9087.

[25] P. Bernardi, A. Rasola, M. Forte & G. Lippe, The Mitochondrial Permeability Transition Pore: Channel Formation by F-ATP Synthase, Integration in Signal Transduction, and Role in Pathophysiology, Physiol.Rev. 95 (2015) 1111-1155.

[26] P. Fernando & L.A. Megeney, Is caspase-dependent apoptosis only cell differentiation taken to the extreme? FASEB J. 21 (2007) 8-17.

[27] T. Miyashita & J.C. Reed, Tumor suppressor p53 is a direct transcriptional activator of the human bax gene, Cell 80 (1995) 293-299.

[28] P. Jiang, W. Du, K. Heese & M. Wu, The Bad guy cooperates with good cop p53: Bad is transcriptionally up-regulated by p53 and forms a Bad/p53 complex at the mitochondria to induce apoptosis, Mol.Cell.Biol. 26 (2006) 9071-9082.

[29] Y.Z. Li, D.Y. Lu, W.Q. Tan, J.X. Wang & P.F. Li, p53 initiates apoptosis by transcriptionally targeting the antiapoptotic protein ARC, Mol.Cell.Biol. 28 (2008) 564-574.

[30] M. Mihara, S. Erster, A. Zaika, O. Petrenko, T. Chittenden, P. Pancoska & U.M. Moll, P53 has a Direct Apoptogenic Role at the Mitochondria, Mol.Cell 11 (2003) 577-590.

[31] N.D. Marchenko, A. Zaika & U.M. Moll, Death signal-induced localization of p53 protein to mitochondria. A potential role in apoptotic signaling, J.Biol.Chem. 275 (2000) 16202-16212.

[32] J.I. Leu, P. Dumont, M. Hafey, M.E. Murphy & D.L. George, Mitochondrial p53 activates Bak and causes disruption of a Bak-Mcl1 complex, Nat.Cell Biol. 6 (2004) 443-450.

[33] J.E. Chipuk, T. Kuwana, L. Bouchier-Hayes, N.M. Droin, D.D. Newmeyer, M. Schuler & D.R. Green, Direct activation of Bax by p53 mediates mitochondrial membrane permeabilization and apoptosis, Science 303 (2004) 1010-1014.

[34] P.F. Li, R. Dietz & R. von Harsdorf, p53 regulates mitochondrial membrane potential through reactive oxygen species and induces cytochrome c-independent apoptosis blocked by Bcl-2, EMBO J. 18 (1999) 6027-6036.

[35] M. Bennett, K. Macdonald, S.W. Chan, J.P. Luzio, R. Simari & P. Weissberg, Cell surface trafficking of Fas: a rapid mechanism of p53-mediated apoptosis, Science 282 (1998) 290-293.

[36] G. Marino, M. Niso-Santano, E.H. Baehrecke & G. Kroemer, Self-consumption: the interplay of autophagy and apoptosis, Nat.Rev.Mol.Cell Biol. 15 (2014) 81-94.

[37] R.J. Kaufman, Orchestrating the unfolded protein response in health and disease, J.Clin.Invest. 110 (2002) 1389-1398.

[38] D. Scheuner, B. Song, E. McEwen, C. Liu, R. Laybutt, P. Gillespie, T. Saunders, S. Bonner-Weir, et al, Translational control is required for the unfolded protein response and in vivo glucose homeostasis, Mol.Cell 7 (2001) 1165-1176.

[39] K.D. McCullough, J.L. Martindale, L.O. Klotz, T.Y. Aw & N.J. Holbrook, Gadd153 sensitizes cells to endoplasmic reticulum stress by down-regulating Bcl2 and perturbing the cellular redox state, Mol.Cell.Biol. 21 (2001) 1249-1259.

[40] C.Y. Liu, M. Schroder & R.J. Kaufman, Ligand-independent dimerization activates the stress response kinases IRE1 and PERK in the lumen of the endoplasmic reticulum, J.Biol.Chem. 275 (2000) 24881-24885.

[41] T. Gotoh, K. Terada, S. Oyadomari & M. Mori, hsp70-DnaJ chaperone pair prevents nitric oxide- and CHOP-induced apoptosis by inhibiting translocation of Bax to mitochondria, Cell Death Differ. 11 (2004) 390-402.

[42] F. Urano, X. Wang, A. Bertolotti, Y. Zhang, P. Chung, H.P. Harding & D. Ron, Coupling of stress in the ER to activation of JNK protein kinases by transmembrane protein kinase IRE1, Science 287 (2000) 664-666.

[43] T. Yoneda, K. Imaizumi, K. Oono, D. Yui, F. Gomi, T. Katayama & M. Tohyama, Activation of caspase-12, an endoplastic reticulum (ER) resident caspase, through tumor necrosis factor receptor-associated factor 2-dependent mechanism in response to the ER stress, J.Biol.Chem. 276 (2001) 13935-13940.

[44] V.I. Rasheva & P.M. Domingos, Cellular responses to endoplasmic reticulum stress and apoptosis, Apoptosis 14 (2009) 996-1007.

[45] R.V. Rao, H.M. Ellerby & D.E. Bredesen, Coupling endoplasmic reticulum stress to the cell death program, Cell Death Differ. 11 (2004) 372-380.

[46] B. Ravikumar, S. Sarkar, J.E. Davies, M. Futter, M. Garcia-Arencibia, Z.W. Green-Thompson, M. Jimenez-Sanchez, V.I. Korolchuk, et al, Regulation of mammalian autophagy in physiology and pathophysiology, Physiol.Rev. 90 (2010) 1383-1435.

[47] S. Alers, A.S. Loffler, S. Wesselborg & B. Stork, Role of AMPK-mTOR-Ulk1/2 in the regulation of autophagy: cross talk, shortcuts, and feedbacks, Mol.Cell.Biol. 32 (2012) 2-11.

[48] C. He & D.J. Klionsky, Regulation mechanisms and signaling pathways of autophagy, Annu.Rev.Genet. 43 (2009) 67-93.

[49] B. Levine & G. Kroemer, Autophagy in the pathogenesis of disease, Cell 132 (2008) 27-42.

[50] M. Komatsu, S. Waguri, T. Ueno, J. Iwata, S. Murata, I. Tanida, J. Ezaki, N. Mizushima, et al, Impairment of starvation-induced and constitutive autophagy in Atg7-deficient mice, J.Cell Biol. 169 (2005) 425-434.

[51] G.M. Fimia, A. Stoykova, A. Romagnoli, L. Giunta, S. Di Bartolomeo, R. Nardacci, M. Corazzari, C. Fuoco, et al, Ambra1 regulates autophagy and development of the nervous system, Nature 447 (2007) 1121-1125.

[52] A. Kuma, M. Hatano, M. Matsui, A. Yamamoto, H. Nakaya, T. Yoshimori, Y. Ohsumi, T. Tokuhisa, et al, The role of autophagy during the early neonatal starvation period, Nature 432 (2004) 1032-1036.

[53] Y.S. Sou, S. Waguri, J. Iwata, T. Ueno, T. Fujimura, T. Hara, N. Sawada, A. Yamada, et al, The Atg8 conjugation system is indispensable for proper development of autophagic isolation membranes in mice, Mol.Biol.Cell 19 (2008) 4762-4775.

[54] T. Saitoh, N. Fujita, T. Hayashi, K. Takahara, T. Satoh, H. Lee, K. Matsunaga, S. Kageyama, et al, Atg9a controls dsDNA-driven dynamic translocation of STING and the innate immune response, Proc.Natl.Acad.Sci.U.S.A. 106 (2009) 20842-20846.

[55] T. Saitoh, N. Fujita, M.H. Jang, S. Uematsu, B.G. Yang, T. Satoh, H. Omori, T. Noda, et al, Loss of the autophagy protein Atg16L1 enhances endotoxin-induced IL-1beta production, Nature 456 (2008) 264-268.

[56] N. Hosokawa, T. Sasaki, S. Iemura, T. Natsume, T. Hara & N. Mizushima, Atg101, a novel mammalian autophagy protein interacting with Atg13, Autophagy 5 (2009) 973-979.

[57] C.H. Jung, C.B. Jun, S.H. Ro, Y.M. Kim, N.M. Otto, J. Cao, M. Kundu & D.H. Kim, ULK-Atg13-FIP200 complexes mediate mTOR signaling to the autophagy machinery, Mol.Biol.Cell 20 (2009) 1992-2003.

[58] I.G. Ganley, H. Lam du, J. Wang, X. Ding, S. Chen & X. Jiang, ULK1.ATG13.FIP200 complex mediates mTOR signaling and is essential for autophagy, J.Biol.Chem. 284 (2009) 12297-12305.

[59] C.H. Jung, S.H. Ro, J. Cao, N.M. Otto & D.H. Kim, mTOR regulation of autophagy, FEBS Lett. 584 (2010) 1287-1295.

[60] D.F. Egan, M.G. Chun, M. Vamos, H. Zou, J. Rong, C.J. Miller, H.J. Lou, D. Raveendra-Panickar, et al, Small Molecule Inhibition of the Autophagy Kinase ULK1 and Identification of ULK1 Substrates, Mol.Cell 59 (2015) 285-297.

[61] R.C. Russell, Y. Tian, H. Yuan, H.W. Park, Y.Y. Chang, J. Kim, H. Kim, T.P. Neufeld, et al, ULK1 induces autophagy by phosphorylating Beclin-1 and activating VPS34 lipid kinase, Nat.Cell Biol. 15 (2013) 741-750.

[62] J. Xu, M. Fotouhi & P.S. McPherson, Phosphorylation of the exchange factor DENND3 by ULK in response to starvation activates Rab12 and induces autophagy, EMBO Rep. 16 (2015) 709-718.

[63] A. Tassa, M.P. Roux, D. Attaix & D.M. Bechet, Class III phosphoinositide 3-kinase--Beclin1 complex mediates the amino acid-dependent regulation of autophagy in C2C12 myotubes, Biochem.J. 376 (2003) 577-586.

[64] B. Ravikumar, K. Moreau, L. Jahreiss, C. Puri & D.C. Rubinsztein, Plasma membrane contributes to the formation of pre-autophagosomal structures, Nat.Cell Biol. 12 (2010) 747-757.

[65] M. Hayashi-Nishino, N. Fujita, T. Noda, A. Yamaguchi, T. Yoshimori & A. Yamamoto, Electron tomography reveals the endoplasmic reticulum as a membrane source for autophagosome formation, Autophagy 6 (2010) 301-303.

[66] ------. A subdomain of the endoplasmic reticulum forms a cradle for autophagosome formation, Nat.Cell Biol. 11 (2009) 1433-1437.

[67] D.W. Hailey, A.S. Rambold, P. Satpute-Krishnan, K. Mitra, R. Sougrat, P.K. Kim & J. Lippincott-Schwartz, Mitochondria supply membranes for autophagosome biogenesis during starvation, Cell 141 (2010) 656-667.

[68] M. Hamasaki, N. Furuta, A. Matsuda, A. Nezu, A. Yamamoto, N. Fujita, H. Oomori, T. Noda, et al, Autophagosomes form at ER-mitochondria contact sites, Nature 495 (2013) 389-393.

[69] T. Garofalo, P. Matarrese, V. Manganelli, M. Marconi, A. Tinari, L. Gambardella, A. Faggioni, R. Misasi, et al, Evidence for the involvement of lipid rafts localized at the ER-mitochondria associated membranes in autophagosome formation, Autophagy 12 (2016) 917-935.

[70] S. Pattingre, A. Tassa, X. Qu, R. Garuti, X.H. Liang, N. Mizushima, M. Packer, M.D. Schneider, et al, Bcl-2 antiapoptotic proteins inhibit Beclin 1-dependent autophagy, Cell 122 (2005) 927-939.

[71] S. Di Bartolomeo, M. Corazzari, F. Nazio, S. Oliverio, G. Lisi, M. Antonioli, V. Pagliarini, S. Matteoni, et al, The dynamic interaction of AMBRA1 with the dynein motor complex regulates mammalian autophagy, J.Cell Biol. 191 (2010) 155-168.

[72] A.R. Young, E.Y. Chan, X.W. Hu, R. Kochl, S.G. Crawshaw, S. High, D.W. Hailey, J. Lippincott-Schwartz, et al, Starvation and ULK1-dependent cycling of mammalian Atg9 between the TGN and endosomes, J.Cell.Sci. 119 (2006) 3888-3900.

[73] H.E. Polson, J. de Lartigue, D.J. Rigden, M. Reedijk, S. Urbe, M.J. Clague & S.A. Tooze, Mammalian Atg18 (WIPI2) localizes to omegasome-anchored phagophores and positively regulates LC3 lipidation, Autophagy 6 (2010) 506-522.

[74] E.L. Axe, S.A. Walker, M. Manifava, P. Chandra, H.L. Roderick, A. Habermann, G. Griffiths & N.T. Ktistakis, Autophagosome formation from membrane compartments enriched in phosphatidylinositol 3-phosphate and dynamically connected to the endoplasmic reticulum, J.Cell Biol. 182 (2008) 685-701.

[75] T. Hanada, N.N. Noda, Y. Satomi, Y. Ichimura, Y. Fujioka, T. Takao, F. Inagaki & Y. Ohsumi, The Atg12-Atg5 conjugate has a novel E3-like activity for protein lipidation in autophagy, J.Biol.Chem. 282 (2007) 37298-37302.

[76] N. Mizushima, A. Kuma, Y. Kobayashi, A. Yamamoto, M. Matsubae, T. Takao, T. Natsume, Y. Ohsumi, et al, Mouse Apg16L, a novel WD-repeat protein, targets to the autophagic isolation membrane with the Apg12-Apg5 conjugate, J.Cell.Sci. 116 (2003) 1679-1688.

[77] I. Tanida, E. Tanida-Miyake, T. Ueno & E. Kominami, The human homolog of Saccharomyces cerevisiae Apg7p is a Protein-activating enzyme for multiple substrates including human Apg12p, GATE-16, GABARAP, and MAP-LC3, J.Biol.Chem. 276 (2001) 1701-1706.

[78] I. Tanida, Y.S. Sou, J. Ezaki, N. Minematsu-Ikeguchi, T. Ueno & E. Kominami, HsAtg4B/HsApg4B/autophagin-1 cleaves the carboxyl termini of three human Atg8 homologues and delipidates microtubule-associated protein light chain 3- and GABAA receptor-associated protein-phospholipid conjugates, J.Biol.Chem. 279 (2004) 36268-36276.

[79] J. Hemelaar, V.S. Lelyveld, B.M. Kessler & H.L. Ploegh, A single protease, Apg4B, is specific for the autophagy-related ubiquitin-like proteins GATE-16, MAP1-LC3, GABARAP, and Apg8L, J.Biol.Chem. 278 (2003) 51841-51850.

[80] Y. Kabeya, N. Mizushima, T. Ueno, A. Yamamoto, T. Kirisako, T. Noda, E. Kominami, Y. Ohsumi, et al, LC3, a mammalian homologue of yeast Apg8p, is localized in autophagosome membranes after processing, EMBO J. 19 (2000) 5720-5728.

[81] Y. Tanaka, G. Guhde, A. Suter, E.L. Eskelinen, D. Hartmann, R. Lullmann-Rauch, P.M. Janssen, J. Blanz, et al, Accumulation of autophagic vacuoles and cardiomyopathy in LAMP-2-deficient mice, Nature 406 (2000) 902-906.

[82] B.D. Manning, A.R. Tee, M.N. Logsdon, J. Blenis & L.C. Cantley, Identification of the tuberous sclerosis complex-2 tumor suppressor gene product tuberin as a target of the phosphoinositide 3-kinase/akt pathway, Mol.Cell 10 (2002) 151-162.

[83] X. Long, Y. Lin, S. Ortiz-Vega, K. Yonezawa & J. Avruch, Rheb binds and regulates the mTOR kinase, Curr.Biol. 15 (2005) 702-713.

[84] X. Gao, Y. Zhang, P. Arrazola, O. Hino, T. Kobayashi, R.S. Yeung, B. Ru & D. Pan, Tsc tumour suppressor proteins antagonize amino-acid-TOR signalling, Nat.Cell Biol. 4 (2002) 699-704.

[85] E. Kim, P. Goraksha-Hicks, L. Li, T.P. Neufeld & K.L. Guan, Regulation of TORC1 by Rag GTPases in nutrient response, Nat.Cell Biol. 10 (2008) 935-945.

[86] Y. Sancak, T.R. Peterson, Y.D. Shaul, R.A. Lindquist, C.C. Thoreen, L. Bar-Peled & D.M. Sabatini, The Rag GTPases bind raptor and mediate amino acid signaling to mTORC1, Science 320 (2008) 1496-1501.

[87] Y. Sancak, L. Bar-Peled, R. Zoncu, A.L. Markhard, S. Nada & D.M. Sabatini, Ragulator-Rag complex targets mTORC1 to the lysosomal surface and is necessary for its activation by amino acids, Cell 141 (2010) 290-303.

[88] D.M. Gwinn, D.B. Shackelford, D.F. Egan, M.M. Mihaylova, A. Mery, D.S. Vasquez, B.E. Turk & R.J. Shaw, AMPK phosphorylation of raptor mediates a metabolic checkpoint, Mol.Cell 30 (2008) 214-226.

[89] K. Inoki, T. Zhu & K.L. Guan, TSC2 mediates cellular energy response to control cell growth and survival, Cell 115 (2003) 577-590.

[90] J. Kim, M. Kundu, B. Viollet & K.L. Guan, AMPK and mTOR regulate autophagy through direct phosphorylation of Ulk1, Nat.Cell Biol. 13 (2011) 132-141.

[91] J.W. Lee, S. Park, Y. Takahashi & H.G. Wang, The association of AMPK with ULK1 regulates autophagy, PLoS One 5 (2010) e15394.

[92] R. Scherz-Shouval, E. Shvets, E. Fass, H. Shorer, L. Gil & Z. Elazar, Reactive oxygen species are essential for autophagy and specifically regulate the activity of Atg4, EMBO J. 26 (2007) 1749-1760.

[93] B. Liu, Y. Cheng, B. Zhang, H.J. Bian & J.K. Bao, Polygonatum cyrtonema lectin induces apoptosis and autophagy in human melanoma A375 cells through a mitochondria-mediated ROS-p38-p53 pathway, Cancer Lett. 275 (2009) 54-60.

[94] L. Cao, J. Xu, Y. Lin, X. Zhao, X. Liu & Z. Chi, Autophagy is upregulated in rats with status epilepticus and partly inhibited by Vitamin E, Biochem.Biophys.Res.Commun. 379 (2009) 949-953.

[95] A. Alexander, S.L. Cai, J. Kim, A. Nanez, M. Sahin, K.H. MacLean, K. Inoki, K.L. Guan, et al, ATM signals to TSC2 in the cytoplasm to regulate mTORC1 in response to ROS, Proc.Natl.Acad.Sci.U.S.A. 107 (2010) 4153-4158.

[96] Y. Chen, E. McMillan-Ward, J. Kong, S.J. Israels & S.B. Gibson, Oxidative stress induces autophagic cell death independent of apoptosis in transformed and cancer cells, Cell Death Differ. 15 (2008) 171-182.

[97] Y. Wei, S. Pattingre, S. Sinha, M. Bassik & B. Levine, JNK1-mediated phosphorylation of Bcl-2 regulates starvation-induced autophagy, Mol.Cell 30 (2008) 678-688.

[98] A.H. Chaanine, D. Jeong, L. Liang, E.R. Chemaly, K. Fish, R.E. Gordon & R.J. Hajjar, JNK modulates FOXO3a for the expression of the mitochondrial death and mitophagy marker BNIP3 in pathological hypertrophy and in heart failure, Cell.Death Dis. 3 (2012) 265.

[99] S. Furuta, E. Hidaka, A. Ogata, S. Yokota & T. Kamata, Ras is involved in the negative control of autophagy through the class I PI3-kinase, Oncogene 23 (2004) 3898-3904.

[100] S. Pattingre, C. Bauvy & P. Codogno, Amino acids interfere with the ERK1/2-dependent control of macroautophagy by controlling the activation of Raf-1 in human colon cancer HT-29 cells, J.Biol.Chem. 278 (2003) 16667-16674.

[101] S. Pankiv, T.H. Clausen, T. Lamark, A. Brech, J.A. Bruun, H. Outzen, A. Overvatn, G. Bjorkoy, et al, p62/SQSTM1 binds directly to Atg8/LC3 to facilitate degradation of ubiquitinated protein aggregates by autophagy, J.Biol.Chem. 282 (2007) 24131-24145.

[102] Y. Ichimura, T. Kumanomidou, Y.S. Sou, T. Mizushima, J. Ezaki, T. Ueno, E. Kominami, T. Yamane, et al, Structural basis for sorting mechanism of p62 in selective autophagy, J.Biol.Chem. 283 (2008) 22847-22857.

[103] D.J. Klionsky, K. Abdelmohsen, A. Abe, M.J. Abedin, H. Abeliovich, A. Acevedo Arozena, H. Adachi, C.M. Adams, et al, Guidelines for the use and interpretation of assays for monitoring autophagy (3rd edition), Autophagy 12 (2016) 1-222.

[104] V. Kirkin, T. Lamark, Y.S. Sou, G. Bjorkoy, J.L. Nunn, J.A. Bruun, E. Shvets, D.G. McEwan, et al, A role for NBR1 in autophagosomal degradation of ubiquitinated substrates, Mol.Cell 33 (2009) 505-516.

[105] S. Carra, S.J. Seguin, H. Lambert & J. Landry, HspB8 chaperone activity toward poly(Q)-containing proteins depends on its association with Bag3, a stimulator of macroautophagy, J.Biol.Chem. 283 (2008) 1437-1444.

[106] M. Gamerdinger, A.M. Kaya, U. Wolfrum, A.M. Clement & C. Behl, BAG3 mediates chaperone-based aggresome-targeting and selective autophagy of misfolded proteins, EMBO Rep. 12 (2011) 149-156.

[107] G. Ashrafi & T.L. Schwarz, The pathways of mitophagy for quality control and clearance of mitochondria, Cell Death Differ. 20 (2013) 31-42.

[108] M.J. Costello, L.A. Brennan, S. Basu, D. Chauss, A. Mohamed, K.O. Gilliland, S. Johnsen, A.S. Menko, et al, Autophagy and mitophagy participate in ocular lens organelle degradation, Exp.Eye Res. 116 (2013) 141-150.

[109] H. Sandoval, P. Thiagarajan, S.K. Dasgupta, A. Schumacher, J.T. Prchal, M. Chen & J. Wang, Essential role for Nix in autophagic maturation of erythroid cells, Nature 454 (2008) 232-235.

[110] J. Sin, A.M. Andres, D.J. Taylor, T. Weston, Y. Hiraumi, A. Stotland, B.J. Kim, C. Huang, et al, Mitophagy is required for mitochondrial biogenesis and myogenic differentiation of C2C12 myoblasts, Autophagy(2015) 0.

[111] E.M. Valente, P.M. Abou-Sleiman, V. Caputo, M.M. Muqit, K. Harvey, S. Gispert, Z. Ali, D. Del Turco, et al, Hereditary early-onset Parkinson's disease caused by mutations in PINK1, Science 304 (2004) 1158-1160.

[112] T. Kitada, S. Asakawa, N. Hattori, H. Matsumine, Y. Yamamura, S. Minoshima, M. Yokochi, Y. Mizuno, et al, Mutations in the parkin gene cause autosomal recessive juvenile parkinsonism, Nature 392 (1998) 605-608.

[113] E. Deas, H. Plun-Favreau, S. Gandhi, H. Desmond, S. Kjaer, S.H. Loh, A.E. Renton, R.J. Harvey, et al, PINK1 cleavage at position A103 by the mitochondrial protease PARL, Hum.Mol.Genet. 20 (2011) 867-879.

[114] S.M. Jin, M. Lazarou, C. Wang, L.A. Kane, D.P. Narendra & R.J. Youle, Mitochondrial membrane potential regulates PINK1 import and proteolytic destabilization by PARL, J.Cell Biol. 191 (2010) 933-942.

[115] D. Narendra, A. Tanaka, D.F. Suen & R.J. Youle, Parkin is recruited selectively to impaired mitochondria and promotes their autophagy, J.Cell Biol. 183 (2008) 795-803.

[116] D.P. Narendra, S.M. Jin, A. Tanaka, D.F. Suen, C.A. Gautier, J. Shen, M.R. Cookson & R.J. Youle, PINK1 is selectively stabilized on impaired mitochondria to activate Parkin, PLoS Biol. 8 (2010) e1000298.

[117] D. Narendra, L.A. Kane, D.N. Hauser, I.M. Fearnley & R.J. Youle, p62/SQSTM1 is required for Parkin-induced mitochondrial clustering but not mitophagy; VDAC1 is dispensable for both, Autophagy 6 (2010) 1090-1106.

[118] S. Geisler, K.M. Holmstrom, D. Skujat, F.C. Fiesel, O.C. Rothfuss, P.J. Kahle & W. Springer, PINK1/Parkin-mediated mitophagy is dependent on VDAC1 and p62/SQSTM1, Nat.Cell Biol. 12 (2010) 119-131.

[119] Y. Kim, J. Park, S. Kim, S. Song, S.K. Kwon, S.H. Lee, T. Kitada, J.M. Kim, et al, PINK1 controls mitochondrial localization of Parkin through direct phosphorylation, Biochem.Biophys.Res.Commun. 377 (2008) 975-980.

[120] K. Shiba-Fukushima, T. Arano, G. Matsumoto, T. Inoshita, S. Yoshida, Y. Ishihama, K.Y. Ryu, N. Nukina, et al, Phosphorylation of mitochondrial polyubiquitin by PINK1 promotes Parkin mitochondrial tethering, PLoS Genet. 10 (2014) e1004861.

[121] V. Sauve, A. Lilov, M. Seirafi, M. Vranas, S. Rasool, G. Kozlov, T. Sprules, J. Wang, et al, A Ubl/ubiquitin switch in the activation of Parkin, EMBO J.(2015).

[122] A. Ordureau, J.M. Heo, D.M. Duda, J.A. Paulo, J.L. Olszewski, D. Yanishevski, J. Rinehart, B.A. Schulman, et al, Defining roles of PARKIN and ubiquitin phosphorylation by PINK1 in mitochondrial quality control using a ubiquitin replacement strategy, Proc.Natl.Acad.Sci.U.S.A. 112 (2015) 6637-6642.

[123] M.A. Fedorowicz, R.L. de Vries-Schneider, C. Rub, D. Becker, Y. Huang, C. Zhou, D.M. Alessi Wolken, W. Voos, et al, Cytosolic cleaved PINK1 represses Parkin translocation to mitochondria and mitophagy, EMBO Rep. 15 (2014) 86-93.

[124] N.C. Chan, A.M. Salazar, A.H. Pham, M.J. Sweredoski, N.J. Kolawa, R.L. Graham, S. Hess & D.C. Chan, Broad activation of the ubiquitin-proteasome system by Parkin is critical for mitophagy, Hum.Mol.Genet. 20 (2011) 1726-1737.

[125] M.E. Gegg, J.M. Cooper, K.Y. Chau, M. Rojo, A.H. Schapira & J.W. Taanman, Mitofusin 1 and mitofusin 2 are ubiquitinated in a PINK1/parkin-dependent manner upon induction of mitophagy, Hum.Mol.Genet. 19 (2010) 4861-4870.

[126] W.X. Ding, H.M. Ni, M. Li, Y. Liao, X. Chen, D.B. Stolz, G.W. Dorn 2nd & X.M. Yin, Nix is critical to two distinct phases of mitophagy, reactive oxygen species-mediated autophagy induction and Parkin-ubiquitin-p62-mediated mitochondrial priming, J.Biol.Chem. 285 (2010) 27879-27890.

[127] K. Okatsu, K. Saisho, M. Shimanuki, K. Nakada, H. Shitara, Y.S. Sou, M. Kimura, S. Sato, et al, p62/SQSTM1 cooperates with Parkin for perinuclear clustering of depolarized mitochondria, Genes Cells 15 (2010) 887-900.

[128] M. Lazarou, D.A. Sliter, L.A. Kane, S.A. Sarraf, C. Wang, J.L. Burman, D.P. Sideris, A.I. Fogel, et al, The ubiquitin kinase PINK1 recruits autophagy receptors to induce mitophagy, Nature 524 (2015) 309-314.

[129] S.R. Yoshii, C. Kishi, N. Ishihara & N. Mizushima, Parkin mediates proteasome-dependent protein degradation and rupture of the outer mitochondrial membrane, J.Biol.Chem. 286 (2011) 19630-19640.

[130] Y. Sun, A.A. Vashisht, J. Tchieu, J.A. Wohlschlegel & L. Dreier, Voltage-dependent anion channels (VDACs) recruit Parkin to defective mitochondria to promote mitochondrial autophagy, J.Biol.Chem. 287 (2012) 40652-40660.

[131] X. Wang, D. Winter, G. Ashrafi, J. Schlehe, Y.L. Wong, D. Selkoe, S. Rice, J. Steen, et al, PINK1 and Parkin target Miro for phosphorylation and degradation to arrest mitochondrial motility, Cell 147 (2011) 893-906.

[132] A. Tanaka, M.M. Cleland, S. Xu, D.P. Narendra, D.F. Suen, M. Karbowski & R.J. Youle, Proteasome and p97 mediate mitophagy and degradation of mitofusins induced by Parkin, J.Cell Biol. 191 (2010) 1367-1380.

[133] Y. Chen & G.W. Dorn 2nd, PINK1-phosphorylated mitofusin 2 is a Parkin receptor for culling damaged mitochondria, Science 340 (2013) 471-475.

[134] G. Twig, A. Elorza, A.J. Molina, H. Mohamed, J.D. Wikstrom, G. Walzer, L. Stiles, S.E. Haigh, et al, Fission and selective fusion govern mitochondrial segregation and elimination by autophagy, EMBO J. 27 (2008) 433-446.

[135] M. Lazarou, S.M. Jin, L.A. Kane & R.J. Youle, Role of PINK1 binding to the TOM complex and alternate intracellular membranes in recruitment and activation of the E3 ligase Parkin, Dev.Cell. 22 (2012) 320-333.

[136] K. Okamoto, N. Kondo-Okamoto & Y. Ohsumi, Mitochondria-anchored receptor Atg32 mediates degradation of mitochondria via selective autophagy, Dev.Cell. 17 (2009) 87-97.

[137] T. Kanki, K. Wang, Y. Cao, M. Baba & D.J. Klionsky, Atg32 is a mitochondrial protein that confers selectivity during mitophagy, Dev.Cell. 17 (2009) 98-109.

[138] T. Murakawa, O. Yamaguchi, A. Hashimoto, S. Hikoso, T. Takeda, T. Oka, H. Yasui, H. Ueda, et al, Bcl-2-like protein 13 is a mammalian Atg32 homologue that mediates mitophagy and mitochondrial fragmentation, Nat.Commun. 6 (2015) 7527.

[139] A. Stolz, A. Ernst & I. Dikic, Cargo recognition and trafficking in selective autophagy, Nat.Cell Biol. 16 (2014) 495-501.

[140] J. Zhang & P.A. Ney, Role of BNIP3 and NIX in cell death, autophagy, and mitophagy, Cell Death Differ. 16 (2009) 939-946.

[141] K. Tracy, B.C. Dibling, B.T. Spike, J.R. Knabb, P. Schumacker & K.F. Macleod, BNIP3 is an RB/E2F target gene required for hypoxia-induced autophagy, Mol.Cell.Biol. 27 (2007) 6229-6242.

[142] S. Rikka, M.N. Quinsay, R.L. Thomas, D.A. Kubli, X. Zhang, A.N. Murphy & A.B. Gustafsson, Bnip3 impairs mitochondrial bioenergetics and stimulates mitochondrial turnover, Cell Death Differ. 18 (2011) 721-731.

[143] A. Hamacher-Brady, N.R. Brady, S.E. Logue, M.R. Sayen, M. Jinno, L.A. Kirshenbaum, R.A. Gottlieb & A.B. Gustafsson, Response to myocardial ischemia/reperfusion injury involves Bnip3 and autophagy, Cell Death Differ. 14 (2007) 146-157.

[144] C. Mammucari, G. Milan, V. Romanello, E. Masiero, R. Rudolf, P. Del Piccolo, S.J. Burden, R. Di Lisi, et al, FoxO3 controls autophagy in skeletal muscle in vivo, Cell.Metab. 6 (2007) 458-471.

[145] G. Bellot, R. Garcia-Medina, P. Gounon, J. Chiche, D. Roux, J. Pouyssegur & N.M. Mazure, Hypoxia-induced autophagy is mediated through hypoxia-inducible factor induction of BNIP3 and BNIP3L via their BH3 domains, Mol.Cell.Biol. 29 (2009) 2570-2581.

[146] R.A. Hanna, M.N. Quinsay, A.M. Orogo, K. Giang, S. Rikka & A.B. Gustafsson, Microtubule-associated protein 1 light chain 3 (LC3) interacts with Bnip3 protein to selectively remove endoplasmic reticulum and mitochondria via autophagy, J.Biol.Chem. 287 (2012) 19094-19104.

[147] I. Novak, V. Kirkin, D.G. McEwan, J. Zhang, P. Wild, A. Rozenknop, V. Rogov, F. Lohr, et al, Nix is a selective autophagy receptor for mitochondrial clearance, EMBO Rep. 11 (2010) 45-51.

[148] M. Schwarten, J. Mohrluder, P. Ma, M. Stoldt, Y. Thielmann, T. Stangler, N. Hersch, B. Hoffmann, et al, Nix directly binds to GABARAP: a possible crosstalk between apoptosis and autophagy, Autophagy 5 (2009) 690-698.

[149] T. Zhang, L. Xue, L. Li, C. Tang, Z. Wan, R. Wang, J. Tan, Y. Tan, et al, BNIP3 Protein Suppresses PINK1 Kinase Proteolytic Cleavage to Promote Mitophagy, J.Biol.Chem. 291 (2016) 21616-21629.

[150] Y. Lee, H.Y. Lee, R.A. Hanna & A.B. Gustafsson, Mitochondrial autophagy by Bnip3 involves Drp1-mediated mitochondrial fission and recruitment of Parkin in cardiac myocytes, Am.J.Physiol.Heart Circ.Physiol. 301 (2011) H1924-31.

[151] L. Liu, D. Feng, G. Chen, M. Chen, Q. Zheng, P. Song, Q. Ma, C. Zhu, et al, Mitochondrial outer-membrane protein FUNDC1 mediates hypoxia-induced mitophagy in mammalian cells, Nat.Cell Biol. 14 (2012) 177-185.

[152] W. Wu, W. Tian, Z. Hu, G. Chen, L. Huang, W. Li, X. Zhang, P. Xue, et al, ULK1 translocates to mitochondria and phosphorylates FUNDC1 to regulate mitophagy, EMBO Rep.(2014).

[153] C.T. Chu, J. Ji, R.K. Dagda, J.F. Jiang, Y.Y. Tyurina, A.A. Kapralov, V.A. Tyurin, N. Yanamala, et al, Cardiolipin externalization to the outer mitochondrial membrane acts as an elimination signal for mitophagy in neuronal cells, Nat.Cell Biol. 15 (2013) 1197-1205.

[154] Y.C. Wong & E.L. Holzbaur, Optineurin is an autophagy receptor for damaged mitochondria in parkin-mediated mitophagy that is disrupted by an ALS-linked mutation, Proc.Natl.Acad.Sci.U.S.A. 111 (2014) E4439-48.

[155] J.M. Heo, A. Ordureau, J.A. Paulo, J. Rinehart & J.W. Harper, The PINK1-PARKIN Mitochondrial Ubiquitylation Pathway Drives a Program of OPTN/NDP52 Recruitment and TBK1 Activation to Promote Mitophagy, Mol.Cell 60 (2015) 7-20.

[156] F. Strappazzon, F. Nazio, M. Corrado, V. Cianfanelli, A. Romagnoli, G.M. Fimia, S. Campello, R. Nardacci, et al, AMBRA1 is able to induce mitophagy via LC3 binding, regardless of PARKIN and p62/SQSTM1, Cell Death Differ. 22 (2015) 419-432.

[157] Q. Li, T. Zhang, J. Wang, Z. Zhang, Y. Zhai, G.Y. Yang & X. Sun, Rapamycin attenuates mitochondrial dysfunction via activation of mitophagy in experimental ischemic stroke, Biochem.Biophys.Res.Commun. 444 (2014) 182-188.

[158] M. Song, G. Gong, Y. Burelle, A.B. Gustafsson, R.N. Kitsis, S.J. Matkovich & G.W. Dorn 2nd, Interdependence of Parkin-Mediated Mitophagy and Mitochondrial Fission in Adult Mouse Hearts, Circ.Res.(2015).

[159] Z. Bhujabal, A.B. Birgisdottir, E. Sjottem, H.B. Brenne, A. Overvatn, S. Habisov, V. Kirkin, T. Lamark, et al, FKBP8 recruits LC3A to mediate Parkin-independent mitophagy, EMBO Rep.(2017).

[160] D.A. Kubli, M.Q. Cortez, A.G. Moyzis, R.H. Najor, Y. Lee & A.B. Gustafsson, PINK1 Is Dispensable for Mitochondrial Recruitment of Parkin and Activation of Mitophagy in Cardiac Myocytes, PLoS One 10 (2015) e0130707.

[161] V. Choubey, M. Cagalinec, J. Liiv, D. Safiulina, M.A. Hickey, M. Kuum, M. Liiv, T. Anwar, et al, BECN1 is involved in the initiation of mitophagy: it facilitates PARK2 translocation to mitochondria, Autophagy 10 (2014) 1105-1119.

[162] V. Gelmetti, P. De Rosa, L. Torosantucci, E.S. Marini, A. Romagnoli, M. Di Rienzo, G. Arena, D. Vignone, et al, PINK1 and BECN1 relocalize at mitochondria-associated membranes during mitophagy and promote ER-mitochondria tethering and autophagosome formation, Autophagy 13 (2017) 654-669.

[163] C. Van Humbeeck, T. Cornelissen, H. Hofkens, W. Mandemakers, K. Gevaert, B. De Strooper & W. Vandenberghe, Parkin interacts with Ambra1 to induce mitophagy, J.Neurosci. 31 (2011) 10249-10261.

[164] S. Michiorri, V. Gelmetti, E. Giarda, F. Lombardi, F. Romano, R. Marongiu, S. Nerini-Molteni, P. Sale, et al, The Parkinson-associated protein PINK1 interacts with Beclin1 and promotes autophagy, Cell Death Differ. 17 (2010) 962-974.

[165] M. Sandri, Autophagy in skeletal muscle, FEBS Lett. 584 (2010) 1411-1416.

[166] J. Zhao, J.J. Brault, A. Schild, P. Cao, M. Sandri, S. Schiaffino, S.H. Lecker & A.L. Goldberg, FoxO3 coordinately activates protein degradation by the autophagic/lysosomal and proteasomal pathways in atrophying muscle cells, Cell.Metab. 6 (2007) 472-483.

[167] S. Mordier, C. Deval, D. Bechet, A. Tassa & M. Ferrara, Leucine limitation induces autophagy and activation of lysosome-dependent proteolysis in C2C12 myotubes through a mammalian target of rapamycin-independent signaling pathway, J.Biol.Chem. 275 (2000) 29900-29906.

[168] N. Mizushima, A. Yamamoto, M. Matsui, T. Yoshimori & Y. Ohsumi, In vivo analysis of autophagy in response to nutrient starvation using transgenic mice expressing a fluorescent autophagosome marker, Mol.Biol.Cell 15 (2004) 1101-1111.

[169] A.L. Bujak, J.D. Crane, J.S. Lally, R.J. Ford, S.J. Kang, I.A. Rebalka, A.E. Green, B.E. Kemp, et al, AMPK activation of muscle autophagy prevents fasting-induced hypoglycemia and myopathy during aging, Cell.Metab. 21 (2015) 883-890.

[170] M.F. O'Leary, A. Vainshtein, H.N. Carter, Y. Zhang & D.A. Hood, Denervation-induced mitochondrial dysfunction and autophagy in skeletal muscle of apoptosis-deficient animals, Am.J.Physiol.Cell.Physiol. 303 (2012) C447-54.

[171] N. Furuya, S. Ikeda, S. Sato, S. Soma, J. Ezaki, J.A. Oliva Trejo, M. Takeda-Ezaki, T. Fujimura, et al, PARK2/Parkin-mediated mitochondrial clearance contributes to proteasome activation during slow-twitch muscle atrophy via NFE2L1 nuclear translocation, Autophagy 10 (2014) 631-641.

[172] T. Ogata, Y. Oishi, M. Higuchi & I. Muraoka, Fasting-related autophagic response in slow- and fast-twitch skeletal muscle, Biochem.Biophys.Res.Commun. 394 (2010) 136-140.

[173] G. Dobrowolny, M. Aucello, E. Rizzuto, S. Beccafico, C. Mammucari, S. Boncompagni, S. Belia, F. Wannenes, et al, Skeletal muscle is a primary target of SOD1G93A-mediated toxicity, Cell.Metab. 8 (2008) 425-436.

[174] F. Pietri-Rouxel, C. Gentil, S. Vassilopoulos, D. Baas, E. Mouisel, A. Ferry, A. Vignaud, C. Hourde, et al, DHPR alpha1S subunit controls skeletal muscle mass and morphogenesis, EMBO J. 29 (2010) 643-654.

[175] T.P. Braun, M. Szumowski, P.R. Levasseur, A.J. Grossberg, X. Zhu, A. Agarwal & D.L. Marks, Muscle atrophy in response to cytotoxic chemotherapy is dependent on intact glucocorticoid signaling in skeletal muscle, PLoS One 9 (2014) e106489.

[176] O. Schakman, M. Dehoux, S. Bouchuari, S. Delaere, P. Lause, N. Decroly, S.E. Shoelson & J.P. Thissen, Role of IGF-I and the TNFalpha/NF-kappaB pathway in the induction of muscle atrogenes by acute inflammation, Am.J.Physiol.Endocrinol.Metab. 303 (2012) E729-39.

[177] R. Troncoso, F. Paredes, V. Parra, D. Gatica, C. Vasquez-Trincado, C. Quiroga, R. Bravo-Sagua, C. Lopez-Crisosto, et al, Dexamethasone-induced autophagy mediates muscle atrophy through mitochondrial clearance, Cell.Cycle 13 (2014) 2281-2295.

[178] S.N. Hussain, M. Mofarrahi, I. Sigala, H.C. Kim, T. Vassilakopoulos, F. Maltais, I. Bellenis, R. Chaturvedi, et al, Mechanical ventilation-induced diaphragm disuse in humans triggers autophagy, Am.J.Respir.Crit.Care Med. 182 (2010) 1377-1386.

[179] D. Taillandier, E. Aurousseau, D. Meynial-Denis, D. Bechet, M. Ferrara, P. Cottin, A. Ducastaing, X. Bigard, et al, Coordinate activation of lysosomal, Ca 2+-activated and ATP-ubiquitin-dependent proteinases in the unweighted rat soleus muscle, Biochem.J. 316 (Pt 1) (1996) 65-72.

[180] S. Lokireddy, I.W. Wijesoma, S. Teng, S. Bonala, P.D. Gluckman, C. McFarlane, M. Sharma & R. Kambadur, The ubiquitin ligase Mul1 induces mitophagy in skeletal muscle in response to muscle-wasting stimuli, Cell.Metab. 16 (2012) 613-624.

[181] C. Jamart, A.V. Gomes, S. Dewey, L. Deldicque, J.M. Raymackers & M. Francaux, Regulation of ubiquitin-proteasome and autophagy pathways after acute LPS and epoxomicin administration in mice, BMC Musculoskelet.Disord. 15 (2014) 166-2474-15-166.

[182] E. Masiero, L. Agatea, C. Mammucari, B. Blaauw, E. Loro, M. Komatsu, D. Metzger, C. Reggiani, et al, Autophagy is required to maintain muscle mass, Cell.Metab. 10 (2009) 507-515.

[183] E.M. McMillan & J. Quadrilatero, Autophagy is required and protects against apoptosis during myoblast differentiation, Biochem.J.(2014).

[184] N. Raben, V. Hill, L. Shea, S. Takikita, R. Baum, N. Mizushima, E. Ralston & P. Plotz, Suppression of autophagy in skeletal muscle uncovers the accumulation of ubiquitinated proteins and their potential role in muscle damage in Pompe disease, Hum.Mol.Genet. 17 (2008) 3897-3908.

[185] M.C. Malicdan, S. Noguchi, I. Nonaka, P. Saftig & I. Nishino, Lysosomal myopathies: an excessive build-up in autophagosomes is too much to handle, Neuromuscul.Disord. 18 (2008) 521-529.

[186] D. Bloemberg, E. McDonald, D. Dulay & J. Quadrilatero, Autophagy is altered in skeletal and cardiac muscle of spontaneously hypertensive rats, Acta Physiol.(Oxf)(2013).

[187] M.J. Drummond, O. Addison, L. Brunker, P.N. Hopkins, D.A. McClain, P.C. LaStayo & R.L. Marcus, Downregulation of E3 ubiquitin ligases and mitophagy-related genes in skeletal muscle of physically inactive, frail older women: a cross-sectional comparison, J.Gerontol.A Biol.Sci.Med.Sci. 69 (2014) 1040-1048.

[188] P. Grumati, L. Coletto, A. Schiavinato, S. Castagnaro, E. Bertaggia, M. Sandri & P. Bonaldo, Physical exercise stimulates autophagy in normal skeletal muscles but is detrimental for collagen VI-deficient muscles, Autophagy 7 (2011) 1415-1423.

[189] C. He, M.C. Bassik, V. Moresi, K. Sun, Y. Wei, Z. Zou, Z. An, J. Loh, et al, Exercise-induced BCL2-regulated autophagy is required for muscle glucose homeostasis, Nature 481 (2012) 511-515.

[190] A.M. Sanchez, H. Bernardi, G. Py & R.B. Candau, Autophagy is essential to support skeletal muscle plasticity in response to endurance exercise, Am.J.Physiol.Regul.Integr.Comp.Physiol. 307 (2014) R956-69.

[191] V.A. Lira, M. Okutsu, M. Zhang, N.P. Greene, R.C. Laker, D.S. Breen, K.L. Hoehn & Z. Yan, Autophagy is required for exercise training-induced skeletal muscle adaptation and improvement of physical performance, FASEB J. 27 (2013) 4184-4193.

[192] F. Lo Verso, S. Carnio, A. Vainshtein & M. Sandri, Autophagy is not required to sustain exercise and PRKAA1/AMPK activity but is important to prevent mitochondrial damage during physical activity, Autophagy 10 (2014) 1883-1894.

[193] A. Vainshtein, L.D. Tryon, M. Pauly & D.A. Hood, Role of PGC-1alpha during acute exercise-induced autophagy and mitophagy in skeletal muscle, Am.J.Physiol.Cell.Physiol. 308 (2015) C710-9.

[194] V. Moresi, M. Carrer, C.E. Grueter, O.F. Rifki, J.M. Shelton, J.A. Richardson, R. Bassel-Duby & E.N. Olson, Histone deacetylases 1 and 2 regulate autophagy flux and skeletal muscle homeostasis in mice, Proc.Natl.Acad.Sci.U.S.A. 109 (2012) 1649-1654.

[195] M.C. Maiuri, G. Le Toumelin, A. Criollo, J.C. Rain, F. Gautier, P. Juin, E. Tasdemir, G. Pierron, et al, Functional and physical interaction between Bcl-X(L) and a BH3-like domain in Beclin-1, EMBO J. 26 (2007) 2527-2539.

[196] E. Tasdemir, M.C. Maiuri, L. Galluzzi, I. Vitale, M. Djavaheri-Mergny, M. D'Amelio, A. Criollo, E. Morselli, et al, Regulation of autophagy by cytoplasmic p53, Nat.Cell Biol. 10 (2008) 676-687.

[197] E. Morselli, S. Shen, C. Ruckenstuhl, M.A. Bauer, G. Marino, L. Galluzzi, A. Criollo, M. Michaud, et al, p53 inhibits autophagy by interacting with the human ortholog of yeast Atg17, RB1CC1/FIP200, Cell.Cycle 10 (2011) 2763-2769.

[198] A. Hoshino, Y. Mita, Y. Okawa, M. Ariyoshi, E. Iwai-Kanai, T. Ueyama, K. Ikeda, T. Ogata, et al, Cytosolic p53 inhibits Parkin-mediated mitophagy and promotes mitochondrial dysfunction in the mouse heart, Nat.Commun. 4 (2013) 2308.

[199] Z. Feng, W. Hu, E. de Stanchina, A.K. Teresky, S. Jin, S. Lowe & A.J. Levine, The regulation of AMPK beta1, TSC2, and PTEN expression by p53: stress, cell and tissue specificity, and the role of these gene products in modulating the IGF-1-AKT-mTOR pathways, Cancer Res. 67 (2007) 3043-3053.

[200] D. Crighton, S. Wilkinson, J. O'Prey, N. Syed, P. Smith, P.R. Harrison, M. Gasco, O. Garrone, et al, DRAM, a p53-induced modulator of autophagy, is critical for apoptosis, Cell 126 (2006) 121-134.

[201] X.D. Zhang, L. Qi, J.C. Wu & Z.H. Qin, DRAM1 regulates autophagy flux through lysosomes, PLoS One 8 (2013) e63245.

[202] M. Ott, J.D. Robertson, V. Gogvadze, B. Zhivotovsky & S. Orrenius, Cytochrome c release from mitochondria proceeds by a two-step process, Proc.Natl.Acad.Sci.U.S.A. 99 (2002) 1259-1263.

[203] F. Gonzalvez, Z.T. Schug, R.H. Houtkooper, E.D. MacKenzie, D.G. Brooks, R.J. Wanders, P.X. Petit, F.M. Vaz, et al, Cardiolipin provides an essential activating platform for caspase-8 on mitochondria, J.Cell Biol. 183 (2008) 681-696.

[204] W. Korytowski, L.V. Basova, A. Pilat, R.M. Kernstock & A.W. Girotti, Permeabilization of the mitochondrial outer membrane by Bax/truncated Bid (tBid) proteins as sensitized by cardiolipin hydroperoxide translocation: mechanistic implications for the intrinsic pathway of oxidative apoptosis, J.Biol.Chem. 286 (2011) 26334-26343.

[205] E. Zalckvar, H. Berissi, L. Mizrachy, Y. Idelchuk, I. Koren, M. Eisenstein, H. Sabanay, R. Pinkas-Kramarski, et al, DAP-kinase-mediated phosphorylation on the BH3 domain of beclin 1 promotes dissociation of beclin 1 from Bcl-XL and induction of autophagy, EMBO Rep. 10 (2009) 285-292.

[206] R.C. Wang, Y. Wei, Z. An, Z. Zou, G. Xiao, G. Bhagat, M. White, J. Reichelt, et al, Akt-mediated regulation of autophagy and tumorigenesis through Beclin 1 phosphorylation, Science 338 (2012) 956-959.

[207] L. del Peso, M. Gonzalez-Garcia, C. Page, R. Herrera & G. Nunez, Interleukin-3-induced phosphorylation of BAD through the protein kinase Akt, Science 278 (1997) 687-689.

[208] Y. Xu, J. Yuan & M.M. Lipinski, Live imaging and single-cell analysis reveal differential dynamics of autophagy and apoptosis, Autophagy 9 (2013) 1418-1430.

[209] T. Pan, P. Rawal, Y. Wu, W. Xie, J. Jankovic & W. Le, Rapamycin protects against rotenone-induced apoptosis through autophagy induction, Neuroscience 164 (2009) 541-551.

[210] B. Ravikumar, Z. Berger, C. Vacher, C.J. O'Kane & D.C. Rubinsztein, Rapamycin pre-treatment protects against apoptosis, Hum.Mol.Genet. 15 (2006) 1209-1216.

[211] Y. Yang, D. Xing, F. Zhou & Q. Chen, Mitochondrial autophagy protects against heat shock-induced apoptosis through reducing cytosolic cytochrome c release and downstream caspase-3 activation, Biochem.Biophys.Res.Commun. 395 (2010) 190-195.

[212] L.P. MacCormac, M.M. Muqit, D.J. Faulkes, N.W. Wood & D.S. Latchman, Reduction in endogenous parkin levels renders glial cells sensitive to both caspase-dependent and caspase-independent cell death, Eur.J.Neurosci. 20 (2004) 2038-2048.

[213] D.A. Kubli, X. Zhang, Y. Lee, R.A. Hanna, M.N. Quinsay, C.K. Nguyen, R. Jimenez, S. Petrosyan, et al, Parkin protein deficiency exacerbates cardiac injury and reduces survival following myocardial infarction, J.Biol.Chem. 288 (2013) 915-926.

[214] Y. Zhu, S. Massen, M. Terenzio, V. Lang, S. Chen-Lindner, R. Eils, I. Novak, I. Dikic, et al, Modulation of serines 17 and 24 in the LC3-interacting region of Bnip3 determines pro-survival mitophagy versus apoptosis, J.Biol.Chem. 288 (2013) 1099-1113.

[215] G. Arena, V. Gelmetti, L. Torosantucci, D. Vignone, G. Lamorte, P. De Rosa, E. Cilia, E.A. Jonas, et al, PINK1 protects against cell death induced by mitochondrial depolarization, by phosphorylating Bcl-xL and impairing its pro-apoptotic cleavage, Cell Death Differ. 20 (2013) 920-930.

[216] C.A. da Costa, C. Sunyach, E. Giaime, A. West, O. Corti, A. Brice, S. Safe, P.M. Abou-Sleiman, et al, Transcriptional repression of p53 by parkin and impairment by mutations associated with autosomal recessive juvenile Parkinson's disease, Nat.Cell Biol. 11 (2009) 1370-1375.

[217] W. Hou, J. Han, C. Lu, L.A. Goldstein & H. Rabinowich, Autophagic degradation of active caspase-8: a crosstalk mechanism between autophagy and apoptosis, Autophagy 6 (2010) 891-900.

[218] S. Saita, M. Shirane & K.I. Nakayama, Selective escape of proteins from the mitochondria during mitophagy, Nat.Commun. 4 (2013) 1410.

[219] S. Luo & D.C. Rubinsztein, Apoptosis blocks Beclin 1-dependent autophagosome synthesis: an effect rescued by Bcl-xL, Cell Death Differ. 17 (2010) 268-277.

[220] E. Wirawan, L. Vande Walle, K. Kersse, S. Cornelis, S. Claerhout, I. Vanoverberghe, R. Roelandt, R. De Rycke, et al, Caspase-mediated cleavage of Beclin-1 inactivates Beclin-1-induced autophagy and enhances apoptosis by promoting the release of proapoptotic factors from mitochondria, Cell.Death Dis. 1 (2010) e18.

[221] V. Pagliarini, E. Wirawan, A. Romagnoli, F. Ciccosanti, G. Lisi, S. Lippens, F. Cecconi, G.M. Fimia, et al, Proteolysis of Ambra1 during apoptosis has a role in the inhibition of the autophagic pro-survival response, Cell Death Differ. 19 (2012) 1495-1504.

[222] O. Oral, D. Oz-Arslan, Z. Itah, A. Naghavi, R. Deveci, S. Karacali & D. Gozuacik, Cleavage of Atg3 protein by caspase-8 regulates autophagy during receptor-activated cell death, Apoptosis 17 (2012) 810-820.

[223] S. Yousefi, R. Perozzo, I. Schmid, A. Ziemiecki, T. Schaffner, L. Scapozza, T. Brunner & H.U. Simon, Calpain-mediated cleavage of Atg5 switches autophagy to apoptosis, Nat.Cell Biol. 8 (2006) 1124-1132.

[224] V.M. Betin & J.D. Lane, Caspase cleavage of Atg4D stimulates GABARAP-L1 processing and triggers mitochondrial targeting and apoptosis, J.Cell.Sci. 122 (2009) 2554-2566.

[225] S. Kahns, M. Kalai, L.D. Jakobsen, B.F. Clark, P. Vandenabeele & P.H. Jensen, Caspase-1 and caspase-8 cleave and inactivate cellular parkin, J.Biol.Chem. 278 (2003) 23376-23380.

[226] Y. Maejima, S. Kyoi, P. Zhai, T. Liu, H. Li, A. Ivessa, S. Sciarretta, D.P. Del Re, et al, Mst1 inhibits autophagy by promoting the interaction between Beclin1 and Bcl-2, Nat.Med. 19 (2013) 1478-1488.

[227] G.P. Leboucher, Y.C. Tsai, M. Yang, K.C. Shaw, M. Zhou, T.D. Veenstra, M.H. Glickman & A.M. Weissman, Stress-induced phosphorylation and proteasomal degradation of mitofusin 2 facilitates mitochondrial fragmentation and apoptosis, Mol.Cell 47 (2012) 547-557.

[228] M.M. Young, Y. Takahashi, O. Khan, S. Park, T. Hori, J. Yun, A.K. Sharma, S. Amin, et al, Autophagosomal membrane serves as platform for intracellular death-inducing signaling complex (iDISC)-mediated caspase-8 activation and apoptosis, J.Biol.Chem. 287 (2012) 12455-12468.

[229] A.D. Rubinstein, M. Eisenstein, Y. Ber, S. Bialik & A. Kimchi, The autophagy protein Atg12 associates with antiapoptotic Bcl-2 family members to promote mitochondrial apoptosis, Mol.Cell 44 (2011) 698-709.

[230] T. Lu, M. Gu, Y. Zhao, X. Zheng & C. Xing, Autophagy contributes to falcarindiol-induced cell death in breast cancer cells with enhanced endoplasmic reticulum stress, PLoS One 12 (2017) e0176348.

[231] J. Hagenbuchner, L. Lungkofler, U. Kiechl-Kohlendorfer, G. Viola, M.G. Ferlin, M.J. Ausserlechner & P. Obexer, The tubulin inhibitor MG-2477 induces autophagy-regulated cell death, ROS accumulation and activation of FOXO3 in neuroblastoma, Oncotarget(2017).

[232] B. Wang, D. Lu, M. Xuan & W. Hu, Antitumor effect of sunitinib in human prostate cancer cells functions via autophagy, Exp.Ther.Med. 13 (2017) 1285-1294.

[233] L.C. Gomes, G. Di Benedetto & L. Scorrano, During autophagy mitochondria elongate, are spared from degradation and sustain cell viability, Nat.Cell Biol. 13 (2011) 589-598.

[234] E. White, Deconvoluting the context-dependent role for autophagy in cancer, Nat.Rev.Cancer. 12 (2012) 401-410.

[235] X.H. Liang, S. Jackson, M. Seaman, K. Brown, B. Kempkes, H. Hibshoosh & B. Levine, Induction of autophagy and inhibition of tumorigenesis by beclin 1, Nature 402 (1999) 672-676.

[236] R. Mathew, S. Kongara, B. Beaudoin, C.M. Karp, K. Bray, K. Degenhardt, G. Chen, S. Jin, et al, Autophagy suppresses tumor progression by limiting chromosomal instability, Genes Dev. 21 (2007) 1367-1381.

[237] A. Duran, J.F. Linares, A.S. Galvez, K. Wikenheiser, J.M. Flores, M.T. Diaz-Meco & J. Moscat, The signaling adaptor p62 is an important NF-kappaB mediator in tumorigenesis, Cancer.Cell. 13 (2008) 343-354.

[238] J.Y. Guo, G. Karsli-Uzunbas, R. Mathew, S.C. Aisner, J.J. Kamphorst, A.M. Strohecker, G. Chen, S. Price, et al, Autophagy suppresses progression of K-ras-induced lung tumors to oncocytomas and maintains lipid homeostasis, Genes Dev. 27 (2013) 1447-1461.

[239] R. Mathew, C.M. Karp, B. Beaudoin, N. Vuong, G. Chen, H.Y. Chen, K. Bray, A. Reddy, et al, Autophagy suppresses tumorigenesis through elimination of p62, Cell 137 (2009) 1062-1075.

[240] K. Degenhardt, R. Mathew, B. Beaudoin, K. Bray, D. Anderson, G. Chen, C. Mukherjee, Y. Shi, et al, Autophagy promotes tumor cell survival and restricts necrosis, inflammation, and tumorigenesis, Cancer.Cell. 10 (2006) 51-64.

[241] K.M. Rosen, C.E. Moussa, H.K. Lee, P. Kumar, T. Kitada, G. Qin, Q. Fu & H.W. Querfurth, Parkin reverses intracellular beta-amyloid accumulation and its negative effects on proteasome function, J.Neurosci.Res. 88 (2010) 167-178.

[242] R. Marongiu, B. Spencer, L. Crews, A. Adame, C. Patrick, M. Trejo, B. Dallapiccola, E.M. Valente, et al, Mutant Pink1 induces mitochondrial dysfunction in a neuronal cell model of Parkinson's disease by disturbing calcium flux, J.Neurochem. 108 (2009) 1561-1574.

[243] Y. Batlevi & A.R. La Spada, Mitochondrial autophagy in neural function, neurodegenerative disease, neuron cell death, and aging, Neurobiol.Dis. 43 (2011) 46-51.

[244] X. Zhang, H. Yan, Y. Yuan, J. Gao, Z. Shen, Y. Cheng, Y. Shen, R.R. Wang, et al, Cerebral ischemia-reperfusion-induced autophagy protects against neuronal injury by mitochondrial clearance, Autophagy 9 (2013) 1321-1333.

[245] J.Y. Ha, J.S. Kim, S.E. Kim & J.H. Son, Simultaneous activation of mitophagy and autophagy by staurosporine protects against dopaminergic neuronal cell death, Neurosci.Lett. 561 (2014) 101-106.

[246] A. Hoshino, S. Matoba, E. Iwai-Kanai, H. Nakamura, M. Kimata, M. Nakaoka, M. Katamura, Y. Okawa, et al, p53-TIGAR axis attenuates mitophagy to exacerbate cardiac damage after ischemia, J.Mol.Cell.Cardiol. 52 (2012) 175-184.

[247] I. Nishino, J. Fu, K. Tanji, T. Yamada, S. Shimojo, T. Koori, M. Mora, J.E. Riggs, et al, Primary LAMP-2 deficiency causes X-linked vacuolar cardiomyopathy and myopathy (Danon disease), Nature 406 (2000) 906-910.

[248] N. Raben, P. Plotz & B.J. Byrne, Acid alpha-glucosidase deficiency (glycogenosis type II, Pompe disease), Curr.Mol.Med. 2 (2002) 145-166.

[249] P. Grumati, L. Coletto, P. Sabatelli, M. Cescon, A. Angelin, E. Bertaggia, B. Blaauw, A. Urciuolo, et al, Autophagy is defective in collagen VI muscular dystrophies, and its reactivation rescues myofiber degeneration, Nat.Med. 16 (2010) 1313-1320.

[250] C. De Palma, F. Morisi, S. Cheli, S. Pambianco, V. Cappello, M. Vezzoli, P. Rovere-Querini, M. Moggio, et al, Autophagy as a new therapeutic target in Duchenne muscular dystrophy, Cell.Death Dis. 3 (2012) e418.

[251] V. Carmignac, M. Svensson, Z. Korner, L. Elowsson, C. Matsumura, K.I. Gawlik, V. Allamand & M. Durbeej, Autophagy is increased in laminin alpha2 chain-deficient muscle and its inhibition improves muscle morphology in a mouse model of MDC1A, Hum.Mol.Genet. 20 (2011) 4891-4902.

[252] L. Garcia-Prat, M. Martinez-Vicente, E. Perdiguero, L. Ortet, J. Rodriguez-Ubreva, E. Rebollo, V. Ruiz-Bonilla, S. Gutarra, et al, Autophagy maintains stemness by preventing senescence, Nature 529 (2016) 37-42.

[253] A. Hoshino, M. Ariyoshi, Y. Okawa, S. Kaimoto, M. Uchihashi, K. Fukai, E. Iwai-Kanai, K. Ikeda, et al, Inhibition of p53 preserves Parkin-mediated mitophagy and pancreatic beta-cell function in diabetes, Proc.Natl.Acad.Sci.U.S.A. 111 (2014) 3116-3121.

[254] A. Ardestani, F. Paroni, Z. Azizi, S. Kaur, V. Khobragade, T. Yuan, T. Frogne, W. Tao, et al, MST1 is a key regulator of beta cell apoptosis and dysfunction in diabetes, Nat.Med. 20 (2014) 385-397.

[255] T. Namba, Y. Takabatake, T. Kimura, A. Takahashi, T. Yamamoto, J. Matsuda, H. Kitamura, F. Niimura, et al, Autophagic Clearance of Mitochondria in the Kidney Copes with Metabolic Acidosis, J.Am.Soc.Nephrol.(2014).

[256] G.C. Higgins & M.T. Coughlan, Mitochondrial dysfunction and mitophagy: the beginning and end to diabetic nephropathy? Br.J.Pharmacol. 171 (2014) 1917-1942.

[257] M. Ishihara, M. Urushido, K. Hamada, T. Matsumoto, Y. Shimamura, K. Ogata, K. Inoue, Y. Taniguchi, et al, Sestrin-2 and BNIP3 regulate autophagy and mitophagy in renal tubular cells in acute kidney injury, Am.J.Physiol.Renal Physiol. 305 (2013) F495-509.

[258] S.J. Kim, M. Khan, J. Quan, A. Till, S. Subramani & A. Siddiqui, Hepatitis B virus disrupts mitochondrial dynamics: induces fission and mitophagy to attenuate apoptosis, PLoS Pathog. 9 (2013) e1003722.

[259] L. HAYFLICK & P.S. MOORHEAD, The serial cultivation of human diploid cell strains, Exp.Cell Res. 25 (1961) 585-621.

[260] L. HAYFLICK, The Limited in Vitro Lifetime of Human Diploid Cell Strains, Exp.Cell Res. 37 (1965) 614-636.

[261] R. Sager, Senescence as a mode of tumor suppression, Environ.Health Perspect. 93 (1991) 59-62.

[262] J. Campisi, Aging, cellular senescence, and cancer, Annu.Rev.Physiol. 75 (2013) 685-705.

[263] G.P. Dimri, X. Lee, G. Basile, M. Acosta, G. Scott, C. Roskelley, E.E. Medrano, M. Linskens, et al, A biomarker that identifies senescent human cells in culture and in aging skin in vivo, Proc.Natl.Acad.Sci.U.S.A. 92 (1995) 9363-9367.

[264] N.E. Sharpless & C.J. Sherr, Forging a signature of in vivo senescence, Nat.Rev.Cancer. 15 (2015) 397-408.

[265] C.B. Harley, A.B. Futcher & C.W. Greider, Telomeres shorten during ageing of human fibroblasts, Nature 345 (1990) 458-460.

[266] J.M. van Deursen, The role of senescent cells in ageing, Nature 509 (2014) 439-446.

[267] S.P. Jackson & J. Bartek, The DNA-damage response in human biology and disease, Nature 461 (2009) 1071-1078.

[268] Y. Chien, C. Scuoppo, X. Wang, X. Fang, B. Balgley, J.E. Bolden, P. Premsrirut, W. Luo, et al, Control of the senescence-associated secretory phenotype by NF-kappaB promotes senescence and enhances chemosensitivity, Genes Dev. 25 (2011) 2125-2136.

[269] B. Ritschka, M. Storer, A. Mas, F. Heinzmann, M.C. Ortells, J.P. Morton, O.J. Sansom, L. Zender, et al, The senescence-associated secretory phenotype induces cellular plasticity and tissue regeneration, Genes Dev. 31 (2017) 172-183.

[270] J.C. Acosta, A. Banito, T. Wuestefeld, A. Georgilis, P. Janich, J.P. Morton, D. Athineos, T.W. Kang, et al, A complex secretory program orchestrated by the inflammasome controls paracrine senescence, Nat.Cell Biol. 15 (2013) 978-990.

[271] W. Xue, L. Zender, C. Miething, R.A. Dickins, E. Hernando, V. Krizhanovsky, C. Cordon-Cardo & S.W. Lowe, Senescence and tumour clearance is triggered by p53 restoration in murine liver carcinomas, Nature 445 (2007) 656-660.

[272] V. Krizhanovsky, W. Xue, L. Zender, M. Yon, E. Hernando & S.W. Lowe, Implications of cellular senescence in tissue damage response, tumor suppression, and stem cell biology, Cold Spring Harb.Symp.Quant.Biol. 73 (2008) 513-522.

[273] A. Lujambio, L. Akkari, J. Simon, D. Grace, D.F. Tschaharganeh, J.E. Bolden, Z. Zhao, V. Thapar, et al, Non-cell-autonomous tumor suppression by p53, Cell 153 (2013) 449-460.

[274] P.J. Hornsby, Cellular senescence and tissue aging in vivo, J.Gerontol.A Biol.Sci.Med.Sci. 57 (2002) B251-6.

[275] R.T. Calado & B. Dumitriu, Telomere dynamics in mice and humans, Semin.Hematol. 50 (2013) 165-174.

[276] D. Munoz-Espin, M. Canamero, A. Maraver, G. Gomez-Lopez, J. Contreras, S. Murillo-Cuesta, A. Rodriguez-Baeza, I. Varela-Nieto, et al, Programmed cell senescence during mammalian embryonic development, Cell 155 (2013) 1104-1118.

[277] M. Storer, A. Mas, A. Robert-Moreno, M. Pecoraro, M.C. Ortells, V. Di Giacomo, R. Yosef, N. Pilpel, et al, Senescence is a developmental mechanism that contributes to embryonic growth and patterning, Cell 155 (2013) 1119-1130.

[278] G.I. Shapiro, C.D. Edwards, L. Kobzik, J. Godleski, W. Richards, D.J. Sugarbaker & B.J. Rollins, Reciprocal Rb inactivation and p16INK4 expression in primary lung cancers and cell lines, Cancer Res. 55 (1995) 505-509.

[279] G.I. Shapiro, J.E. Park, C.D. Edwards, L. Mao, A. Merlo, D. Sidransky, M.E. Ewen & B.J. Rollins, Multiple mechanisms of p16INK4A inactivation in non-small cell lung cancer cell lines, Cancer Res. 55 (1995) 6200-6209.

[280] A.K. Witkiewicz, K.E. Knudsen, A.P. Dicker & E.S. Knudsen, The meaning of p16(ink4a) expression in tumors: functional significance, clinical associations and future developments, Cell.Cycle 10 (2011) 2497-2503.

[281] D.J. Baker, B.G. Childs, M. Durik, M.E. Wijers, C.J. Sieben, J. Zhong, R.A. Saltness, K.B. Jeganathan, et al, Naturally occurring p16(Ink4a)-positive cells shorten healthy lifespan, Nature 530 (2016) 184-189.

[282] D.J. Baker, T. Wijshake, T. Tchkonia, N.K. LeBrasseur, B.G. Childs, B. van de Sluis, J.L. Kirkland & J.M. van Deursen, Clearance of p16Ink4a-positive senescent cells delays ageing-associated disorders, Nature 479 (2011) 232-236.

[283] D.A. Gewirtz, Autophagy and senescence: a partnership in search of definition, Autophagy 9 (2013) 808-812.

[284] A.R. Young, M. Narita, M. Ferreira, K. Kirschner, M. Sadaie, J.F. Darot, S. Tavare, S. Arakawa, et al, Autophagy mediates the mitotic senescence transition, Genes Dev. 23 (2009) 798-803.

[285] R.W. Goehe, X. Di, K. Sharma, M.L. Bristol, S.C. Henderson, K. Valerie, F. Rodier, A.R. Davalos, et al, The autophagy-senescence connection in chemotherapy: must tumor cells (self) eat before they sleep? J.Pharmacol.Exp.Ther. 343 (2012) 763-778.

[286] Y. Wang, X.D. Wang, E. Lapi, A. Sullivan, W. Jia, Y.W. He, I. Ratnayaka, S. Zhong, et al, Autophagic activity dictates the cellular response to oncogenic RAS, Proc.Natl.Acad.Sci.U.S.A. 109 (2012) 13325-13330.

[287] C. Ott, J. Konig, A. Hohn, T. Jung & T. Grune, Macroautophagy is impaired in old murine brain tissue as well as in senescent human fibroblasts, Redox Biol. 10 (2016) 266-273.

[288] H.T. Kang, K.B. Lee, S.Y. Kim, H.R. Choi & S.C. Park, Autophagy impairment induces premature senescence in primary human fibroblasts, PLoS One 6 (2011) e23367.

[289] S. Fujii, H. Hara, J. Araya, N. Takasaka, J. Kojima, S. Ito, S. Minagawa, Y. Yumino, et al, Insufficient autophagy promotes bronchial epithelial cell senescence in chronic obstructive pulmonary disease, Oncoimmunology 1 (2012) 630-641.

[290] M.O. Grootaert, P.A. da Costa Martins, N. Bitsch, I. Pintelon, G.R. De Meyer, W. Martinet & D.M. Schrijvers, Defective autophagy in vascular smooth muscle cells accelerates senescence and promotes neointima formation and atherogenesis, Autophagy 11 (2015) 2014-2032.

[291] C.F. Zhang, F. Gruber, C. Ni, M. Mildner, U. Koenig, S. Karner, C. Barresi, H. Rossiter, et al, Suppression of autophagy dysregulates the antioxidant response and causes premature senescence of melanocytes, J.Invest.Dermatol. 135 (2015) 1348-1357.

[292] E.C. Filippi-Chiela, M.M. Bueno e Silva, M.P. Thome & G. Lenz, Single-cell analysis challenges the connection between autophagy and senescence induced by DNA damage, Autophagy 11 (2015) 1099-1113.

[293] H. Tai, Z. Wang, H. Gong, X. Han, J. Zhou, X. Wang, X. Wei, Y. Ding, et al, Autophagy impairment with lysosomal and mitochondrial dysfunction is an important characteristic of oxidative stress-induced senescence, Autophagy 13 (2017) 99-113.

[294] C. Kang, Q. Xu, T.D. Martin, M.Z. Li, M. Demaria, L. Aron, T. Lu, B.A. Yankner, et al, The DNA damage response induces inflammation and senescence by inhibiting autophagy of GATA4, Science 349 (2015) aaa5612.

[295] J. Kaiser, Hormesis. Sipping from a poisoned chalice, Science 302 (2003) 376-379.

[296] D.C. Rubinsztein, G. Marino & G. Kroemer, Autophagy and aging, Cell 146 (2011) 682-695.

[297] M. Ristow & K. Zarse, How increased oxidative stress promotes longevity and metabolic health: The concept of mitochondrial hormesis (mitohormesis), Exp.Gerontol. 45 (2010) 410-418.

[298] L. Portt, G. Norman, C. Clapp, M. Greenwood & M.T. Greenwood, Anti-apoptosis and cell survival: a review, Biochim.Biophys.Acta 1813 (2011) 238-259.

[299] K. Przyklenk & R.A. Kloner, Ischemic preconditioning: exploring the paradox, Prog.Cardiovasc.Dis. 40 (1998) 517-547.

[300] X.Q. Liu, R. Sheng & Z.H. Qin, The neuroprotective mechanism of brain ischemic preconditioning, Acta Pharmacol.Sin. 30 (2009) 1071-1080.

[301] R. Sullivan, G.C. Pare, L.J. Frederiksen, G.L. Semenza & C.H. Graham, Hypoxia-induced resistance to anticancer drugs is associated with decreased senescence and requires hypoxia-inducible factor-1 activity, Mol.Cancer.Ther. 7 (2008) 1961-1973.

[302] J. Haendeler, V. Tischler, J. Hoffmann, A.M. Zeiher & S. Dimmeler, Low doses of reactive oxygen species protect endothelial cells from apoptosis by increasing thioredoxin-1 expression, FEBS Lett. 577 (2004) 427-433.

[303] B. Shi & R.R. Isseroff, Arsenite pre-conditioning reduces UVB-induced apoptosis in corneal epithelial cells through the anti-apoptotic activity of 27 kDa heat shock protein (HSP27), J.Cell.Physiol. 206 (2006) 301-308.

[304] B. Jiang, W. Xiao, Y. Shi, M. Liu & X. Xiao, Heat shock pretreatment inhibited the release of Smac/DIABLO from mitochondria and apoptosis induced by hydrogen peroxide in cardiomyocytes and C2C12 myogenic cells, Cell Stress Chaperones 10 (2005) 252-262.

[305] P. Pallepati & D. Averill-Bates, Mild thermotolerance induced at 40 degrees C increases antioxidants and protects HeLa cells against mitochondrial apoptosis induced by hydrogen peroxide: Role of p53, Arch.Biochem.Biophys. 495 (2010) 97-111.

[306] M.I. Bhuiyan, M.N. Islam, S.Y. Jung, H.H. Yoo, Y.S. Lee & C. Jin, Involvement of ceramide in ischemic tolerance induced by preconditioning with sublethal oxygen-glucose deprivation in primary cultured cortical neurons of rats, Biol.Pharm.Bull. 33 (2010) 11-17.

[307] Y. Chen, I. Ginis & J.M. Hallenbeck, The protective effect of ceramide in immature rat brain hypoxia-ischemia involves up-regulation of bcl-2 and reduction of TUNEL-positive cells, J.Cereb.Blood Flow Metab. 21 (2001) 34-40.

[308] A. Liu, H. Fang, W. Wei, O. Dirsch & U. Dahmen, Ischemic preconditioning protects against liver ischemia/reperfusion injury via heme oxygenase-1-mediated autophagy, Crit.Care Med. 42 (2014) e762-71.

[309] H.K. Park, K. Chu, K.H. Jung, S.T. Lee, J.J. Bahn, M. Kim, S.K. Lee & J.K. Roh, Autophagy is involved in the ischemic preconditioning, Neurosci.Lett. 451 (2009) 16-19.

[310] C. Gao, Y. Cai, X. Zhang, H. Huang, J. Wang, Y. Wang, X. Tong, J. Wang, et al, Ischemic Preconditioning Mediates Neuroprotection against Ischemia in Mouse Hippocampal CA1 Neurons by Inducing Autophagy, PLoS One 10 (2015) e0137146.

[311] F. Madeo, A. Zimmermann, M.C. Maiuri & G. Kroemer, Essential role for autophagy in life span extension, J.Clin.Invest. 125 (2015) 85-93.

[312] C. Lee & V. Longo, Dietary restriction with and without caloric restriction for healthy aging, F1000Res 5 (2016) 10.12688/f1000research.7136.1. eCollection 2016.

[313] R.W. Powers 3rd, M. Kaeberlein, S.D. Caldwell, B.K. Kennedy & S. Fields, Extension of chronological life span in yeast by decreased TOR pathway signaling, Genes Dev. 20 (2006) 174-184.

[314] D.E. Harrison, R. Strong, Z.D. Sharp, J.F. Nelson, C.M. Astle, K. Flurkey, N.L. Nadon, J.E. Wilkinson, et al, Rapamycin fed late in life extends lifespan in genetically heterogeneous mice, Nature 460 (2009) 392-395.

[315] R.A. Miller, D.E. Harrison, C.M. Astle, J.A. Baur, A.R. Boyd, R. de Cabo, E. Fernandez, K. Flurkey, et al, Rapamycin, but not resveratrol or simvastatin, extends life span of genetically heterogeneous mice, J.Gerontol.A Biol.Sci.Med.Sci. 66 (2011) 191-201.

[316] R.A. Miller, D.E. Harrison, C.M. Astle, E. Fernandez, K. Flurkey, M. Han, M.A. Javors, X. Li, et al, Rapamycin-mediated lifespan increase in mice is dose and sex dependent and metabolically distinct from dietary restriction, Aging Cell. 13 (2014) 468-477.

[317] A. Bitto, T.K. Ito, V.V. Pineda, N.J. LeTexier, H.Z. Huang, E. Sutlief, H. Tung, N. Vizzini, et al, Transient rapamycin treatment can increase lifespan and healthspan in middle-aged mice, Elife 5 (2016) 10.7554/eLife.16351.

[318] R.J. Colman, T.M. Beasley, J.W. Kemnitz, S.C. Johnson, R. Weindruch & R.M. Anderson, Caloric restriction reduces age-related and all-cause mortality in rhesus monkeys, Nat.Commun. 5 (2014) 3557.

[319] J.A. Mattison, G.S. Roth, T.M. Beasley, E.M. Tilmont, A.M. Handy, R.L. Herbert, D.L. Longo, D.B. Allison, et al, Impact of caloric restriction on health and survival in rhesus monkeys from the NIA study, Nature 489 (2012) 318-321.

[320] J.A. Mattison, R.J. Colman, T.M. Beasley, D.B. Allison, J.W. Kemnitz, G.S. Roth, D.K. Ingram, R. Weindruch, et al, Caloric restriction improves health and survival of rhesus monkeys, Nat.Commun. 8 (2017) 14063.

[321] R.S. Sohal & M.J. Forster, Caloric restriction and the aging process: a critique, Free Radic.Biol.Med. 73 (2014) 366-382.

[322] S.R. Urfer, T.L. Kaeberlein, S. Mailheau, P.J. Bergman, K.E. Creevy, D.E.L. Promislow & M. Kaeberlein, A randomized controlled trial to establish effects of short-term rapamycin treatment in 24 middle-aged companion dogs, Geroscience 39 (2017) 117-127.

[323] A. Hartmann, S. Hunot, P.P. Michel, M.P. Muriel, S. Vyas, B.A. Faucheux, A. Mouatt-Prigent, H. Turmel, et al, Caspase-3: A vulnerability factor and final effector in apoptotic death of dopaminergic neurons in Parkinson's disease, Proc.Natl.Acad.Sci.U.S.A. 97 (2000) 2875-2880.

[324] J.H. Su, M. Zhao, A.J. Anderson, A. Srinivasan & C.W. Cotman, Activated caspase-3 expression in Alzheimer's and aged control brain: correlation with Alzheimer pathology, Brain Res. 898 (2001) 350-357.

[325] M. Vila, V. Jackson-Lewis, S. Vukosavic, R. Djaldetti, G. Liberatore, D. Offen, S.J. Korsmeyer & S. Przedborski, Bax ablation prevents dopaminergic neurodegeneration in the 1-methyl- 4-phenyl-1,2,3,6-tetrahydropyridine mouse model of Parkinson's disease, Proc.Natl.Acad.Sci.U.S.A. 98 (2001) 2837-2842.

[326] M.V. Karpuj, M.W. Becher, J.E. Springer, D. Chabas, S. Youssef, R. Pedotti, D. Mitchell & L. Steinman, Prolonged survival and decreased abnormal movements in transgenic model of Huntington disease, with administration of the transglutaminase inhibitor cystamine, Nat.Med. 8 (2002) 143-149.

[327] B. Halliwell, Oxidative stress and neurodegeneration: where are we now? J.Neurochem. 97 (2006) 1634-1658.

[328] L.I. Bruijn, M.K. Houseweart, S. Kato, K.L. Anderson, S.D. Anderson, E. Ohama, A.G. Reaume, R.W. Scott, et al, Aggregation and motor neuron toxicity of an ALS-linked SOD1 mutant independent from wild-type SOD1, Science 281 (1998) 1851-1854.

[329] S. Zhu, I.G. Stavrovskaya, M. Drozda, B.Y. Kim, V. Ona, M. Li, S. Sarang, A.S. Liu, et al, Minocycline inhibits cytochrome c release and delays progression of amyotrophic lateral sclerosis in mice, Nature 417 (2002) 74-78.

[330] M. Chen, V.O. Ona, M. Li, R.J. Ferrante, K.B. Fink, S. Zhu, J. Bian, L. Guo, et al, Minocycline inhibits caspase-1 and caspase-3 expression and delays mortality in a transgenic mouse model of Huntington disease, Nat.Med. 6 (2000) 797-801.

[331] A. Degterev, Z. Huang, M. Boyce, Y. Li, P. Jagtap, N. Mizushima, G.D. Cuny, T.J. Mitchison, et al, Chemical inhibitor of nonapoptotic cell death with therapeutic potential for ischemic brain injury, Nat.Chem.Biol. 1 (2005) 112-119.

[332] C. Piot, P. Croisille, P. Staat, H. Thibault, G. Rioufol, N. Mewton, R. Elbelghiti, T.T. Cung, et al, Effect of cyclosporine on reperfusion injury in acute myocardial infarction, N.Engl.J.Med. 359 (2008) 473-481.

[333] A. Saraste, K. Pulkki, M. Kallajoki, K. Henriksen, M. Parvinen & L.M. Voipio-Pulkki, Apoptosis in human acute myocardial infarction, Circulation 95 (1997) 320-323.

[334] Y. Fujio, T. Nguyen, D. Wencker, R.N. Kitsis & K. Walsh, Akt promotes survival of cardiomyocytes in vitro and protects against ischemia-reperfusion injury in mouse heart, Circulation 101 (2000) 660-667.

[335] R.S. Whelan, V. Kaplinskiy & R.N. Kitsis, Cell death in the pathogenesis of heart disease: mechanisms and significance, Annu.Rev.Physiol. 72 (2010) 19-44.

[336] G. Olivetti, R. Abbi, F. Quaini, J. Kajstura, W. Cheng, J.A. Nitahara, E. Quaini, C. Di Loreto, et al, Apoptosis in the failing human heart, N.Engl.J.Med. 336 (1997) 1131-1141.

[337] D. Wencker, M. Chandra, K. Nguyen, W. Miao, S. Garantziotis, S.M. Factor, J. Shirani, R.C. Armstrong, et al, A mechanistic role for cardiac myocyte apoptosis in heart failure, J.Clin.Invest. 111 (2003) 1497-1504.

[338] J. Quadrilatero, S.E. Alway & E.E. Dupont-Versteegden, Skeletal muscle apoptotic response to physical activity: potential mechanisms for protection, Appl.Physiol.Nutr.Metab. 36 (2011) 608-617.

[339] M.C. Lee, G.R. Wee & J.H. Kim, Apoptosis of skeletal muscle on steroid-induced myopathy in rats, J.Nutr. 135 (2005) 1806S-1808S.

[340] M. Girgenrath, J.A. Dominov, C.A. Kostek & J.B. Miller, Inhibition of apoptosis improves outcome in a model of congenital muscular dystrophy, J.Clin.Invest. 114 (2004) 1635-1639.

[341] D.M. Yellon & J.M. Downey, Preconditioning the myocardium: from cellular physiology to clinical cardiology, Physiol.Rev. 83 (2003) 1113-1151.

[342] R. Sheng, L.S. Zhang, R. Han, X.Q. Liu, B. Gao & Z.H. Qin, Autophagy activation is associated with neuroprotection in a rat model of focal cerebral ischemic preconditioning, Autophagy 6 (2010) 482-494.

[343] C. Huang, A.M. Andres, E.P. Ratliff, G. Hernandez, P. Lee & R.A. Gottlieb, Preconditioning involves selective mitophagy mediated by Parkin and p62/SQSTM1, PLoS One 6 (2011) e20975.

[344] C. Huang, S. Yitzhaki, C.N. Perry, W. Liu, Z. Giricz, R.M. Mentzer Jr & R.A. Gottlieb, Autophagy induced by ischemic preconditioning is essential for cardioprotection, J.Cardiovasc.Transl.Res. 3 (2010) 365-373.

[345] J. Campisi & F. d'Adda di Fagagna, Cellular senescence: when bad things happen to good cells, Nat.Rev.Mol.Cell Biol. 8 (2007) 729-740.

[346] C.Y. Pang, R.Z. Yang, A. Zhong, N. Xu, B. Boyd & C.R. Forrest, Acute ischaemic preconditioning protects against skeletal muscle infarction in the pig, Cardiovasc.Res. 29 (1995) 782-788.

[347] M.H. Theus, L. Wei, L. Cui, K. Francis, X. Hu, C. Keogh & S.P. Yu, In vitro hypoxic preconditioning of embryonic stem cells as a strategy of promoting cell survival and functional benefits after transplantation into the ischemic rat brain, Exp.Neurol. 210 (2008) 656-670.

[348] R. Thuret, T. Saint Yves, X. Tillou, N. Chatauret, R. Thuillier, B. Barrou & C. Billault, Ischemic pre- and post-conditioning: current clinical applications, Prog.Urol. 24 Suppl 1 (2014) S56-61.

[349] R.A. Forbes, C. Steenbergen & E. Murphy, Diazoxide-induced cardioprotection requires signaling through a redox-sensitive mechanism, Circ.Res. 88 (2001) 802-809.

[350] M. Ristow, K. Zarse, A. Oberbach, N. Kloting, M. Birringer, M. Kiehntopf, M. Stumvoll, C.R. Kahn, et al, Antioxidants prevent health-promoting effects of physical exercise in humans, Proc.Natl.Acad.Sci.U.S.A. 106 (2009) 8665-8670.

[351] C. Grimm, A. Wenzel, M. Groszer, H. Mayser, M. Seeliger, M. Samardzija, C. Bauer, M. Gassmann, et al, HIF-1-induced erythropoietin in the hypoxic retina protects against light-induced retinal degeneration, Nat.Med. 8 (2002) 718-724.

[352] R. Carini, M. Grazia De Cesaris, R. Splendore & E. Albano, Stimulation of p38 MAP kinase reduces acidosis and Na(+) overload in preconditioned hepatocytes, FEBS Lett. 491 (2001) 180-183.

[353] H.M. Brown-Borg, Longevity in mice: is stress resistance a common factor? Age (Dordr) 28 (2006) 145-162.

[354] E. Le Bourg, Hormesis, aging and longevity, Biochim.Biophys.Acta 1790 (2009) 1030-1039.

[355] S.R. Spindler & J.M. Dhahbi, Conserved and tissue-specific genic and physiologic responses to caloric restriction and altered IGFI signaling in mitotic and postmitotic tissues, Annu.Rev.Nutr. 27 (2007) 193-217.

[356] R. de Cabo, D. Carmona-Gutierrez, M. Bernier, M.N. Hall & F. Madeo, The search for antiaging interventions: from elixirs to fasting regimens, Cell 157 (2014) 1515-1526.

[357] D. Bloemberg & J. Quadrilatero, Caspase activity and apoptotic signaling in proliferating C2C12 cells following cisplatin or A23187 exposure, Data Brief 7 (2016) 1024-1030.

[358] U.T. Ruegg & G.M. Burgess, Staurosporine, K-252 and UCN-01: potent but nonspecific inhibitors of protein kinases, Trends Pharmacol.Sci. 10 (1989) 218-220.

[359] M. Enari, H. Sakahira, H. Yokoyama, K. Okawa, A. Iwamatsu & S. Nagata, A caspase-activated DNase that degrades DNA during apoptosis, and its inhibitor ICAD, Nature 391 (1998) 43-50.

[360] R.U. Janicke, M.L. Sprengart, M.R. Wati & A.G. Porter, Caspase-3 is required for DNA fragmentation and morphological changes associated with apoptosis, J.Biol.Chem. 273 (1998) 9357-9360.

[361] J. Yang, X. Liu, K. Bhalla, C.N. Kim, A.M. Ibrado, J. Cai, T.I. Peng, D.P. Jones, et al, Prevention of apoptosis by Bcl-2: release of cytochrome c from mitochondria blocked, Science 275 (1997) 1129-1132.

[362] M.C. Wei, W.X. Zong, E.H. Cheng, T. Lindsten, V. Panoutsakopoulou, A.J. Ross, K.A. Roth, G.R. MacGregor, et al, Proapoptotic BAX and BAK: a requisite gateway to mitochondrial dysfunction and death, Science 292 (2001) 727-730.

[363] J. Gil, S. Almeida, C.R. Oliveira & A.C. Rego, Cytosolic and mitochondrial ROS in staurosporine-induced retinal cell apoptosis, Free Radic.Biol.Med. 35 (2003) 1500-1514.

[364] I. Kruman, Q. Guo & M.P. Mattson, Calcium and reactive oxygen species mediate staurosporine-induced mitochondrial dysfunction and apoptosis in PC12 cells, J.Neurosci.Res. 51 (1998) 293-308.

[365] C.A. Belmokhtar, J. Hillion & E. Segal-Bendirdjian, Staurosporine induces apoptosis through both caspase-dependent and caspase-independent mechanisms, Oncogene 20 (2001) 3354-3362.

[366] B. Fitzner, S. Muller, M. Walther, M. Fischer, R. Engelmann, B. Muller-Hilke, B.M. Putzer, M. Kreutzer, et al, Senescence determines the fate of activated rat pancreatic stellate cells, J.Cell.Mol.Med. 16 (2012) 2620-2630.

[367] M.E. Caldwell, G.M. DeNicola, C.P. Martins, M.A. Jacobetz, A. Maitra, R.H. Hruban & D.A. Tuveson, Cellular features of senescence during the evolution of human and murine ductal pancreatic cancer, Oncogene 31 (2012) 1599-1608.

[368] Y. Johmura, J. Sun, K. Kitagawa, K. Nakanishi, T. Kuno, A. Naiki-Ito, Y. Sawada, T. Miyamoto, et al, SCF(Fbxo22)-KDM4A targets methylated p53 for degradation and regulates senescence, Nat.Commun. 7 (2016) 10574.

[369] D. Bloemberg & J. Quadrilatero, Mitochondrial pro-apoptotic indices do not precede the transient caspase activation associated with myogenesis, Biochim.Biophys.Acta 1843 (2014) 2926-2936.

[370] Y. Fuchs & H. Steller, Live to die another way: modes of programmed cell death and the signals emanating from dying cells, Nat.Rev.Mol.Cell Biol. 16 (2015) 329-344.

[371] C. Zeng, Y. Fan, J. Wu, S. Shi, Z. Chen, Y. Zhong, C. Zhang, K. Zen, et al, Podocyte autophagic activity plays a protective role in renal injury and delays the progression of podocytopathies, J.Pathol. 234 (2014) 203-213.

[372] Y.T. Wu, H.L. Tan, Q. Huang, Y.S. Kim, N. Pan, W.Y. Ong, Z.G. Liu, C.N. Ong, et al, Autophagy plays a protective role during zVAD-induced necrotic cell death, Autophagy 4 (2008) 457-466.

[373] R. Varshney, S. Gupta & P. Roy, Cytoprotective effect of kaempferol against palmitic acid-induced pancreatic beta-cell death through modulation of autophagy via AMPK/mTOR signaling pathway, Mol.Cell.Endocrinol. 448 (2017) 1-20.

[374] Z. Liu, B. Ren, Y. Wang, C. Zou, Q. Qiao, Z. Diao, Y. Mi, D. Zhu, et al, Sesamol Induces Human Hepatocellular Carcinoma Cells Apoptosis by Impairing Mitochondrial Function and Suppressing Autophagy, Sci.Rep. 7 (2017) 45728.

[375] J. Xu, Y. Wu, G. Lu, S. Xie, Z. Ma, Z. Chen, H.M. Shen & D. Xia, Importance of ROS-mediated autophagy in determining apoptotic cell death induced by physapubescin B, Redox Biol. 12 (2017) 198-207.

[376] H.K. Sung, Y.K. Chan, M. Han, J.W.S. Jahng, E. Song, E. Danielson, T. Berger, T.W. Mak, et al, Lipocalin-2 (NGAL) Attenuates Autophagy to Exacerbate Cardiac Apoptosis Induced by Myocardial Ischemia, J.Cell.Physiol. 232 (2017) 2125-2134.

[377] M. Hu, Z. Liu, P. Lv, H. Wang, Y. Zhu, Q. Qi & J. Xu, Autophagy and Akt/CREB signalling play an important role in the neuroprotective effect of nimodipine in a rat model of vascular dementia, Behav.Brain Res. 325 (2017) 79-86.

[378] K.A. Whelan, P.M. Chandramouleeswaran, K. Tanaka, M. Natsuizaka, M. Guha, S. Srinivasan, D.S. Darling, Y. Kita, et al, Autophagy supports generation of cells with high CD44 expression via modulation of oxidative stress and Parkin-mediated mitochondrial clearance, Oncogene(2017).

[379] Y. Liu, W. Gong, Z.Y. Yang, X.S. Zhou, C. Gong, T.R. Zhang, X. Wei, D. Ma, et al, Quercetin induces protective autophagy and apoptosis through ER stress via the p-STAT3/Bcl-2 axis in ovarian cancer, Apoptosis 22 (2017) 544-557.

[380] F. Cecconi & B. Levine, The role of autophagy in mammalian development: cell makeover rather than cell death, Dev.Cell. 15 (2008) 344-357.

[381] T. Tomoda, R.S. Bhatt, H. Kuroyanagi, T. Shirasawa & M.E. Hatten, A mouse serine/threonine kinase homologous to C. elegans UNC51 functions in parallel fiber formation of cerebellar granule neurons, Neuron 24 (1999) 833-846.

[382] R. Baerga, Y. Zhang, P.H. Chen, S. Goldman & S. Jin, Targeted deletion of autophagy-related 5 (atg5) impairs adipogenesis in a cellular model and in mice, Autophagy 5 (2009) 1118-1130.

[383] H.H. Pua, I. Dzhagalov, M. Chuck, N. Mizushima & Y.W. He, A critical role for the autophagy gene Atg5 in T cell survival and proliferation, J.Exp.Med. 204 (2007) 25-31.

[384] M. Mortensen, D.J. Ferguson, M. Edelmann, B. Kessler, K.J. Morten, M. Komatsu & A.K. Simon, Loss of autophagy in erythroid cells leads to defective removal of mitochondria and severe anemia in vivo, Proc.Natl.Acad.Sci.U.S.A. 107 (2010) 832-837.

[385] W.J. Yan, H.L. Dong & L.Z. Xiong, The protective roles of autophagy in ischemic preconditioning, Acta Pharmacol.Sin. 34 (2013) 636-643.

[386] S. Khan, F. Salloum, A. Das, L. Xi, G.W. Vetrovec & R.C. Kukreja, Rapamycin confers preconditioning-like protection against ischemia-reperfusion injury in isolated mouse heart and cardiomyocytes, J.Mol.Cell.Cardiol. 41 (2006) 256-264.

[387] B. Levine, N. Mizushima & H.W. Virgin, Autophagy in immunity and inflammation, Nature 469 (2011) 323-335.

[388] A.D. Dam, A.S. Mitchell & J. Quadrilatero, Induction of mitochondrial biogenesis protects against caspase-dependent and caspase-independent apoptosis in L6 myoblasts, Biochim.Biophys.Acta(2013).

[389] I. Valle, A. Alvarez-Barrientos, E. Arza, S. Lamas & M. Monsalve, PGC-1alpha regulates the mitochondrial antioxidant defense system in vascular endothelial cells, Cardiovasc.Res. 66 (2005) 562-573.

[390] J. St-Pierre, S. Drori, M. Uldry, J.M. Silvaggi, J. Rhee, S. Jager, C. Handschin, K. Zheng, et al, Suppression of reactive oxygen species and neurodegeneration by the PGC-1 transcriptional coactivators, Cell 127 (2006) 397-408.

[391] M.G. Apps, E.H. Choi & N.J. Wheate, The state-of-play and future of platinum drugs, Endocr.Relat.Cancer 22 (2015) R219-33.

[392] G. Bjorkoy, T. Lamark, A. Brech, H. Outzen, M. Perander, A. Overvatn, H. Stenmark & T. Johansen, p62/SQSTM1 forms protein aggregates degraded by autophagy and has a protective effect on huntingtin-induced cell death, J.Cell Biol. 171 (2005) 603-614.

[393] M. Gamerdinger, P. Hajieva, A.M. Kaya, U. Wolfrum, F.U. Hartl & C. Behl, Protein quality control during aging involves recruitment of the macroautophagy pathway by BAG3, EMBO J. 28 (2009) 889-901.

[394] S. Shaid, C.H. Brandts, H. Serve & I. Dikic, Ubiquitination and selective autophagy, Cell Death Differ. 20 (2013) 21-30.

[395] I. Kim, S. Rodriguez-Enriquez & J.J. Lemasters, Selective degradation of mitochondria by mitophagy, Arch.Biochem.Biophys. 462 (2007) 245-253.

[396] Y. Ishida, A. Yamamoto, A. Kitamura, S.R. Lamande, T. Yoshimori, J.F. Bateman, H. Kubota & K. Nagata, Autophagic elimination of misfolded procollagen aggregates in the endoplasmic reticulum as a means of cell protection, Mol.Biol.Cell 20 (2009) 2744-2754.

[397] M. Ogata, S. Hino, A. Saito, K. Morikawa, S. Kondo, S. Kanemoto, T. Murakami, M. Taniguchi, et al, Autophagy is activated for cell survival after endoplasmic reticulum stress, Mol.Cell.Biol. 26 (2006) 9220-9231.

[398] Y.B. Zhang, W. Zhao & R.X. Zeng, Autophagic degradation of caspase-8 protects U87MG cells against H2O2-induced oxidative stress, Asian Pac.J.Cancer.Prev. 14 (2013) 4095-4099.

[399] M. Komatsu, H. Kurokawa, S. Waguri, K. Taguchi, A. Kobayashi, Y. Ichimura, Y.S. Sou, I. Ueno, et al, The selective autophagy substrate p62 activates the stress responsive transcription factor Nrf2 through inactivation of Keap1, Nat.Cell Biol. 12 (2010) 213-223.

[400] X. Wu, A. Fleming, T. Ricketts, M. Pavel, H. Virgin, F.M. Menzies & D.C. Rubinsztein, Autophagy regulates Notch degradation and modulates stem cell development and neurogenesis, Nat.Commun. 7 (2016) 10533.

[401] T. Liu, Q. Tang, K. Liu, W. Xie, X. Liu, H. Wang, R.F. Wang & J. Cui, TRIM11 Suppresses AIM2 Inflammasome by Degrading AIM2 via p62-Dependent Selective Autophagy, Cell.Rep. 16 (2016) 1988-2002.

[402] T. Kimura, A. Jain, S.W. Choi, M.A. Mandell, K. Schroder, T. Johansen & V. Deretic, TRIM-mediated precision autophagy targets cytoplasmic regulators of innate immunity, J.Cell Biol. 210 (2015) 973-989.

[403] C. Park, Y. Suh & A.M. Cuervo, Regulated degradation of Chk1 by chaperone-mediated autophagy in response to DNA damage, Nat.Commun. 6 (2015) 6823.

[404] M. Niida, M. Tanaka & T. Kamitani, Downregulation of active IKK beta by Ro52-mediated autophagy, Mol.Immunol. 47 (2010) 2378-2387.

[405] T. Copetti, C. Bertoli, E. Dalla, F. Demarchi & C. Schneider, p65/RelA modulates BECN1 transcription and autophagy, Mol.Cell.Biol. 29 (2009) 2594-2608.

[406] S. Bhatnagar, A. Mittal, S.K. Gupta & A. Kumar, TWEAK causes myotube atrophy through coordinated activation of ubiquitin-proteasome system, autophagy, and caspases, J.Cell.Physiol. 227 (2012) 1042-1051.

[407] A. Criollo, F. Chereau, S.A. Malik, M. Niso-Santano, G. Marino, L. Galluzzi, M.C. Maiuri, V. Baud, et al, Autophagy is required for the activation of NFkappaB, Cell.Cycle 11 (2012) 194-199.

[408] Y. Feng, Z. Yao & D.J. Klionsky, How to control self-digestion: transcriptional, post-transcriptional, and post-translational regulation of autophagy, Trends Cell Biol. 25 (2015) 354-363.

[409] J. Heitman, N.R. Movva & M.N. Hall, Targets for cell cycle arrest by the immunosuppressant rapamycin in yeast, Science 253 (1991) 905-909.

[410] E.J. Brown, M.W. Albers, T.B. Shin, K. Ichikawa, C.T. Keith, W.S. Lane & S.L. Schreiber, A mammalian protein targeted by G1-arresting rapamycin-receptor complex, Nature 369 (1994) 756-758.

[411] F.J. Dumont, M.R. Melino, M.J. Staruch, S.L. Koprak, P.A. Fischer & N.H. Sigal, The immunosuppressive macrolides FK-506 and rapamycin act as reciprocal antagonists in murine T cells, J.Immunol. 144 (1990) 1418-1424.

[412] R.T. Abraham & G.J. Wiederrecht, Immunopharmacology of rapamycin, Annu.Rev.Immunol. 14 (1996) 483-510.

[413] L. Shu & P.J. Houghton, The mTORC2 complex regulates terminal differentiation of C2C12 myoblasts, Mol.Cell.Biol. 29 (2009) 4691-4700.

[414] L. Shu, X. Zhang & P.J. Houghton, Myogenic differentiation is dependent on both the kinase function and the N-terminal sequence of mammalian target of rapamycin, J.Biol.Chem. 277 (2002) 16726-16732.

[415] R. Conejo, A.M. Valverde, M. Benito & M. Lorenzo, Insulin produces myogenesis in C2C12 myoblasts by induction of NF-kappaB and downregulation of AP-1 activities, J.Cell.Physiol. 186 (2001) 82-94.

[416] S.A. Coolican, D.S. Samuel, D.Z. Ewton, F.J. McWade & J.R. Florini, The mitogenic and myogenic actions of insulin-like growth factors utilize distinct signaling pathways, J.Biol.Chem. 272 (1997) 6653-6662.

[417] E. Erbay & J. Chen, The mammalian target of rapamycin regulates C2C12 myogenesis via a kinase-independent mechanism, J.Biol.Chem. 276 (2001) 36079-36082.

[418] A. Cuenda & P. Cohen, Stress-activated protein kinase-2/p38 and a rapamycin-sensitive pathway are required for C2C12 myogenesis, J.Biol.Chem. 274 (1999) 4341-4346.

[419] H.M. Kauffman, W.S. Cherikh, Y. Cheng, D.W. Hanto & B.D. Kahan, Maintenance immunosuppression with target-of-rapamycin inhibitors is associated with a reduced incidence of de novo malignancies, Transplantation 80 (2005) 883-889.

[420] C. Porta, C. Paglino & A. Mosca, Targeting PI3K/Akt/mTOR Signaling in Cancer, Front.Oncol. 4 (2014) 64.

[421] H.A. Burris 3rd, Overcoming acquired resistance to anticancer therapy: focus on the PI3K/AKT/mTOR pathway, Cancer Chemother.Pharmacol. 71 (2013) 829-842.

[422] B. Levine, M. Packer & P. Codogno, Development of autophagy inducers in clinical medicine, J.Clin.Invest. 125 (2015) 14-24.

[423] G. Kroemer, Autophagy: a druggable process that is deregulated in aging and human disease, J.Clin.Invest. 125 (2015) 1-4.

[424] L. Yang, P. Li, S. Fu, E.S. Calay & G.S. Hotamisligil, Defective hepatic autophagy in obesity promotes ER stress and causes insulin resistance, Cell.Metab. 11 (2010) 467-478.

[425] K.L. Poulin, R.M. Lanthier, A.C. Smith, C. Christou, M. Risco Quiroz, K.L. Powell, R.W. O'Meara, R. Kothary, et al, Retargeting of adenovirus vectors through genetic fusion of a single-chain or single-domain antibody to capsid protein IX, J.Virol. 84 (2010) 10074-10086.

[426] G. Gouspillou & R.T. Hepple, Facts and controversies in our understanding of how caloric restriction impacts the mitochondrion, Exp.Gerontol. 48 (2013) 1075-1084.

[427] L. Galluzzi, O. Kepp & G. Kroemer, Mitochondria: master regulators of danger signalling, Nat.Rev.Mol.Cell Biol. 13 (2012) 780-788.

[428] R. Rizzuto, D. De Stefani, A. Raffaello & C. Mammucari, Mitochondria as sensors and regulators of calcium signalling, Nat.Rev.Mol.Cell Biol. 13 (2012) 566-578.

[429] Q. Zhang, M. Raoof, Y. Chen, Y. Sumi, T. Sursal, W. Junger, K. Brohi, K. Itagaki, et al, Circulating mitochondrial DAMPs cause inflammatory responses to injury, Nature 464 (2010) 104-107.

[430] P. Boya, R.A. Gonzalez-Polo, N. Casares, J.L. Perfettini, P. Dessen, N. Larochette, D. Metivier, D. Meley, et al, Inhibition of macroautophagy triggers apoptosis, Mol.Cell.Biol. 25 (2005) 1025-1040.

[431] L. Vucicevic, M. Misirkic-Marjanovic, V. Paunovic, T. Kravic-Stevovic, T. Martinovic, D. Ciric, N. Maric, S. Petricevic, et al, Autophagy inhibition uncovers the neurotoxic action of the antipsychotic drug olanzapine, Autophagy 10 (2014) 2362-2378.

[432] S. Saez-Atienzar, L. Bonet-Ponce, J.R. Blesa, F.J. Romero, M.P. Murphy, J. Jordan & M.F. Galindo, The LRRK2 inhibitor GSK2578215A induces protective autophagy in SH-SY5Y cells: involvement of Drp-1-mediated mitochondrial fission and mitochondrial-derived ROS signaling, Cell.Death Dis. 5 (2014) e1368.

[433] J.F. Rivera, S. Costes, T. Gurlo, C.G. Glabe & P.C. Butler, Autophagy defends pancreatic beta cells from human islet amyloid polypeptide-induced toxicity, J.Clin.Invest. 124 (2014) 3489-3500.

[434] S.P. Elmore, T. Qian, S.F. Grissom & J.J. Lemasters, The mitochondrial permeability transition initiates autophagy in rat hepatocytes, FASEB J. 15 (2001) 2286-2287.

[435] M. Priault, B. Salin, J. Schaeffer, F.M. Vallette, J.P. di Rago & J.C. Martinou, Impairing the bioenergetic status and the biogenesis of mitochondria triggers mitophagy in yeast, Cell Death Differ. 12 (2005) 1613-1621.

[436] H. Abeliovich, M. Zarei, K.T. Rigbolt, R.J. Youle & J. Dengjel, Involvement of mitochondrial dynamics in the segregation of mitochondrial matrix proteins during stationary phase mitophagy, Nat.Commun. 4 (2013) 2789.

[437] N. Gurusamy, I. Lekli, N.V. Gorbunov, M. Gherghiceanu, L.M. Popescu & D.K. Das, Cardioprotection by adaptation to ischaemia augments autophagy in association with BAG-1 protein, J.Cell.Mol.Med. 13 (2009) 373-387.

[438] A.M. Andres, G. Hernandez, P. Lee, C. Huang, E.P. Ratliff, J. Sin, C.A. Thornton, M.V. Damasco, et al, Mitophagy is required for acute cardioprotection by simvastatin, Antioxid.Redox Signal. 21 (2014) 1960-1973.

[439] A.Z. Saadet Turkseven, Determination of mitochondrial fragmentation and autophagosome formation in C2C12 skeletal muscle cells, Turkish Journal of Medical Sciences, Turk J Med Sci 43 (2013) 775-781.

[440] Q. Zhang, H. Kuang, C. Chen, J. Yan, H.C. Do-Umehara, X.Y. Liu, L. Dada, K.M. Ridge, et al, The kinase Jnk2 promotes stress-induced mitophagy by targeting the small mitochondrial form of the tumor suppressor ARF for degradation, Nat.Immunol. 16 (2015) 458-466.

[441] M. Frank, S. Duvezin-Caubet, S. Koob, A. Occhipinti, R. Jagasia, A. Petcherski, M.O. Ruonala, M. Priault, et al, Mitophagy is triggered by mild oxidative stress in a mitochondrial fission dependent manner, Biochim.Biophys.Acta 1823 (2012) 2297-2310.

[442] A.S. Rambold, B. Kostelecky, N. Elia & J. Lippincott-Schwartz, Tubular network formation protects mitochondria from autophagosomal degradation during nutrient starvation, Proc.Natl.Acad.Sci.U.S.A. 108 (2011) 10190-10195.

[443] B.G. Drew, V. Ribas, J.A. Le, D.C. Henstridge, J. Phun, Z. Zhou, T. Soleymani, P. Daraei, et al, HSP72 is a mitochondrial stress sensor critical for Parkin action, oxidative metabolism, and insulin sensitivity in skeletal muscle, Diabetes 63 (2014) 1488-1505.

[444] J.M. Boyd, S. Malstrom, T. Subramanian, L.K. Venkatesh, U. Schaeper, B. Elangovan, C. D'Sa-Eipper & G. Chinnadurai, Adenovirus E1B 19 kDa and Bcl-2 proteins interact with a common set of cellular proteins, Cell 79 (1994) 341-351.

[445] G. Chen, R. Ray, D. Dubik, L. Shi, J. Cizeau, R.C. Bleackley, S. Saxena, R.D. Gietz, et al, The E1B 19K/Bcl-2-binding protein Nip3 is a dimeric mitochondrial protein that activates apoptosis, J.Exp.Med. 186 (1997) 1975-1983.

[446] C. Vande Velde, J. Cizeau, D. Dubik, J. Alimonti, T. Brown, S. Israels, R. Hakem & A.H. Greenberg, BNIP3 and genetic control of necrosis-like cell death through the mitochondrial permeability transition pore, Mol.Cell.Biol. 20 (2000) 5454-5468.

[447] R. Ray, G. Chen, C. Vande Velde, J. Cizeau, J.H. Park, J.C. Reed, R.D. Gietz & A.H. Greenberg, BNIP3 heterodimerizes with Bcl-2/Bcl-X(L) and induces cell death independent of a Bcl-2 homology 3 (BH3) domain at both mitochondrial and nonmitochondrial sites, J.Biol.Chem. 275 (2000) 1439-1448.

[448] M. Bauer, A.C. Hamm, M. Bonaus, A. Jacob, J. Jaekel, H. Schorle, M.J. Pankratz & J.D. Katzenberger, Starvation response in mouse liver shows strong correlation with life-span-prolonging processes, Physiol.Genomics 17 (2004) 230-244.

[449] D. Glick, W. Zhang, M. Beaton, G. Marsboom, M. Gruber, M.C. Simon, J. Hart, G.W. Dorn 2nd, et al, BNip3 regulates mitochondrial function and lipid metabolism in the liver, Mol.Cell.Biol. 32 (2012) 2570-2584.

[450] C.W. Park, S.M. Hong, E.S. Kim, J.H. Kwon, K.T. Kim, H.G. Nam & K.Y. Choi, BNIP3 is degraded by ULK1-dependent autophagy via MTORC1 and AMPK, Autophagy 9 (2013) 345-360.

[451] R. Dhingra, V. Margulets, S.R. Chowdhury, J. Thliveris, D. Jassal, P. Fernyhough, G.W. Dorn 2nd & L.A. Kirshenbaum, Bnip3 mediates doxorubicin-induced cardiac myocyte necrosis and mortality through changes in mitochondrial signaling, Proc.Natl.Acad.Sci.U.S.A. 111 (2014) E5537-44.

[452] H. Zhang, M. Bosch-Marce, L.A. Shimoda, Y.S. Tan, J.H. Baek, J.B. Wesley, F.J. Gonzalez & G.L. Semenza, Mitochondrial autophagy is an HIF-1-dependent adaptive metabolic response to hypoxia, J.Biol.Chem. 283 (2008) 10892-10903.

[453] Y. Zhang, H. Qi, R. Taylor, W. Xu, L.F. Liu & S. Jin, The role of autophagy in mitochondria maintenance: characterization of mitochondrial functions in autophagy-deficient S. cerevisiae strains, Autophagy 3 (2007) 337-346.

[454] A. Nakai, O. Yamaguchi, T. Takeda, Y. Higuchi, S. Hikoso, M. Taniike, S. Omiya, I. Mizote, et al, The role of autophagy in cardiomyocytes in the basal state and in response to hemodynamic stress, Nat.Med. 13 (2007) 619-624.

[455] H.H. Pua, J. Guo, M. Komatsu & Y.W. He, Autophagy is essential for mitochondrial clearance in mature T lymphocytes, J.Immunol. 182 (2009) 4046-4055.

[456] M. Mortensen, E.J. Soilleux, G. Djordjevic, R. Tripp, M. Lutteropp, E. Sadighi-Akha, A.J. Stranks, J. Glanville, et al, The autophagy protein Atg7 is essential for hematopoietic stem cell maintenance, J.Exp.Med. 208 (2011) 455-467.

[457] Y. Zhang, S. Goldman, R. Baerga, Y. Zhao, M. Komatsu & S. Jin, Adipose-specific deletion of autophagy-related gene 7 (atg7) in mice reveals a role in adipogenesis, Proc.Natl.Acad.Sci.U.S.A. 106 (2009) 19860-19865.

[458] J.J. Wu, C. Quijano, E. Chen, H. Liu, L. Cao, M.M. Fergusson, I.I. Rovira, S. Gutkind, et al, Mitochondrial dysfunction and oxidative stress mediate the physiological impairment induced by the disruption of autophagy, Aging (Albany NY) 1 (2009) 425-437.

[459] M.J. Kim, O.K. Choi, K.S. Chae, M.K. Kim, J.H. Kim, M. Komatsu, K. Tanaka, H. Lee, et al, Mitochondrial Complexes I and II Are More Susceptible to Autophagy Deficiency in Mouse Î²-Cells, Endocrinol.Metab.(Seoul) 30 (2015) 65-70.

[460] M.A. Johnson, S. Vidoni, R. Durigon, S.F. Pearce, J. Rorbach, J. He, G. Brea-Calvo, M. Minczuk, et al, Amino Acid Starvation Has Opposite Effects on Mitochondrial and Cytosolic Protein Synthesis, PLoS One 9 (2014) . doi:10.1371/journal.pone.0093597.

[461] E. Nisoli, C. Tonello, A. Cardile, V. Cozzi, R. Bracale, L. Tedesco, S. Falcone, A. Valerio, et al, Calorie restriction promotes mitochondrial biogenesis by inducing the expression of eNOS, Science 310 (2005) 314-317.

[462] F.M. Cerqueira, F.R. Laurindo & A.J. Kowaltowski, Mild mitochondrial uncoupling and calorie restriction increase fasting eNOS, akt and mitochondrial biogenesis, PLoS One 6 (2011) e18433.

[463] A. Zimmermann, M.A. Bauer, G. Kroemer, F. Madeo & D. Carmona-Gutierrez, When less is more: hormesis against stress and disease, Microb.Cell. 1 (2014) 150-153.

[464] W. Martinet, G.R. De Meyer, A.G. Herman & M.M. Kockx, Amino acid deprivation induces both apoptosis and autophagy in murine C2C12 muscle cells, Biotechnol.Lett. 27 (2005) 1157-1163.

[465] H.Y. Nam, M.W. Han, H.W. Chang, Y.S. Lee, M. Lee, H.J. Lee, B.W. Lee, H.J. Lee, et al, Radioresistant cancer cells can be conditioned to enter senescence by mTOR inhibition, Cancer Res. 73 (2013) 4267-4277.

[466] K. Singh, S. Matsuyama, J.A. Drazba & A. Almasan, Autophagy-dependent senescence in response to DNA damage and chronic apoptotic stress, Autophagy 8 (2012) 236-251.

[467] S. Patschan, J. Chen, O. Gealekman, K. Krupincza, M. Wang, L. Shu, J.A. Shayman & M.S. Goligorsky, Mapping mechanisms and charting the time course of premature cell senescence and apoptosis: lysosomal dysfunction and ganglioside accumulation in endothelial cells, Am.J.Physiol.Renal Physiol. 294 (2008) F100-9.

[468] F.A. Mar, J. Debnath & B.A. Stohr, Autophagy-independent senescence and genome instability driven by targeted telomere dysfunction, Autophagy 11 (2015) 527-537.

[469] Z.N. Demidenko, S.G. Zubova, E.I. Bukreeva, V.A. Pospelov, T.V. Pospelova & M.V. Blagosklonny, Rapamycin decelerates cellular senescence, Cell.Cycle 8 (2009) 1888-1895.

[470] R.M. Laberge, Y. Sun, A.V. Orjalo, C.K. Patil, A. Freund, L. Zhou, S.C. Curran, A.R. Davalos, et al, MTOR regulates the pro-tumorigenic senescence-associated secretory phenotype by promoting IL1A translation, Nat.Cell Biol. 17 (2015) 1049-1061.

[471] M. Laplante & D.M. Sabatini, mTOR signaling in growth control and disease, Cell 149 (2012) 274-293.

[472] T.W. Kensler, N. Wakabayashi & S. Biswal, Cell survival responses to environmental stresses via the Keap1-Nrf2-ARE pathway, Annu.Rev.Pharmacol.Toxicol. 47 (2007) 89-116.

[473] L. Zhu, E.C. Barrett, Y. Xu, Z. Liu, A. Manoharan & Y. Chen, Regulation of Cigarette Smoke (CS)-Induced Autophagy by Nrf2, PLoS One 8 (2013) e55695.

[474] S. Yoon, S.U. Woo, J.H. Kang, K. Kim, H.J. Shin, H.S. Gwak, S. Park & Y.J. Chwae, NF-kappaB and STAT3 cooperatively induce IL6 in starved cancer cells, Oncogene 31 (2012) 3467-3481.

[475] C.A. Wu, D.Y. Huang & W.W. Lin, Beclin-1-independent autophagy positively regulates internal ribosomal entry site-dependent translation of hypoxia-inducible factor 1alpha under nutrient deprivation, Oncotarget 5 (2014) 7525-7539.

[476] O. Puig & R. Tjian, Transcriptional feedback control of insulin receptor by dFOXO/FOXO1, Genes Dev. 19 (2005) 2435-2446.

[477] C.A. Wu, Y. Chao, S.G. Shiah & W.W. Lin, Nutrient deprivation induces the Warburg effect through ROS/AMPK-dependent activation of pyruvate dehydrogenase kinase, Biochim.Biophys.Acta 1833 (2013) 1147-1156.

[478] T. Kimura, Y. Takabatake, A. Takahashi & Y. Isaka, Chloroquine in cancer therapy: a double-edged sword of autophagy, Cancer Res. 73 (2013) 3-7.

[479] A. Safdar, J.M. Bourgeois, D.I. Ogborn, J.P. Little, B.P. Hettinga, M. Akhtar, J.E. Thompson, S. Melov, et al, Endurance exercise rescues progeroid aging and induces systemic mitochondrial rejuvenation in mtDNA mutator mice, Proc.Natl.Acad.Sci.U.S.A. 108 (2011) 4135-4140.

[480] S. Someya, G.C. Kujoth, M.J. Kim, T.A. Hacker, M. Vermulst, R. Weindruch & T.A. Prolla, Effects of calorie restriction on the lifespan and healthspan of POLG mitochondrial mutator mice, PLoS One 12 (2017) e0171159.

[481] U.B. Pajvani, M.E. Trujillo, T.P. Combs, P. Iyengar, L. Jelicks, K.A. Roth, R.N. Kitsis & P.E. Scherer, Fat apoptosis through targeted activation of caspase 8: a new mouse model of inducible and reversible lipoatrophy, Nat.Med. 11 (2005) 797-803.

[482] P.M. Peixoto, S.Y. Ryu, A. Bombrun, B. Antonsson & K.W. Kinnally, MAC inhibitors suppress mitochondrial apoptosis, Biochem.J. 423 (2009) 381-387.

[483] P.M. Peixoto, O. Teijido, O. Mirzalieva, L.M. Dejean, E.V. Pavlov, B. Antonsson & K.W. Kinnally, MAC inhibitors antagonize the pro-apoptotic effects of tBid and disassemble Bax / Bak oligomers, J.Bioenerg.Biomembr. 49 (2017) 65-74.

Appendix A – Complete Methods

Cell Culture

C2C12 mouse skeletal myoblasts, L6 rat skeletal myoblasts, NIH 3T3 mouse fibroblasts, MCF7 human breast cancer (ATCC), SH-SY5Y human neuroblastoma and HEK 293-A cells (generously provided by Dr. Robin Duncan, University of Waterloo) were cultured in growth media (GM) consisting of low-glucose Dulbecco's Modified Eagles Medium (DMEM; Hyclone, ThermoFisher) containing 10% fetal bovine serum (FBS; ThermoFisher) and 1% penicillin/streptomycin (ThermoFisher) on polystyrene culture dishes (BD Biosciences), as previously performed (369). For microscopy experiments, cells were grown on Cultrex-coated (3432-005-001; R&D Systems) glass coverslips. Coverslip-coating was performed by thawing Cultrex on ice, diluting the stock 1:100 (resulting in a concentration of 120-180 µg/mL) in high-glucose DMEM, incubating coverslip surfaces in an appropriate volume of this diluted solution for 1 hour at room temperature, and plating cells immediately after aspirating the coating solution. C2C12 and L6 cells were appropriately sub-cultured using trypsin (0.25% solution with EDTA, ThermoFisher) to ensure all appropriate treatments and analyses were performed before cells reached confluence to avoid the potential side-effects of spontaneous differentiation. In appropriate situations, myogenic differentiation was induced by switching 80-90% confluent C2C12 or L6 cells to differentiation media consisting of DMEM with 2% horse serum (ThermoFisher) and 1% penicillin/streptomycin. Cells were collected for subsequent experimental analyses via trypsinization and centrifuged at 1000g.

Materials

Cells were treated as indicated with various chemicals/solutions to induce or measure cell stress. These include: Hank's Balanced Salt Solution (HBSS; Gibco formulation: 140mg/L $CaCl_2$, 100mg/L $MgCl_2$-$6H_2O$, 100mg/L $MgSO_4$-7H2O, 400mg/L KCl, 60mg/L KH_2PO_4, 350mg/L $NaHCO_3$, 8.0g/L NaCl, 48mg/L Na_2HPO_4, 1.0g/L D-glucose, with 1% penicillin/streptomycin), chloroquine (Cq, 30-200 µM; Sigma-Aldrich C6628),

leupeptin (Leu, 250 μM; Sigma Aldrich L2884), staurosporine (STS, 15 nM, 125 nM, 0.5 μM or 2.0 μM; Alexis Biochemicals 380-014-C100), cisplatin (CisPL, 25 μM; Enzo Life Sciences 400-40-M250), hydrogen peroxide (H_2O_2, 2.5-5 mM; Sigma Aldrich), the caspase inhibitor z-VAD-FMK (10 or 25 M μM; Enzo Life Sciences ALX-260-020-M005), N-acetyl-L-cysteine (NAC, 10, 20, or 50 μM; Sigma Aldrich A-7250), tiron (1, 2, or 5 mM; Sigma Aldrich), 2',7'-dichlorodihydrofluorescein diacetate (DCF, 25 μM; Sigma Aldrich D399), carbonyl cyanide 3-chlorophenylhydrazone (CCCP, 30 μM; Sigma-Aldrich C2759), rapamycin (Rap, 0.5-10 μM; Enzo Life Sciences BML-A275-0005), mdivi-1 (20 μM; Enzo Life Sciences BML-CM127-0050), the calcium ionophore A23187 (5, 10, or 15 μM; BioVision 1501), oligomycin (oligo, 2.5 μM; Cayman Chemical Company 11341), and doxorubicin (Doxo, 10 μM; Sigma Aldrich D1515).

Vectors, Cloning, and Adenovirus

Vectors encoding shRNA against mouse Atg7 were used as previously described (183). Vectors were purchased from Origene containing an shRNA sequence targeting Atg7 (TG504956) or a scramble control sequence (TR30013).

Adenovirus coding for human Atg7 protein (adAtg7) was generously provided by Dr. Gokhan S. Hotamisligil, Department of Genetics and Complex Diseases, T.H. Chan School of Public Health, Harvard (424). Control adenoviral constructs encoding GFP (adAVH6/adGFP) were a gift from Dr. Robin Parks, Ottawa Hospital Research Institute (425). Virus were amplified using HEK 293A cells and viral particles were isolated/concentrated through repeated freeze-thaw cycles as indicated in the ViraPower Adenoviral Expression System protocol (Life Technologies). AdAtg7 stock volumes were titred to recover Atg7 protein content in Atg7-deficient cells to the levels observed in control/SCR cells (Appendix B Figure 20).

CRISPR/Cas9 vectors targeting mouse Bnip3 were constructed as follows. The region immediately upstream of the transcription start site was mined for candidate guide RNA (gRNA) targets using several available online tools including: Zhang Lab, MIT (http://crispr.mit.edu/), CCTop (http://crispr.cos.uni-heidelberg.de/), and Off-Spotter (https://cm.jefferson.edu/Off-Spotter/). From these, two common gRNA sequences were identified (PAM in brackets): First: 5'GAGCCACCATGTCGCAGAGC(GGG), and Second: 5'GGAGGAGAACCTGCAGGGTG(AGG). The scramble sequence used in Origene CRISPR products was used as a control: 5'GCACTACCAGAGCTAACTCA. Corresponding oligonucleotides were constructed (Sigma Aldrich) to allow cloning into the CRISPR/Cas9 vector pSpCas9(BB)-2A-Puro (PX459) V2.0 (Addgene #62988), which uses a single gRNA. Correct gRNA cloning was confirmed by sequencing constructed vectors (The Center for Applied Genomics, Hospital for Sick Kids, Toronto, Ontario, Canada).

For visualization of mitochondrial morphology and autophagic puncta, cells were co-transfected with the vectors pDsRed2-Mito and pGFP-LC3, generously provided by Dr. D. R. Green (St. Jude's Children's Research Hospital, Memphis, Tennessee) and Dr. Terje Johansen (Department of Medical Biology, UiT, Tromso, Norway), respectively.

Transfections and Gene Knockdown

C2C12 cells were transfected using Lipofectamine 2000 (Life Technologies), optimized according to the manufacturer's instructions, as previously performed (183,369). Briefly, appropriate vector DNA and Lipofectamine was diluted in 100 µL Opti-MEM (Gibco) at a ratio of 1µg: 3µL, and incubated for 5 min at room temperature. This mixture was added to 50-60% confluent cells with media containing 5% FBS in Opti-MEM and incubated for 6 hours, after which cells were washed with PBS and regular growth media was added.

For generating C2C12 cells with stable knockdown of Atg7, cells grown in 12-well plates were transfected with vectors encoding either an shRNA against Atg7 or a scramble control sequence using Lipofectamine 2000 (ThermoFisher) as previously performed (183). 24 hours later, cells were transferred to 10 cm culture plates and those with stable incorporation of each vector were selected by growing cells in GM with 2 μg/mL puromycin (Sigma Aldrich). Surviving clones were individually isolated and assessed for Atg7 protein expression using immunoblotting.

For generating Bnip3 knockout C2C12s, cells grown in 12-well plates were transfected either with the aforementioned Bnip3 CRISPR or scramble control vector. 24 hours later, cells were transferred to 10 cm culture plates and those with incorporation of each vector were selected by growing cells in GM with 2 μg/mL puromycin (Sigma Aldrich). Surviving clones were individually isolated and assessed for Bnip3 protein expression using immunoblotting.

Subcellular Fractionation

Cells were additionally separated into cytosolic-, mitochondrial-, and nuclear-enriched fractions (369). After collection via trypsinization, cells were incubated in digitonin buffer (PBS with 250 mM sucrose, 80 mM KCl, and 50 μg/mL digitonin, Sigma Aldrich D141) for 5 min on ice. Cells were centrifuged at 1000g for 10 min, the supernatant was collected and centrifuged at 16,000g for 10 minutes to pellet any mitochondrial contamination, and the supernatant from this spin kept as the cytosolic-enriched fraction. The pellet (P1) remaining from the 1000g spin was suspended in PBS, centrifuged at 1000g for 5 min, the pellet suspended in lysis buffer (LB, pH 7.4; 20mM HEPES, 10mM NaCl, 1.5mM $MgCl_2$, 1 mM DTT, 20% glycerol, and 0.1% Triton-X100), and allowed to sit on ice for 5 min. This was then centrifuged at 1000g for 5 min, resulting in a pellet (P2) containing nuclei, and a supernatant (S2) containing mitochondria. S2 was centrifuged at 1000g for 10 min to pellet nuclear contamination, with the resulting supernatant

kept as the mitochondrial-enriched fraction. The P2 pellet was suspended in LB, centrifuged at 1000g for 10 min, the pellet again suspended in LB, sonicated for 12 seconds on ice, and kept as the nuclear-enriched fraction.

Immunoblotting

Immunoblotting was performed as previously described (357,369). Whole-cell lysates were generated by adding ice-cold lysis buffer with protease inhibitors (Complete Cocktail; Roche) to cell pellets followed by sonication for 12 seconds. Protein content was measured using the BCA protein assay method. Briefly, equal amounts of protein were loaded into and separated using 10-12% SDS-PAGE, transferred onto PVDF membranes (Bio-Rad Laboratories), and blocked for 1 hr at room temperature with 5% non-fat dry milk in TBS-T. Membranes were then probed with primary antibodies against: ANT (sc-9299, 1:100), Bcl2 (sc-7382, 1:200), Bax (sc-493, 1:1000), cytochrome c (sc-13156, 1:2000), parkin (sc-32282, 1:500), PARP (sc-7150, 1:200), PGC1 (sc-13067, 1:200), PINK1 (sc-33796, 1:500), p21 (sc-397, 1:1000), p53 (sc-6243, 1:500), phosphorylated histone H2AX (pH2AX, sc-101696, 1:1000; Santa Cruz), Atg7 (8558, 1:1000), Atg4B (5299, 1:1000), Atg12/5 (4180, 1:1000), Beclin1 (3738, 1:1000), LC3 (2775, 1:1000), AMPKα (5831, 1:1000), pAMPKα Thr172 (2535, 1:1000), AMPKβ1/2 (4150, 1:1000), pAMPKβ1 Ser108 (4181, 1:1000), ACC (3676, 1:1000), pACC Ser79 (11818, 1:1000; Cell Signaling Technologies), histone H2B (07-371, 1:2000; Millipore), MnSOD (SOD-110, 1:4000), Smac (ADI-905-244, 1:2000), XIAP (ADI-AAM-050, 1:1000; Enzo Life Sciences), actin (A-2066, 1:2000), Bnip3 (B7931, 1:1000), cleaved caspase-3 (C8487, 1:1000; Sigma Aldrich), myosin (MF-20, 1:2000), myogenin (F5D, 1:200), Pax7 (PAX7, 1:200; Developmental Studies Hybridoma Bank), or p62 (PM045, 1:2000; MBL) overnight at 4^{o}C. Membranes were then incubated with the appropriate horseradish peroxidase- (HRP) conjugated secondary antibody (anti-rabbit: sc-2004, anti-mouse: sc-2005, anti-goat: sc-2020; Santa Cruz), and bands visualized using ECL immunoblotting substrates (BioVision) or Clarity ECL substrates (Bio-Rad) and

the ChemiGenius 2 Bio-Imaging System (Syngene). The approximate molecular weight for each protein was estimated using Precision Plus Protein WesternC Standards and Precision Protein Strep-Tactin HRP Conjugate (Bio-Rad Laboratories).

Proteolytic Enzyme Activity

Enzymatic activity of caspases-3, -8, and -9 was determined using the substrates Ac-DEVD-AFC , Ac-IETD-AMC, and Ac-LEHD-AMC (Enzo Life Sciences), respectively, as previously performed (357,369). Calpain activity was determined similarly, using the substrate Suc-LLVY-AMC. To account for proteasomal cleavage of this substrate, each sample was also analyzed with 25 µM of the calpain inhibitor Z-LL-CHO and the difference in fluorescence was taken as calpain activity. Cell lysates were prepared using lysis buffer without addition of protease inhibitors and incubated in duplicate with 20 µM of the appropriate fluorogenic substrate. Caspase and calpain activity measurements were performed in an assay buffer of 20 mM HEPES, 10 mM DTT, and 10% glycerol.

Lysosomal enzyme activity was measured using the substrate z-FR-AFC (Enzo Life Sciences), generally considered to indicate the activities of cathepsins L and B (357,369). Cell lysates were prepared similar to caspase/calpain assays and analyzed in duplicate with 25 µM of z-FR-AFC in a buffer containing 50 mM sodium acetate, 8 mM DTT, 4 mM EDTA, and 1 mM Pefabloc at pH 5.0. For all activities, fluorescence was measured at 30^{o}C using a Synergy H1 microplate reader (BioTek) with excitation and emission wavelengths of 360 nm and 440 nm for AMC substrates, and 400 nm and 505 nm for AFC substrates, respectively. All enzyme activities are presented normalized to total protein content measured using BCA and expressed as fluorescence intensity in arbitrary units (AU) per milligram protein.

Microscopy

Giemsa

Cell morphology was visualized using Giemsa staining, as previously performed (357). Briefly, after fixing in ice-cold methanol for 10 min and air-drying, cells were incubated with 1:20 dilution of 0.45 µm filtered Giemsa staining solution (Sigma Aldrich 48900) in PBS (pH 6.0) for 45 min at room temperature. Cells were then washed with distilled water and mounted with Permount (ThermoFisher).

Immunofluorescence

Cell and nuclear morphology was also determined using immunofluorescent identification of actin and DAPI. After fixing in 4% formaldehyde for 5 min and permeabilizing in 0.5% Triton-X 100 in PBS for 5 min, cells were blocked in 5% goat serum for 1 hr and incubated with an anti-actin antibody (A-2066, 1:200; Sigma Aldrich) overnight at room temperature. Cells were then incubated with anti-rabbit AlexaFluor 488 secondary antibody for 1 hr (ThermoFisher A-11008), counterstained in 300 nM DAPI (ThermoFisher), and mounted with Prolong Gold (ThermoFisher). ImageJ was used to analyze cell and nuclear shape parameters, with at least 100 cells measured per trial. After masking nuclei by colour threshold, Area and Shape Descriptors measurements were performed. Calculations of these measurements can be found under the Analyze heading of the ImageJ user guide.

β-galactosidase Staining

Senescence-associated β-galactosidase activity staining (SA-Bgal) was performed as previously indicated by others (263). After washing with PBS, cells were fixed in 2% formaldehyde for 5 min at room temperature, washed again with PBS, and then incubated at 37^{o}C for 48 hours in the staining solution consisting of PBS with 1 mg/mL X-gal, 40 mM citric acid, 5 mM potassium ferrocyanide, 5 mM potassium ferricyanide, 150 mM NaCl, and 2 mM $MgCl_2$ at pH 6.0. For all microscopy experiments, cells were grown

on Cultrex- (R&D Systems) coated glass coverslips. All fluorescent microscopy was performed using a Zeiss Laser Scanning Microscope (LSM) 780. All light microscope images were acquired with a Nikon microscope equipped with a PixeLink digital camera.

Flow Cytometry

Mitochondrial Measurements

Cells were collected as described above and suspended in HBSS. Mitochondrial membrane potential and mitochondrial permeability transition pore formation were measured using JC-1 and calcein, respectively, as previously performed (369). Mitochondrial membrane depolarization can be monitored by changes in the JC-1 red:green fluorescence ratio, where a decreased ratio is indicative of decreased mitochondrial membrane potential. After removing from culture, cells were incubated with 2 µM JC-1 in 100 µL HBSS for 15 min at 37 °C, washed by centrifugation, and suspended in HBSS. Mitochondrial permeability transition pore (mPTP) formation occurs during mitochondrial-mediated apoptosis prior to mitochondrial apoptotic protein release. The fluorescent dye calcein AM accumulates in intact mitochondria, but is quenched by cobalt if the mitochondrial membrane becomes permeable to cobalt. Thus a decrease in calcein fluorescence indicates mPTP formation. Briefly, cells were incubated with 1 µM calcein AM and 1 mM $CoCl_2$ in 100 µL HBSS for 15 min at 37°C, washed by centrifugation, and resuspended in 500 µl HBSS. Mitochondria-specific resistance to calcium stress was tested by concomitantly incubating cells with 2.5, 5, or 10 µM of the calcium ionophore A23187 along with JC-1/calcein.

Cell Death

In cell culture experiments, Annexin-V/PI staining was performed to assess the degree and type of cell death occurring after various stressors (388). After treatment, cells were removed from culture dishes

and suspended in Annexin Binding Buffer (10 mM HEPES/NaOH, 150 mM NaCl, 1.8 mM $CaCl_2$, pH 7.4) and incubated with 1 µL of Annexin V-FITC (BioLegend, 640906) and 1 µL of 500 µg/mL propidium iodide (PI, Sigma Aldrich P-4170). Cells were incubated for 20 min at room temperature, after which they were washed and suspended in HBSS. Cells negative for both annexin and PI were classified as healthy, those positive for annexin and negative for PI were considered to be in early stages of cell death, and those positive for both annexin and PI were considered to be in late stages of cell death.

Cell Cycle

After collection, cells were fixed by slowly suspending them in ice-cold 70% ethanol in PBS. Following at least 24 hr fixation, cells were washed with PBS and suspended in PI staining solution containing 40 µg/mL PI, 0.1% Triton-X, and 20 µg/mL RNAse in PBS for 30 minutes at room temperature. For each flow cytometry analysis, the cells from 1 well of a 12-well plate were measured. All flow cytometry analyses were performed on a BD FACSCalibur flow cytometer equipped with Cell Quest Pro software (BD Bioscience).

Mitochondrial Respirometry

Analyses of C2C12 mitochondrial bioenergetics were performed using high resolution respirometry measurement of oxygen consumption (O2K, Oroboros Instruments). After collection via trypsinization, cells were centrifuged at 100g and permeabilized using digitonin buffer (PBS with 250 mM sucrose, 80 mM KCl, and 50 µg/mL digitonin) for 3 min while agitating at room temperature. After centrifuging once more at 200g to remove digitonin, cells were suspended in mitochondrial respiration buffer (Mir06: 0.5 mM EGTA, 3 mM $MgCL_2$-$6H_2O$, 60 mM lactobionic acid, 20 mM taurine, 10 mM KH_2PO_4, 20 mM HEPES, 110 mM sucrose, 1 g/L fatty acid-free BSA, and 100 mg/L catalase; pH 7.1) and transferred into O2K chambers. Respiration was performed in Mir06 at 37^{o}C under hyperoxygenated conditions (350 µM) in

the presence of glutamate (10 mM), pyruvate (5 mM), and malate (2 mM). The sensitivity and maximal response to complex I-supported ADP-stimulated respiration were then measured by conducting an ADP titration with the following concentrations: 1.0 µM, 2.5 µM, 5.0 µM, 10 µM, 20 µM, 50 µM, 100 µM, 200 µM, 500 µM, and 1.0 mM. Succinate was then added in excess (10 mM) to determine maximal complex-II supported respiration. Finally, cytochrome c was added (10 µM) after achieving maximal respiration to test the integrity of the outer mitochondrial membrane. Data is presented normalized to total protein content of the O2K chambers, calculated by aspirating and collecting a portion of the chamber volume upon protocol completion. GraphPad Prism was used to calculate Vmax and EC50 values on ADP titration curves, using the allosteric sigmoidal enzyme kinetics equation: Y=Vmax*X^h/(Khalf^h + X^h).

Reactive Oxygen Species

ROS production was assessed by measuring DCF fluorescence. The day before the experiment, 20,000 cells were plated in each well of a black-walled 96-well cell culture plate. The following day, cells were pre-loaded with dye by incubating them in HBSS with 25 µM DCF for 45 minutes at 37^{o}C/5% CO_2. Cells were then washed twice with warmed PBS and treated as indicated with or without HBSS, STS, NAC, and tiron for 4 hours. After washing again in PBS, HBSS was added to all wells and fluorescence was measured at 37^{o}C using a Synergy H1 microplate reader (BioTek) with excitation and emission wavelengths of 395 nm and 528 nm, respectively. Data is reported as arbitrary fluorescence units after subtracting treatment-specific background fluorescence of wells which did not receive DCF.

Cell Counting

A Beckman-Coulter Z2 particle analyzer was used to assess cell numbers. Events from 12-23 µm were counted as cells.

Statistical Analyses

Results are presented as means ± SEM, where n=3-6 independent experiments. GraphPad Prism was used to perform 1-way and 2-way ANOVA analyses with Tukey post-hoc tests where appropriate with significance indicated when $p<0.05$. Microsoft Excel was used to perform T-tests with significance indicated when $p<0.05$.

Appendix B - Supplementary Data

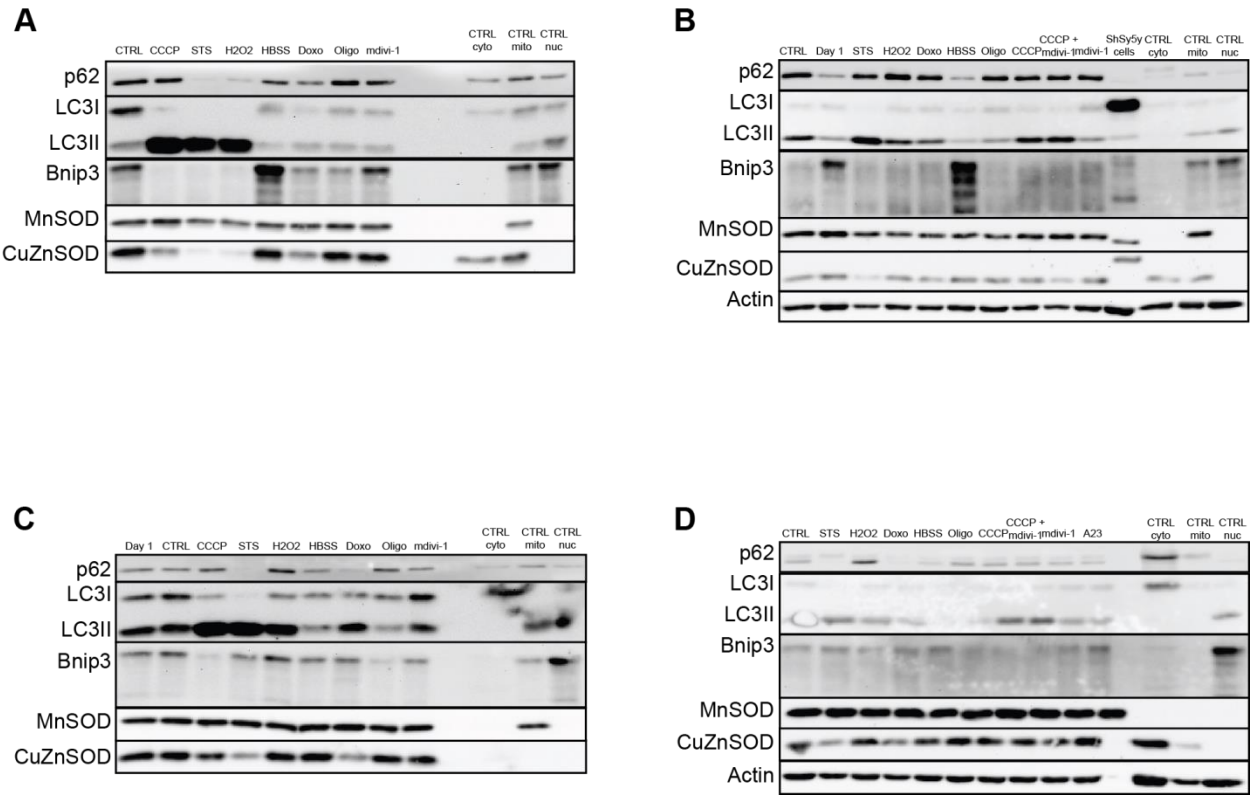

Figure 1. Autophagic signaling induced by various stressors in subconfluent and differentiated C2C12 cells. Subconfluent (A & B) and differentiated (C & D) C2C12 cells were treated as indicated and immunoblotted for autophagy-related proteins. Day 1 = 24 hours after inducing differentiation, CCCP = 30 µM 4 hours, STS = 2 µM 4 hours, H_2O_2 = 2.5 mM (A & B) or 5 mM (C & D) 6 hours, HBSS = 6 hours, Doxo = 10 µM 6 hours, oligo = 2.5 µM 6 hours, mdivi-1 = 20 µM 6 hours, A23 = 1 nM 8 hours.

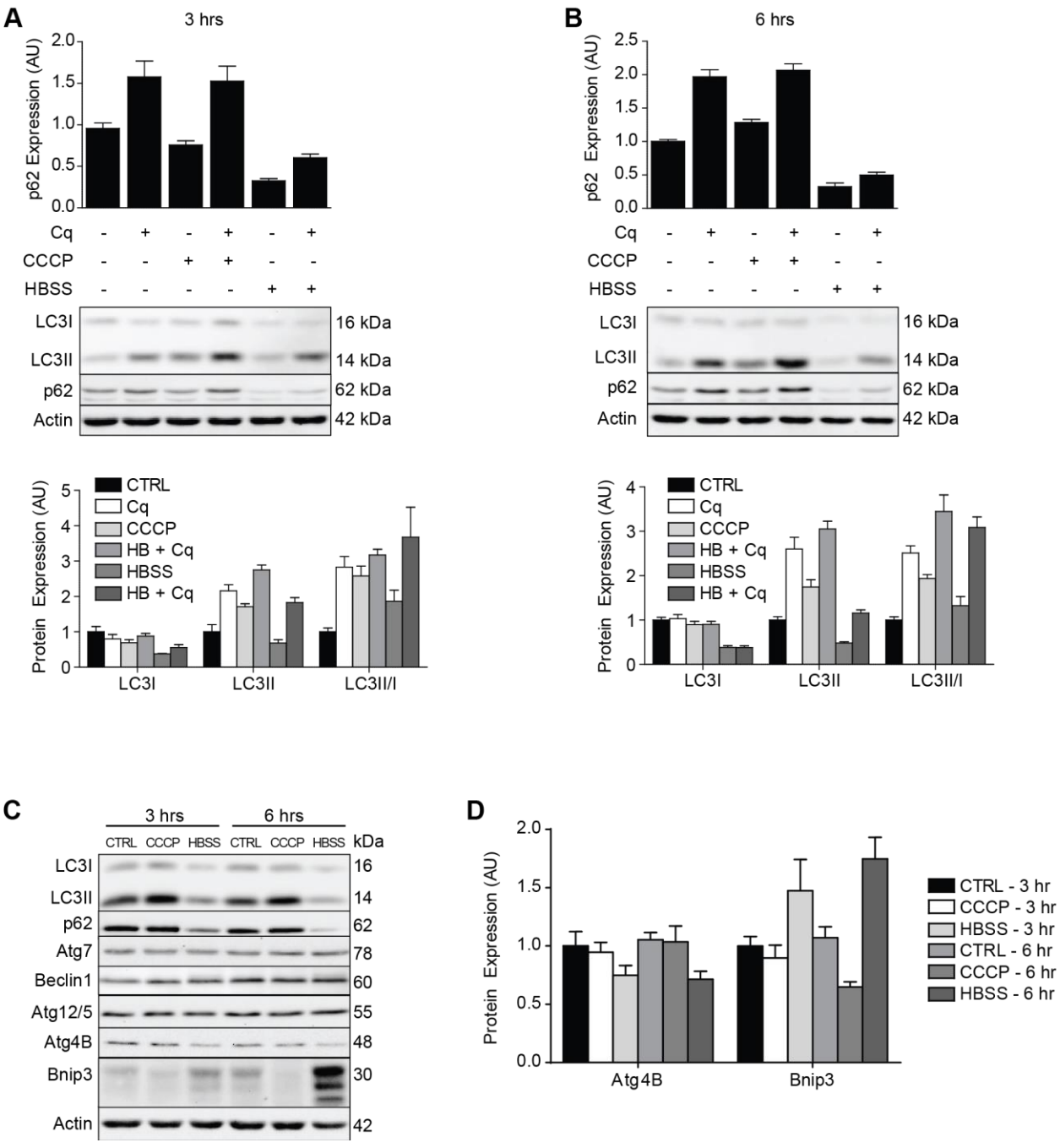

Figure 2. Characterizing autophagy induced by CCCP and HBSS. C2C12 cells were treated with 30 µM CCCP in GM, HBSS, and/or 30 µM chloroquine (Cq) for 3 hours (A) or 6 hours (B) and collected for assessing autophagic flux by p62 and LC3 immunoblotting. (C & D) C2C12 cells were similarly treated with CCCP or HBSS and immunoblotted for various autophagy-related proteins. Apart from the predicted changes to LC3 and p62 protein contents, HBSS decreased Atg4B while Bnip3 was reduced by CCCP and increased by HBSS. N=4. Note, some of this data is presented in Chapter IV, Figure 1.

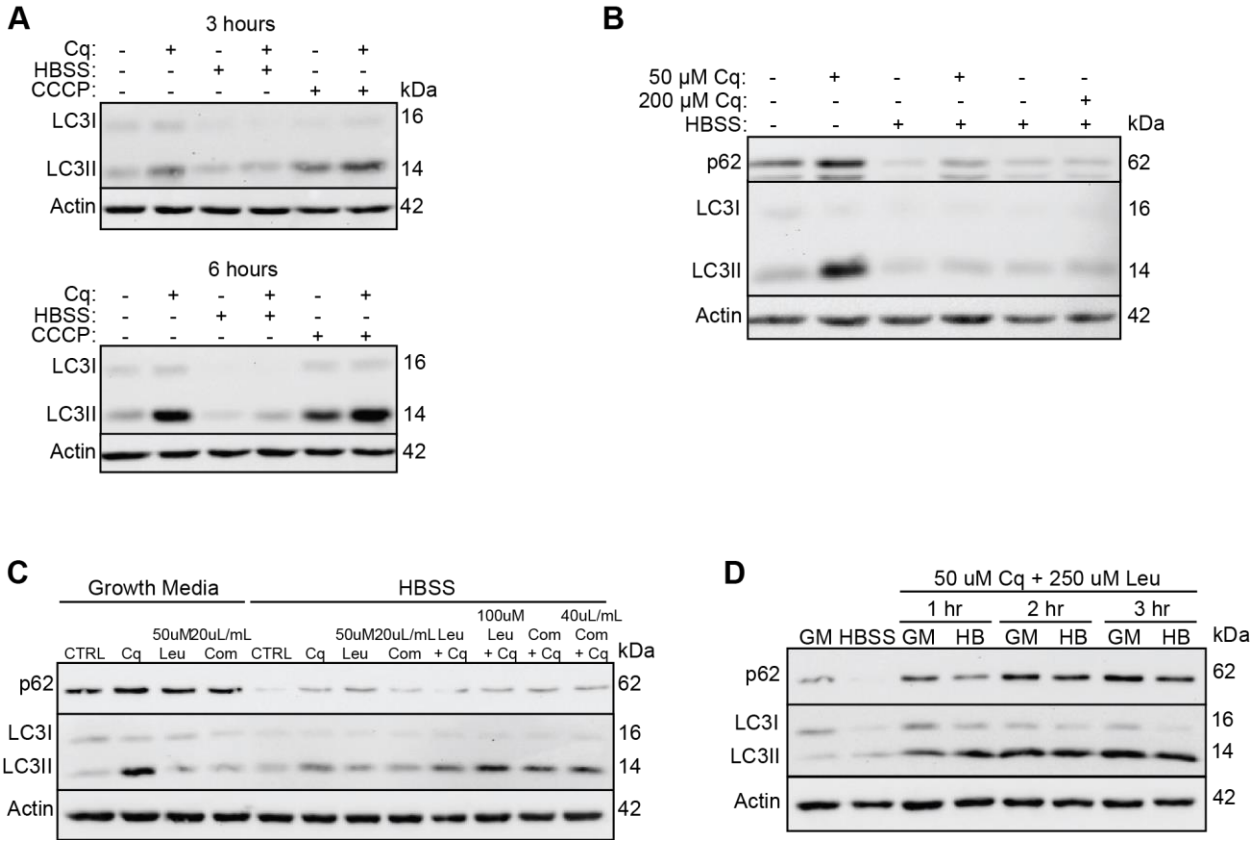

Figure 3. Autophagy flux analyses with various lysosomal enzyme inhibiting chemicals. C2C12 cells were treated as indicated and immunoblotted for LC3 and p62 to quantitatively analyze autophagic flux. (A) Initial assays were performed with 10 µM chloroquine (Cq, which impairs degradative enzymes by altering lysosomal pH levels), although this concentration was unable to prevent p62 and LC3II degradation during HBSS treatments, presumably due to the high amount of autophagy induction. (B) Up to 200 µM Cq was unable to fully prevent HBSS-induced p62 and LC3II degradation during a 3 hour treatment. (C) Leupeptin (Leu, a serine and cysteine protease inhibitor that doesn't affect pepsin or cathepsins A/D) and Complete Cocktail (a proprietary collection of serine, cysteine, metalloproteinase, and calpain inhibitors) were tested for their ability to prevent p62 and LC3II degradation caused by 3 hours of HBSS. (D) A combination of 50 µM Cq and 250 µM Leu was able to prevent HBSS-induced LC3II degradation during shorter time periods. Note that the "gold standard" for performing an LC3/p62 autophagic flux assay is to treat cells with 1-10 µM pepstatin (aspartic protease inhibitor) and 1-10 µM E64 (cysteine protease inhibitor) along with the chemical/treatment of interest

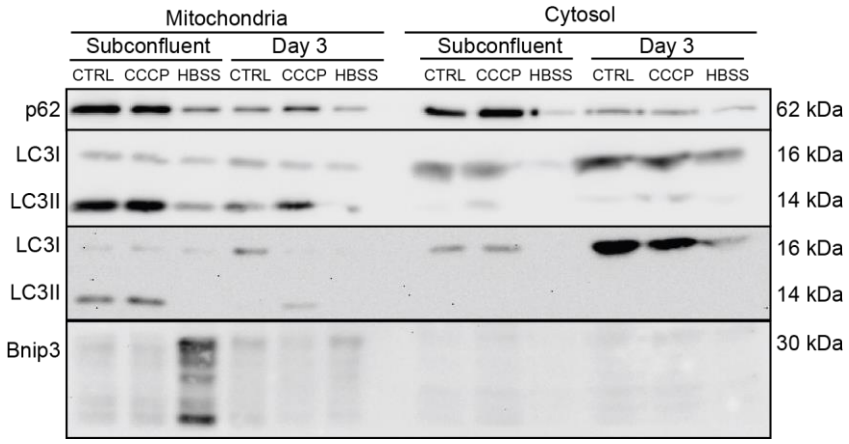

Figure 4. Assessing autophagy-related signaling induced by CCCP and HBSS in subcellular fractions. Subconfluent C2C12 cells and those on Day 3 of differentiation were treated with 30 µM CCCP or HBSS for 6 hours and separated into mitochondrial and cytosolic fractions prior to immunoblotting. A trial of this experiment is presented in Chapter IV, Figure 1.

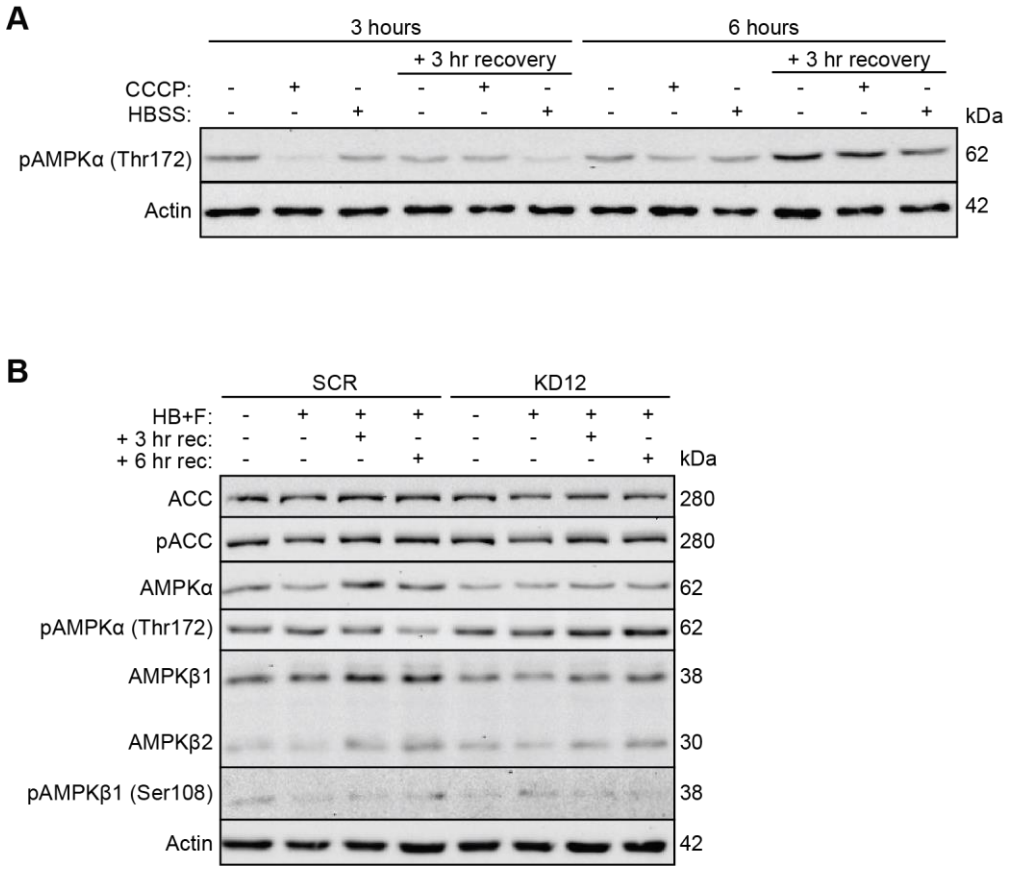

Figure 5. AMPK-related signaling is not induced by HBSS or altered by Atg7 deficiency. (A) C2C12 cells were treated as indicated with 30 μM CCCP or HBSS for 3 or 6 hours and collected immediately or after spending 3 additional hours in regular GM (+3 hr recovery). Immunoblotting of phosphorylated AMPKα was performed to assess AMPK signaling activation. (B) Control (SCR) and Atg7-deficient cells (shAtg7) were treated as indicated with HB+F for 1.5 hours and cells were collected immediately or after spending 3 or 6 additional hours in regular GM. Immunoblotting of various AMPK-related targets was performed to assess AMPK signaling. There were no significant changes in any protein content, suggesting amino acid and serum starvation does not activate AMPK in C2C12 cells.

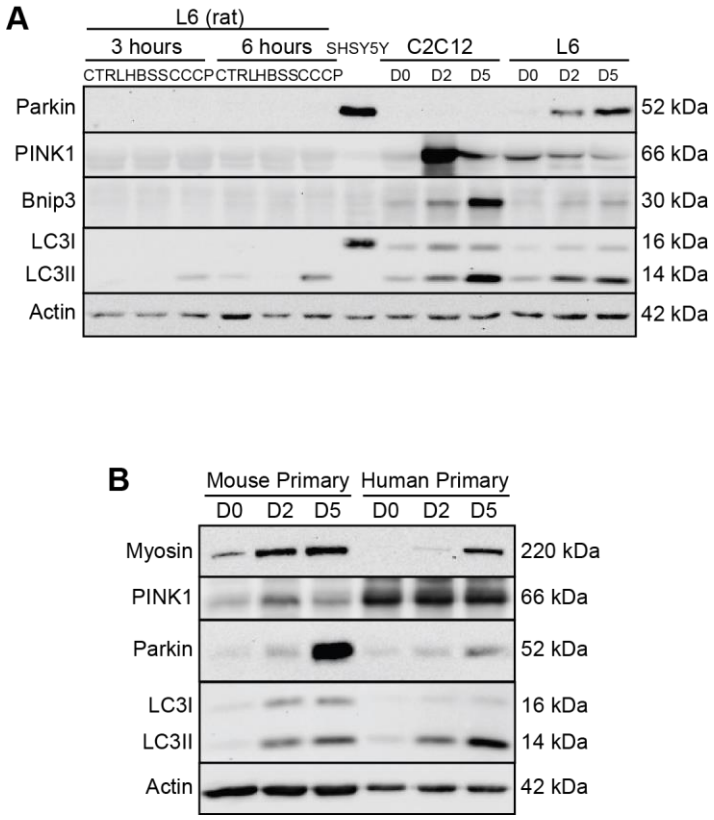

Figure 6. Comparing autophagy signaling in C2C12, L6, SHSY5Y, mouse primary, and human primary myoblasts. (A) L6 myoblasts were treated as indicated with 30 μM CCCP or HBSS for 3 or 6 hours and C2C12 and L6 cells were collected during various time points during differentiation and collected for immunoblotting. Notably, PINK1 demonstrates massive induction in C2C12 but not L6 cells on Day 1 of differentiation. Surprisingly, C2C12s possessed undetectable levels of Parkin protein. (B) Despite this, Parkin protein is expressed in mouse and human primary myoblasts and dramatically increases during differentiation.

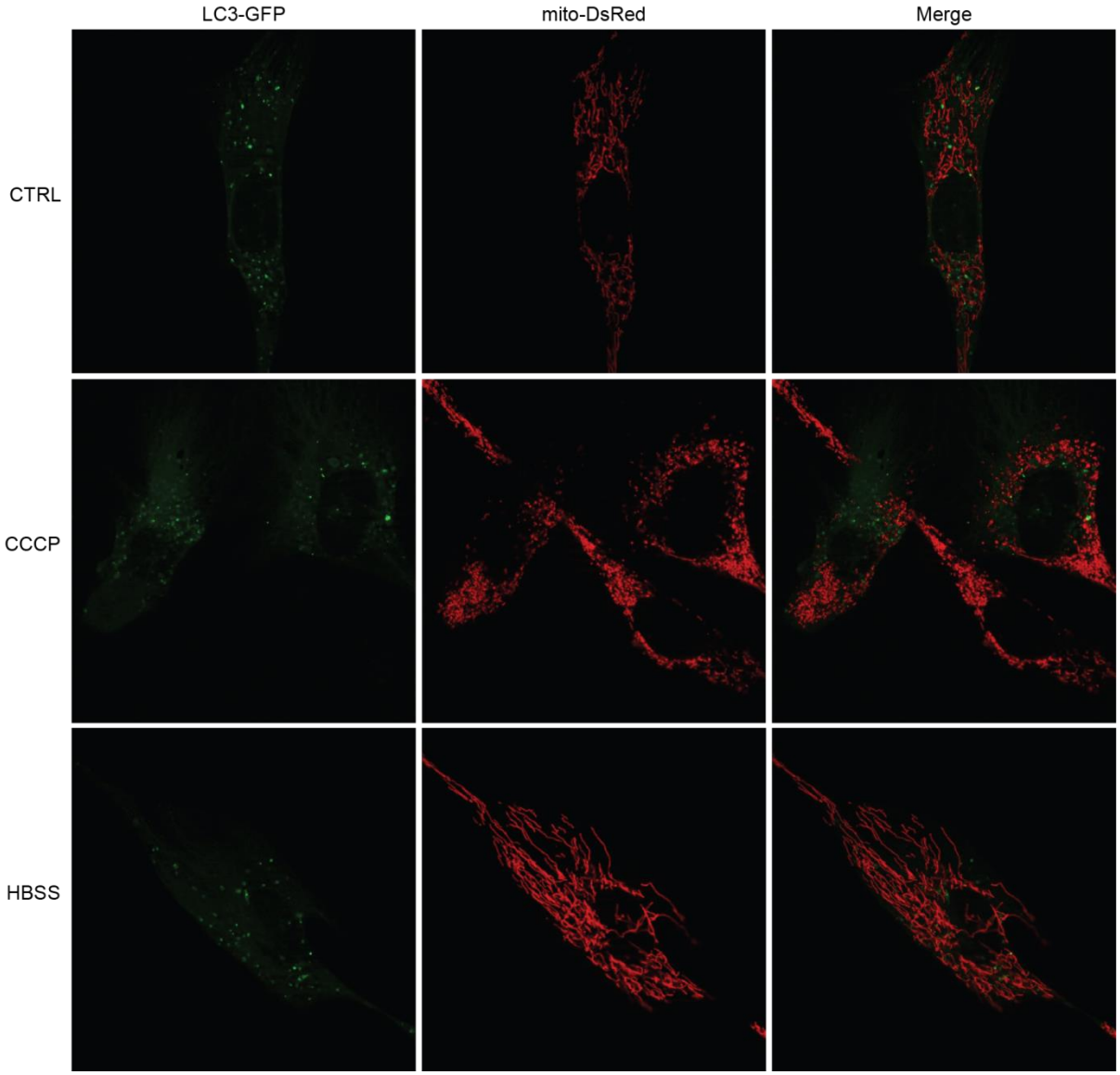

Figure 7. Mitochondria and autophagosome visualization during CCCP and HBSS treatments. C2C12 cells were co-transfected with LC3-GFP and mito-DsRed vectors and imaged live using fluorescent microscopy. Cells were left untreated (CTRL) or administered 30 µM CCCP or HBSS for 6 hours.

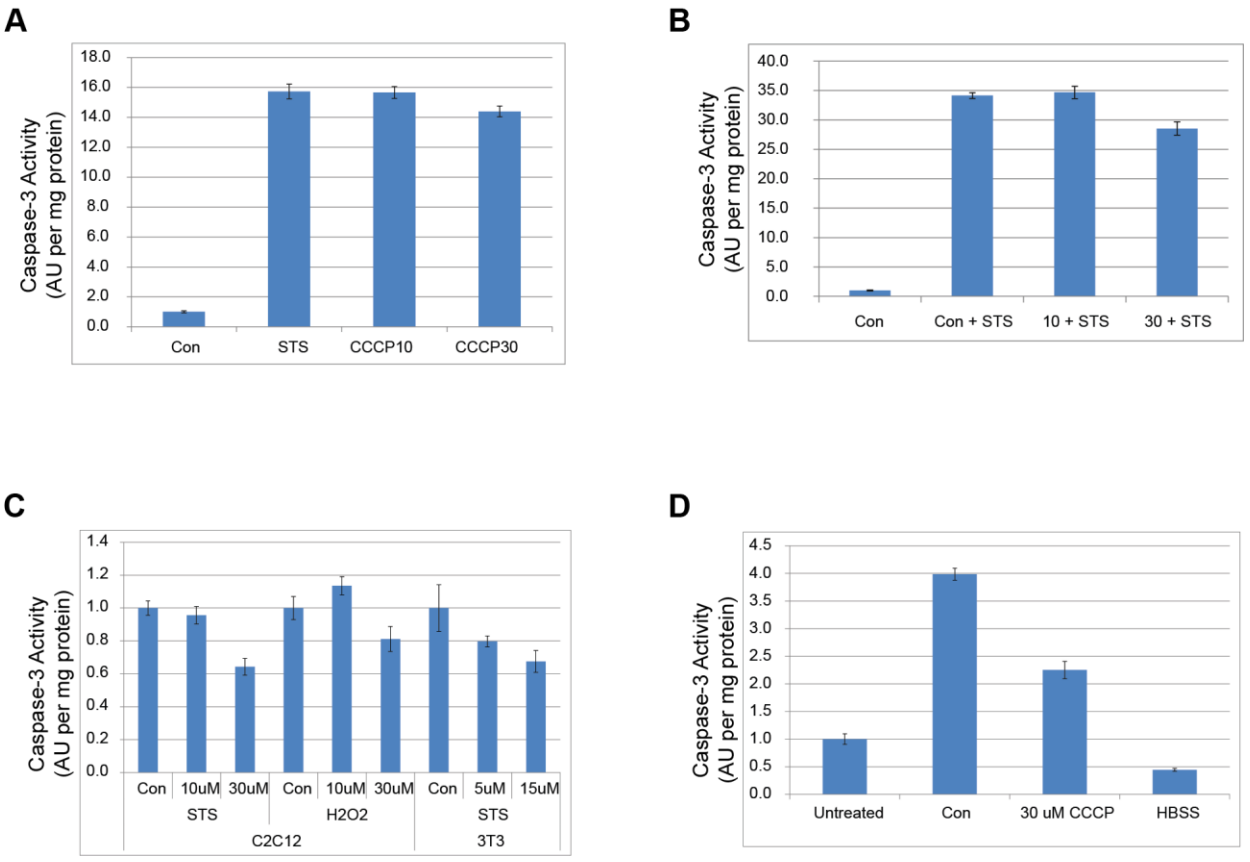

Figure 8. Determining appropriate conditions for repeated treatments in various cell types. Cells were administered CCCP or incubated in HBSS, treated with STS to induce cell death, and assessed for caspase-3 activity to determine whether repeated treatments led to cyto-protection. (A) Differentiating C2C12 cells were administered 10 or 30 µM CCCP for 3 hours per day for 3 consecutive days and given 2.0 µM STS 20 hours following the final treatment. (B) Similar experiment to (A) performed in proliferative C2C12 cells. (C) Proliferative C2C12 and NIH3T3 cells were administered the indicated concentrations of CCCP for 5 hours per day for 3 consecutive days and given 1 µM STS 20 hours following the final treatment. (D) Proliferative C2C12 cells were administered 30 µM CCCP or incubated in HBSS for 5 hours per day for 3 consecutive days and given 0.5 µM STS 20 hours following the final treatment. Error bars are SEM, n=3.

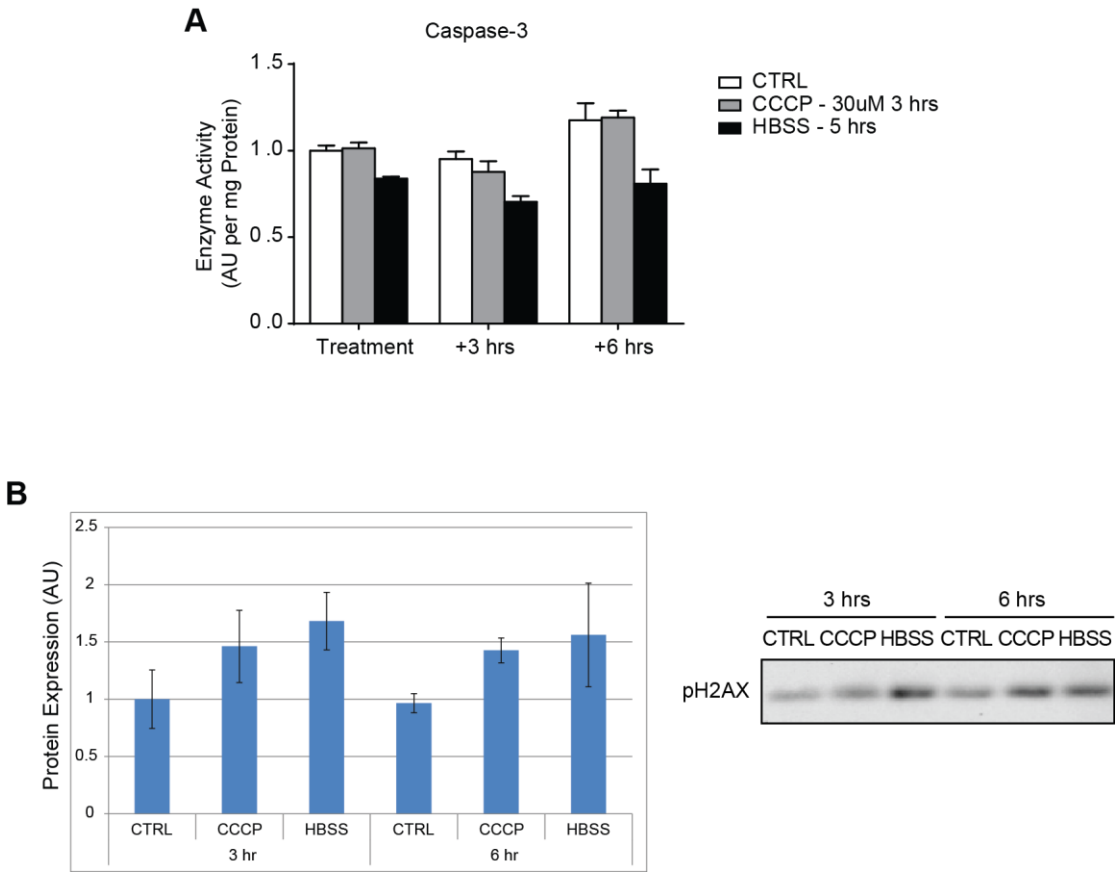

Figure 9. Cell death signaling caused by individual CCCP and HBSS treatments. (A) C2C12 cells were treated as indicated and assessed for caspase-3 activity. +3/6 hours refers to cells given regular growth media following treatments and allowed to "recover" for 3 or 6 hours. (B) C2C12 cells were treated as indicated and immunoblotted for pH2AX protein content. Error bars are SEM, n=3.

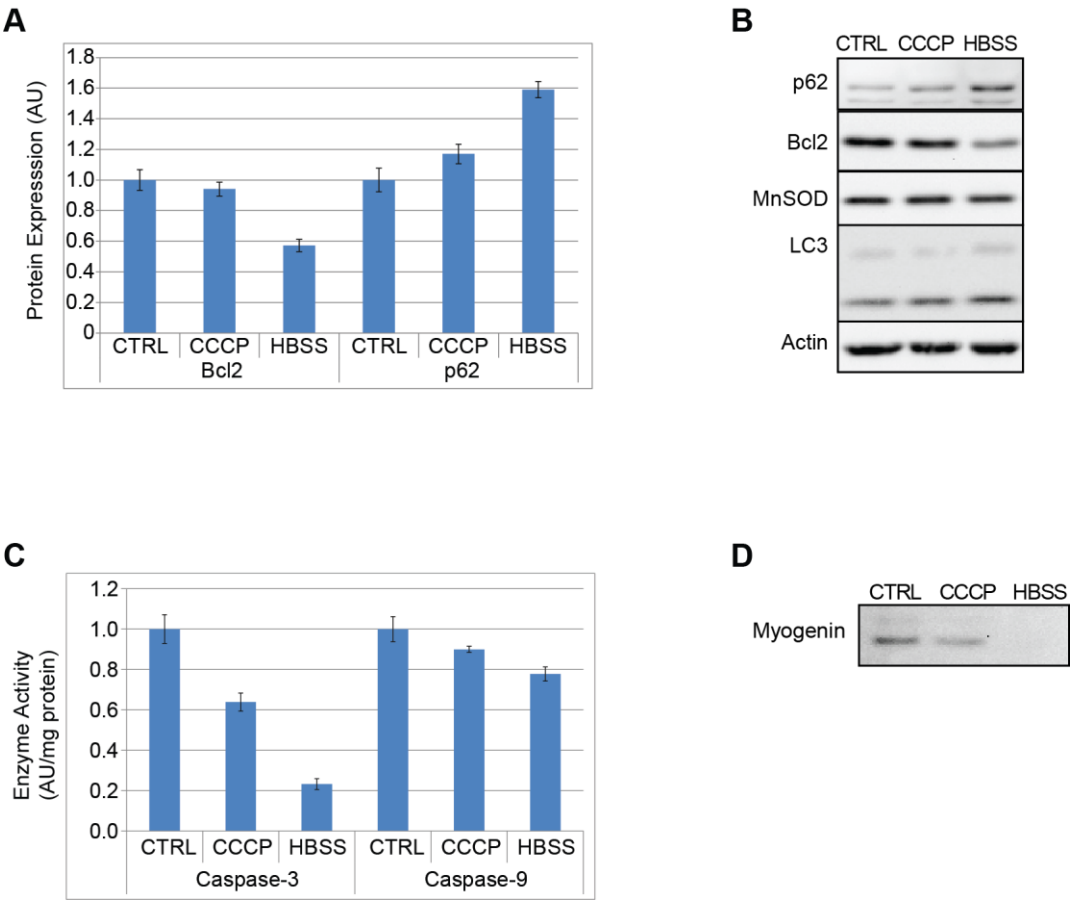

Figure 10. Effect of repeated CCCP and HBSS treatments on cell death and autophagy signaling. C2C12 cells were administered 30 µM CCCP or incubated in HBSS for 5 hours per day for 3 consecutive days and collected 20 hours following the final treatment. (A) Quantitative analyses of Bcl2 and p62 protein expression. (B) Representative immunoblots. (C) Enzyme activity of caspase-3 and caspase-9. (D) As the changes depicted in (A, B, & C) can be explained by CTRL cells being over-confluent and HBSS cells being under-confluent, immunoblotting of myogenin was performed to determine the onset of myogenic differentiation. As suspected, CTRL expressed increased myogenin protein. Error bars are SEM, n=3.

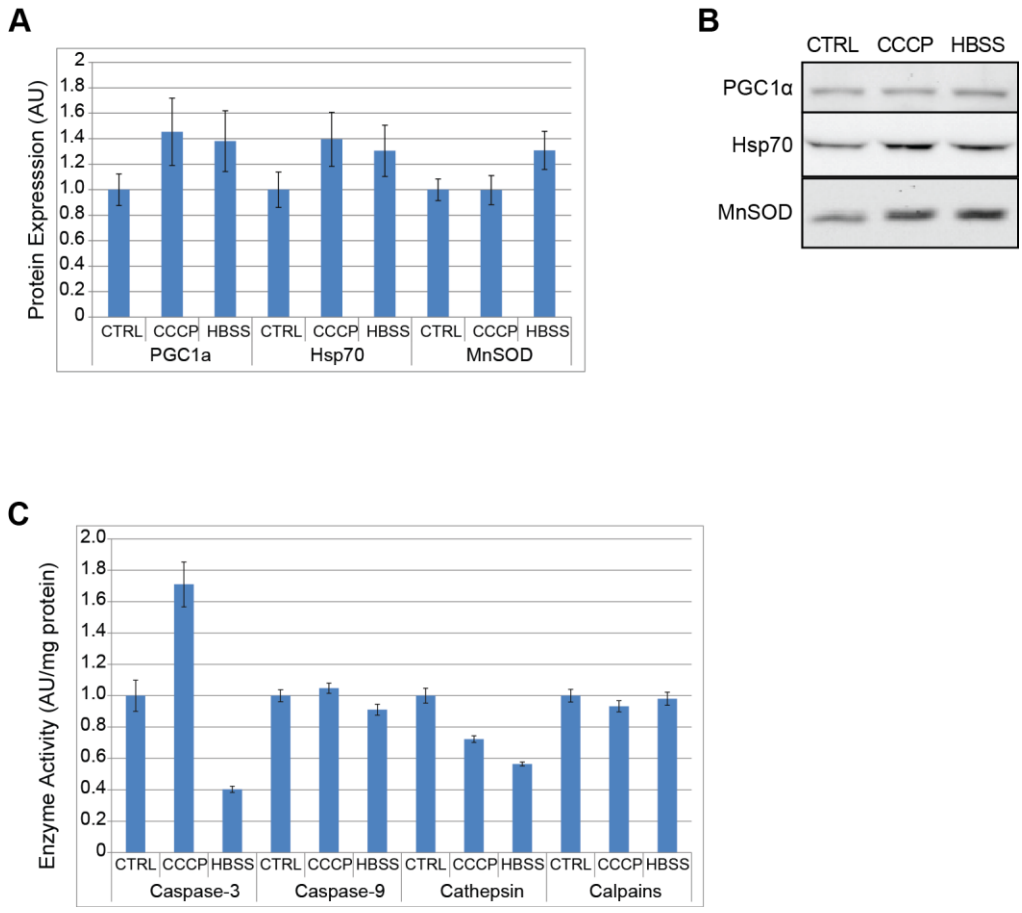

Figure 11. Effect of repeated CCCP and HBSS exposure on proteolytic enzyme activity and select stress-related protein markers. C2C12 cells were treated as in the previous Figure, but seeded at treatment-specific densities that resulted in similar confluence between groups after 3 days of repeated CCCP or HBSS. (A) Quantitative analyses of PGC1α, Hsp70, and MnSOD protein expression. (B) Representative immunobots. (C) Enzyme activity of several proteolytic enzymes. Error bars are SEM, n=3.

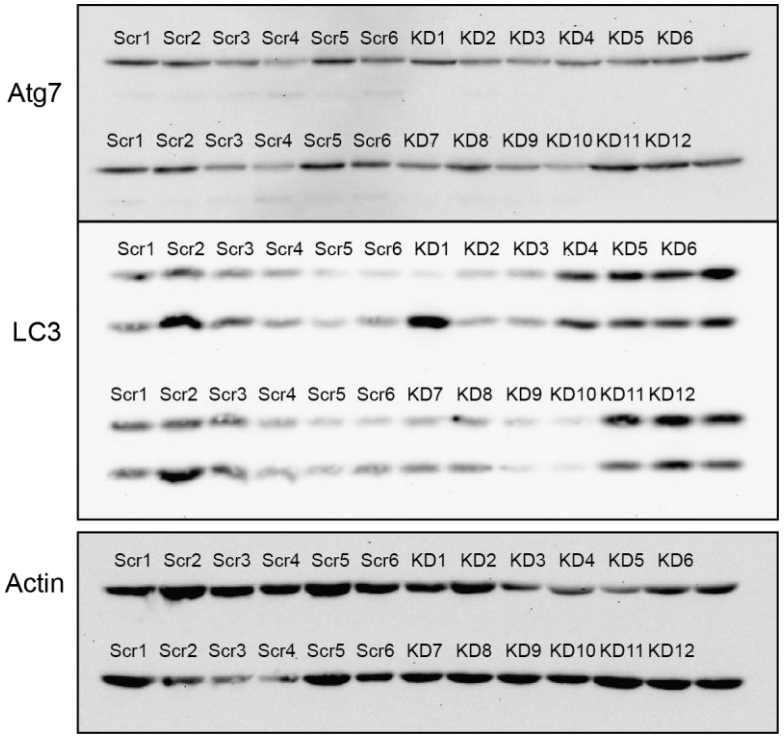

Figure 12. Generating C2C12 cells with stable Atg7 knockdown: Attempt #1. C2C12 cells were transfected with vectors coding for either an shRNA against Atg7 (KD) or a scramble control sequence (Scr), stably-incorporated colonies were selected using puromycin, and individual clones were isolated and assessed for Atg7 protein expression using immunoblotting, as previously performed (183).

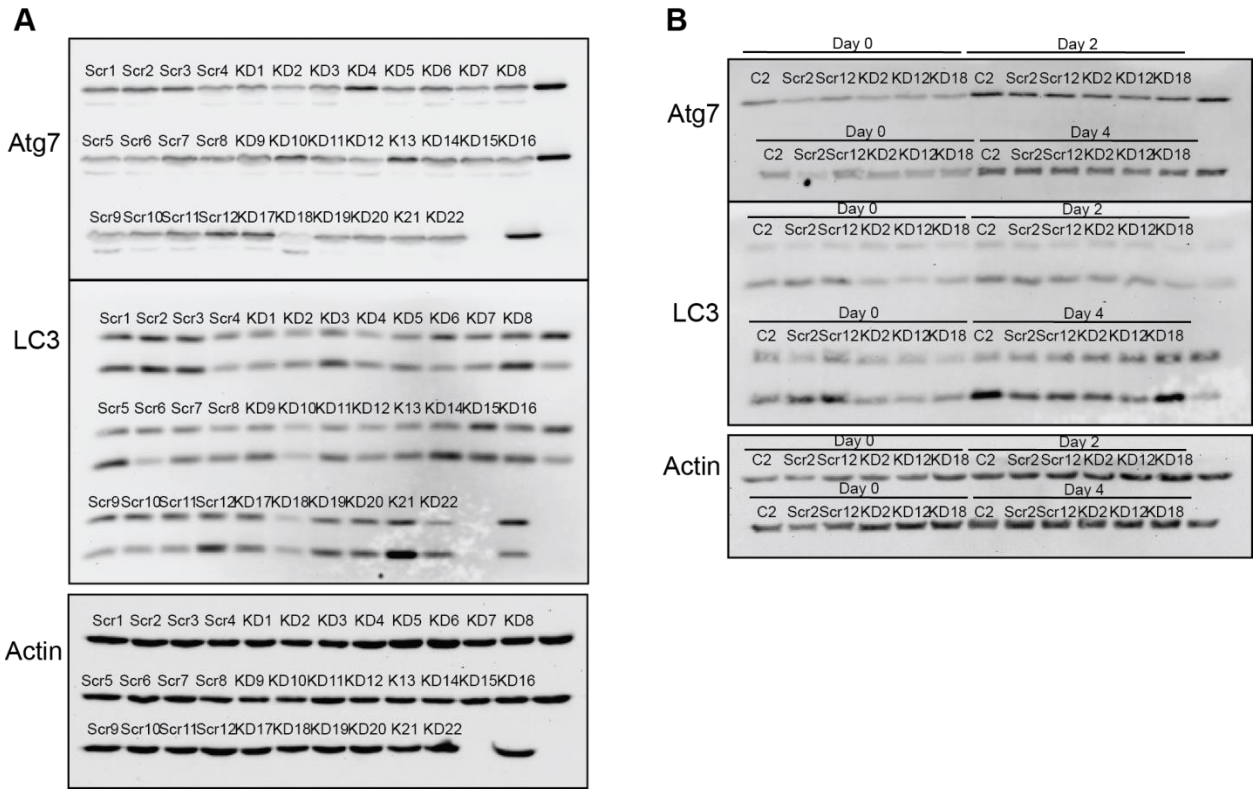

Figure 13. Generating C2C12 cells with stable Atg7 knockdown: Attempt #2. (A) Cells were transfected and isolated similar to Figure 6. (B) Select clones were re-plated into culture and differentiated to confirm Atg7 protein knockdown. C2 represents non-transfected, low-pass C2C12 cells.

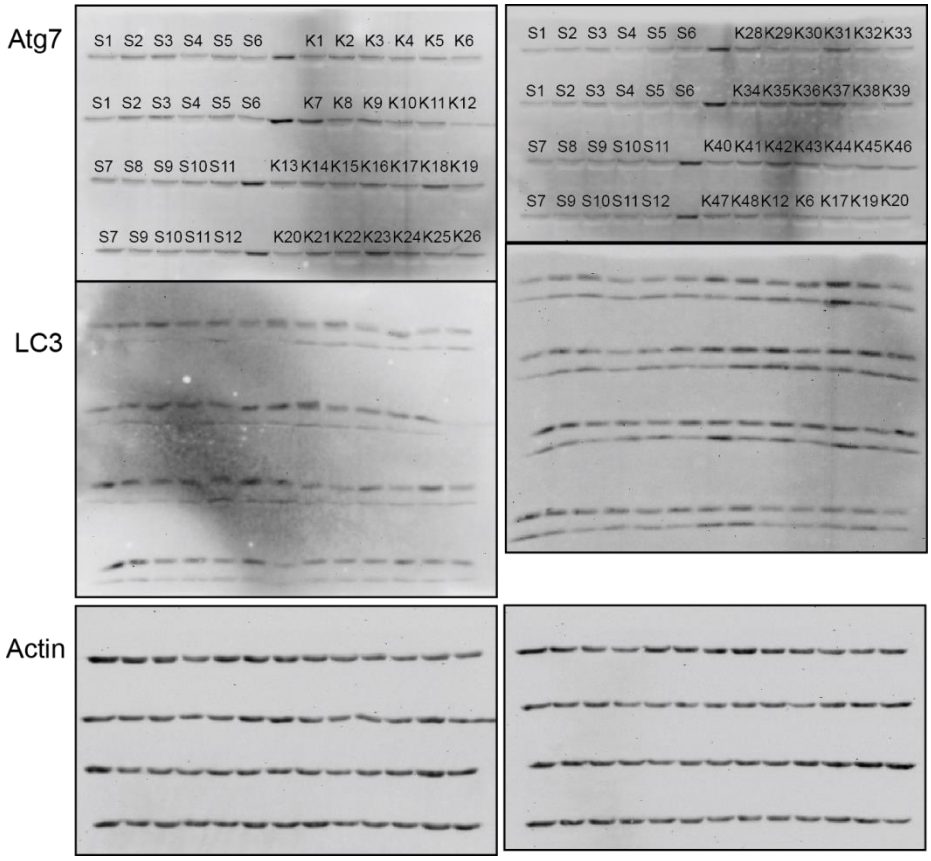

Figure 14. Generating C2C12 cells with stable Atg7 knockdown: Attempt #3. Phoenix helper-free retrovirus-producing cells were used to package virus particles containing either Atg7-targeting or scramble shRNA vectors. After isolation, viral particles were introduced into C2C12 cultures with Polybrene (Santa Cruz), and individual cell clones with stable vector incorporation were selected using puromycin as in previous Figures. Atg7 protein content was then assessed using immunoblotting. Scramble/control clones are labelled with “S” and Atg7-targeting vector clones are labelled with “K”.

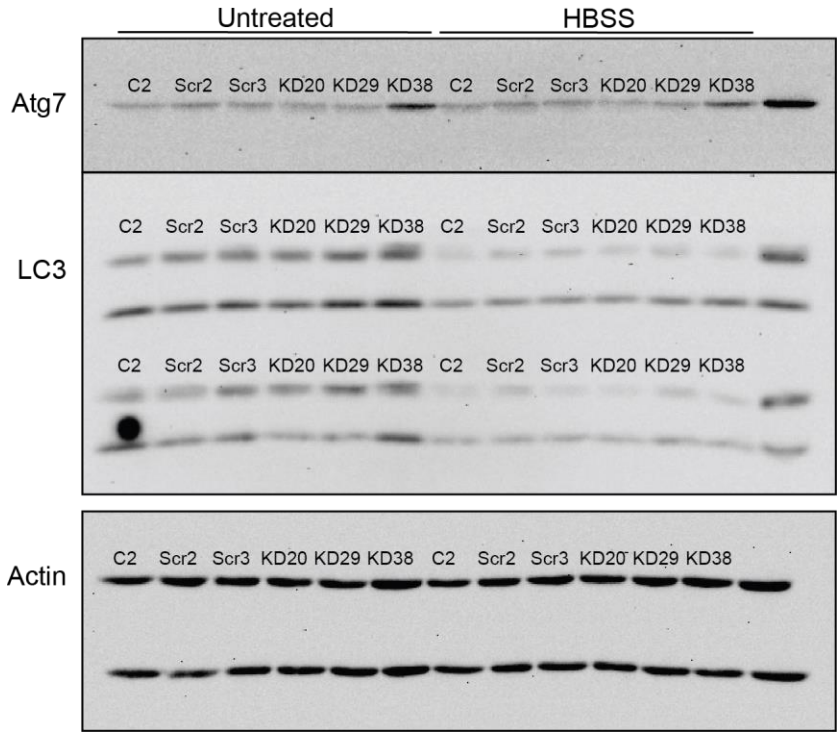

Figure 15. Evaluating Atg7 expression in cell clones from Attempt #3. Select clones were re-plated into culture and administered HBSS to confirm Atg7 protein knockdown. C2 represents non-transfected, low-pass C2C12 cells.

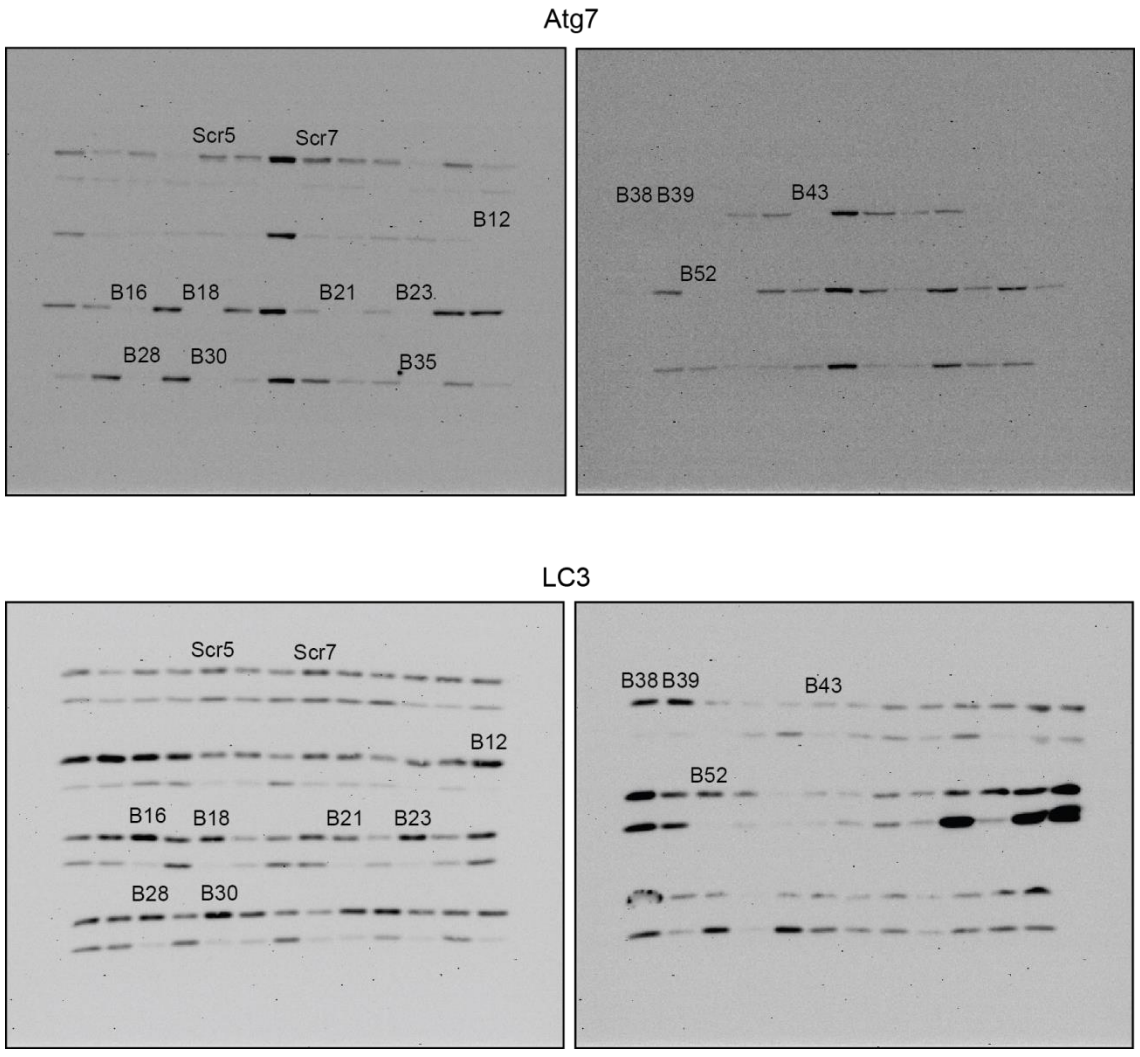

Figure 16. Generating C2C12 cells with stable Atg7 knockdown: Attempt #4. Using fresh vector DNA, C2C12 cells were transfected with either Atg7 or scramble vectors and clones were isolated as in Attempts 1 and 2. This time, numerous clones transfected with Atg7-specific shRNA demonstrated reduced Atg7 and LC3II protein content compared to SCR and C2C12 cells.

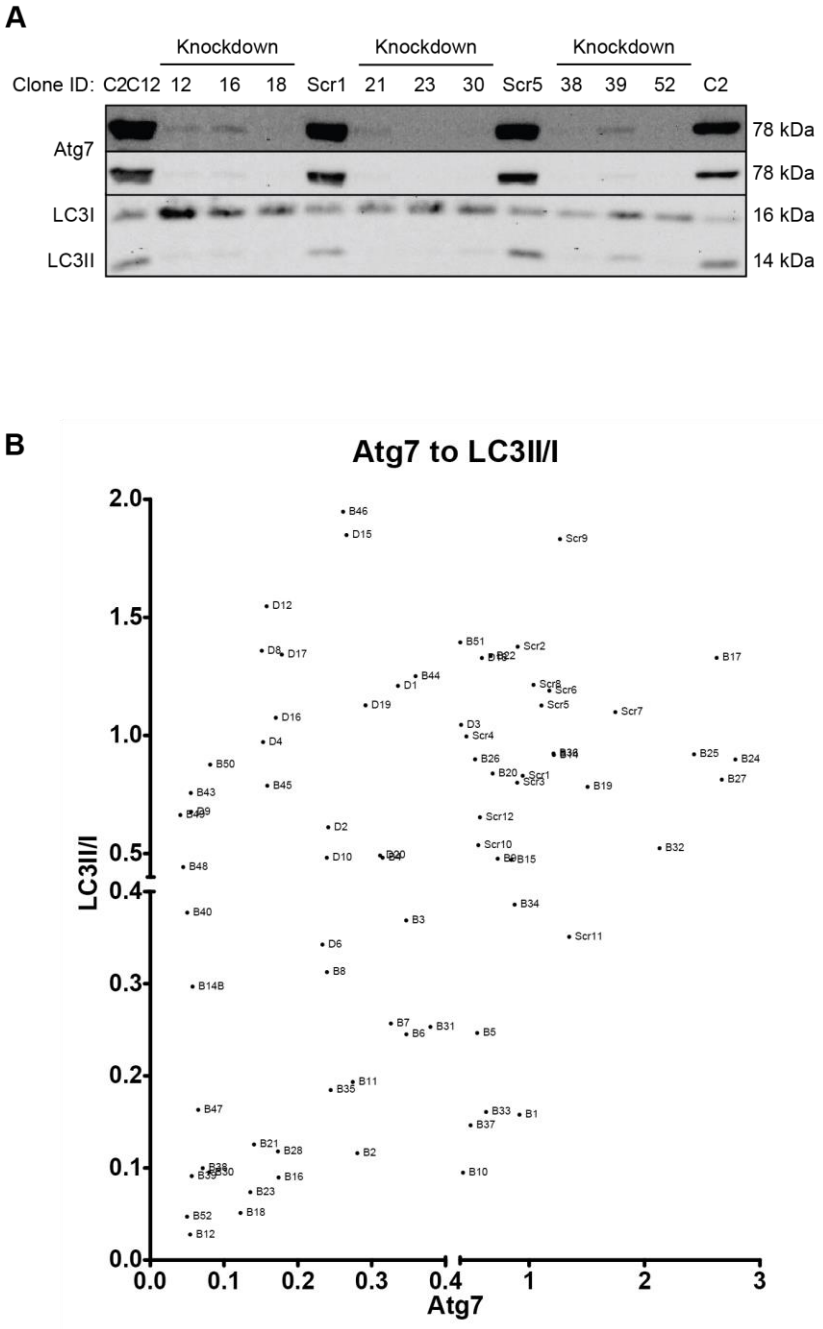

Figure 17. Selecting experimental Atg7 knockdown cell lines. (A) Immunoblot demonstrating reduced Atg7 and LC3II protein content in several knockdown clones compared to low-pass non-transfected C2C12 and scramble control cells (SCR). (B) To select clones with "effective" Atg7 protein knockdown, the relative expression of Atg7 was plotted against the LC3II/I ratio, with the intention of selecting clones in which these two parameters were related: decreased Atg7 should result in less LC3 lipidation. As can be seen, clones 12, 18, and 52 have drastically lower Atg7 levels and LC3II/I ratios. In other parts of this thiesis, Atg7-knockdown clone 12 is referred to as shAtg7-#1, clone 16 as shAtg7-#2, and clone 18 as shAtg7-#3.

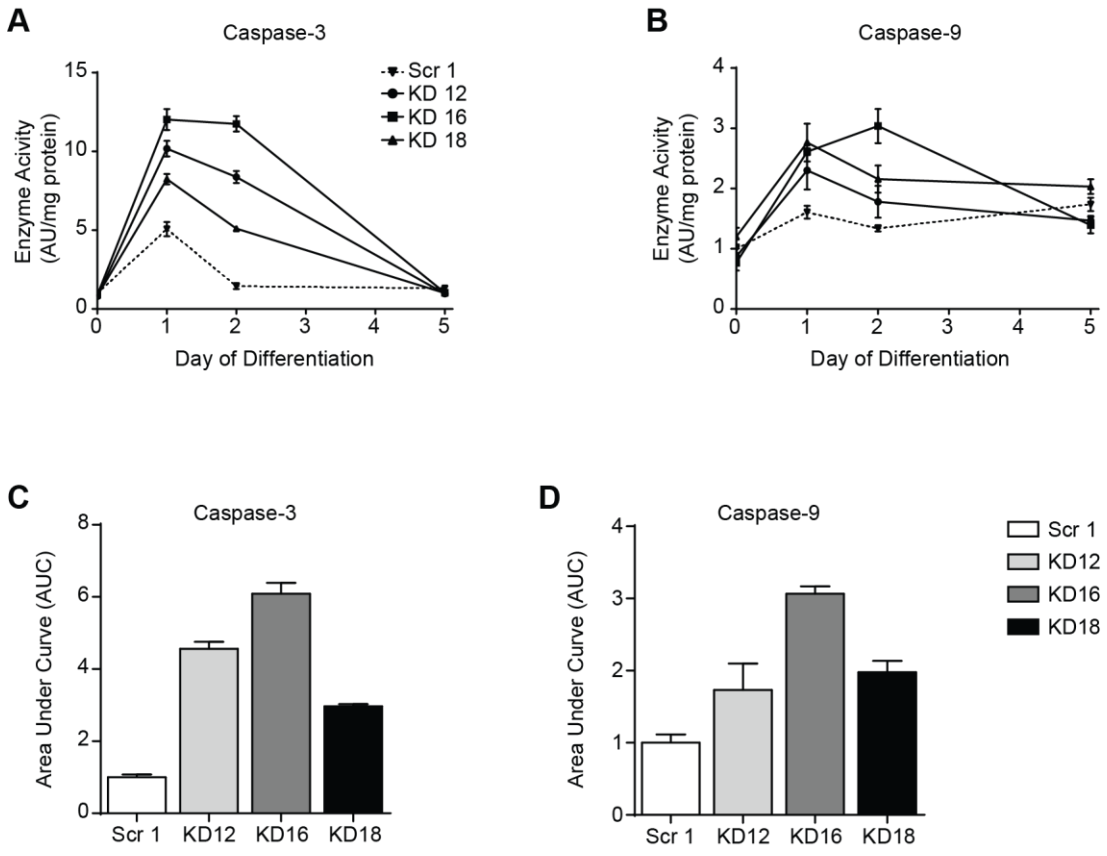

Figure 18. Effect of Atg7 knockdown on caspase activity during myogenic differentiation. To corroborate previous findings regarding the role of autophagy during myogenic differentiation (183), several knockdown clones were differentiated. Cells were assessed for caspase-3 (A) and caspase-9 (B) activity at several time points during the differentiation process. Area under the curve (AUC) calculations highlight increased caspase-3 (C) and caspase-9 (D) activation during differentiation in the absence of Atg7. Error bars represent SEM, n=3.

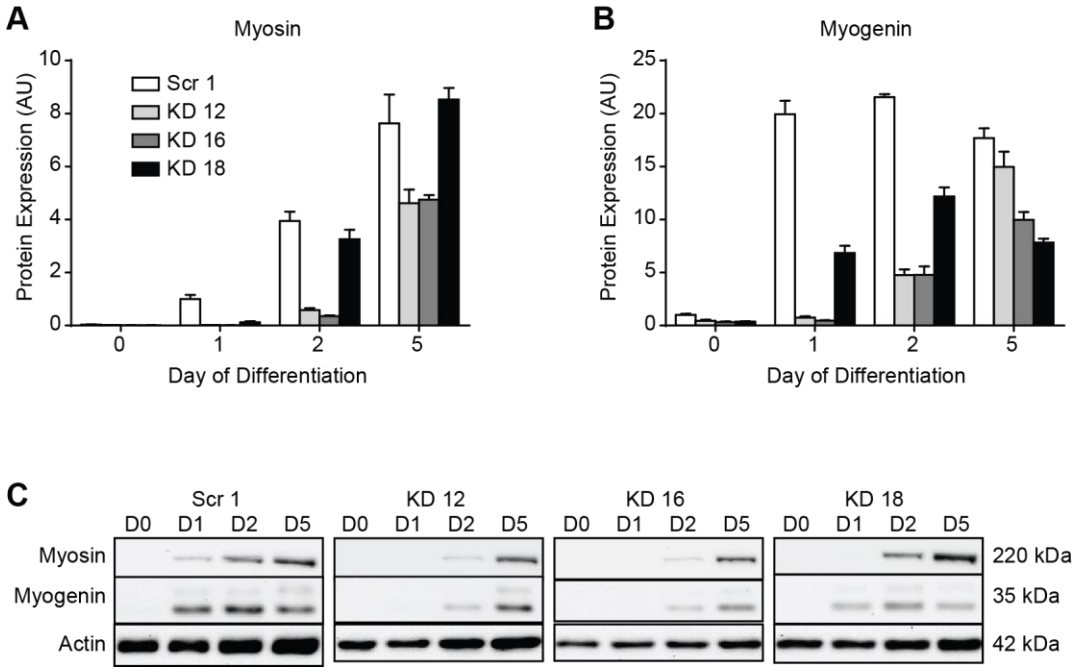

Figure 19. Effect of Atg7 knockdown on myogenic differentiation. Similar to Figure 18, several Atg7-knockdown cell lines were differentiated and collected at various time points. (A) Quantitative analysis of myosin protein content. (B) Quantitative analysis of myogenin protein content. Knockdown clones #1 and #2 demonstrate significantly reduced expression of these two myogenic-specific proteins. (C) Representative immunoblots. Error bars represent SEM, n=3.

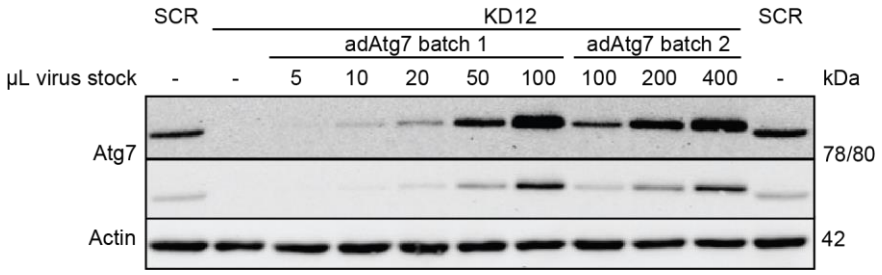

Figure 20. Adenoviral recovery of Atg7 protein content in Atg7-deficient C2C12 cells. Adenovirus coding for human Atg7 (adAtg7) was generated in two batches, each of which was titred for its ability to induce Atg7 protein expression. The indicated volumes of virus stock was incubated on 40-50% confluent shAtg7 cells in 12-well plates for 24 hours, cells were washed in PBS and grown in regular GM for 48 hours, and cells were collected and analyzed for Atg7 protein content using immunoblotting. Note that the human Atg7 protein created by adAtg7 is 2 kDa larger than endogenous mouse Atg7. Recovery of Atg7 protein to SCR levels apparent in both adAtg7-receiving groups.

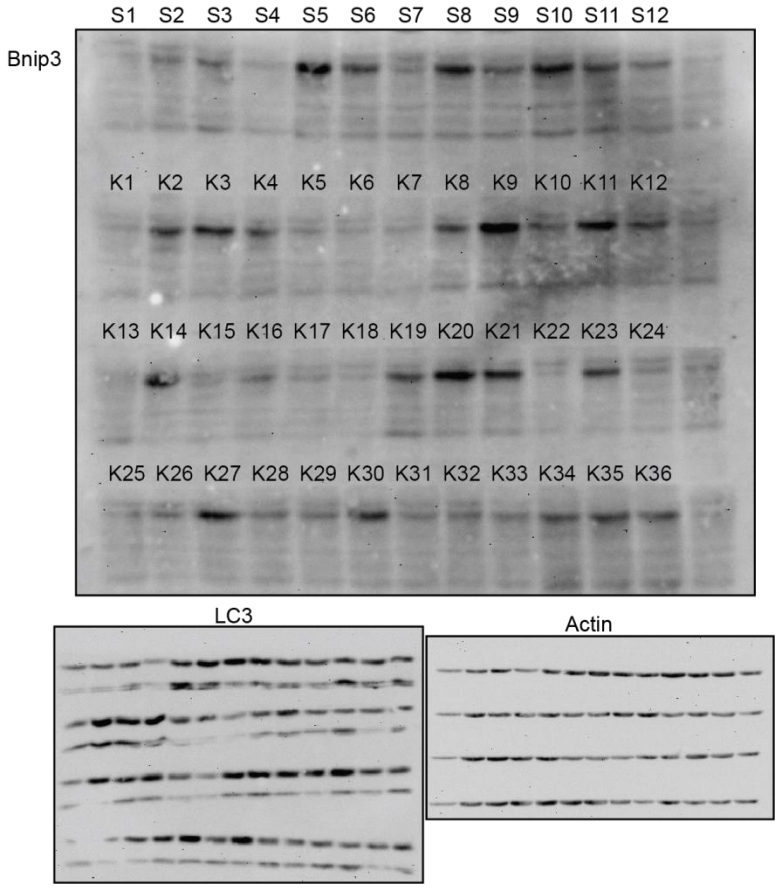

Figure 21. Generating C2C12 cells with stable Bnip3 knockdown: Attempt #1. C2C12 cells were transfected with vectors coding for either an shRNA against Bnip3 (K) or a scramble control sequence (S), stably-incorporated colonies were selected using puromycin, and individual clones were isolated and assessed for Bnip3 protein expression using immunoblotting.

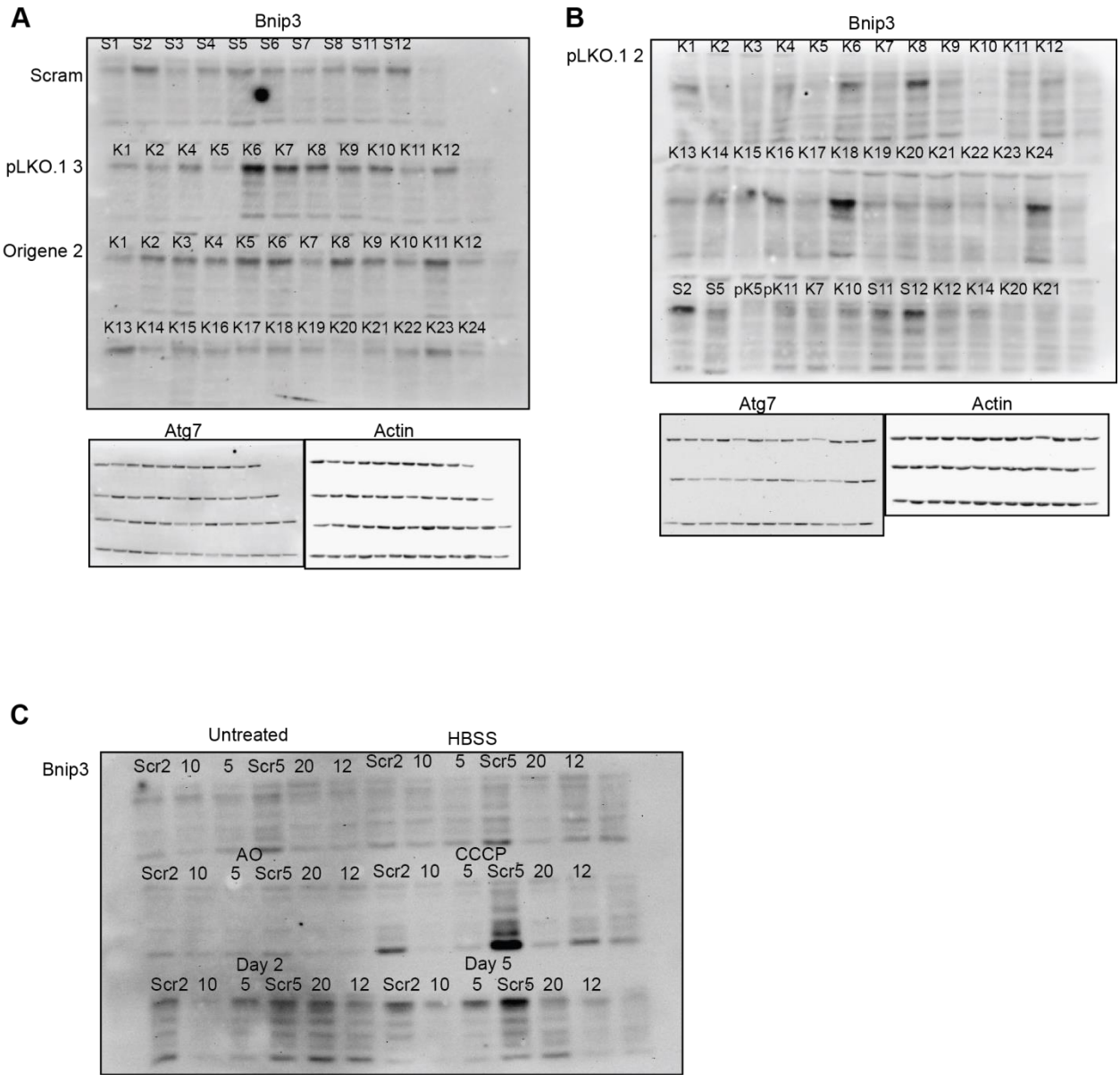

Figure 22. Generating C2C12 cells with stable Bnip3 knockdown: Attempt #2. (A & B) C2C12 cells were transfected with one of three vectors coding for shRNA against Bnip3 (K) or a vector targeting a scramble control sequence (S), stably-incorporated colonies were selected using puromycin, and individual clones were isolated and assessed for Bnip3 protein expression using immunoblotting. (C) Select clones were re-introduced into culture and left untreated or incubated in HBSS to verify Bnip3 protein knockdown.

Designing Bnip3 CRISPR gene knockout targets in mouse

Zhang Lab's tool: http://crispr.mit.edu/
Boutros Lab's tool (E-CRISP): http://www.e-crisp.org/E-CRISP/designcrispr.html
CCTop: http://crispr.cos.uni-heidelberg.de/
Off-Spotter: https://cm.jefferson.edu/Off-Spotter/

Basically, these programs allow you to analyze DNA sequences for CRISPR targets. Each works by searching for 20mer targets (this is standard CRISPR sgRNA (single guide RNA) size used by Zhang's px330 family of CRISPR/Cas9 vectors) with correct PAM locationality (-NGG) in your given sequence.

- Note that the E-CRISP tool can accept GeneID/FASTA information and then pull the sequence data to be analyzed from NCBI's gene database, while the other programs have to be manually provided relatively smaller (up to 250-500bp) DNA sequences.

After potential target sequences are attained, the programs essentially "BLAST" these identified sequences against the rest of the genome (from NCBI) to determine how specific they are to your gene of interest. Each then provides some sort of "score" informing how good/useful the identified targets are.

The Zhang lab also suggests the following when using CRISPR to target things specifically for knock-out experiments: aim for a protein coding region of the genome near the beginning of the resulting mRNA sequence, have your target sequence begin 5'-G...-3'.

To make confirming these designs more complicated, it's important to note that since we're making a double-strand break, it doesn't matter which direction or which "side" of the DNA sequence is targeted: we just want to make a cut. Additionally, Bnip3 is actually positioned "backwards" on the genome (it uses the reverse complement DNA strand according to NCBI's sequencing direction).

Anyways, I inserted the following 50bp of genomic DNA located roughly around the transcriptional start site for Bnip3 into the above programs (or GeneID Bnip3 for E-CRISPR):

CTGCCTCACCCTGCAGGTTCTCCTCCCCGCTCTGCGACATGGTGGCTCGG

This is in the *forward* direction according to NCBI around the transcriptional start site, noting that Cas9 should make cuts 3-4 bp upstream (towards the 5' end) of the PAM. The sequence is described here:

NCBI forward
5'-C TGC CTC ACC CTG CAG GTT CTC CTC CCC GCT CTG CGA **CAT** GGT GGC TCG G-3'

Reverse complement (in the direction that Bnip3 is made)
5'-C CGA GCC ACC **ATG** TCG CAG AGC GGG GAG GAG AAC CTG CAG GGT GAG GCA G-3'

Bold = start. Gray = exon. Green = protein coding. Yellow = intron.

The following numbers of potential targets were identified:
Zhang: 10
CCTop: 3

Off-Spotter: 10
E-CRISP: 60 (but, 5084 potential targets were identified across the entire 18,683 bases that make up the Bnip3 mouse gene, 561 hit a specific target, and 501 were removed for being redundant).

So, 3 or 10 is not a lot of targets. In fact, 1 of CCTop's actually targets 4 other regions of the genome, and only 2 of Zhang's are classified as "good" and they're only different by a single base. But, all four programs identified two similar target sequences with the best chances of working (PAM in brackets):

```
First: GAGCCACCATGTCGCAGAGC (GGG)
Second: GGAGGAGAACCTGCAGGGTG (AGG)
```

Both of these sequences in the same direction as Bnip3 is made:

```
5'-C CGA GCC ACC ATG TCG CAG AGC GGG GAG GAG AAC CTG CAG GGT GAG GCA G-3'
1st:   GA GCC ACC ATG TCG CAG AGC(GGG)
2nd:                                 G GAG GAG AAC CTG CAG GGT G(AG G)
```

Alrighty then. Now we need oligos to insert into the spCas9 vectors we have. Note these have small overhangs for cloning: as specified by Zhang Lab's cloning protocol.

```
First forward: 5'- CACC GAGCCACCATGTCGCAGAGC -3'
      reverse: 5'- AAAC GCTCTGCGACATGGTGGCTC -3'

Second forward: 5'- CACC GGAGGAGAACCTGCAGGGTG -3'
       reverse: 5'- AAAC CACCCTGCAGGTTCTCCTCC -3'
```

Here is a scramble sequence for control. This is actually the sequence that Origene uses in their control CRISPR products. According to the gRNA design tools, there is a greater chance of an off-target hit with either of the above Bnip3 sequences than with this scramble sequence:

```
Scramble forward: 5'- CACC GCACTACCAGAGCTAACTCA -3'
Scramble reverse: 5'- AAAC TGAGTTAGCTCTGGTAGTGC -3'
```

Well, it looks like we need a few things yes to do this: two restriction enzymes (Robin doesn't have these) and a nucleotide phosphorylating kinase (the annealed oligos need to be phosphorylated for ligating). New England BioLabs or ThermoFisher/Invitrogen/Fermentas has this stuff (NEB is cheaper).

- *BbsI*
- *AgeI*
- T4 Polynucleotide Kinase (PNK)

And maybe two for mouse Atg7? (we didn't end up getting these – they are *great* gRNA according to the design tool guidelines):

```
First: forward: 5'- CACC GGCCTCACCACTGTGCTCGT -3'
      reverse: 5'- AAAC ACGAGCACAGTGGTGAGGCC -3'
```

Second: forward: 5′- CACC GAAAATTCCCACGAGCACAG -3′
reverse: 5′- AAAC CTGTGCTCGTGGGAATTTTC -3′

Zhang Lab Target Sequence Cloning Protocol

PX330-based plasmids, including PX458-462 – SpCas9 (or SpCas9n D10A nickase) + single guide RNA:

The Quadrilatero Lab has pSpCas9(BB)-2A-Puro(px459) which makes double-strand breaks and pSpCas9n(BB)-2A-Puro(px462) which makes single-strand nicks

To clone the guide sequence into the sgRNA scaffold, synthesize two oligos *(Standard de-salted oligos are sufficient)* of the form:

5' – CACCGNNNNNNNNNNNNNNNNNN – 3'
3' – CNNNNNNNNNNNNNNNNNNNCAAA – 5'

PX260 and PX334 – SpCas9 (or SpCas9n D10A nickase) + CRISPR array + tracrRNA:

To clone the guide sequence into the sgRNA scaffold, synthesize two oligos of the form:

5' – AAACNNNNNNNNNNNNNNNNNNNNNNNNNNNNGT – 3'
3' – NNNNNNNNNNNNNNNNNNNNNNNNNNNNNCAAAAT – 5'

Oligo annealing and cloning into backbone vectors:

1. Digest 1ug of plasmid with *Bbs*I for 30 min at 37°C:

1 ug	Plasmid
1 ul	FastDigest *Bbs*I (Fermentas)
1 ul	FastAP (Fermentas)
2 ul	10X FastDigest Buffer
X ul	ddH_2O
20 ul	total

2. Gel purify digested plasmid using QIAquick Gel Extraction Kit and elute in EB.

3. Phosphorylate and anneal each pair of oligos:

1 ul	oligo 1 (100mM)
1 ul	oligo 2 (100mM)
1 ul	10X T4 Ligation Buffer (NEB)
6.5 ul	ddH_2O
0.5 ul	T4 PNK (NEB)
10 ul	total

Anneal in a thermocycler using the following parameters:

37°C	30 min
95°C	5 min and then ramp down to 25°C at 5°C/min

4. Set up ligation reaction and incubate at room temperature for 10 min:

X ul	*Bbs*I digested plasmid from step 2 (50ng)
1 ul	phosphorylated and annealed oligo duplex from step 3 (1:200 dilution)
5 ul	2X Quickligation Buffer (NEB)
X ul	ddH_2O
10 ul	subtotal
1 ul	Quick Ligase (NEB)
11 ul	total

5. Transformation.

Bnip3 CRISPR vectors

Vector Backbone (on AddGene, from distributor)
>U6::sgRNA(BbsI)

Gagggcctatttcccatgattccttcatatttgcatatacgatacaag
gctgttagagagataattggaattaatttgactgtaaacacaaagatattagtacaaaatacgtgacgta
gaaagtaataatttcttgggtagtttgcagttttaaaattatgttttaaaatggactatcatatgcttac
cgtaacttgaaagtatttcgatttcttggctttatatatcttGTGGAAAGGACGAAACACCggGTCTTCg
aGAAGACctgttttagagctaGAAAtagcaagttaaaataaggctagtccgttatcaacttgaaaaagtg
gcaccgagtcggtgcTTTTTT

Sequencing from The Center For Applied Genomics

Overlapping region
Cloned-in restriction site
CRISPR sgRNA
Edited per FinchTV

Scram sequence from Origene
>BS2-U6-fwd CHROMAT_ID=417757
~~Atttgmawtacgatama~~c
gctgttagagagataattggaattaatttgactgtaaacacaaagatattagtacaaaatacgtgacgt
agaaagtaataatttcttgggtagtttgcagttttaaaattatgttttaaaatggactatcatatgctt
accgtaacttgaaagtatttcgatttcttggctttatatatcttgtggaaaggacgaaacaccgcacta
ccagagctaactcagttttagagctagaaatagcaagttaaaataaggctagtccgttatcaacttgaa
aaagtggcaccgagtcggtgctttttgttttagagctagaaatagcaagttaaaataaggctagtccg
tttttagcgcgtgcgccaattctgcagacaaatggctctagaggtacccgttacataacttacggtaaa
tggcccgcctggctgaccgcccaacgacccccgcccattgacgtcaatagtaacgccaatagggacttt
ccattgacgtcaatgggtggagtatttacggtaaactgcccacttggcagtacatcaagtgtatcatat
gccaagtacgccccctattgacgtcaatgacggtaaatggcccgcctggcattgtgcccagtacatgac
cttatgggactttcctacttggcagtacatctacgtattagtcatcgctattaccatggtcgaggtgag
ccccacgttctgcttcactctccccatctccccccccctccccacccccaattttgtatttatttatttt
ttaattattttgtgcagcgatgggggcgggggggggggtccscscmccatgykgkgcrkgmygggcry
ggygctkkgckkgtmkakcygaaagtgcacrscayymatcaragmgykccyyackaaygtttcytttay
ggca

Bnip3 targeting sequence #1
>B12-U6-fwd CHROMAT_ID=417770
~~Awttgcwtacgat~~acac
Gctgttagagagataattggaattaatttgactgtaaacacaaagatattagtacaaaatacgtgacgt
agaaagtaataatttcttgggtagtttgcagttttaaaattatgttttaaaatggactatcatatgctt
accgtaacttgaaagtatttcgatttcttggctttatatatcttgtggaaaggacgaaacaccgagcca
ccatgtcgcagagcgttttagagctagaaatagcaagttaaaataaggctagtccgttatcaacttgaa
aaagtggcaccgagtcggtgctttttgttttagagctagaaatagcaagttaaaataaggctagtccg
tttttagcgcgtgcgccaattctgcagacaaatggctctagaggtacccgttacataacttacggtaaa
tggcccgcctggctgaccgcccaacgacccccgcccattgacgtcaatagtaacgccaatagggacttt

ccattgacgtcaatgggtggagtatttacggtaaactgcccacttggcagtacatcaagtgtatcatat
gccaagtacgccccctattgacgtcaatgacggtaaatggcccgcctggcattgtgcccagtacatgac
cttatgggactttcctacttggcagtacatctacgtattagtcatcgctattaccatggtcgaggtgag
ccccacgttctgcttcactctccccatctccccccccctccccacccccaattttgtatttatttatttt
ttaattattttgtgcagcgatgggggcgggggggggggggggggcgcrccyccwagcggsscwgtgmy
agtcwagssrcgsgackgtccmagsckaaaaggtgcggcgtcwsccaaawcassggmgcsmtccgaaag
ttccyytrwwggrgrasw

Bnip3 targeting sequence #1 – other clone
>B16-U6-fwd CHROMAT_ID=417733
aatttgcwtwcgatacac
gctgttagagagataattggaattaatttgactgtaaacacaaagatattagtacaaaatacgtgacgt
agaaagtaataatttcttgggtagtttgcagttttaaaattatgttttaaaatggactatcatatgctt
accgtaacttgaaagtatttcgatttcttggctttatatatcttgtggaaaggacgaaacaccgagcca
ccatgtcgcagagcgttttagagctagaaatagcaagttaaaataaggctagtccgttatcaacttgaa
aaagtggcaccgagtcggtgctttttttgttttagagctagaaatagcaagttaaaataaggctagtccg
tttttagcgcgtgcgccaattctgcagacaaatggctctagaggtacccgttacataacttacggtaaa
tggcccgcctggctgaccgcccaacgacccccgcccattgacgtcaatagtaacgccaatagggacttt
ccattgacgtcaatgggtggagtatttacggtaaactgcccacttggcagtacatcaagtgtatcatat
gccaagtacgccccctattgacgtcaatgacggtaaatggcccgcctggcattgtgcccagtacatgac
cttatgggactttcctacttggcagtacatctacgtattagtcatcgctattaccatggtcgaggtgag
ccccacgttctgcttcactctccccatctccccccccctccccacccccaattttgtatttatttatttt
ttaattattttgtgcagcgatgggggcggggtgggggggtcccsgcsccagccgggcggggcgggcga
ggggcgggcgggccaagcgaaagktgcgscgcmgccmatmraagcggcgcgctccraagkttyccttttt
wwrggcrragg

Bnip3 targeting sequence #2
>B23-U6-fwd CHROMAT_ID=417745
Attkgmwtacgatacag
gctgttagagagATaattggaattaatttgactgtaaacacaaagatattagtacaaaatacgtgacgt
agaaagtaataatttcttgggtagtttgcagttttaaaattatgttttaaaatggactatcatatgctt
accgtaacttgaaagtatttcgatttcttggctttatatatcttgtggaaaggacgaaacaccggagga
gaacctgcagggtgttttagagctagaaatagcaagttaaaataaggctagtccgttatcaacttgaa
aaagtggcaccgagtcggtgctttttttgttttagagctagaaatagcaagttaaaataaggctagtccg
tttttagcgcgtgcgccaattctgcagacaaatggctctagaggtacccgttacataacttacggtaaa
tggcccgcctggctgaccgcccaacgacccccgcccattgacgtcaatagtaacgccaatagggacttt
ccattgacgtcaatgggtggagtatttacggtaaactgcccacttggcagtacatcaagtgtatcatat
gccaagtacgccccctattgacgtcaatgacggtaaatggcccgcctggcattgtgcccagtacatgac
cttatgggactttcctacttggcagtacatctacgtattagtcatcgctattaccatggtcgaggtgag
ccccacgttctgcttcactctccccatctccccccccctccccacccccaattttgtatttatttatttt
ttaattattttgtgcagcgatgggggcggatcgggggggaccycgcgccaggcggggcgggcgrgcragr
gcgggcgggcagkcaaaaggtgcgcggcaccaatcaragcggsgcgctcckaaagtttctttttakggs
sgaggcgg

Anti-Bnip3 Antibody from Sigma

Our antibody's epitope

Bnip3 mouse amino acids

MSQSGEENLQ GSWVELHFSN GNGSSVPASV SIYNGDMEKI LLDAQHESGR SSSKSSHCDS
PPRSQTPQDT NRAEIDSHSF GEKNSTLSEE DYIERRREVE SILKKNSDWI WDWSSRPENI
PPKEFLFKHP KRTATLSMRN TSVMKKGGIF SADFLKVFLP SLLLSHLLAI GLGIYIGRRL
TTSTSTF

Nix mouse Amino Acids

MSHLVEPPPP LHNNNNNCEE GEQPLPPPAG LNSSWVELPM NSSNGNENGN GKNGGLEHVP
SSSSIHNGDM EKILLDAQHE SGQSSSRGSS HCDSPSPQED GQIMFDVEMH TSRDHSSQSE
EEVVEGEKEV EALKKSADWV SDWSSRPENI PPKEFHFRHP KRAASLSMRK SGAMKKGGIF
SAEFLKVFIP SLFLSHVLAL GLGIYIGKRL STPSASTY

Bnip3 Human Amino Acids

MGDAAADPPG PALPCEFLRP GCGAPLSPGA QLGRGAPTSA FPPPAAEAHP AARRGLRSPQ
LPSGAMSQNG APGMQEESLQ GSWVELHFSN NGNGGSVPAS VSIYNGDMEK ILLDAQHESG
RSSSKSSHCD SPPRSQTPQD TNRASETDTH SIGEKNSSQS EEDDIERRKE VESILKKNSD
WIWDWSSRPE NIPPKEFLFK HPKRTATLSM RNTSVMKKGG IFSAEFLKVF LPSLLLSHLL
AIGLGIYIGR RLTTSTSTF

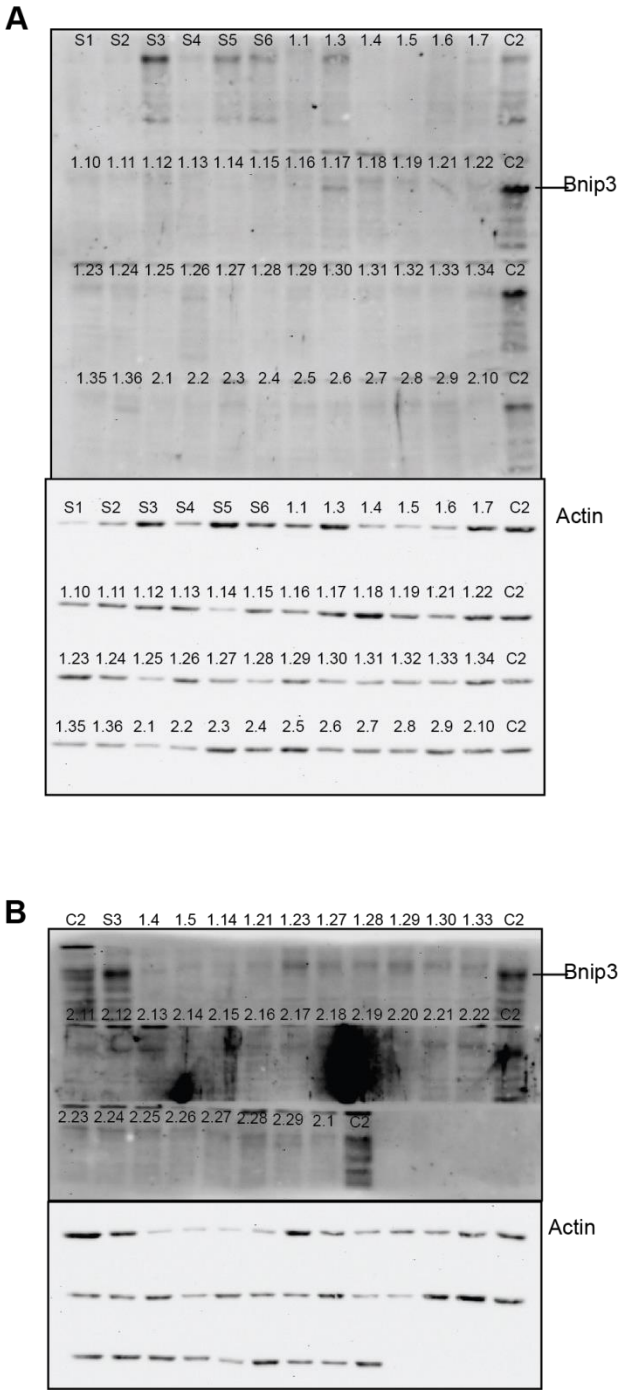

Figure 23. Generating Bnip3-knockout C2C12 cells using CRISPR/Cas9: Attempt #1. (A) C2C12 cells were transfected with CRISPR/Cas9 vectors containing one of two gRNAs targeting Bnip3 (1.N or 2.N) or a scramble control sequence (S) and more successfully transfected clones were selected with puromycin and individually isolated for assessment of Bnip3 protein content using immunoblotting. (B) Select clones were immunoblotted again to facilitate protein expression comparisons. C2 represents non-transfected, low pass C2C12 cells.

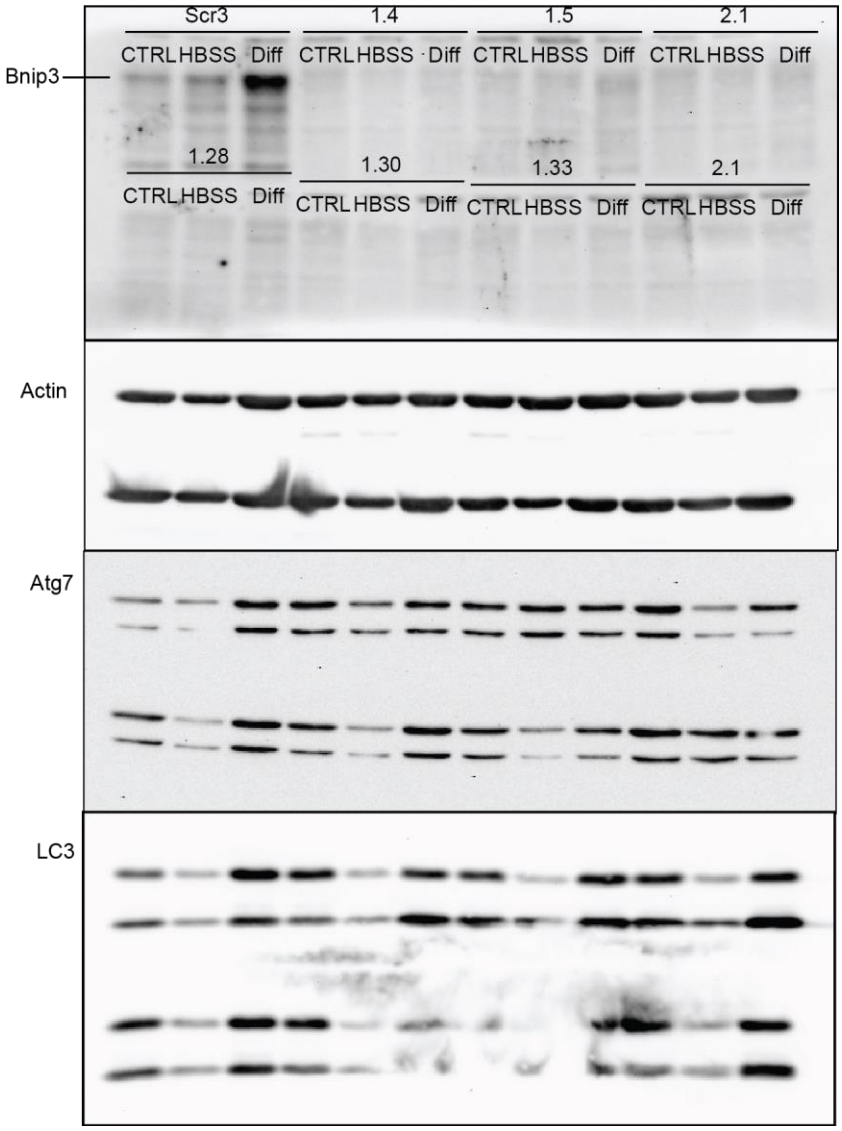

Figure 24. Evaluating Bnip3 expression in cell clones from CRISPR Attempt #1. Select clones from Figure 18 were re-introduced into culture and left untreated (CTRL), differentiated for 4 days (Diff), or treated with HBSS (HBSS) to further assess Bnip3 protein content.

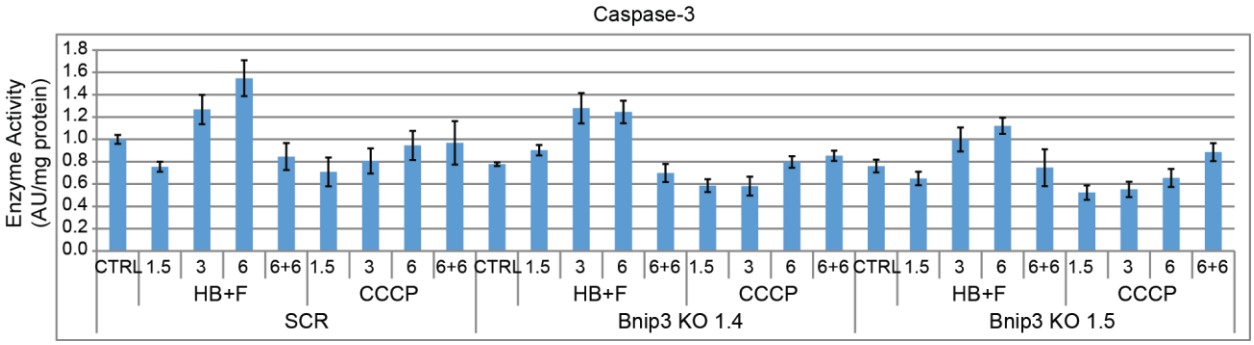

Figure 25. Selecting experimental Bnip3-knockout cell clones. Select Bnip3-CRISPR clones were incubated in HB+F or 30 µM CCCP for 1.5, 3, or 6 hours and collected immediately or after spending an additional 6 hours in GM (6+6) and assessed for caspase-3 activity.

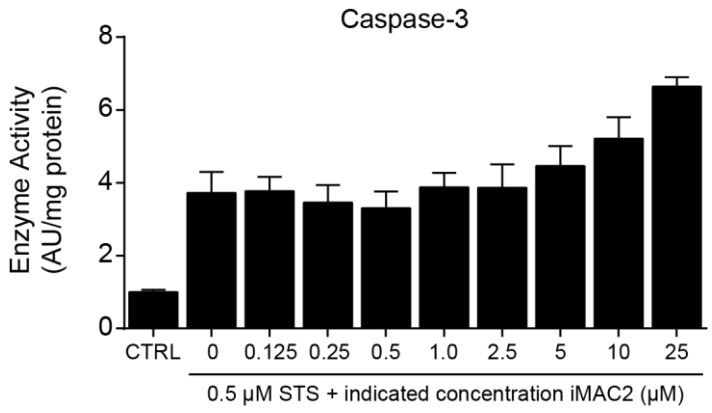

Figure 26. Preventing STS-induced caspase-3 activity with iMAC2. To implicate mitochondrial-mediated mechanisms involved in autophagy-induced protective cellular remodelling, the mitochondrial pore inhibiting chemical iMAC2 was tested for its ability to prevent STS-induced caspase-3 activity. Although caspase-3 activity was slightly reduced by 0.5 µM iMAC2, this was not significant enough to justify performing a full experiment. However, "iMAC2-mediated reduction in STS-induced caspase-3 activation" is the exact experiment performed when initially developing this chemical, where its IC50 was observed to be 2.5 µM (482). In an additional study, these researchers conducted similar experiments with 0.5-5.0 µM iMAC2 (483).

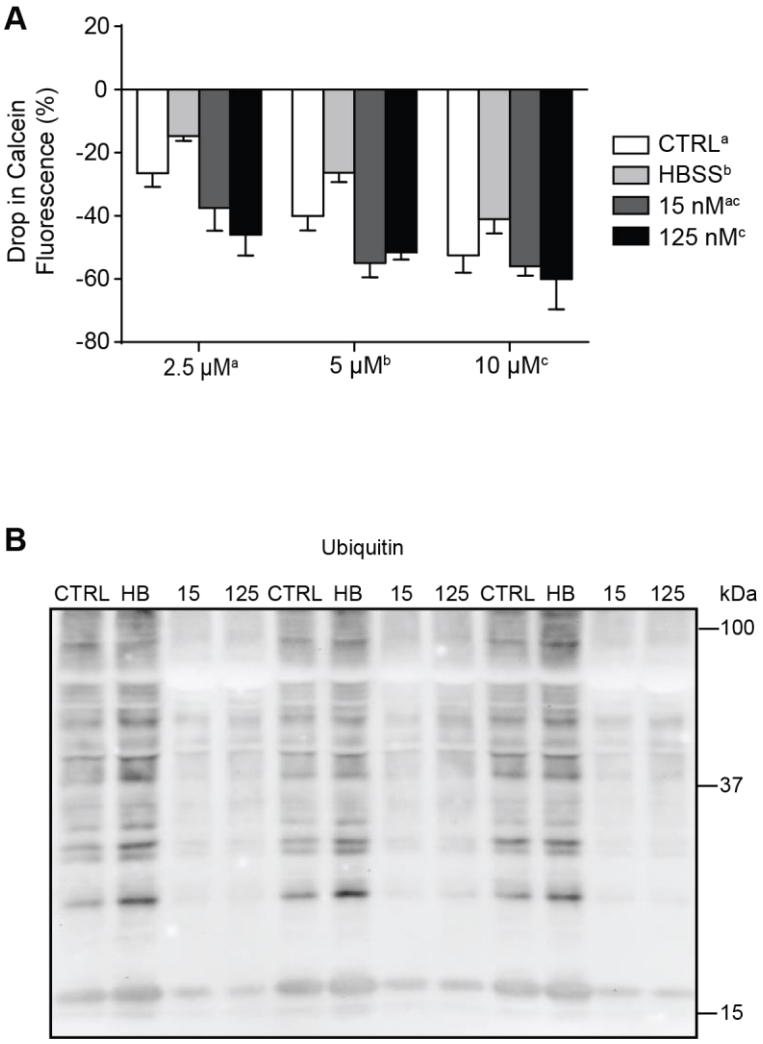

Figure 27. Repeated HBSS treatments protect mitochondria from while senescent cells are sensitized to Ca^{2+} stress. (A) To specifically test the stress-resistance of mitochondria, mitochondrial permeability transition pore (mPTP) formation was measured with flow cytometry analysis of calcein fluorescence after inducing calcium stress with the Ca^{2+} ionophore A23187. Here, increasing concentrations of A23187 caused progressive drops in calcein fluorescence ($p<0.05$), indicating mitochondrial permeabilization. However, cells repeatedly given HBSS displayed relatively smaller ($p<0.05$) decreases in fluorescence compared to CTRL, signifying partial protection from Ca^{2+} stress. This contrasts the response of STS-treated cells, as 125 nM STS administration let to larger ($p<0.05$) decreases in calcein fluorescence compared to CTRL. Bars represent SEM, n=4, comparisons made with 2-way ANOVA. (B) Ubiquitin immunoblot, demonstrating reduced ubiquitination of proteins between 15 and 100 kDa.

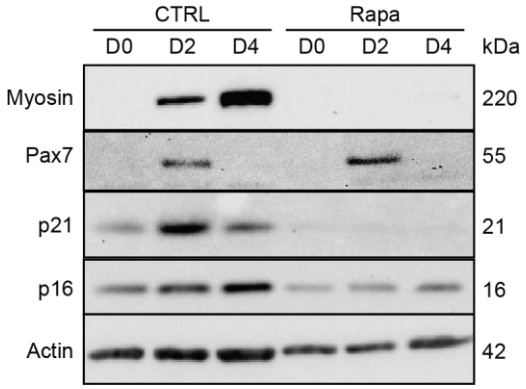

Figure 28. Repeated rapamycin administration prevents C2C12 myogenic differentiation. In this pilot experiment, C2C12 cells were grown in regular GM (CTRL) or administered 1.0 µM rapamycin (Rapa) for 8 hours per day for 3 consecutive days and myogenic differentiation was induced 20 hours following the final treatment by switching to low growth-factor DM. Cells were collected at the media-switching moment (D0) as well as after spending 2 days (D2) and 4 days (D4) in DM and subsequently immunoblotted for various myogenic factors. While expected transient p21 and progressive myosin protein content increases occur in CTRL, these are absent in Rapa.

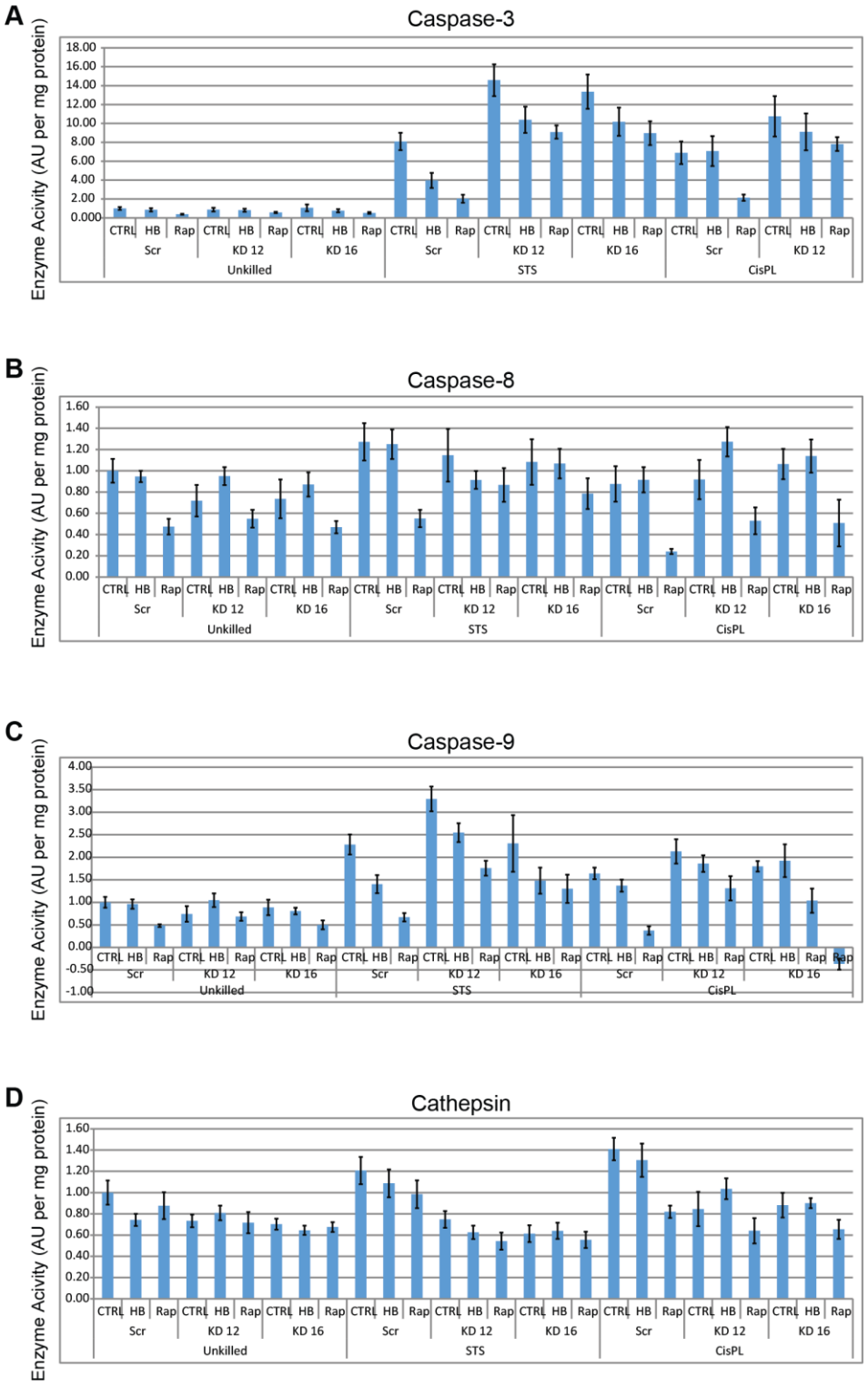

Figure 29. Proteolytic enzyme activity assessment in Atg7-deficient C2C12 cells repeatedly incubated in HBSS or rapamycin and subsequently killed with STS or CisPL. Full panels of caspase-3 (A), caspase-8 (B), caspase-9 (C), and cathepsin (D) activity measurements as previously depicted in Chapter II, Figure 4, including data for KD16.

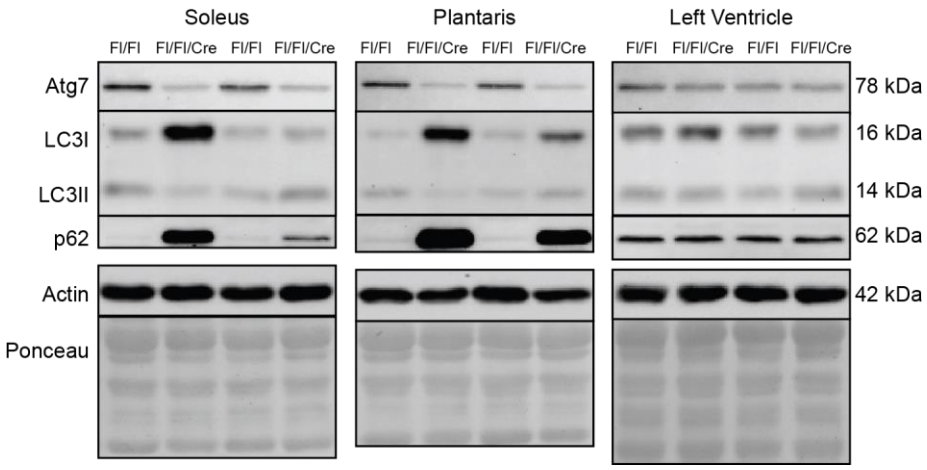

Figure 30. Assessing autophagy signaling alterations 10 weeks after inducing skeletal muscle-specific knockdown of Atg7 in mice. Mice with floxed Atg7 genomic regions (Fl/Fl) with/without additional skeletal muscle-specific (driven by human skeletal muscle actin promoter) tamoxifen-inducible Cre-recombinase expression (Fl/Fl/Cre) were intraperitoneally-injected with 2 mg of 10 mg/mL tamoxifen dissolved in sunflower seed oil once per day for 5 consecutive days. 10 weeks later, mice were sacrificed, soleus, plantaris, and left ventricle muscles were dissected and snap-frozen in liquid nitrogen, and tissues were assessed for Atg7, LC3, p62, and actin protein expression using immunoblotting. As expected, Fl/Fl/Cre mice displayed reduced Atg7 but increased LC3I and p62 protein levels compared to Fl/Fl control mice only in their skeletal muscles.

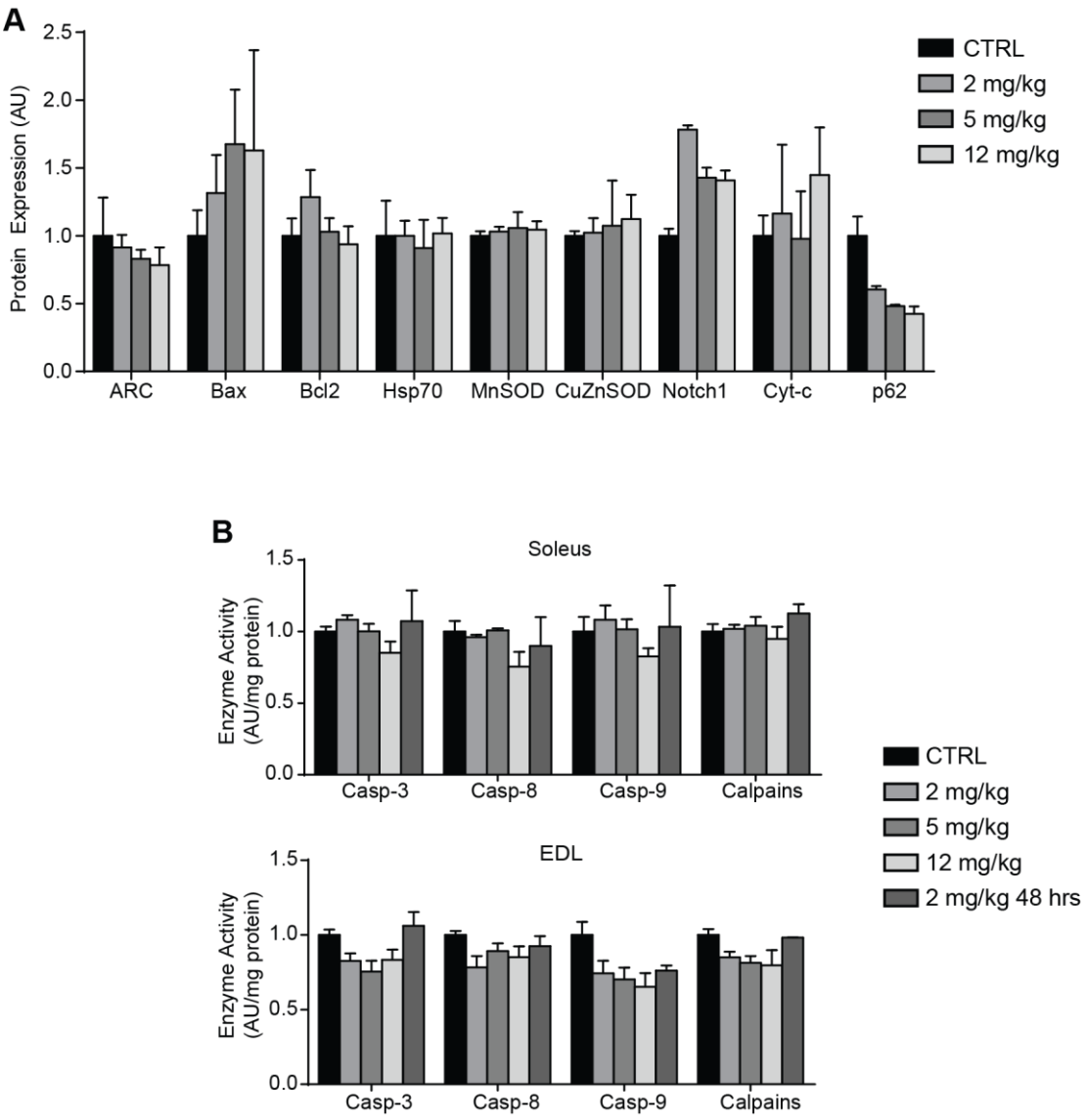

Figure 31. Effect of endotoxin/LPS on skeletal muscle cell death, antioxidant, and autophagy signaling protein contents and proteolytic enzyme activity. C57 mice were intraperitoneally-injected with the indicated concentrations of endotoxin/LPS, sacrificed 24 hours later, and select hindlimb skeletal muscles were dissected and snap-frozen in liquid nitrogen. (A) Mixed-type gastrocnemius muscles were used for immunoblotting analyses of several stress-related proteins. Proteolytic enzyme activity measurements were performed in soleus (B) and extensor digitorum longus (EDL) (C) muscle homogenates. Error bars represent SEM, n=3.

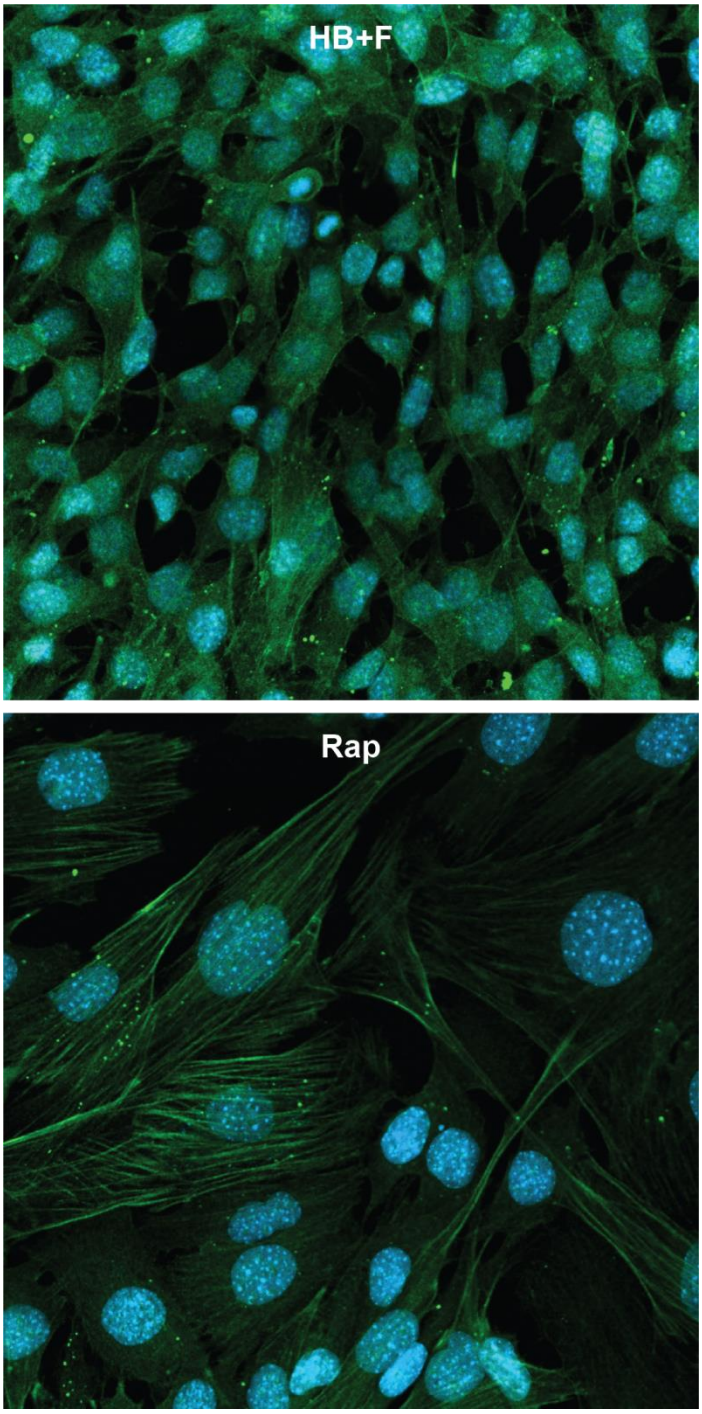

Figure 32. Morphological assessment of C2C12 cells repeatedly incubated in amino acid starvation media or administered rapamycin. Cells were incubated in HB+F for 3 hours or given 1.0 µM rapamycin in GM for 8 hours per day for 3 consecutive days and immunofluorescently stained for actin (green) and DAPI (blue). Note these images were acquired with the same microscope objective: this highlight the odd/enlarged morphology caused by repeated rapamycin administration.